The University of Nottingham

GROUTED MACADAM – MATERIAL CHARACTERISATION FOR PAVEMENT DESIGN

Joel Ricardo Martins de Oliveira

Thesis submitted to the University of Nottingham
For the degree of Doctor of Philosophy

May 2006

ABSTRACT

A new type of pavement has been gaining popularity over the last few years in the U.K. It comprises a surface course with a semi-flexible material that provides significant advantages in comparison to both concrete and conventional asphalt, having both rut resistance and a degree of flexibility. It also provides good protection against the ingress of water to the foundation, since it has an impermeable surface.

The semi-flexible material, generally known as grouted macadam, comprises an open-graded asphalt skeleton with 25 to 35% voids into which a cementitious slurry is grouted. This hybrid mixture provides good rut resistance and a surface highly resistant to fuel and oil spillage. Such properties allow it to be used in industrial areas, airports and harbours, where those situations are frequently associated with heavy and slow traffic.

Grouted Macadams constitute a poorly understood branch of pavement technology and have generally been relegated to a role in certain specialist pavements whose performance is predicted on purely empirical evidence. Therefore, the main objectives of this project were related to better understanding the properties of this type of material, in order to predict its performance more realistically and to design pavements incorporating grouted macadam more accurately.

Based on a standard mix design, which has been used in the U.K. for the past few years, several variables were studied during this project in order to characterise the behaviour of grouted macadams in general, and the influence of those variables on the fundamental properties of the final mixture.

In this research project, two approaches were used to the design of pavements incorporating grouted macadams: a traditional design method, based on laboratory determined fatigue life and; an iterative approach, taking into account the degradation of the mixture properties with load applications. A half-scale pavement was constructed in the laboratory Pavement Test Facility, in order to study the performance of the main mixtures used during the project, following the appearance and degradation of cracks.

ACKNOWLEDGEMENTS

LIST OF CONTENTS

LIST OF FIGURES

LIST OF TABLES

1 INTRODUCTION

1.1 Background

Road construction and rehabilitation in the UK is normally undertaken by the use of three main types of pavement: flexible, rigid and semi-rigid (or composite). Flexible pavements are characterised by their immediate serviceability, good riding quality and absence of joints. On the other hand, rigid pavements have an increased bearing capacity and a longer life span when properly designed. However, in terms of comfort (riding quality and noise) for the users, rigid pavements have been losing popularity, largely due to the presence of transverse joints, required to combat thermal movements of the concrete slab. Actually, most rigid pavements in the UK are nowadays being overlaid by bituminous materials (one or more layers), becoming in effect semi-rigid pavements, i.e., the third type of pavements where the base comprises hydraulically bound materials and the surface comprises bituminous material. The asphalt surface improves the riding quality of the pavement and, when thick enough, minimises the occurrence of reflective cracking which is often associated with thermal movements (expansion and contraction) of the rigid support. The formation of cracks through the whole thickness of the bound layers allows the ingress of water to the granular layers and subgrade, contributing to a premature pavement failure.

However, a new type of pavement, which is the main subject of this dissertation, has been used in the last few years. It is known as semi-flexible pavement, where the surface course comprises a semi-flexible material that has the potential to combine some of the best qualities of flexible and rigid pavements, namely absence of joints, long life and high bearing capacity. It also provides good protection against water ingress to the foundation since it has an impermeable surface.

The semi-flexible material, generally known as grouted macadam, comprises an open-graded asphalt skeleton with 25 to 35% voids into which a cementitious slurry is grouted. This hybrid mixture provides a very rut resistant material, for use in heavy-duty pavements, and a surface highly resistant to fuel and oil spillage that allows it to be used in industrial areas, airports and harbours, where those situations frequently occur, associated with heavy and slow traffic.

Construction of grouted macadams is a two-stage operation, normally carried out on two consecutive days. First the open-graded asphalt is applied, using the normal equipment for construction of flexible pavements. On the following day (or after the asphalt has cooled down), the grout is spread over the surface, with the help of rubber scrapers (squeegees), penetrating the voids of the asphalt until it reaches the bottom of the layer. The beneficial properties of this material depend on good void connectivity, in order to allow the grout to flow through them and an adequate workability of the grout to completely fill the voids. Unfilled voids may cause premature pavement failure.

The first development of a semi-flexible material was carried out in the 1950's, in France (van de Ven and Molenaar, 2004). This material, known as Salviacim, was further developed by the construction company *Jean Lefebvre Enterprises*, as a cost effective alternative to Portland cement concrete (Anderton, 2000). Several other products have been developed since, with different 'brands' but with the same construction and working principle.

Grouted Macadams constitute a poorly understood branch of pavement technology and have generally been relegated to a role in certain specialist pavements whose performance is predicted on purely empirical evidence. On the other hand, and based on its enhanced properties, these specialist pavements include aircraft stands, bus stations, port pavements, industrial hard-standings and warehouse floors, and it is clear that grouted macadam is used by industry as a real alternative in all circumstances where Portland Cement Concrete might normally be used. Yet grouted macadams are rarely 'designed'; they tend to be specified based on successful past performance.

These facts justify the need for the research carried out during the present project, and the outcomes will definitely constitute a step forward in the design of pavements incorporating grouted macadam mixtures.

1.2 Research aims

Most of grouted macadam applications in the UK, in the last few years, are based on a standard mixture, designed for surface courses. However, a further exploitation of its characteristics, which has not been investigated, is the possibility of using it as a structural layer (base or binder course) in a pavement. Thus, the main objectives of this project are related to better understanding the properties of this type of material, in order to be able to predict its performance more realistically and to design pavements incorporating grouted macadams more accurately.

In terms of the specific research objectives of this investigation, they can be identified as follows:

- Optimise grouted macadam mixture design, according to the application of the material;
- Check whether thermally-induced cracking is an issue, in pavements with grouted macadam surface courses;
- Determine the benefits of including a reinforcing grid under a grouted macadam surface course;
- Quantify the deterioration rate of grouted macadam surface courses following the appearance of cracking;
- Verify the relationship between laboratory fatigue performance of grouted macadams and their fatigue life in a pavement;
- Develop a design method which realistically predicts the life of a pavement including a grouted macadam layer.

1.3 Thesis outline

This dissertation is organised in nine chapters, including an initial literature review, regarding road pavements and grouted macadams, and a description of the work carried out under the present research project. In Chapter 1 an introduction to the project is presented and the objectives of the research are identified.

Chapter 2 reviews the types of pavement and materials that are used in road construction and other paved areas. A brief description of each type of pavement is made and pavement design methods are presented and analysed.

Previous research and applications of semi-flexible pavements and grouted macadam materials are reviewed in Chapter 3. Although limited literature is available regarding grouted macadams, mix designs and the main properties of mixtures used by several researchers are presented and discussed in this chapter.

In Chapter 4, a purpose-designed laboratory test equipment is described. This equipment was developed with the objective of studying the properties of grouted macadams (stiffness and fatigue resistance) to be used in pavement design. It can be described as a four-point bending equipment and represents more realistically the bending of a pavement layer than the Nottingham Asphalt Tester (NAT) equipment, routinely used to characterise stiffness. Hence it allows the determination of the phase angle, a property not possible to obtain from the NAT.

Chapter 5 is used to introduce all the materials used in the present project, namely the aggregates, the binders and the grouts. The main properties of a standard grouted macadam mixture (resulting from the 'standard' mix design in use for the past few years in the UK) are presented in this chapter. The effect of issues like temperature, binder ageing and testing strain level, as well as the type of test, in the determination of mixture stiffness and fatigue life are discussed.

A mix design study, based on fundamental properties of grouted macadams, is presented in Chapter 6. The influence of variables such as binder type and content, aggregate type and grading, and grout type, on the performance of the final mixture

is discussed. The main properties studied in this investigation include stiffness and resistance to fatigue and thermally induced cracking. In the latter case, the benefits of using a reinforcing grid were assessed.

Chapter 7 is dedicated to the presentation of the results obtained from a half-scale pavement constructed in the laboratory. A Pavement Test Facility (PTF) was used to apply traffic loads on top of the pavement, in order to follow the appearance and degradation of cracks, due to the traffic. The performance of the pavement, which was monitored regularly, namely in terms of temperature, surface deflection, permanent deformation, and crack length, is discussed.

The design of pavements incorporating grouted macadam layers is discussed in Chapter 8. A study carried out to establish the relationship between laboratory fatigue performance of grouted macadams and their fatigue life in a pavement is also discussed in this chapter. To conclude, an iterative approach to the design of pavements including grouted macadams is presented, where the results are compared with those obtained for pavements comprising traditional asphalt layers.

A summary of the main findings and conclusions is presented in Chapter 9, together with some recommendations for future research on this subject.

2 REVIEW OF "TRADITIONAL" ROAD PAVEMENT TYPES AND DESIGN

2.1 Introduction

In this chapter, a review of the pavement types traditionally used in road construction is presented. Additionally, a description of the materials used in each of the construction types is discussed. The main pavement design methods are also described in order to support the work carried out during the present project.

A road pavement can be defined as a structure that provides support to the vehicles using the road. Since the route selection process for the road does not usually take into account the bearing capacity of the foundation (soil, in most cases), also known as the subgrade, a structure is necessary to withstand the vehicle loads and to guarantee a surface with adequate evenness and skid resistance to be used by vehicles, with sufficient comfort and safety for the users. In the absence of this protective structure, the repetitive loads applied by the vehicles, together with adverse climatic conditions, would cause permanent deformation or even failure of the subgrade. To minimize the damage, a set of layers is normally built on top of the subgrade to spread the loads and dissipate the stresses, at the subgrade level, to an acceptable value.

The surface layer, also known as the surface course, has to provide good riding quality for the users (skid resistance, noise, spray, etc.) and also prevent the ingress of water through the pavement structure and ultimately into the subgrade. Thus, the surface course should ideally be impermeable, otherwise the water that penetrates through the voids or cracks can alter the structural properties of the layers underneath, thus decreasing the bearing capacity of the pavement.

Depending upon the constitution of materials used in the top layers of the pavement and their behaviour, pavements are normally classified into three main types, i.e.

flexible, rigid and semi-rigid. A fourth type of pavement, which will be referred to hereafter as semi-flexible, has been gradually gaining acceptance over the last few decades, although in more specific applications, and was selected for a detailed study in this research project. The lower layers of all four types of pavements normally comprise granular materials, which are mechanically stabilised, allowing the road to be trafficable during the construction phase whilst simultaneously increasing the bearing capacity of the pavements without significantly increasing the costs. In some cases, cement or slag stabilisation is used to further increase the bearing capacity of these layers. A more detailed description of these types of pavements is given in Section 2.2.

2.2 "Traditional" road pavement types

The nature of the material that comprises the upper layers is the criterion used to classify road pavements. Therefore, in a flexible pavement, also known as an asphalt pavement, the top layers are constructed with bituminous materials. This type of pavement has a high recoverable deformation and provides a good riding quality, since asphalt surfacings do not require joints to accommodate differential expansion/contraction movements, due to temperature variations, as in the case of rigid pavements, constructed with concrete. Rigid pavements also require a longer time before opening to traffic, in order to allow the concrete to achieve an adequate strength. However, as far as durability, in terms of design life, is concerned, rigid pavements perform better than flexible pavements, provided that the pavement is correctly constructed.

A third type of pavement, known as semi-rigid (or composite), comprises a combination of bituminous and concrete (or cement bound) layers. The former are used as the upper layers and the latter as a base. This type of pavement can also be considered as a long life pavement provided that the cracking of the cementitious base is controlled. In such a scenario, the pavement will combine the good bearing capacity of rigid pavements and the good riding quality of flexible pavements. However, if the cracking of the base is not controlled, the phenomenon of reflective cracking will take place and the surface of the pavement will start to exhibit early degradation.

The fourth type of pavement is known as semi-flexible pavement and is characterised by the composition of the surface course, which includes semi-flexible materials, i.e., grouted macadams. In essence, this composite material comprises a porous asphalt skeleton into which a cementitious grout is poured, completely filling the voids. This type of pavement has the potential to combine the best qualities of flexible and rigid pavements, namely the absence of joints that characterises asphalt and the long life and high bearing capacity of concrete. The impermeable surface of a grouted macadam mixture provides good protection to the foundation against the ingress of water. This type of pavement demands a two stage construction. Nonetheless, the time required before opening to traffic is still considerably less than that needed when using concrete.

Table 2.1 presents a summary of the main advantages and disadvantages of each type of pavement previously discussed.

<p align="center">Table 2.1 – Basic qualities of various road pavement types
(Adapted from Setyawan, 2003)</p>

Type of pavement	Advantages	Disadvantages
Flexible Pavements (Bitumen based)	Flexible, jointless, quickly serviceable, good riding quality	Limited service life, limited static bearing capacity
Rigid Pavement (Concrete)	High strength, high bearing capacity	Slow setting, joints, cracks, large layer thickness
Semi-rigid Pavement (Concrete and Asphalt)	High overall bearing capacity, good riding quality	Cracked base, reflective cracking, surface rutting susceptible
Semi-flexible pavement (Grouted macadams)	High strength, enhanced durability, flexible, jointless, quickly serviceable	Two stage construction of surface course

The semi-flexible pavement type of construction has been selected for a detailed investigation in this project. A detailed characterisation of Grouted Macadam properties is therefore presented separately in Chapter 3. For the remainder of this chapter, a description of the materials used in flexible, rigid and semi-rigid pavements and their main properties is made in the following sections.

2.2.1 Flexible Pavements

In a flexible pavement the upper layers are composed of bituminous materials. There are several types of bituminous mixtures that can be used in those layers, depending upon the function of the layer. The surface course usually has to be relatively impermeable, to protect the layers underneath from the ingress of water (except in the case of porous asphalt), and has to provide adequate skid resistance for the traffic. The base and binder courses are essentially structural layers contributing to the spread of loads applied by the traffic. Figure 2.1 represents a typical flexible pavement structure. The surfacing layers are made of bituminous materials; the base may be bituminous or granular; and the foundation, made up sub-base and the capping (if used), is generally made of granular materials.

The foundation provides a platform on to which the more expensive layers are placed. Its function is to distribute the stresses imposed by the traffic loading in order to transmit them to the subgrade without causing any form of distress to it. It can also be used to provide frost protection, in countries where it is necessary, to protect the subgrade from heave. The foundation is an important part of the pavement not only in its service life but also during the construction phase, where the stress level imposed by the construction traffic can be even higher then those generated in service (Read and Whiteoak, 2003).
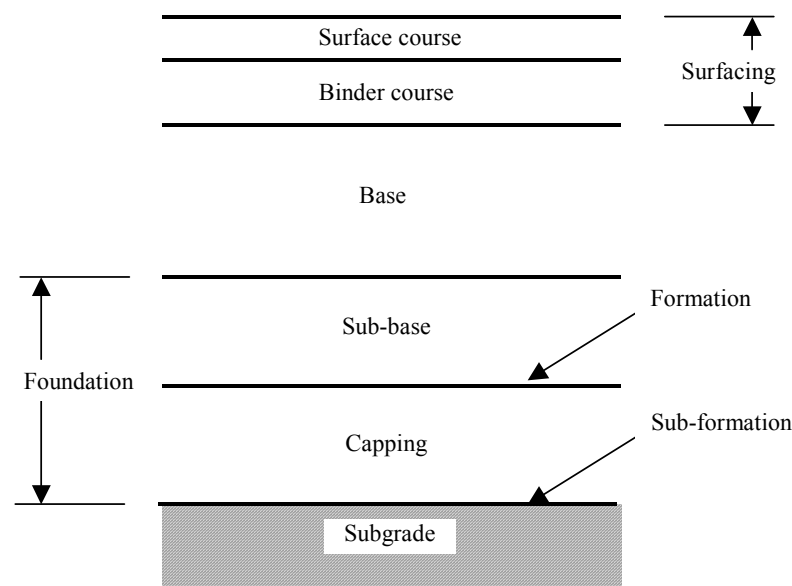
Figure 2.1 – Layers in a flexible pavement (Adapted from Read and Whiteoak, 2003 and Highways Agency, 1999)

Regarding the bituminous mixtures composition, there are infinite possibilities. Traditionally, the types of mixes used in U.K. could be broadly classified as asphalts or macadams. However, nowadays, most of asphalt mixtures are being replaced by Stone Mastic Asphalt (SMA) Mixtures (Taherkhani and Collop, 2005). The difference between the first two is apparently the quantity and particle size distribution of the coarse aggregate. The main features of an Asphalt are the high proportion of mortar to coarse aggregate and the relatively large distances between adjacent coarse aggregate particles. This type of mixture is then referred to as gap-graded. Macadams, however, are referred to as continuously graded and are made up of a wide range of aggregate sizes (BACMI, 1992).

Asphalts rely on a stiff fine aggregate/binder mortar for its strength and stability, as opposed to macadams, which utilise their internal friction and mechanical interlock between the aggregate particles to provide these properties (BACMI, 1992).

Macadams generally provide better resistance to permanent deformation than asphalts and can be stiffer, depending on the grade and type of bitumen used in the mixture.

Due to the greater quantity of fine material present in asphalts (compared to macadams) the amount of binder needed is higher, since the surface area of the aggregates is greater, which increases the production costs. However, the increased binder content improves the fatigue resistance of asphalts and it also makes them more impermeable to air and water, increasing their durability.

The main examples of asphalts are Mastic Asphalt and Hot Rolled Asphalt (HRA). Macadam mixture types can be divided into Dense Bitumen Macadam (DBM), Porous Asphalt (PA) and Asphalt Concrete (AC). There is also a mixture type that combines the properties of the asphalts and the macadams, known as Stone Mastic Asphalt (SMA), which could be described as a very high stone content asphalt and uses the addition of fibres to keep the binder content at a comparable level to traditional asphalts (BACMI, 1992; Hunter, 1994).

Regarding macadams, there are many types, ranging from 3 mm fine graded surface course to 40 mm Heavy Duty Macadam. The differences between the mixture types are obtained by varying the nominal maximum aggregate size, the bitumen grade and the filler content. An asphaltic concrete is a dense bituminous surfacing of the macadam type, deriving much of its strength and stability from its continuously-graded aggregate (BACMI, 1992). Porous asphalts are used as surface courses so that any water deposited on the surface can percolate rapidly into the interconnected voids and drain laterally through the mixture. A typical porous asphalt mixture is composed of about 75% by mass of coarse aggregate, 4% of binder and the remainder, 21%, fine aggregate and filler (Setyawan, 2003).

The type of mixture to be used in a road should, ideally, be chosen according to the type of loads that will be imposed on the pavement, i.e. mixtures with high resistance to permanent deformation (macadams) should be used on roads with heavy slow-moving traffic or mixtures more resistant to fatigue (asphalts) should be used in roads with intense traffic. If the bituminous mixture is not well chosen, early degradation of the pavement may happen.

The main types of degradation observed in flexible pavements are cracking, permanent deformation and loss or movement of materials. These types can be sub-divided as presented in Table 2.2.

Table 2.2 – Types of degradations in pavements

Types of Degradation	Sub-divisions
Cracking	Load associated cracking Thermal cracking Reflective cracking
Permanent Deformation	Rutting Settlement Local deformations
Loss of material	Fretting Ravelling
Movement of materials	Fatting-up

Cracking, loss and movement of materials are types of degradation that only affect the bituminous layers whereas permanent deformation can be observed in bituminous and granular layers or even in the subgrade.

Most of pavement cracking is known as fatigue cracking because it grows slowly with repeated load applications, i.e. the material fatigues. In pavements with thin bituminous layers, load associated cracking starts at the underside of the bituminous layer(s) due to the tensile stresses induced by the traffic. Once the crack is formed, it will propagate towards the surface with repeated load applications. In thicker pavements the cracks may also start at the surface and propagate towards the bottom of the bound layers.

Thermal cracking is normally associated with a significant temperature variation. During periods of cooling, bituminous mixtures try to contract; however, due to the constraint of the layer within the road structure, the material cannot change its length. As a result, tensile stresses develop in the layer, which may result in a transverse crack if the tensile strength of the asphalt is exceeded. This type of cracking normally starts at the surface and grows towards the bottom of the layer since the temperature gradient gives greater contraction at the surface.

Reflective cracking is a degradation associated with pavement overlays. When a new bituminous layer is overlaid on top of a cracked pavement, the relative movements of the blocks underneath will induce a crack in the overlay, directly over the existing cracks, producing a reflection of the original crack pattern onto the surface of the new layer. In Figure 2.2 two proposed mechanisms of reflective cracking are shown.

All types of cracking previously mentioned could be observed in pavements as top-down cracking (TDC), a designation given to pavement cracking initiating at the surface and progressing towards the bottom of the bound layer(s). In flexible pavements, this phenomenon is normally observed in thick bituminous layers. Although the deterioration mechanism is far from being fully understood, climatic conditions, traffic, mix ageing, structure and construction quality are the main causes pointed out for the initiation and propagation of TDC (Freitas et al., 2003). The traffic-induced stresses at the surface of the pavements may have tensile components

due to tyre shape and pressure. Tensile induced surface stresses under the new wide-base tyres (super-singles) are predicted, under certain circumstances, to be *much larger* than those at the underside of the base (Jacobs, 1995) (see Nunn, 1997, p. 9).
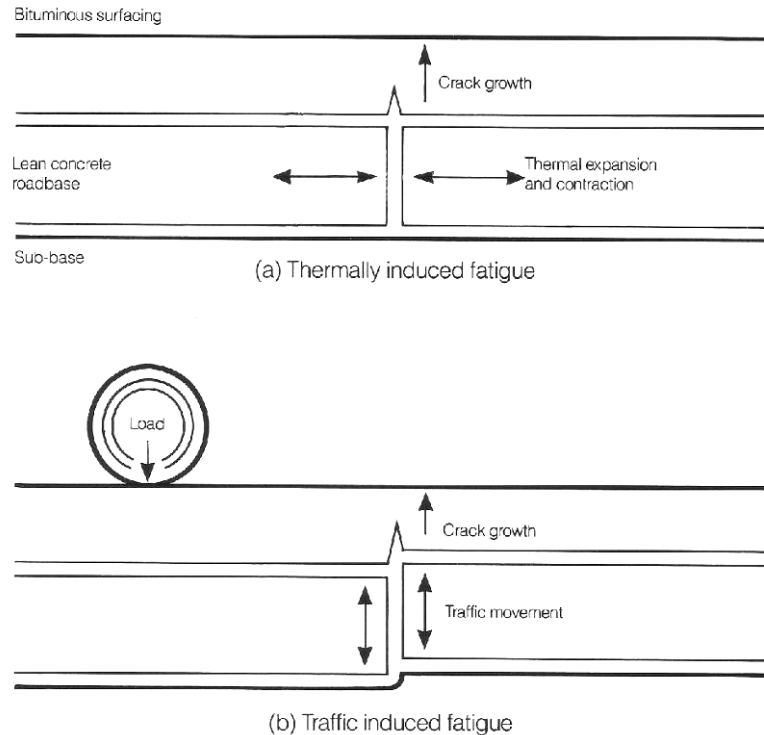
Figure 2.2 – Mechanisms of reflective cracking (Adapted from Whiteoak, 1990)

Thermally generated stresses will also contribute towards the initiation and propagation of surface cracks. This is especially so for transverse cracking where thermal stresses are likely to be the principal cause of the tensile condition required for crack initiation. Age hardening of the binder in the surface course will also play a part, with hardening over time progressively reducing the ability of the surface course to withstand the thermal and traffic-generated stresses at the surface (Nunn, 1997).

Permanent deformation is usually observed in pavements in the form of rutting. This phenomenon takes place in the wheel-tracks of the vehicles and may be caused by permanent deformation in all the layers of the pavement (structural damage) or by permanent deformation only in the bituminous layers (plastic deformation of the bituminous layers). As can be observed in Figure 2.3, the development of the rut arises from the accumulation of permanent strain throughout the structure (Whiteoak,

1990). The former mechanism is typically associated with excessive permanent deformation in the subgrade and represents failure of the pavement, while the latter is confined to the bituminous layers and can be corrected by the replacement of the top layers only.
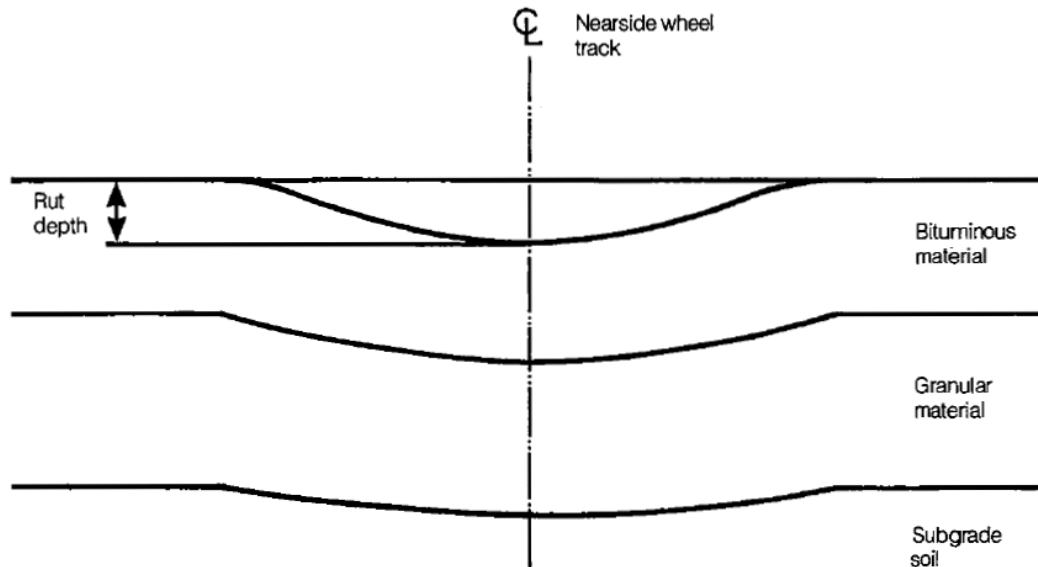
Figure 2.3 – Permanent deformation under the wheel track
(Adapted from Whiteoak, 1990)

In most thick flexible pavements constructed in the U.K. rutting is associated mainly with permanent deformation within the bituminous layers. It usually occurs at high service temperature and is a result of the cumulative load applications by heavy vehicles. This can occur under moving or stationary traffic, and particularly under high shearing stresses. The primary factor influencing plastic deformations is the mix composition, namely, the voids content, the bitumen type and content and the aggregate interlock but, for a given composition, the behaviour will be governed by the viscosity of the bitumen (Whiteoak, 1990). According to Taherkhani and Collop (2005), in the UK, traditional Hot Rolled Asphalt (HRA), although still used for surfacings, is rapidly being replaced by Stone Mastic Asphalt (SMA), since this new mixture appears to offer better rut resistance.

In dense graded mixtures the voids content may be an important factor to be controlled. Sousa (1994) has found that when the voids content drops below 2 to 3%, the binder acts as a lubricant between the aggregates and reduces point-to-point contact pressures. Without the aggregate skeleton resisting the shear stresses, which appear near the edge of the tyres, the mixture rapidly develops large permanent shear

strains, which cause the development of the rut. During the majority of the pavement life, as traffic densifies the mixture, it steadily develops better aggregate interlock and resistance to shear stresses. Only when the reduction of the voids content causes the binder to prevent point-to-point contact in the aggregate does the mix lose stability. Figure 2.4 illustrates the variation of rut depth with the variation of voids content.
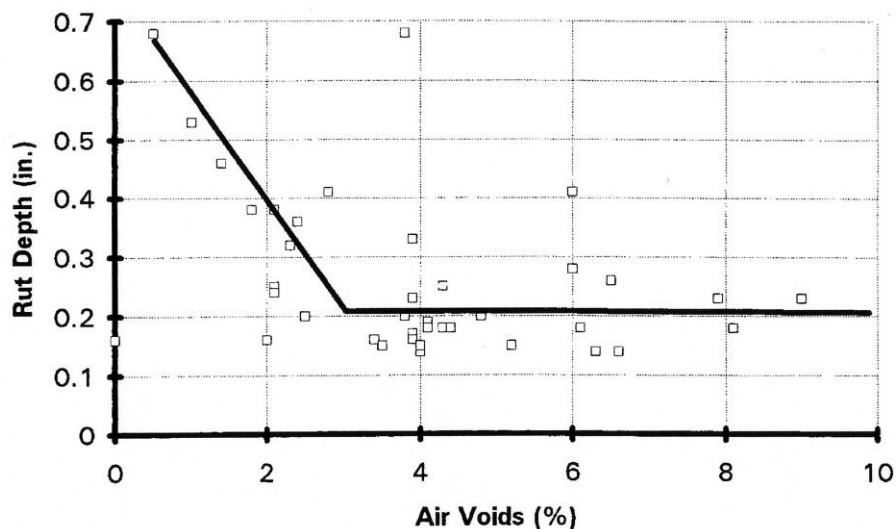
Figure 2.4 – Variation of Rut depth with variation of voids content (Sousa, 1994)

Less common forms of permanent deformation in flexible pavements are settlements and local deformations. In the first case, the deformation is normally associated with movements of material in the subgrade, due to the presence of water, or with post-compaction of the subgrade and granular layers over a large area, producing a considerable depression on the pavement. Localised deformations comprise a smaller deformed area at the surface of the pavement, usually due to localised problems in the bituminous layers, generally associated with construction defects.

Among the degradations presented in Table 2.2, the last two categories are associated with surface distress, decreasing the riding quality and the safety for the road users. Fretting is the progressive loss of interstitial fines from the road surface. It occurs when traffic stresses exceed the breaking strength of the asphalt itself or the asphalt mortar depending on the nature of the mixture. Fretting is more likely to occur at low temperatures and at short loading times when the stiffness of the bitumen is high.

The major factors influencing fretting are the bitumen content of the mixture and the degree of compaction. Loss of aggregate can be due to either loss of adhesion between the aggregate and the bitumen or brittle fracture of the bitumen film connecting particles of aggregate (Read and Whiteoak, 2003).

Ravelling differs from the above in that it involves the plucking out of surface aggregate by traffic without any loss of cohesion of internal fines. It occurs when individual aggregate particles move under the action of traffic. If the tensile stress (induced in the bitumen as a result of the movement) exceeds the breaking strength of the bitumen, cohesive fracture of the bitumen will occur and the aggregate particle will be detached from the road surface. Thus, ravelling is most likely to occur at low temperatures and at short loading times when the stiffness of the bitumen is high (Read and Whiteoak, 2003).

Another type of degradation visible at the surface of pavements is the fatting-up of bitumen. This occurs in over-rich bituminous mixtures, i.e., with too high a binder content, or with too low a voids content. An eventual consolidation of the aggregates in the mixture may force the bitumen to move to the surface. In this case, it would result in a smooth, shiny surface that has poor skidding resistance in wet weather.

2.2.2 Rigid Pavements

Rigid pavements (or concrete pavements) normally consist of two structural layers, the concrete slab and the sub-base. The slab may be laid in composite form using different aggregates in the upper and lower layers. Upper and lower sub-base layers and a capping layer may also be used (Croney and Croney, 1991). Capping is used to improve and protect weak subgrades, by using a relatively cheap material between the subgrade and the sub-base. The aim is to increase the stiffness modulus and strength of the formation, on which the sub-base will be placed (Highways Agency, 1994$_a$).

In a rigid pavement, the concrete slab should be strong enough to support the traffic loads and to protect the subgrade and the sub-base. Thus, a separate base layer is not

necessary to reduce the stresses in the pavement. The sub-base is used as a drainage layer and also to protect the subgrade during the construction of the concrete slab and to protect it from the action of frost.

The pavement structure may vary, depending upon the type of concrete slab used, but the main composition of the pavement is similar in all cases (Figure 2.5). The concrete slab can be reinforced or unreinforced and it can be constructed with or without joints.
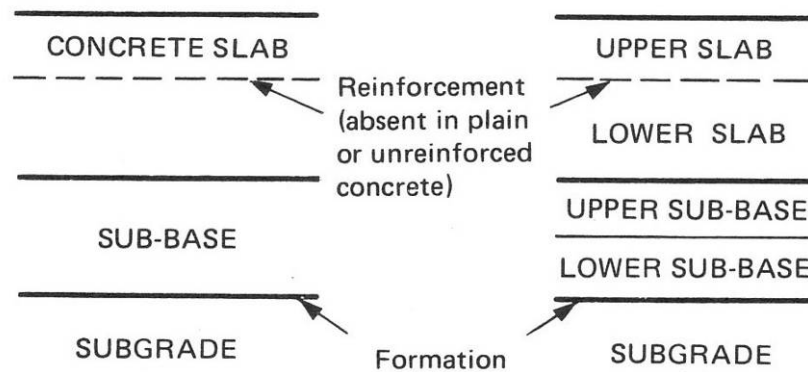
Figure 2.5 – Components of concrete pavements
(Adapted from Croney and Croney, 1991)

An unreinforced concrete pavement (UCP), often referred to as jointed plain concrete pavement (JPCP), has no reinforcement and is normally constructed with induced joints (spaced at 5 m or less) to reduce the probability of thermal cracking. It is designed to be thick enough to resist traffic induced cracking. If a crack occurs, it tends to widen rapidly and granular interlock is lost (Figure 2.6). Detritus entering the crack tends to cause spalling and water entering the crack results in loss of strength in the sub-base and sometimes pumping of fines. The commonest cause of such cracking may be low-strength concrete (Croney and Croney, 1991).

The transverse joints are usually induced by saw cutting the concrete slab over at least one third of the thickness of the slab. Expansion joints are used only in particular locations such as on approaching bridges or other structures and sometimes in winter construction. If the width of the surface is greater than 4.50 m, a longitudinal joint is always placed between lanes of traffic, to prevent the appearance of a longitudinal crack along the road axis. Except on roads with light traffic, the

joints are generally sealed with a bituminous sealant, after creating a groove of an appropriate size in the upper part of the joint (Lemlin, 1997).
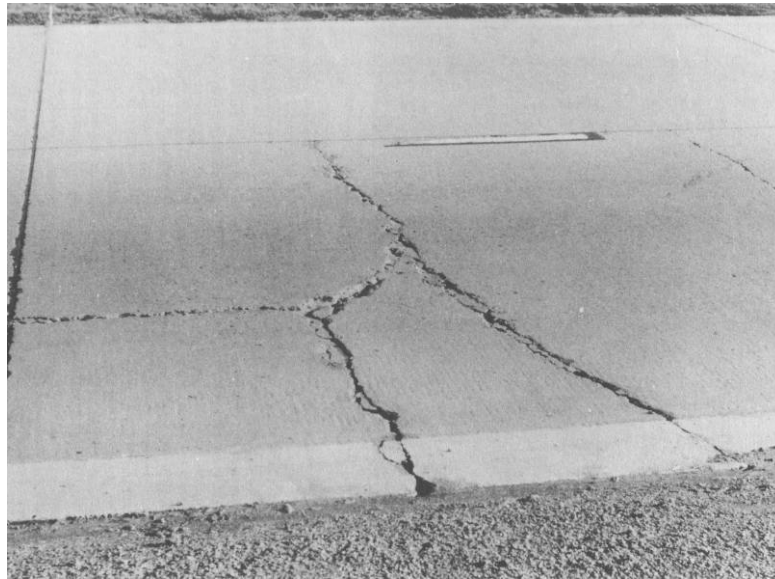
Figure 2.6 – Cracks in an unreinforced concrete pavement
(Croney and Croney, 1991)

On major roads, the transverse joints are normally constructed with dowel bars to prevent vertical movement between slabs from occurring under traffic loading, transferring the load to the next slab. The dowel bars allow, however, horizontal movements of the slabs, due to thermal expansion or contraction.

Rigid pavements may also be constructed with steel reinforcement of the concrete slab. In this case there are two types of pavements, jointed reinforced concrete pavement (JRCP) and continuously reinforced concrete pavements (CRCP).

Jointed reinforced concrete pavements are made of slabs with a length three or four times greater than the width and with reinforcement in the longitudinal direction. Opening of eventual transverse cracks is prevented by the reinforcement, concentrating it at the end of the slabs, where there is no continuity of the reinforcement. The joints are sealed and water and detritus are, therefore, prevented from entering the structure of the pavement and creating any kind of distress.

Continuously reinforced concrete pavements (CRCP) rely on heavy reinforcement, without gaps or joints, to uniformly distribute a large number of cracks, which are

held closed by the reinforcement. This requires much heavier reinforcement than is normally used in jointed reinforced concrete pavements. Figure 2.7 shows the type of cracking expected on a well-designed and constructed pavement using continuous reinforcement. Even a single wide crack in a pavement of this type represents failure and requires urgent attention. The normal cause is fracture of the welds in the reinforcement or the use of a low-strength batch of concrete. The whole area around the crack must be broken out and the broken bars rewelded prior to the relaying of the concrete (Croney and Croney, 1991).

Figure 2.7 – Typical cracking in continuously reinforced concrete pavement
(Croney and Croney, 1991)

The principle behind continuously reinforced concrete pavements consists of letting the surface crack freely, since that cracking is controlled by a carefully dimensioned reinforcement grid to obtain a network of fine cracks, which do not threaten the performance of the surface. The cracks should be spaced between 1 and 3 m on average and the width should not exceed 0.5 mm (Lemlin, 1997).

Rigid pavements are normally designed for a service life of 30 or 40 years (some pavements may be designed for indeterminate life), during which it is expected to maintain its structural properties. However, during their lifetime, these pavements are often subjected to a surface treatment to restore the riding properties, namely the skid resistance. The failure criterion is generally associated with the development of wide

cracks across the full width of a slab. According to the Highways Agency (1994$_b$), the width of cracks in concrete pavements may be classified in three categories: (i) narrow cracks (< 0.5 mm wide – full aggregate interlock and load transfer); (ii) medium cracks (between 0.5 and 1.5 mm – partial load transfer, permits ingress of water); (iii) wide cracks (>1.5 mm – no load transfer, permits ingress of water and fine detritus).

In contrast to flexible pavements, rutting is not applicable to rigid pavements, due to the rigid behaviour of concrete. Thus, the degradation of rigid pavements is normally by thermal or traffic induced cracking or settlement of the concrete slabs. This last case is a result of problems at the level of the subgrade, namely movement (pumping) of fines, due to the presence of water, and consequent settlement.

A well-designed and properly constructed concrete road has the potential for a very long structural life with low maintenance costs. Experience shows that such a road designed for a 40-year life is in fact likely to have a much longer structural life, although a renewable bituminous overlay may be necessary to maintain adequate skid resistance (Croney and Croney, 1991). However, rehabilitation of localised distress of concrete pavements (shallow spalling, loss of joint seal) is usually more costly and difficult, compared with flexible pavements, since it is necessary, in many cases, to do a full depth repair. This situation is even more difficult in continuously reinforced pavements due to the large quantity of heavy steel reinforcement in the slab.

When a rigid pavement reaches the end of its life, it may be overlaid with new concrete or bituminous layers, after being cracked and seated, or removed, crushed and re-used as a base (Darter, 1992). A concrete pavement overlaid with bituminous layers is referred as a semi-rigid (or composite) pavement.

2.2.3 Semi-rigid Pavements

A semi-rigid pavement is normally composed of a cementitious base and a bituminous surface (Figure 2.8). Depending upon the material used as a base, the

pavement may also be called flexible composite or rigid composite. The former comprises a base made of an old concrete pavement that has reached the end of its life, and the latter comprises a new layer of cement bound material (CBM), used as a base (Highways Agency, 1999).

CBMs are extensively used as sub-bases and bases in flexible composite pavements. They are also widely used as sub-bases for concrete pavements. In CBMs, cement is used as a binder, the amount depending on the desired strength level, and a water content, compatible with compaction by rolling, is chosen. CBMs are normally produced on site in mobile batching plants, and are laid by a paver or by a grader (Shahid, 1997).

Bituminous surfacing

CBM

Sub-base

Subgrade
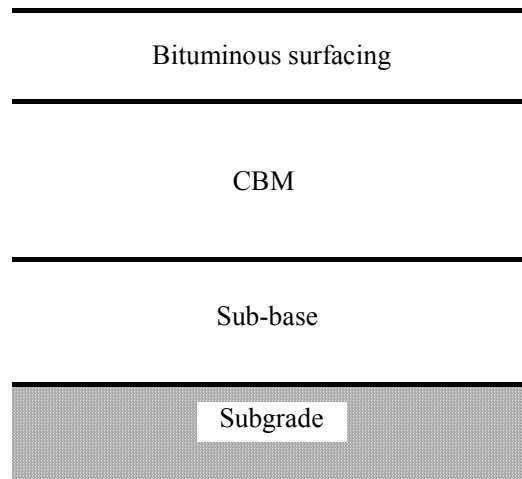
Figure 2.8 – Semi-rigid pavement structure
(Adapted from Croney and Croney, 1991)

According to Parry et al. (1999), a typical UK flexible composite pavement comprises a lean concrete base with 250 mm surfaced with up to 150 mm of asphalt layers. This design is expected to support 20 million standard (80 kN) axles (msa). Increasing the thickness of the asphalt layers up to 190 mm, the pavement life is defined as indeterminate and is greater than 20 msa (Highways Agency, 2001). The lean concrete used in these designs is cement bound material, class 3 (CBM3) with a seven-day compressive strength of 10 MPa.

Up to the end of 2004, cement bound materials (CBMs) were classified in the UK into seven categories based on their 7 day cube compressive strength and on their composition. However, a new European classification has been adopted since (BSI, 2004), where cement bound granular mixtures (CBGM) are classified by the strength

properties of the job standard mixture either by: (i) the characteristic compressive strength R_{ck} of specimen (System I); (ii) the characteristic direct tensile strength R_{tk} or the indirect tensile strength R_{itk} and the modulus of elasticity (E) of specimen (System II). Table 2.3 shows the new classification regarding System I. Classification according to System II is presented in Figure 2.9 and Table 2.4. Similar classifications can also be found, for slag and fly ash bound mixtures, in BSI (2004[a], 2004[b]), as well as for hydraulic road binder bound mixtures (BSI, 2004[c]).

Table 2.3 – Characteristic compressive strength of CBGM – System I (BSI, 2004)

28 days compressive strength (MPa)		Strength class
Characteristic strength R_{ck}		
Cylinders H/D[a] = 2.0	Cylinders or Cubes H/D[a] = 1.0[b]	
No requirement		C_0
1.5	2.0	$C_{1.5/2.0}$
3.0	4.0	$C_{3/4}$
5.0	6.0	$C_{5/6}$
8.0	10.0	$C_{8/10}$
12	15	$C_{12/15}$
16	20	$C_{16/20}$
20	25	$C_{20/25}$
[a] H/D = ratio between the height and the diameter of the specimen. [b] H/D = 0.80 to 1.21.		

Table 2.4 – Characterisation of CBGM by tensile strength and modulus of elasticity at 28 days – System II (BSI, 2004)

Category	R_t (MPa) for category curve					
E (MPa)	1600	2000	5000	10000	20000	40000
Category	R_t (MPa)					
T5	0.64	0.70	1.00	1.23	1.46	1.59
T4	0.45	0.49	0.68	0.83	0.97	1.09
T3	0.33	0.36	0.48	0.58	0.68	0.75
T2	0.21	0.23	0.32	0.38	0.44	0.49
T1	0.12	0.13	0.18	0.22	0.26	0.29
Note: The table gives the values of R_t and E used to draw the curves limiting the categories T5, T4, T3, T2 and T1 in Figure 2.9						

Transverse cracks often occur in the surface of composite pavements as a reflection of either the cracks in an existing concrete pavement or the naturally occurring or induced thermal stress cracks in the new CBM base (Figures 2.10 and 2.11). Cracking in a CBM base is mainly the result of its failure in tension. It is well established that a pavement layer, whether cement bound, concrete or asphalt, will crack when the induced stresses, either externally applied or internally developed,

exceed the tensile strength of the material. Externally applied stresses may be due to traffic and drag resulting from the movement of an adjacent layer (sub-base or subgrade), whereas internally induced stresses are associated with shrinkage (primary cracking, caused by self-desiccation due to hydration of cement and drying of the material) and with thermal cracking (Shahid and Thom, 1996).

Key

R_t Direct tensile strength R_t at 28 days, in MPa

E Elastic modulus E at 28 days, in Mpa
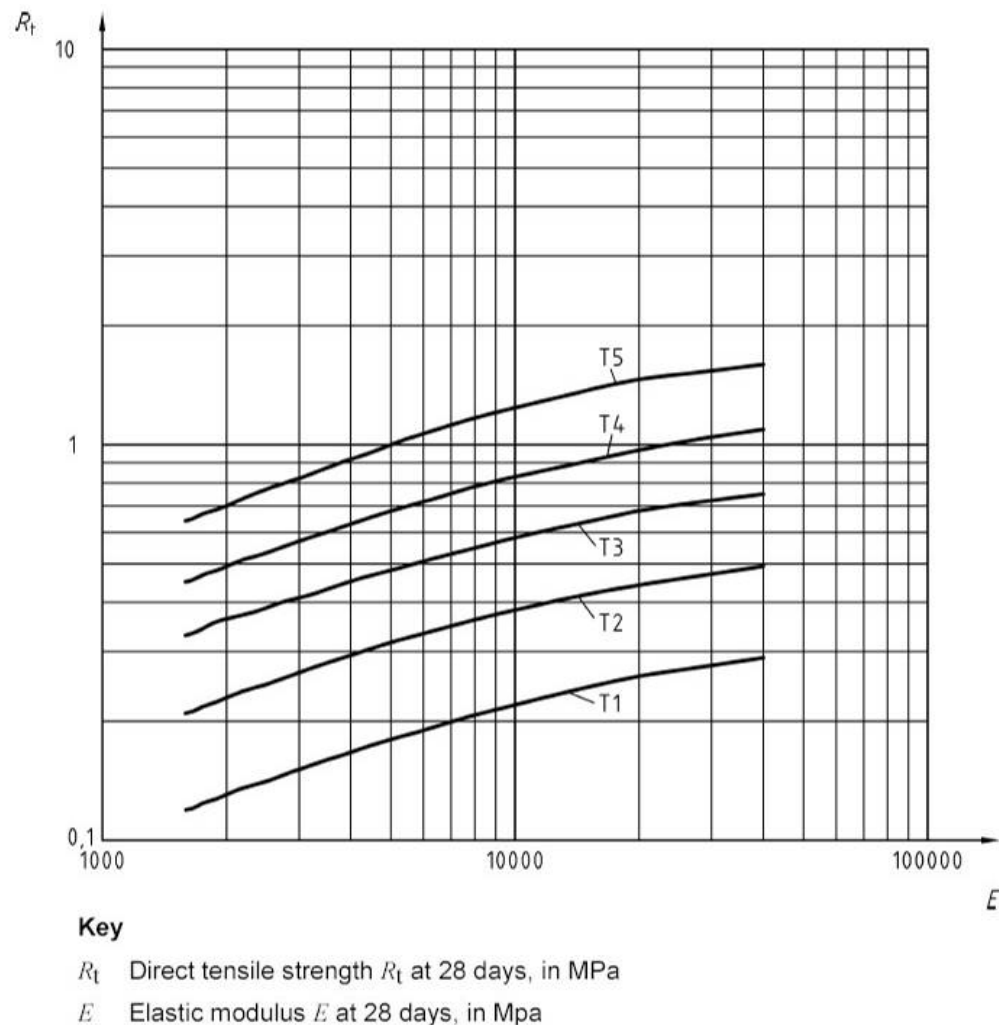
Figure 2.9 – Characterisation of CBGM by tensile strength and modulus of elasticity at 28 days – System II (BSI, 2004)

In this type of pavement, the opening and closing of a crack is caused by temperature changes in the concrete and the amount of movement depends on the length of the concrete slabs each side of the crack, the thermal properties of the concrete and the frictional restraint between base and sub-base (Nunn and Potter, 1993). Traffic loading is also responsible for the relative movement of adjacent concrete slabs. These movements will impose concentrated strains and stresses in the new layer

(Figure 2.12) and the crack will propagate through its thickness. Figure 2.13 represents the two modes of crack propagation of transverse cracks in a pavement.

Figure 2.10 – Reflective cracking in a composite pavement with a jointed concrete base (Saraf, 1998)

Figure 2.11 – Transverse reflective crack in a composite pavement with an unjointed concrete base (Saraf, 1998)
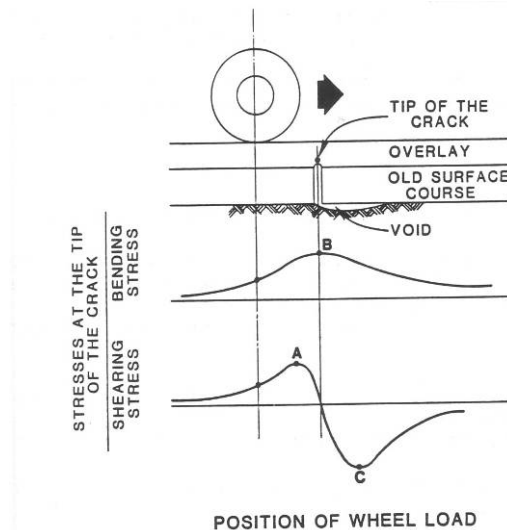
Figure 2.12 – Stresses induced at the cracked section of an overlay due to a moving wheel load (Francken, 1993)
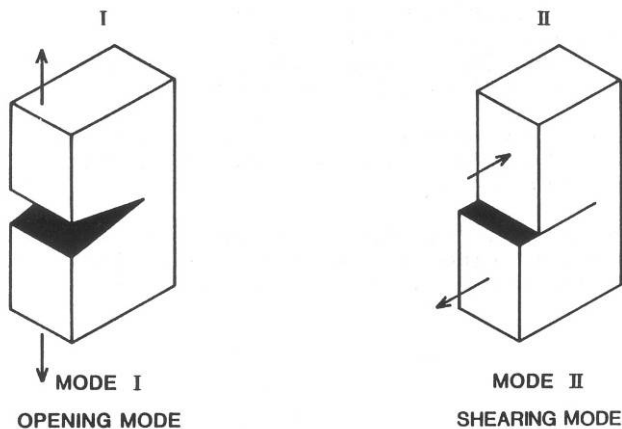
Figure 2.13 – Typical modes of propagation of transverse cracks (Francken, 1993)

To prevent or delay the reflection of the cracks, when applying new overlays on top of old concrete pavements, several measures have been used. Nunn and Potter (1993) refer the following methods as solutions to inhibit reflective cracking:

- Stress absorbing membrane interlayers (SAMI);
- Reinforcement of the bituminous overlay;
- Increasing the thickness of the bituminous overlay;
- Modifying the bituminous materials;
- Treating the existing concrete.

A stress absorbing membrane interlayer is designed to act as a slip layer to prevent crack movements in the cement bound base from being transferred to the overlay.

SAMIs can be laid as continuous membranes like geotextiles or they can comprise thin layers ($\cong$ 10 mm) of a modified type of asphalt (Nunn and Potter, 1993). However, this kind of solution is only effective in situations where no vertical movement occurs between the edges of a crack.

Reinforcement of the asphalt overlay is generally made with geogrids (manufactured with steel, glass fibres or polymers). The reinforcement can either be applied at the interface between the cracked pavement (or base) and the new overlay or closer to the surface, depending on the type of movement of the cracks (Nunn and Potter, 1993).

Increasing the thickness of the bituminous overlay is another method to delay the reflection of the cracks at the surface of the new layer. In fact, the current practice to minimise reflective cracking in UK is to lay thick, and therefore expensive, bituminous surfacing making this type of construction less competitive (Ellis et al., 1997). According to Thom (2003$_a$), the inclusion of reinforcement in new overlays generally reduces their required thickness by 25 to 70 mm, which represents a considerable saving in the cost of the new material.

The use of polymer modified bituminous mixtures represents a way of reducing the appearance of reflective cracks in the surface of composite pavements, due to the increased flexibility of the material, associated with improved temperature susceptibility. Softer bitumens can also be used although these may lead to permanent deformation of the layer if not well chosen (Nunn and Potter, 1993).

A way of treating the existing concrete pavement or base is to deliberately introduce cracks at a closer spacing than the naturally occurring thermal transverse cracking. Thus, the magnitude of the thermal movements at each individual crack will be reduced. Hence the tensile strains in the asphalt will also be reduced, minimising the occurrence of reflective cracking. Any reflected cracks should be much finer and less likely to lead to deterioration in the surface layer. Minimising the size of the surface crack, by controlling its location and severity, gives a longer pavement life and reduces future maintenance costs, both in terms of maintenance works and in the cost

to the road user by reducing the delays due to roadworks (Ellis et al., 1997; Ellis et al., 2000).

According to the work of Colombier and Marchand (1993), the space between the artificially produced cracks is chosen so as to be very short (2 to 3 m) by comparison with that observed between cracks which occur naturally, namely 15 to 30 m after the first winter and 5 to 10 m in the final stages of cracking. A spacing of 3 m corresponds, according to these researchers, to a technical and economical optimum value. They have also concluded that to prevent the rise of the cracks towards the surface, a minimum of 5 or 6 cm of bituminous mixture is necessary.

In the UK, most of the semi-rigid pavements are flexible composite. According to Parry et al. (1999) and Highways Agency (2001), for long-life designs, the asphalt thickness is held constant at 190 mm in order to limit the severity of reflective cracking. Increasing the thickness, the strains and stresses are reduced and, therefore, the propagation rate of a crack will be slower; the length of the crack will also be longer, increasing the time for it to reach the surface of the pavement.

Induced cracking in cement bound material used as a base, normally at 3 m centres, has been in use in the last few years in the construction of new hydraulically bound layers, as part of composite pavements. Regarding the maintenance of rigid pavements, namely jointed concrete pavements, developments in maintenance techniques, such as "crack and seat" have been evaluated and used in the last few years, in order to overlay it, with bituminous materials, without excessively increasing the thickness of the overlay (Potter et al., 2000; Highways agency, 2001).

The Transportation Research Laboratory (TRL) has also investigated flexible composite roads that have used induced cracking techniques in the construction of cement bound bases in full-scale trials in the UK. Three years after construction, reflective cracking was observed within a control section, but not on the sections constructed with induced cracks. In this work, the load transfer efficiency of the induced cracks has also been evaluated and it has shown good behaviour, not affecting the overall pavement strength (Ellis et al., 2000).

In another study carried out in Spain, the application of pre-cracking techniques in cement treated layers was investigated with different spacings between the cracks. As a final conclusion from this study, it can be stated that wet-forming of joints at short distances (2.5 to 3.5 m) is probably the most effective measure to minimise the problems associated with reflective cracking (Jofré et al., 2000).

Nowadays, some pavements are constructed with a surface course made of semi-flexible materials and are therefore classified as semi-flexible pavements (Mayer and Thau, 2001). In the next chapter, a description of these materials and results from previous research are presented.

2.3 Design of Pavements

The design of a pavement comprises the establishment of a structure that ensures a good performance of the pavement under load applications and adverse climatic conditions. With the experience obtained over the years by researchers and institutions, several methods have been developed for the design of pavements. These methods are generally classified in three types, the empirical, the analytical and the mechanistic methods, although some methods use a combination of two types (AMADEUS, 2000).

Current UK pavement design and structural maintenance practice has been developed by a combination of practical experience, laboratory research and full-scale road trials. Structural design standards for roads were first set out in Road Note 29, which was published in three editions in 1960, 1965 and 1970. It used the observed performance of a number of experimental constructions within the public road network as a basis for design curves relating traffic loading to subgrade strength (Hunter, 2000).

In 1984, Transport Road Research Laboratory (TRRL) published the Laboratory Report LR 1132, where a new approach to pavement design was made. That report was based not only on empirical knowledge but also on theoretical concepts of pavement design. At that time, the empirical design method used in Road Note 29

was no longer providing a satisfactory basis upon which to design pavements, due to the rapid growth in the number and damaging power of heavy goods vehicles, since they were so far in excess of those observed on the Road Note 29 experimental roads (Powell et al., 1984).

In the study undertaken by Powell et al. (1984) at the TRRL, the approach adopted was to develop a standard set of designs based on the structural performance of numerous sections of experimental roads. Those standards were then interpreted in terms of theoretical design concepts leading to a design method that could take advantage of the advances in theoretical methods of analysis of that time.

In order to ensure a satisfactory service of the pavement, the design criteria adopted in LR 1132 were the following (Powell et al., 1984):

  a) the subgrade must be able to sustain traffic loading without excessive deformation; this is controlled by the vertical compressive stress or strain at formation level (Figure 2.14);

  b) bituminous materials and cement-bound materials used in base designs for long life must not crack under the influence of traffic; this is controlled by the horizontal tensile stress or strain at the bottom of the base;

  c) in pavements containing a considerable thickness of bituminous materials the internal deformation of these materials must be limited; their deformation is a function of their creep characteristics;

  d) the load spreading ability of granular sub-bases and capping layers must be adequate to provide a satisfactory construction platform.

Design life was defined as the traffic to be carried up to the time when preventive strengthening would be necessary to extend the life of the pavement. Recommendations were made for the design thickness of sub-base and capping layers, based on evidence of the ability of these layers to carry construction traffic. The study was developed furthest for roads with bituminous bases, creating design curves for the thickness of the bituminous layers, of which Figure 2.15 is an example. Those design curves were created for a probability of survival of 85% (this value being chosen because it provided a typical basis upon which maintenance

interventions were judged). Design curves for granular and lean concrete bases were also created, but the design concepts were less developed (Powell et al., 1984).
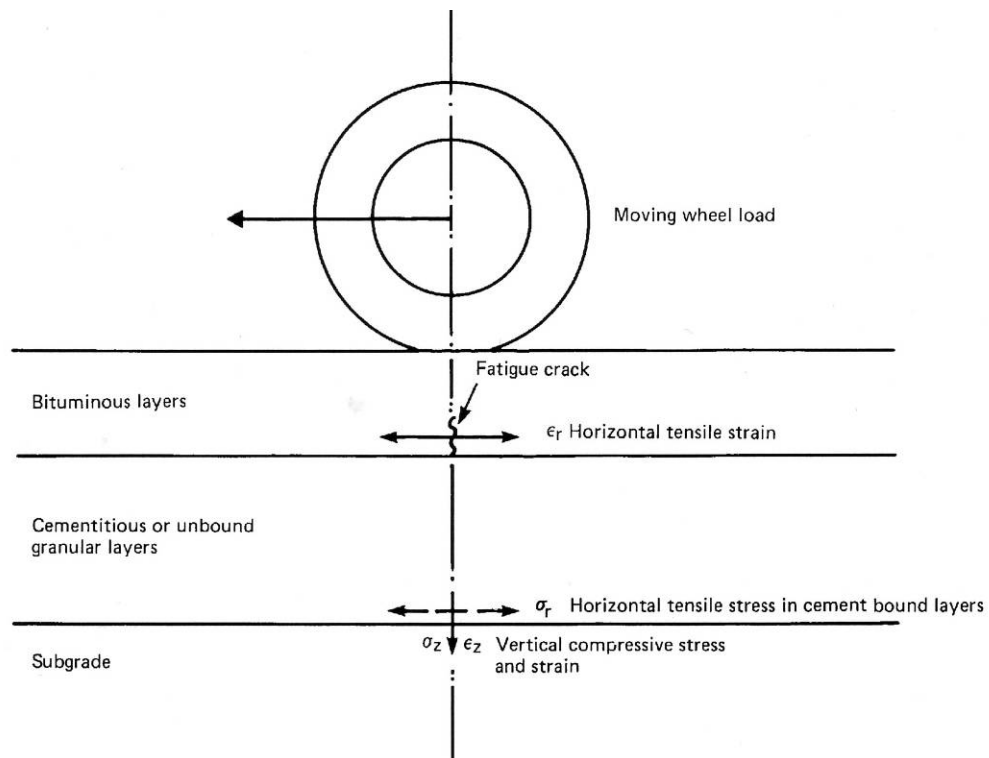
Figure 2.14 – Critical stresses and strains in a bituminous pavement
(Powell et al., 1984)
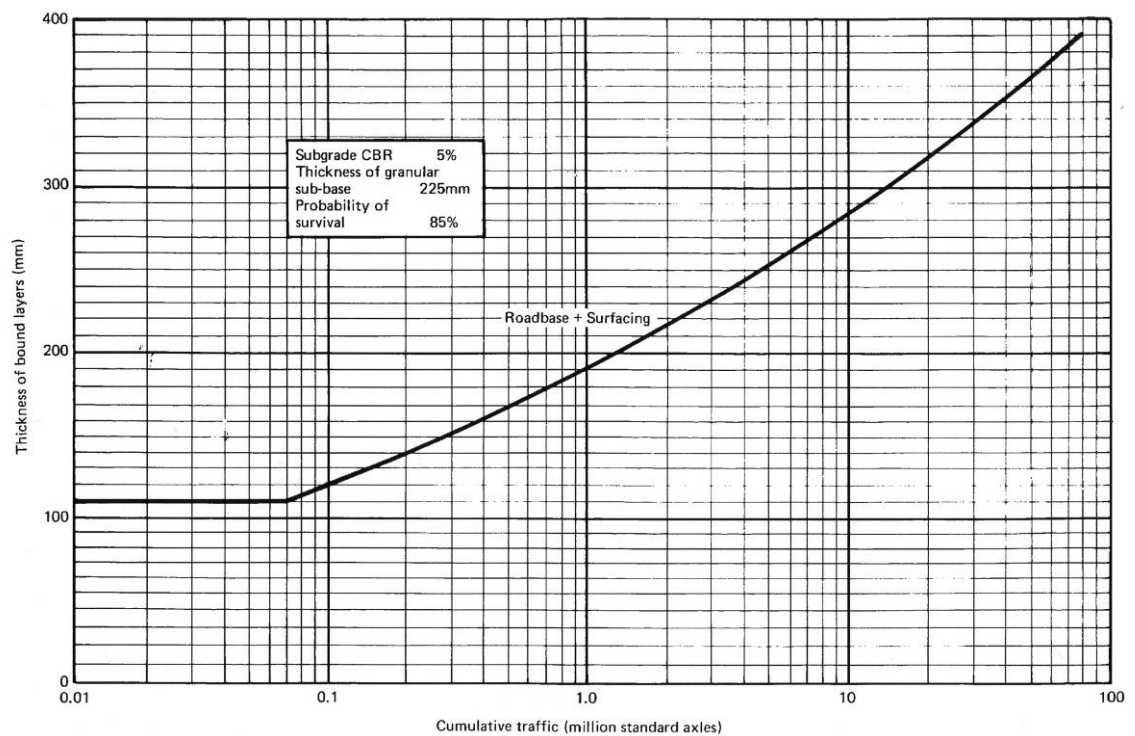
Figure 2.15 – Design curve for roads with bituminous base (Powell et al., 1984)

The design curves were based on a subgrade strength characterized by a value of 5% in the California Bearing Ratio (CBR) test and the sub-base thickness was assumed to be at least 225 mm. A capping layer underneath the sub-base was recommended on subgrades weaker than 5% CBR. This was to provide an adequate construction platform and also to reduce the dynamic vertical strain at formation level.

For pavements with a high bituminous thickness, used in heavily trafficked roads, or for the introduction of new bituminous materials, Powell et al. (1984) suggested the use of a uniaxial creep test to determine the creep characteristics of the material, in order to assess the permanent deformation susceptibility of the pavement within the bituminous layers.

The concept of a design life is particularly important for pavements, since they do not fail suddenly but gradually deteriorate over a period of time. This is essentially a fatigue phenomenon, in the sense that the deterioration results from both the magnitude and the number of load applications the pavement experiences (Brown and Brunton, 1985).

Due to the limitations in the design of pavements using the empirical methods, an analytical approach was developed in the University of Nottingham. The philosophy behind that approach is that the structure should be treated in the same way as other civil engineering structures, the procedure for which may be summarised as follows (Brown and Brunton, 1985):

1. Specify the loading;
2. Estimate the size of components;
3. Consider the materials available;
4. Carry out a structural analysis using theoretical principles;
5. Compare critical stresses, strains or deflections with allowable values;
6. Make adjustments to materials or geometry until a satisfactory design is achieved;
7. Consider the economic feasibility of the result.

The development of analytical design methods has been based on two failure modes and their respective critical strains. Thus, the failure modes considered are the

permanent deformation (by the development of rutting at the surface of the pavement) and the cracking of the bituminous layers. To avoid the appearance of such distresses, the design criteria used in the analytical methods are the maximum tensile strain in the underside of the asphalt (ε_t or ε_r) and the maximum compressive subgrade strain (ε_z), as was illustrated in Figure 2.14.

The development of a rut is the result of the accumulation of permanent deformation throughout the pavement structure. Within the asphalt layers this can be minimised by an adequate mixture design and by a good compaction of all layers. According to Brown and Brunton (1985) if the vertical strain in the subgrade is kept below a certain level, experience has shown that excessive rutting will not occur, unless poor mix design or inadequate compaction are involved.

Cracking of the asphalt layer arises from repeated tensile strain, the maximum of which occurs at the bottom of the layer, as shown in Figure 2.14. The crack, once initiated, propagates upwards causing gradual weakening of the structure (Brown and Brunton, 1985). More recently, a different concept has been studied and discussed among researchers, where a crack may initiate at the surface and propagate downwards, especially in pavements with thick bound layers (Freitas et al., 2003).

The design procedure would consist of proportioning the pavement structure so that, for the chosen materials, it would not present values of strain higher than the critical levels stipulated for the design life. The analytical methods have been used with computer programs that determine the stresses and strains in the various layers, according to the mechanical properties of the materials used, i.e. stiffness modulus and Poisson's ratio. Different response models have been used, e.g., semi-infinite half-space[†] and layered analytical models[*], based on linear elastic theory and isotropic layers (AMADEUS, 2000). For new materials, those properties may be determined by laboratory tests, adjusted in some cases for loading rate, temperature, confinement and/or age.

[†] Usually associated with Boussinesq's equations, using the method of equivalent thicknesses to transform the layered system into a semi-infinite linear isotropic half-space.
[*] Generally based on Burmister's work, using a multi-layered, linear elastic pavement in which the layers are treated as being horizontally infinite and resting on a semi-infinite subgrade.

Figure 2.16 illustrates the flow diagram of the analytical design procedure developed by Brown and Brunton (1985), which is based on the design criteria mentioned above. The thickness chosen for each of the layers would be the minimum value that satisfies both criteria.

Current UK pavement design practice is based on a combination of practical experience, laboratory research and full-scale road trials. Findings have been translated into departmental standards and advice notes for many years. Since 1994, this advice has been consolidated into Volume 7 of the Design Manual for Roads and Bridges (DMRB), published by the Highways Agency. Local Highway Authorities and private sector clients accept the DMRB as a "best practice" document and use it as a basis for most highway-related construction and maintenance contracts (Hunter, 2000). Figure 2.17 illustrates the various parts into which Volume 7 is divided as well as the links between them.
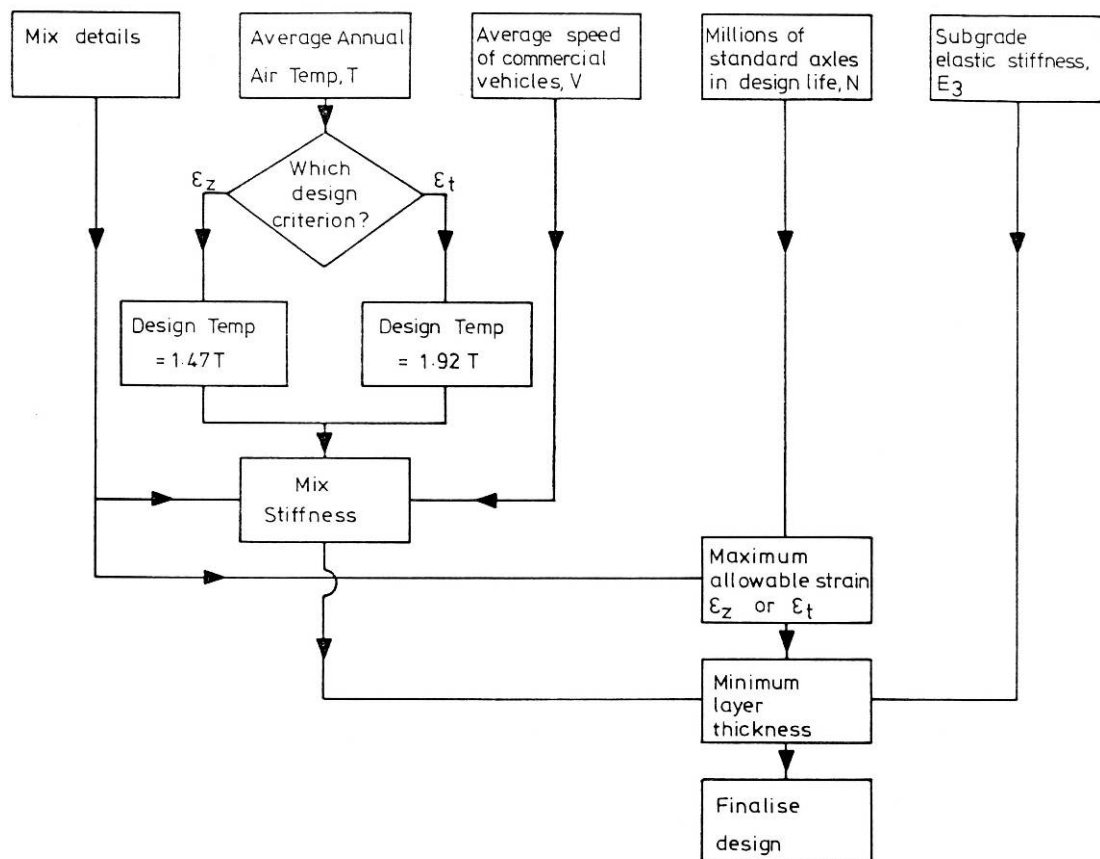
Figure 2.16 – Flow diagram of design procedure (Brown and Brunton, 1985)
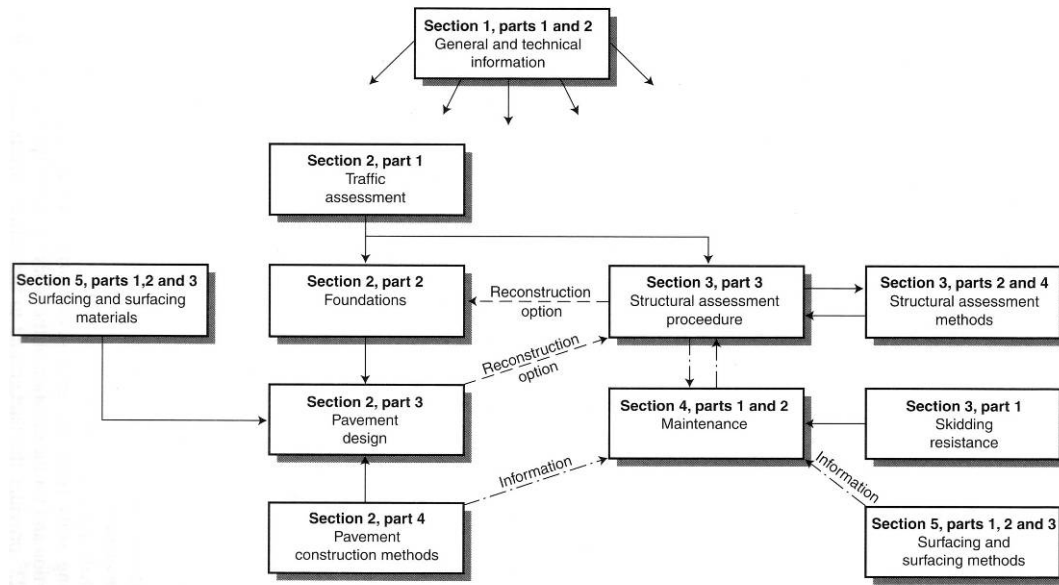
Figure 2.17 – Use of Volume 7 of the Design Manual for Roads and Bridges
(Hunter, 2000)

Pavement designs for flexible, composite or rigid pavements are obtained, according to Section 2, Part 3 of Volume 7, from graphs for a specific design traffic (as illustrated in Figure 2.18 - an example for flexible composite pavement design).

In the last few years an effort has been made to contribute to the development of a new European design method for flexible and composite roads. Several researchers from twenty European countries have been involved in the COST Action 333 (1999) in order to work towards the development of this new method, which should be based on the latest research findings and the latest developments in pavement modelling.

The majority of design methods currently used are analytically based. They use a simple response model to calculate stresses and strains induced by an axle load at critical locations in the pavement structure. These stresses or strains are normally related to the permissible number of load applications, using empirical data, before the pavements deteriorate to an unacceptable level (COST 333, 1999).

The third type of design method is known as mechanistic. It is based on a fundamental understanding of the behaviour of materials in the road pavement. A completely mechanistic approach will use analytical models of the physical

processes that lead to pavement deterioration and these models will require input data on fundamental materials properties which are obtained from laboratory tests carried out under carefully controlled conditions. This method should be able to predict the performance of pavements under specified traffic and climatic conditions. This goal has yet to be achieved and the design methods in regular use are either analytically based or empirical (COST 333, 1999).

R   =   Roadbase having a coefficient of thermal expansion less than 10 x 10⁻⁶ per °C, containing crushed rock aggregate.

G   =   Roadbase containing gravel aggregate or Roadbase that has a coefficient of thermal expansion more than 10 x 10⁻⁶ per °C, containing crushed rock aggregate.
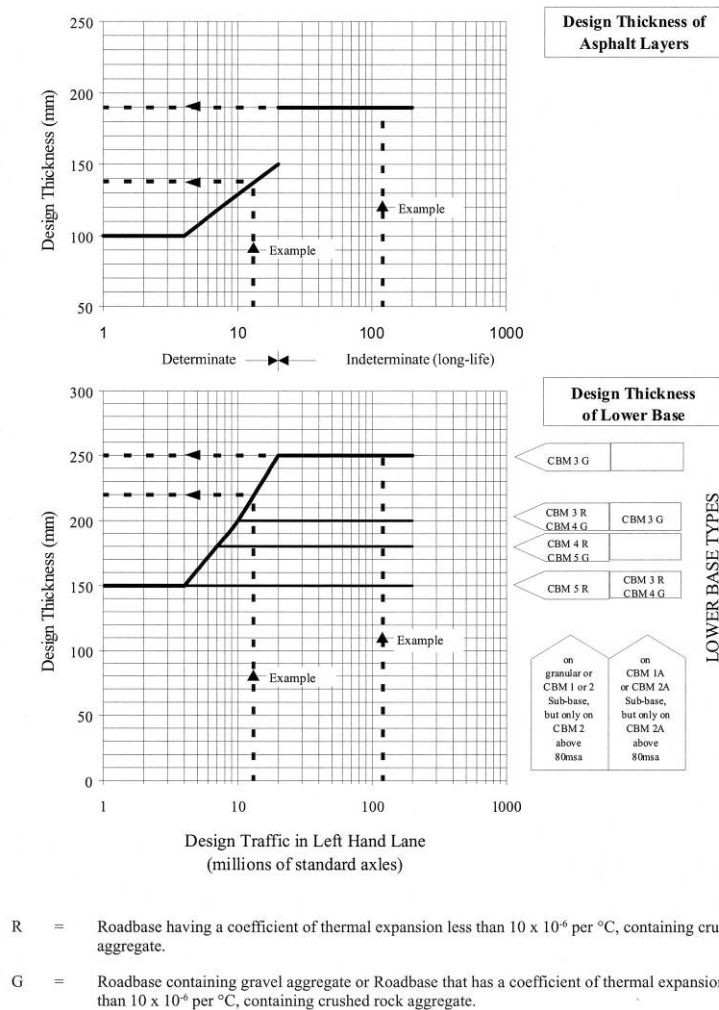
Figure 2.18 – Design thickness for flexible composite (i.e. semi-rigid) pavements (Highways Agency, 2001)

According to the researchers involved in the COST 333 Action, the ideal design method should be able to describe the behaviour of bituminous materials, soils and granular materials under different climatic conditions, and under traffic induced dynamic loads, with complex tyre contact stress distributions. More knowledge is required on the behaviour of pavement materials under these conditions, in order to

produce the advanced pavement deterioration models required for the development of a design method based on a fundamental understanding of pavement deterioration.

Figure 2.19 illustrates the procedure for a fundamental design method proposed by COST 333 (1999). An incremental approach has been chosen due to the complexity of predicting the evolution of the behaviour of the materials used in the pavements. Material properties are often non-linear and they can change with time, t, either due to exposure to environmental effects or due to damage by traffic, D, and these issues should be considered in the design process.

As a complement to the work undertaken in the COST 333 Action, another research programme, Advanced Models for Analytical Design of EUropean pavement Structures (AMADEUS), was established in January 1998 under the co-ordination of BRRC, the Belgian Road Research Centre, to provide a thorough and well-documented evaluation of existing, advanced, design models and to recommend whether these models are suitable as design elements for a comprehensive mechanistic design method, in which a large number of distress phenomena are integrated (AMADEUS, 2000).
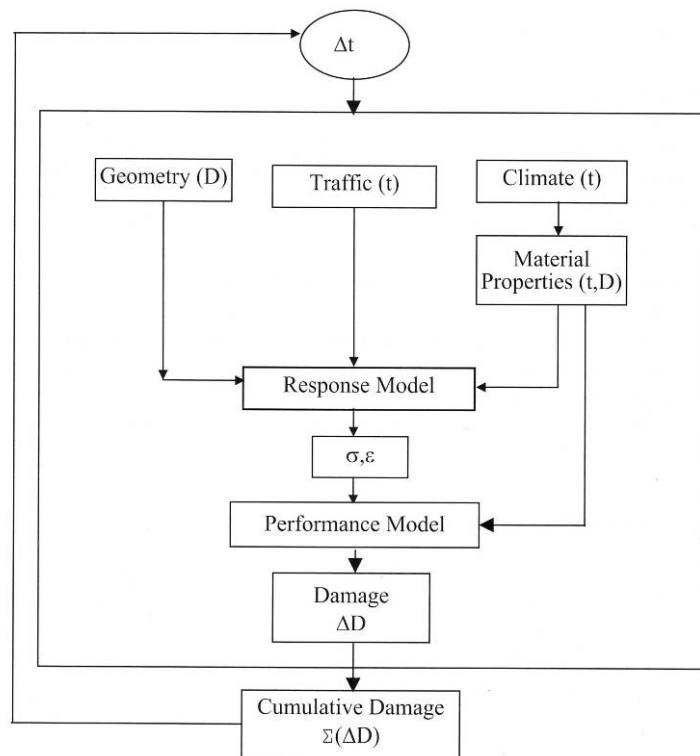
Figure 2.19 – Procedure for a fundamental design method (COST 333, 1999)

The main objectives of AMADEUS were:

- To evaluate existing, advanced, analytical pavement design models by comparing their predictions using standard inputs. The ability of these models to deal with different materials, pavement construction, climate and traffic characteristics would be considered.

- To issue recommendations and guidelines to promote appropriate use of these design models.

- To set up the elements for a comprehensive design method integrating a number of distress phenomena with their evolution and mutual interactions.

In the frame of COST 333 action an inquiry was made in 1997, by Mike Nunn and Darren Merrill (TRL), on current design methods used in Europe. As shown below the two criteria that are generally taken for structural pavement design, i.e. fatigue cracking and permanent deformation of the subgrade, are located far below in the ranking of the observed pavement deteriorations (AMADEUS, 2000):

1. Rutting in asphalt;
2. Loss of skidding resistance;
3. Surface cracking;
4. Longitudinal unevenness;
5. Wheel-path cracking;
6. Cracking from bottom of base;
7. Ravelling;
8. Rutting in subgrade;
9. Frost heave/ low temperature cracking/ studded tyre wear.

In fact, some frequently observed deterioration mechanisms, such as rutting originating in the bituminous layers, and cracking initiated in the surface, are not directly taken into account in current pavement design methods. It is recommended that more research effort is put into developing new improved models for pavement design, which provide better explanation to the observed deterioration mechanisms (AMADEUS, 2000).

The main conclusions drawn from AMADEUS are presented below:

- Models based on multi-layer elastic theory are easy to use and they give generally similar results;

- Multi-layer elastic models can be used for non-linear elastic materials (with stress dependent stiffness) provided they are included in an iterative loop;

- Linear visco-elastic models describe better the shape of the stress and strain waves generated by moving loads;

- Models based on finite element approaches are more difficult to apply unless users have a thorough knowledge of basic principles. In the context of pavement analysis, 2D FE axi-symmetrical methods have little advantage over multi-layer elastic models. True 3D methods are worth applying in situations where particular boundary conditions and local discontinuities must be modelled, which is the case with crack propagation and reflective cracking;

- An incremental procedure is recommended as a new design method, as shown in Figure 2.19, including not only the initial stage but also future maintenance and rehabilitation strategies;

- Other relevant forms of deterioration (e.g., cracking initiating at the surface; rutting initiating at the surface layers; thermal cracking) should be included in the pavement design methods.

2.4 Summary

In this Chapter, the main types of pavement traditionally used in road construction have been described, together with the main forms of distress. A new type of pavement, which is the main subject of this dissertation, has been introduced, with further details presented in Chapter 3. Finally, the main types of pavement design methods have been presented. They were used as a basis for the analysis made in Chapter 8. Particular interest was given to the fundamental design approach discussed at the end of the chapter, where the changes of the material properties during the pavement service life are taken into account during the design process. This principle is also used in the iterative approach to pavement design presented in Chapter 8.

3 REVIEW OF GROUTED MACADAMS

3.1 Introduction

Roads or paved areas subjected to heavy and slow loads, often canalised traffic, such as bus lanes, airport aprons and taxiways or distribution centres, are susceptible to develop permanent deformation within the pavement structure when they comprise flexible layers at the top. Hence these areas are often constructed as rigid pavements. The major disadvantages of rigid pavements, in comparison with flexible pavements, are related with the construction time and the necessity of joints to allow the thermal movements of the concrete layer, in order to prevent scattered cracks from developing in the pavement due to the restraint of such movements. Thus, a third type of material has been devised to create a semi-flexible surface layer, rut resistant and free from joints or cracks.

The first development of the semi-flexible process was carried out in the 1950's, in France, as a protection of asphalt concrete surface course against the attack of waste oils and fuels (van de Ven and Molenaar, 2004). This process, known as *Salviacim*, was further developed by the French construction company *Jean Lefebvre Enterprises* as a cost-effective alternative to Portland cement concrete (Anderton, 2000; Setyawan, 2003). After the *Salviacim* process became successful, its usage spread throughout various countries including Great Britain, South Africa, Japan, Australia and Saudi Arabia (Ahlrich and Anderton, 1991). Since then, similar products have been used with different designations, according to the location. Thus, in the United States it is known as *Resin Modified Pavement (RMP)* (Anderton, 2000). In Europe, products include *Hardicrete Heavy Duty Surfacing* (BBA, 1994), *Worthycim Heavy Duty Paving* (BBA, 1996), *Densiphalt*® (Densit, 2000) or *Confalt*® (Contec, 2005), to mention some of the *brand* names. In Japan, this type of material is known as *RP-Pavement* (Rut Proof Pavement) (Watanabegumi, 2005). In general terms, it is classified as "grouted macadam" although some authors have also referred to it as 'combi-layer' (van de Ven and Molenaar, 2004).

3.2 Application fields

Based on the properties of pavements with this type of surfacing layer, normally referred to as semi-flexible pavements, namely their high bearing capacity and rut resistance, the most common application fields are heavy duty areas, e.g. industrial floors, warehouses, distribution centres, workshops, harbours, roads, road crossings, bus terminals, parking areas with heavy traffic, airport pavements, holding bays, hangar pavements, cargo centres and other areas subjected to slow and heavy loads (Zoorob et al., 2002; Setyawan, 2003). As an example, between 1988 and 2000, 165000 m2 of grouted macadams were constructed in Copenhagen Airport (Mayer and Thau, 2001).

3.3 Constitution of grouted macadams

A typical semi-flexible material is used as a surface course and is composed of a combination of an asphalt mixture and a cementitious grout in the same layer. In essence, grouted macadams comprise an open-graded asphalt mixture (usually single sized), containing 25 to 35 percent air voids, which forms the skeleton into which a cementitious grout is poured (Figures 3.1 and 3.2). The final product combines part of the best qualities of concrete and asphalt pavements, namely the flexibility and freedom from joints that characterise asphalt and the high static bearing capacity and wear resistance of concrete. The impervious grouted macadam layer protects the underlying layers and its high strength effectively reduces the stress level in the base layer. The speed of construction of grouted macadam surfacing and the period of time required ahead of opening to traffic is a significant advance over conventional concrete (Setyawan, 2003). This type of surface layer is normally applied with a thickness of 30 to 60 mm (Densit, 2000), although some work has been done with thicknesses in the region of 80 mm (van de Ven and Molenaar, 2004) and some grout suppliers claim it is possible to use thicknesses of up to 200 mm (Contec, 2005).

The construction of a grouted macadam is a two stage procedure, since it is necessary to allow the asphalt layer to cool down before applying the grout into its voids. Thus, construction is normally carried out on two consecutive days. The porous asphalt

layer is applied using a normal asphalt paver and is then lightly compacted using a steel roller without vibration to avoid the formation of cracks or tracks in the material. As soon as the porous asphalt mixture has cooled down, its voids can be filled with the selected high fluidity cementitious grout (Zoorob et al., 2002). The grout is spread on the surface, with the help of rubber scrapers (squeegees). Depending upon the powder type used to produce the grout and the producer's specification, a light steel roller may be used in the vibration mode to make sure that the voids of the asphalt are completely filled with the grout. After filling the voids, the surface may be treated to improve its properties, namely skid resistance, durability and aesthetics.
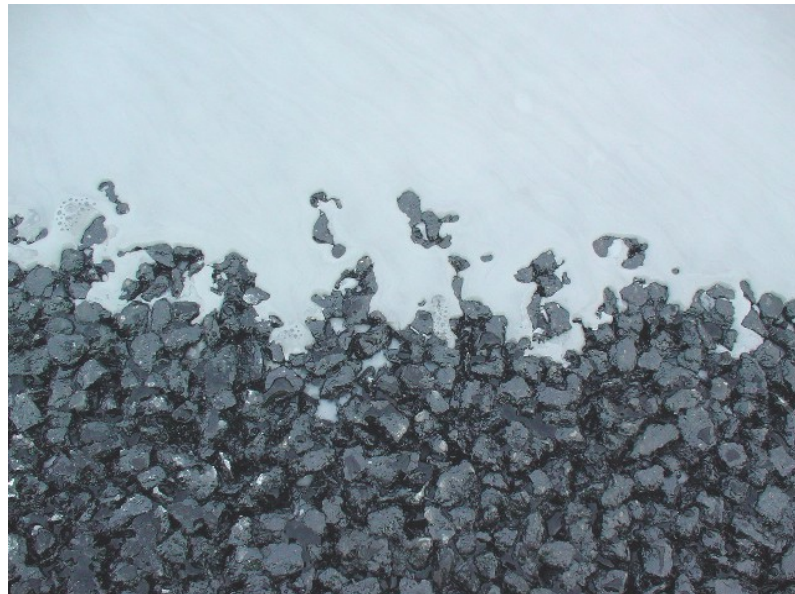
Figure 3.1 – Cementitious grout during the process of penetrating the voids of a porous asphalt skeleton

Figure 3.2 – Core extracted from a typical grouted macadam slab

3.4 Properties of grouted macadams

Although grouted macadams have been used since the 1960's, not much has been published about this type of material. In this section, a review is made of the main properties of grouted macadams, according to the results available in the literature, specifically the fundamental properties of grouted macadams relevant to pavement design, e.g., stiffness and resistance to fatigue and permanent deformation.

In 1979, a research project was undertaken at the University of Nottingham by Boundy (1979), regarding the assessment of the mechanical properties of a heavy duty road surfacing, patented under the name of *Hardicrete*. According to this author, it consists of a conventionally laid open-graded bituminous macadam (usually 40 mm thick), which is fully grouted with a high fluidity resin/cement grout. In this project the stiffness and the fatigue properties of *Hardicrete* were evaluated and will be presented later in this section. Permanent deformation was also studied and was considered negligible due to its very small magnitude. The Poisson's ratio was also determined and the value suggested by Boundy (1979) was 0.25 at 20 ºC.

According to Anderton (2000), other studies (made by Blight, 1984; TARMAC, 1986; Al-Qadi et al., 1993 and 1994) have shown good performance of *Salviacim* and *RMP* materials in relation to impact loads, hot spillage and fuel and chemical spillage. Their mechanical properties were found to fall in a range between the normal values for hot rolled asphalt and Portland cement concrete. The skid resistance of these surface materials was found to be relatively low after construction when wet, but improved significantly after trafficking to a point fully acceptable to British pavement standards.

A summary of some test results from the work carried out by Al-Qadi et al. (1993 and 1994) (see Anderton, 2000, pp.19) for the Strategic Highway Research Program (SHRP) is listed in Table 3.1. These data show that the RMP material has mechanical properties and durability characteristics equal to or better than a high quality hot mix asphalt (HMA).

Table 3.1 – Summary of laboratory results from SHRP evaluation (Anderton, 2000)

Material Property	HMA	RMP
Marshall Stability (kN)	8.7	19.0
Indirect Tensile Strength (kPa)	715	985
Tensile Strength Ratio		
Water Sensitivity	0.87	0.72
Freeze-Thaw	0.70	0.66 – 0.89
Resilient Modulus (MPa)	2040	4937
Resilient Modulus Ratio		
Water Sensitivity	0.83	0.82
Freeze-Thaw	0.68	0.51 – 0.78
Compressive Strength (MPa)	1.2	5.5

Some of the results presented in the table above may be slightly conservative for most grouted macadams, notably the Resilient Modulus, since it is possible to obtain values in the range 6000 to 10000 MPa at 20 °C, depending upon the composition of the mixture and the type of test used.

Ahlrich and Anderton (1991) studied the deterioration of RMP, in an experimental section constructed at the U.S. Army Engineer Waterways Experiment Station (WES), under trafficking with an Accelerated Loading Facility (ALF) and with military tanks. Areas of the test section were also subjected to controlled fuel and oil spillage. The evaluation indicated that no significant deterioration was observed due to the trafficking and that the material had resisted satisfactorily the fuel and oil spillage.

The RMP process is generally applied in a 50 mm thick layer over an asphalt or concrete base. The air voids content of the asphalt skeleton used as a target in the mentioned study was 30% (with acceptable values in the range of 25 to 35%). Until the year 2000, the construction experience with this material in the United States could be divided into two distinct 5-year periods. The first period, from 1987 through early-1991, generally included smaller-scale test sections and some pilot projects. The second period, from mid-1991 through 1996, is when the larger, full-scale projects were constructed at nine military sites and one private industrial site (Anderton, 2000).

Visual inspections were made by Anderton (2000) of some of the projects mentioned above. These inspections were made to provide observations of RMP with different ages, pavement design conditions, traffic, environmental conditions and pavement distress, in order to direct laboratory testing towards the most critical failure modes.

The main conclusions obtained from those inspections included the good properties of the material in resisting permanent deformation, as no evidence of wheel path rutting was found at any RMP location. However, reflective cracks from underlying concrete slabs were found at several locations, reinforcing the idea that the design of pavements incorporating such material must consider the conditions of the supporting layers. Hence, this highlights the need to better understand the behaviour of grouted macadams in general, in order to predict, more accurately, the life of a pavement incorporating such material.

The last observation from the inspections carried out by Anderton (2000) pointed out the importance of determining the skid resistance of RMP. In fact, according to this author, the lack of definitive skid resistance data has limited RMP usage to only low-speed traffic applications.

During the late eighties, a new generation of special slurry grout emerged in Denmark, which brought about extensive developments of Semi-Flexible Pavement (SFP) structures demonstrating high potentials for very heavy loads and, in particular, static loads. This second generation of SFP was optimised in two ways. First, the open-graded asphalt concrete was optimised to get a higher fraction of the total voids penetrable by the slurry grout. Second, a new type of high performance slurry grout based on micro silica technology was developed which exhibited superior properties to penetrate the void structure of the open-graded asphalt concrete (Mayer and Thau, 2001).

Collop and Elliott (1999) carried out a research study to evaluate the fundamental properties of *Densiphalt*® produced in a laboratory situation. The open-graded asphalt composition used in that study is presented in Table 3.2.

Table 3.2 – Composition of the open-graded asphalt used in *Densiphalt*[®]
(Collop and Elliott, 1999)

Material	Proportion by mass (%)
10 mm nominal size crushed aggregate	91.75
200 pen bitumen	4.1
Limestone filler	4.0
Cellulose fibres	0.15

In a more recent publication, the grout supplier has specified the reference values (shown in Table 3.3) to be used as guidelines. The final asphalt mixture should also comply with the following requirements (Densit, 2000):

Air voids (AASHTO T269):   25-30%

Cantabro Abrasion: Max. 15%

Binder drain-off   Max. 0.3%

Table 3.3 – Specification values for open-graded asphalt (Densit, 2000)

Material	Proportion by mass (%)
Coarse crushed aggregate	91.2-92.2
Bitumen	3.6-4.6
Limestone filler	4.0
Cellulose fibres	0.2

In the study carried out by Collop and Elliott (1999), *Densiphalt*[®] specimens were produced to test compressive strength, flexural strength, stiffness modulus, fatigue and permanent deformation. The compressive strength was determined in accordance with BS1881: Part 116 using three cubes at each of 1, 7 and 28 days age. To determine the flexural strength, tests were carried out at the same ages (using three beams at each age) and according to BS1881: Part 118. The results of these tests are shown in Table 3.4 (Collop and Elliott, 1999). The results obtained, regarding stiffness and fatigue, are discussed in Section 3.4.2.1.

Table 3.4 – Summary of average compressive and flexural strengths
(Collop and Elliott, 1999)

Age (Days)	Cube compressive Strength (MPa)	Beam flexural strength (MPa)
1	5.5	1.3
7	7.0	1.4
28	7.0	1.5

According to the authors, cube compressive strength and beam flexural strength tests showed that 79% and 87% of the respective 28 day compressive and flexural strengths were achieved within 24 hours of grouting, which suggests that early age trafficking would not be detrimental to ultimate performance.

The resistance to permanent deformation of the material was assessed using the Repeated Load Axial Test (RLAT) in accordance with British Standard Draft for Development DD226, at 28 days and at 40 ºC, where the material was likely to be most susceptible to permanent deformation. The results are summarised in Table 3.5. It can be seen from this table that low cumulative permanent strains were recorded on the specimens tested. This indicates that, as expected, the permanent deformation resistance of the material was very good (Collop and Elliott, 1999). The results are actually far below the maximum allowable values recommended in clause 952 of the Specification for Highway Works (Highways Agency, 2004).

Table 3.5 – Results from the permanent deformation tests (RLAT)
(Collop and Elliott, 1999)

Core Number	Cumulative % Strain at 40 ºC, 3600 cycles Stress applied = 100 kPa
1	0.2
2	0.4
3	0.1
4	0.2
5	0.1
6	0.3

More recently, Setyawan (2003) studied various types of grouted macadams, with variations in the binder type used in the cementitious grout and also with different bituminous binders for production of the open-graded asphalt macadams.

The following sections summarise the main results obtained by the authors previously mentioned, during their research projects.

3.4.1 The influence of material characteristics

3.4.1.1 Aggregate

The type, size and properties of the aggregate used for production of grouted macadams vary according to the patent or the guidelines produced by authors or grout suppliers. Some examples of aggregate gradations and specification values are given below.

According to Anderton (1996) the aggregates used in the open-graded asphalt concrete must consist of sound, tough, durable particles crushed and sized to provide a relatively uniform gradation. In the study published in 2000, Anderton used crushed limestone to produce laboratory specimens, used in the characterisation of the Resin Modified Pavement for mechanistic design. The physical properties of the aggregates, as well as the specification values are presented in Table 3.6. Table 3.7 shows the gradation of the aggregate used and the corresponding specification limits for the open-graded asphalt concrete.

Table 3.6 – Coarse aggregate physical properties (Anderton, 2000)

Test Method	ASTM Designation	Specification Requirement	Test Result
Los Angeles Abrasion	C131	≤ 40% loss	23.2%
Sodium Sulphate Soundness	C88	≤ 9% loss	2.7%
Flat or Elongated Particles	D4791	≤ 8%	0%

Table 3.7 – Blending formula for open-graded asphalt concrete aggregates
(Adapted from Anderton, 2000)

Sieve Size	Percent passing	
	Spec. Limits	Optimum Blend
19.0 mm	100	100
12.5 mm	54 – 76	62.8
9.5 mm	38 – 60	51.5
4.75 mm	10 – 26	17.6
2.36 mm	8 – 16	11.1
1.18 mm	--	7.3
600 μm	4 – 10	6.6
300 μm	--	2.4
150 μm	--	1.2
75 μm	1 – 3	1.1

The gradation of the aggregate used by Boundy (1979) is presented in Table 3.8.

Table 3.8 – Gradation of the Hardicrete Aggregate (Boundy, 1979)

Sieve Size (mm)	Aggregate percentage passing
20	100
12.5	95
9.5	35
6.2	10
2.5	6
1.2	0

The aggregate used in the production of the open-graded asphalt by Collop and Elliot (1999) was the 10 mm single sized aggregate specified in British Standard BS63: Part 1 (BSI, 1987). The specified gradation envelope of the aggregate is shown in Table 3.9.

Table 3.9 – Gradation of 10 mm Nominal single size aggregate (BSI, 1987)

BS Sieve Size (mm)	Cumulative Percentage Passing by mass (%) BS 63: Part 1 Requirements
14	100
10	85-100
6.3	0-35
5.0	0-10
2.36	0-2

Densit a/s specifies two types of gradation to be used according to the thickness of the *Densiphalt*® layer. Thus, a Type 8 aggregate is specified for thickness in the range of 30 to 50 mm and a Type 12 is specified for thickness of about 40 to 60 mm (Densit, 2000). Further details are given in Table 3.10.

Table 3.10 – Gradation of *Densiphalt*® asphalt (Densit, 2000)

Sieve size (mm)	Percentage passing	
	Type 8	Type 12
19		100
12.5	100	95-100
8	95-100	<20
4.75	<30	<12
2	<10	<10
0.075	4-5	4-5

The Densit a/s specification states that the aggregate shall consist of clean, sound, durable, angular particles produced by crushing rock or gravel. The aggregate shall

be free from organic matter, clay and other detrimental material. The percentage of friable particles, clay lumps, and other deleterious matter should not exceed 0.5% as determined by AASHTO T112. The aggregate should also comply with the following requirements (Densit, 2000):

Los Angeles Abrasion:	AASHTO T96	<25%
Angularity:	ASTM D5821	100/100
Flakiness Index:	BS 812	<25%
Sodium Sulphate Soundness:	AASHTO T104	<10%
Water Absorption:	BS 812	<2%
Apparent Specific Gravity:	AASHTO T85	>2.6 g/cm^3

The aggregate gradation used by Setyawan (2003) in his study is presented in Table 3.11.

Table 3.11 – Gradation of the aggregate used to produce the grouted macadams (Setyawan, 2003)

Sieve (mm)	% Passing
14	100
10	90
6.3	38
4.75	8
2036	5
0.075	3

Figure 3.3 summarises the various gradations used in the past by the above mentioned authors. It is possible to see that most of the gradations are highly single sized, with the exception of the aggregate used in the RMP process. This may be the reason why it demands vibration on the surface of the pavement to guarantee a full penetration of the grout throughout the whole thickness of the layer. The main difference between the remaining gradations is the aggregate nominal size.

Anderton (2000) has analysed the effect of the aggregate type on the coefficient of thermal expansion. Two sets of RMP samples were used: one made with crushed limestone and one made with crushed siliceous gravel. These two aggregates were chosen due to their different coefficient of thermal expansion (limestone – 6×10^{-6}/°C and gravel – 11×10^{-6}/°C, according to Mindess and Young, 1981) (see Anderton, 2000, p.99). Table 3.12 shows the results obtained for this test.
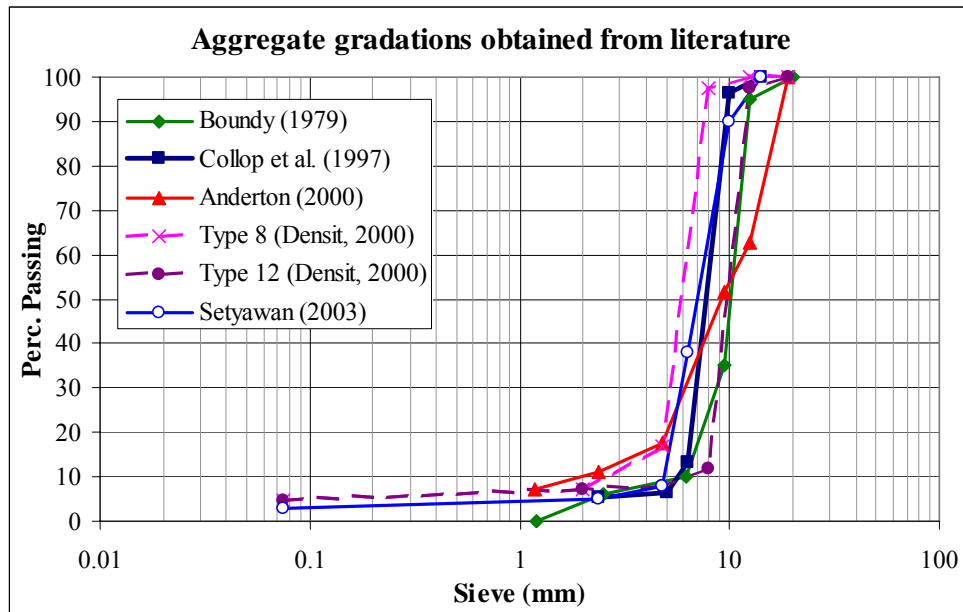
Figure 3.3 – Summary of the aggregate gradations obtained from literature

Table 3.12 – Test Results for the Coefficient of Thermal Expansion of RMP
(Anderton, 2000)

Specimen	Aggregate	Thermal Coefficient ($\times 10^{-6}$/ºC)	Average
1	Gravel	11.8	12.0
2		11.8	
3		12.3	
4	Limestone	10.7	10.9
5		10.7	
6		10.9	

Mindess and Young (1981) and Janoo et al. (1995) have determined the coefficient of thermal expansion for concrete and asphalt concrete materials. The values reported for concrete made with limestone are of about 8×10^{-6}/ºC, while for concrete made with gravel the value is suggested to be of about 12×10^{-6}/ºC. For various asphalt concrete materials measured in different research studies, the thermal coefficient values were reported to be in the 17 to 30×10^{-6}/ºC range (see Anderton, 2000, p.99).

Setyawan (2003), producing two types of cold mix grouted macadams, investigated the effect of aggregate type on the Indirect Tensile Stiffness Modulus (ITSM) of grouted macadams. One was obtained using carboniferous limestone (CL/SF-GM) and for the other a dolomitic limestone (CD/SF-GM) was used. Both porous asphalt

skeletons were grouted using the same silica fume (SF) cementitious grout. The results are presented in Table 3.13. The effect of aggregate type on ITSM at several test temperatures was similarly investigated by performing the test at different temperatures at 28 days. The results are summarised in Figure 3.4.

Table 3.13 – The effect of aggregate type on ITSM at several curing ages (Setyawan, 2003)

Material	Indirect tensile stiffness modulus at 20 ºC (MPa)		
	1 day curing	7 days curing	28 days curing
CL/SF-GM	4350	8440	10320
CD/SF-GM	2320	6970	9280
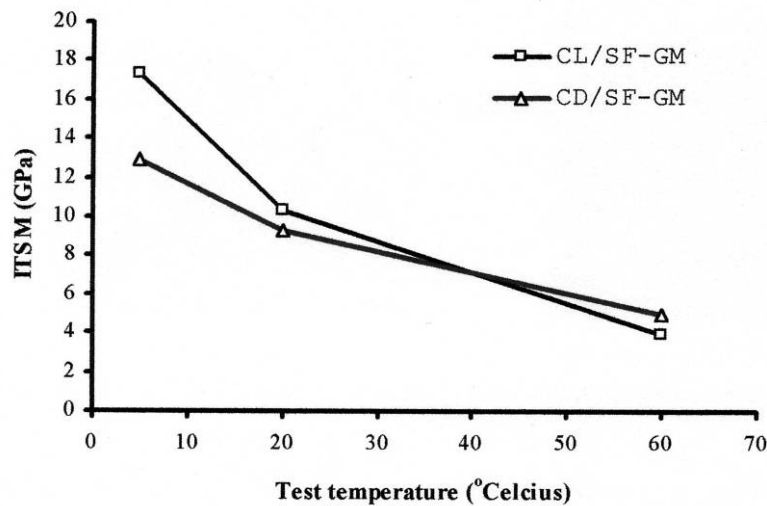
Figure 3.4 – Effect of aggregate types on the indirect tensile stiffness modulus of grouted macadam at different test temperatures at 28 days (Setyawan, 2003)

Based on the previous results, it is possible to say that the aggregate type seems to have an effect on the final properties of grouted macadams, namely in the stiffness modulus, the effect being more significant for lower temperatures, indicating that the temperature susceptibility of grouted macadams may also depend on the type of aggregate used. The aggregate type may also influence the thermal cracking properties of grouted macadams as the type of aggregate used influences the coefficient of thermal expansion of the material (e.g., limestone seems to have better thermal properties than granite).

In the U.K., some contractors have used exclusively crushed granite as the aggregate of their grouted macadams (usually applied as a surface course), due to its improved

wearing properties, when comparing it with limestone, as can be observed in Figure 3.5, regarding the Polished Stone Value (PSV).
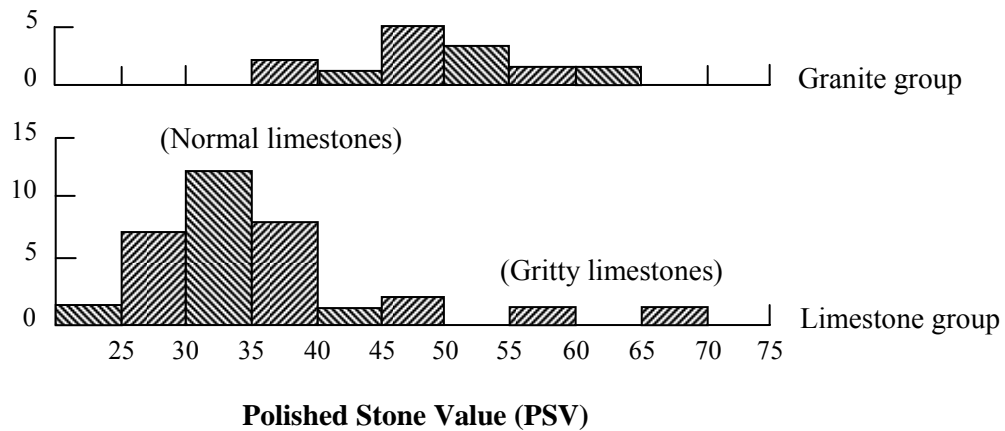
Polished Stone Value (PSV)
Figure 3.5 – Distribution of polished stone values in Granite and Limestone rocks (Adapted from Collis and Fox, 1985 (after Hartley, 1970, 1971))

3.4.1.2   Binder

As for the aggregate, the binder type used in the production of the open-graded asphalt varies according to the authors. Anderton (2000) suggests that the bitumen should have a penetration value, at 25 °C, in the range of 40 to 100 pen. In the particular case of the mentioned study, the penetration value of the bitumen used was 89.

Densit (2000) suggests that the bitumen type should be chosen according to the location of the site (indoors or outdoors) and the weather conditions (for colder climates, a softer bitumen should be used). The penetration value of the bitumen should be between the 85-100 pen and the 120-150 pen specified by the ASTM D946 standard.

However, other types of bitumen have been used in the past, e.g., Boundy (1979) used a 60/70 pen bitumen, while Collop and Elliott (1999) have used a 200 pen binder.

Regarding the binder content of the open-graded asphalt, better consensus seems to be found amongst the various authors, with values ranging from 3.5 to 4.6% by mass

of mixture (Boundy, 1979; Collop and Elliott, 1999; Anderton, 2000; Densit, 2000; Setyawan, 2003).

According to the work carried out by Roffe (1989), the optimum asphalt (i.e. binder) content (OAC), to be used in the production of the open-graded asphalt mixture, should be determined from the Equation 2.1 (see Anderton, 2000, p. 54).

$$OAC = 3.25(\alpha)\Sigma^{0.2} \tag{3.1}$$

where:

α	=	$2.65/G_{sb}$;
G_{sb}	=	apparent specific gravity of aggregate blend;
Σ	=	conventional specific surface area = $0.21G + 5.4S + 7.2s + 135f$;
G	=	percentage of material retained on 4.75 mm sieve;
S	=	percentage of material passing 4.75 mm sieve and retained on 600 μm sieve;
s	=	percentage of material passing 600 μm sieve and retained on 75 μm sieve;
f	=	percentage of material passing 75 μm sieve.

The effect of bitumen type on the Indirect Tensile Stiffness Modulus (ITSM) of grouted macadams was investigated by Setyawan (2003) using a 50 pen straight-run bitumen (HL) and a 62% cationic bituminous emulsion (CL) to produce the open-graded asphalt macadam skeleton. Both of the porous asphalt skeletons were then filled with an identical silica fume cementitious grout (SF). The results are plotted in Figure 3.6.
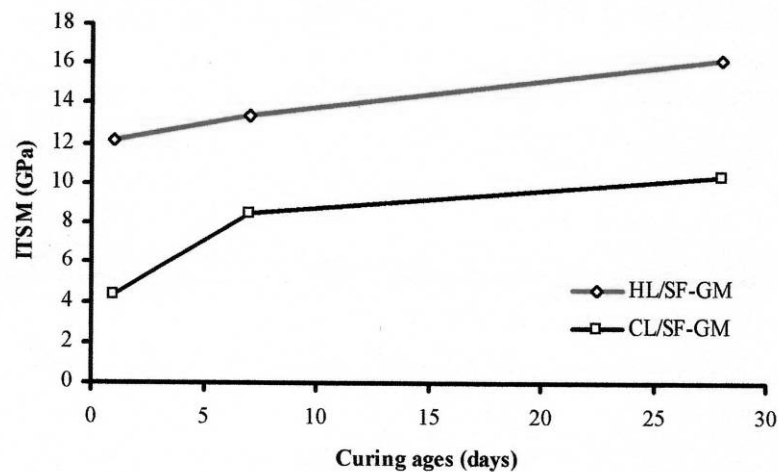
Figure 3.6 – Effect of bitumen type on the Indirect Tensile Stiffness Modulus of grouted macadam at different curing ages (Setyawan, 2003)

The effects of the two bitumen types at different temperatures were also evaluated at 28 days. The results are graphically illustrated in Figure 3.7.
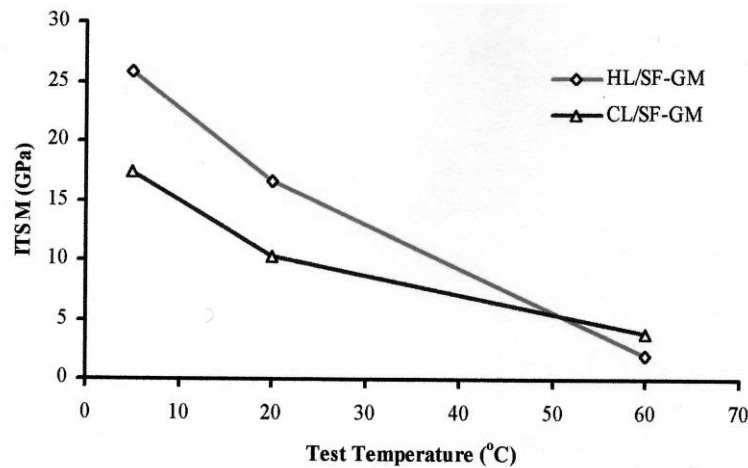
Figure 3.7 – Effect of bitumen type on the Indirect Tensile Stiffness Modulus of grouted macadam at different test temperatures (Setyawan, 2003)

From the previous figures it is possible to appreciate that grouted macadams produced with bituminous emulsions are generally less stiff than grouted macadams produced with hot bituminous mixtures, especially at early ages (less than 7 days), due to the fact that the cold mix porous asphalt skeletons have developed less strength (Setyawan, 2003). At the same time, the emulsion bound grouted macadam showed a reduced temperature susceptibility, with higher ITSM values at 60 ºC.

To determine the fatigue life of the grouted macadams studied, Setyawan (2003) carried out Indirect Tensile Fatigue Tests (ITFT) using the Nottingham Asphalt Tester (NAT). The tests were performed at 20 ºC and the results are presented in Figure 3.8 and Table 3.14.
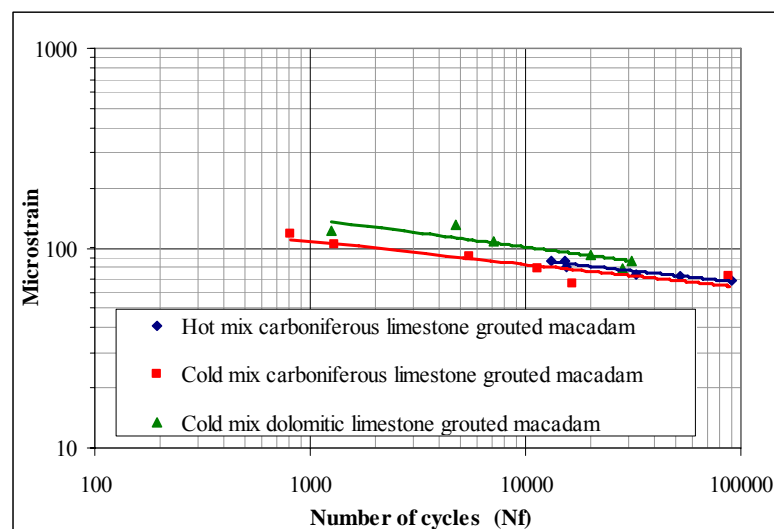
Figure 3.8 – Fatigue lines of grouted macadams based on initial strain
(Adapted from Setyawan, 2003)

Table 3.14 – ITFT results of various grouted macadams
(Adapted from Setyawan, 2003)

Grouted Macadam Type	Specimen	Strain (x 10^{-6})	Number of cycles to failure (N_f)
Hot mix carboniferous limestone grouted macadam	1	69	90000
	2	73	52000
	3	74	32767
	4	87	15300
	5	81	15461
	6	86	13216
Cold mix carboniferous limestone grouted macadam	1	72	88512
	2	67	16465
	3	79	11440
	4	91	5486
	5	105	1292
	6	117	806
Cold mix dolomitic limestone grouted macadam	1	123	1255
	2	87	31040
	3	109	7143
	4	131	4755
	5	93	20148
	6	79	28389

3.4.1.3 Grout

The establishment of grout composition is usually based on the need to produce a material that is easily flowable into the voids of the asphalt skeleton. Furthermore, the grout should also be strong enough to resist the application of stresses and strains without failing. However, limited data is available in the literature regarding grout composition, as many grouts have been established for commercial purposes and, therefore, the producers keep their formulations confidential. In this section, the available grout compositions are presented, together with the properties usually controlled, according to the specifications. The influence of the grout type on the properties of grouted macadams is also presented, according to available data.

According to Anderton (2000), in the RMP process, the Corps of Engineers guide specification was followed for the grout mixture design. The constituents, their proportions and tolerances are given in Table 3.15. To fulfil the viscosity

requirement, one litre of grout should flow through a standard funnel, the Marsh flow cone (Figure 3.9), within 8 to 10 seconds immediately after mixing.

Table 3.15 – Required and Used RMP Grout Mixture Proportions (Anderton, 2000)

Material	Percent by Weight	
	Specification	Blend used
Type I Cement	34 – 40	36.6
Fly Ash	16 – 20	17.1
Sand	16 – 20	17.1
Water	22 – 26	25.7
Resin Modifier	2.5 – 3.5	3.5
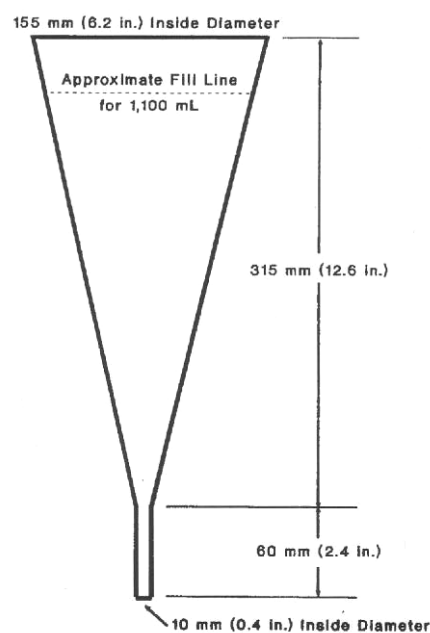
Figure 3.9 – Marsh flow cone (Anderton, 2000)

The constituents of the cementitious grout used by Boundy (1979) are shown in Table 3.16. In order to reduce the amount of water necessary to make the grout flowable enough to penetrate the voids of the porous asphalt, chemical admixtures are usually used. They can be referred as *Resin Modifiers* or *Superplasticisers* (Boundy, 1979; Anderton, 2000; Setyawan, 2003). An *accelerator* may also be used to improve the strength of the grout in the early curing ages (Setyawan, 2003).

The exact composition of commercial grouts is difficult (if not impossible) to obtain. According to Collop and Elliott (1999) it is understood that the commercial grout used in their project contains a microsilica improved cement binder, which allows easier penetration of the void structure of the open-graded asphalt, and hence greater

achievement of the theoretical packing density than grouts manufactured exclusively with cement. In that project, the powder was manufactured by Densit a/s from Denmark.

Table 3.16 – Composition of the Grout used in Hardicrete (Boundy, 1979)

Material	Percentage by mass
Cement	44.3
Sand	14.8
Silica Flour	14.8
Resin	6.3
Water	19.8

The *Densiphalt*® grout is produced by adding just water to the Densit powder to obtain a grout fluid enough to fill the voids in the asphalt. As a guideline, Densit (2000) suggests the use of 16.2% of water by mass of powder used. However, the fluidity should be controlled using the standard *Densiphalt*® funnel (Figure 3.10). The flow time for one litre of grout should be 12 to 16 seconds (the acceptable limits are 10 to 18 seconds).

Figure 3.10 – *Densiphalt*® funnel (Densit, 2000)

Collop and Elliott (1999) used 17.5% of water by mass of powder in the laboratory study where the fundamental properties of *Densiphalt*® were determined.

In his project "Development of semi-flexible heavy-duty pavements", Setyawan (2003) has studied different grouts to be used in grouted macadams. The types of

grout used in this study comprised three combinations of hydraulic binders (ordinary Portland cement (OPC), silica fume (SF) and fly ash (FA)). The first type (OPC) was composed of 100% OPC; the second (SF) comprised 95% OPC and 5% SF; and the third (FA&SF) was made of 65% OPC, 30% FA and 5% SF.

To investigate the effect of cementitious grout type at different test temperatures, ITSM tests were conducted by Setyawan (2003) using a single hot mixture porous macadam produced with limestone (HL). Testing of all samples was carried out after 28 days of curing. The results are presented in Figure 3.11, where very little difference can be observed in the stiffness modulus of the mixtures manufactured with different types of grout.
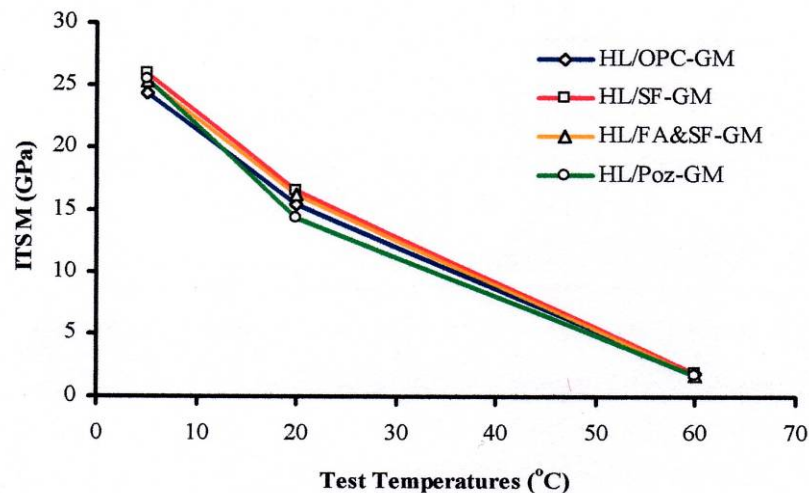
Figure 3.11 – Effect of cementitious grout on the indirect tensile stiffness modulus of 28 days cured grouted macadam at different test temperatures (Setyawan, 2003)

3.4.2 The influence of testing conditions

According to the characteristics of each component, composite materials like grouted macadams, will present specific properties. These properties may be dependent or independent of the testing conditions. Since grouted macadams are a material that combines properties of both bituminous and cementitious materials, it would be interesting to assess how close grouted macadams perform to either of those materials.

It is generally accepted that bituminous materials change their properties according to the testing conditions, e.g., temperature, loading rate and amplitude, due to the viscous nature of the binder. On the other hand, cementitious materials, like concrete, tend to behave in a more elastic manner. Therefore, their properties are less susceptible to the testing conditions.

In this section, a review is made of the available literature, in order to try to establish which type of behaviour is more characteristic of grouted macadams. An analysis of the type of tests used to determine their main properties is also made to assess the influence of such properties on pavement design.

In the project carried out by Boundy (1979), cylindrical specimens were produced in the laboratory to be used in stiffness and fatigue tests using cyclic axial tension and compression.

Anderton (2000) produced cylindrical cores and beams in the laboratory to be used in several test configurations to determine their fundamental properties, i.e., indirect tensile strength, flexural strength, compressive strength, resilient modulus (indirect tensile test), coefficient of thermal expansion, freezing and thawing resistance and fatigue resistance. Friction tests were also conducted in field applications of RMP to determine its skid resistance.

In the work carried out by Collop and Elliott (1999), the stiffness modulus and the fatigue resistance of *Densiphalt*[®] were determined using the Nottingham Asphalt Tester (NAT) to test 10 cores with 100 mm nominal diameter. The Indirect Tensile Stiffness Modulus test (ITSM) was performed at 1, 7 and 28 days, at a range of temperatures between 0 and 40 °C, in accordance with British Standard Draft for Development DD213, and the Indirect Tensile Fatigue Test (ITFT) was performed in accordance with British Standard Draft for Development DD ABF, at 40 °C after 28 days.

Regarding the work carried out by Setyawan (2003), the influence of the testing conditions on the results has already been presented in Section 3.4.1, together with the influence of the materials.

3.4.2.1   Temperature, loading time and frequency

A summary of the stiffness results obtained by Boundy (1979) at different temperatures and different stress levels for 30-days old specimens is represented in Figure 3.12. Some complementary tests were conducted to analyse the effect of very early trafficking and it was observed that a reduction in stiffness was noted even for relatively low stress levels (Figure 3.13).
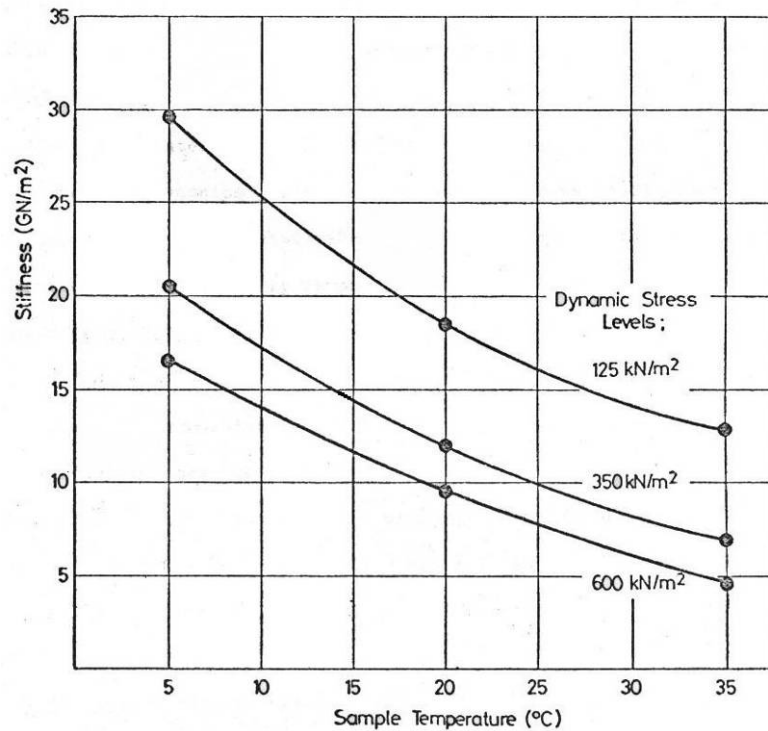
Figure 3.12 – Summary of stiffness modulus of Hardicrete vs temperature at different stress levels (Boundy, 1979)

To assess the fatigue properties of Hardicrete, the specimens were subjected to dynamic load applications (tension and compression) in controlled stress mode, for different stress levels. Figure 3.14 shows the fatigue results obtained for the three temperatures studied (5, 20 and 35 °C), plotted as initial measured strain against cycles to failure.

Results of the Resilient Modulus and Poisson's Ratio of RMP material, obtained from the indirect tensile test, are presented in Table 3.17. This test was done at three different temperatures using specimens produced in the laboratory and cored from two field sites (Altus and McChord air force bases) (Anderton, 2000).
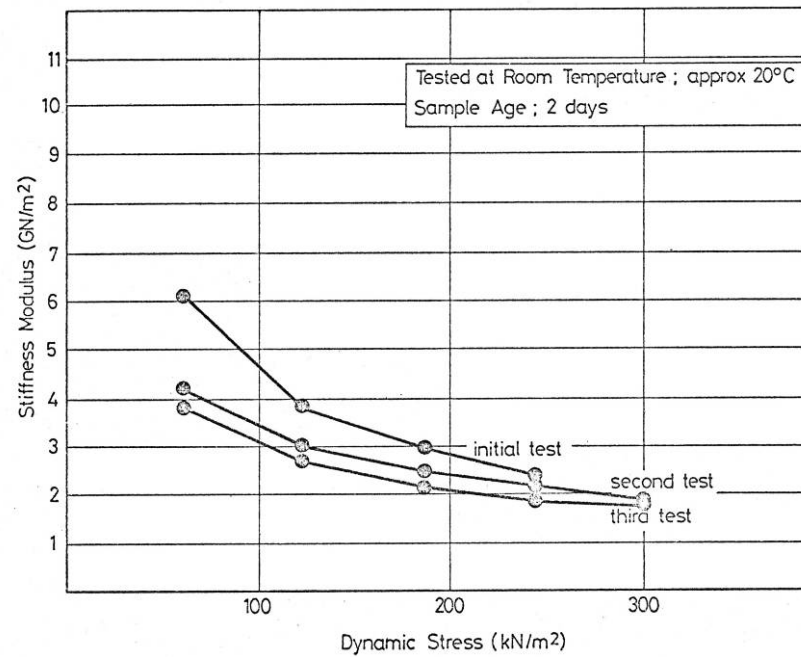
Figure 3.13 – Reduction in stiffness modulus of Hardicrete with repeated testing –
2-day samples (Boundy, 1979)
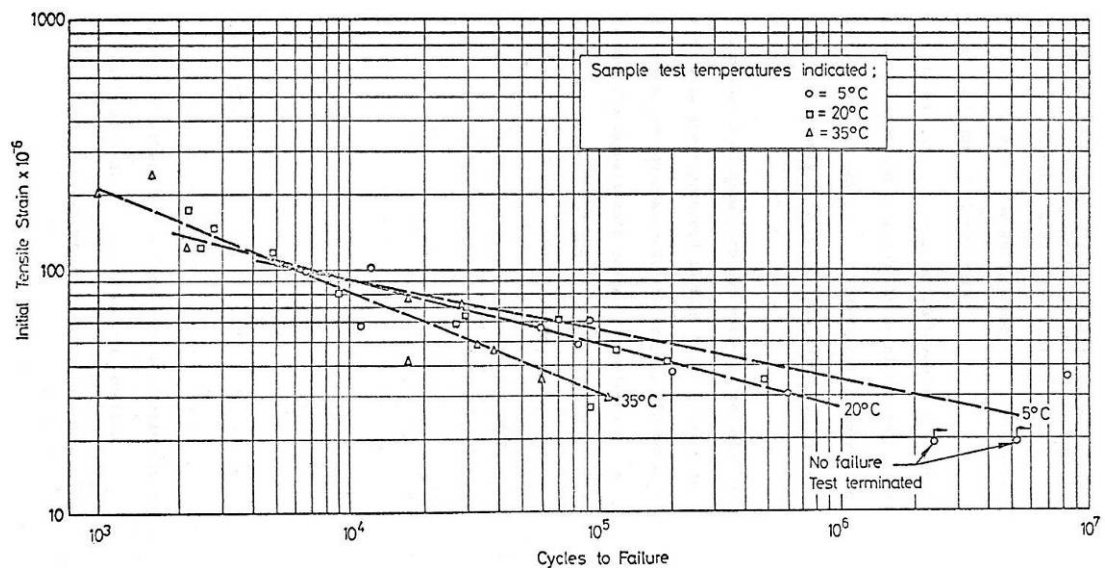
Figure 3.14 – Initial tensile strain vs Fatigue life of Hardicrete (Boundy, 1979)

According to this author, the reduction in the modulus and the increase of the
Poisson's ratio with increasing temperature provides further evidence of RMP's
visco-elastic nature, allowing for direct comparisons to the stiffness characteristics of
traditional asphalt concrete (i.e., bituminous) mixtures. Analysing the results for
Poisson's ratio, Anderton suggests the use of an average value (0.27) for RMP if the
design method requires a single Poisson's ratio value.

Table 3.17 – Summary of Resilient Modulus Test Results (Anderton, 2000)

Specimen Origin	Test Temperature (ºC)	Resilient Modulus (GPa)	Poisson's Ratio
Lab	5	19.2	0.20
	25	11.2	0.26
	40	5.8	0.28
Altus	5	21.7	0.15
	25	10.3	0.24
	40	5.0	0.24
McChord	5	21.4	0.20
	25	8.6	0.29
	40	4.2	0.30

To characterise the fatigue resistance of RMP, laboratory produced beams were tested in repetitive flexure tests. The test method is generally described as a four-point bending test. It was performed in controlled strain mode and the fatigue failure has been identified, in this case, when the beam samples reached a 50% reduction in stiffness during testing. The tests were carried out at three temperatures (5, 20 and 30 ºC) and two strain levels (250 and 400 microstrain). The results are presented in Figure 3.15.
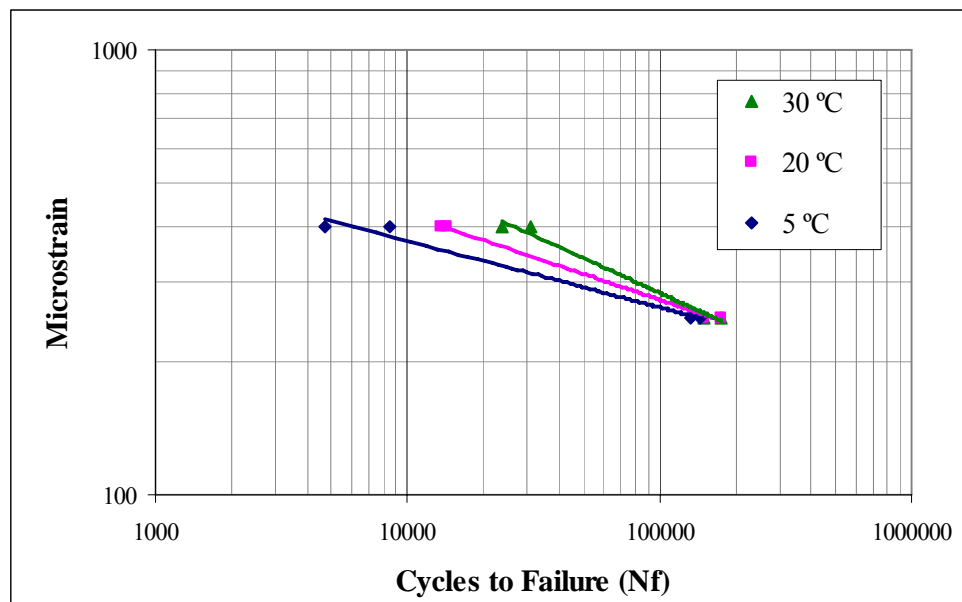
Figure 3.15 – RMP fatigue curves at three test temperatures
(Adapted from Anderton, 2000)

Table 3.18 shows the results obtained by Collop and Elliott (1999) from stiffness tests, and the results from fatigue resistance tests are presented in Figure 3.16, where

a comparison with results previously obtained for typical Hot Rolled Asphalt is made.

Table 3.18 – Summary of average stiffness moduli (Collop and Elliott, 1999)

Age (Days)	Stiffness (ITSM), MPa				
	0 ºC	10 ºC	20 ºC	30 ºC	40 ºC
3	17750	10590	6510	3980	2790
7	19230	11700	6920	4080	2520
28	19870	12570	7110	4280	2600
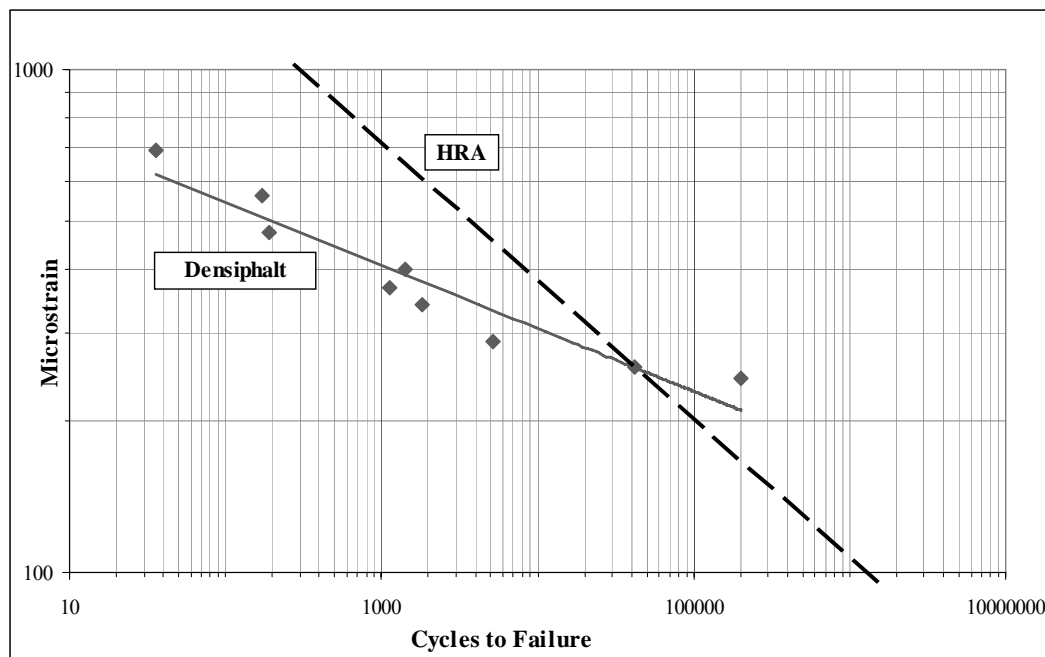
Figure 3.16 – Initial strain vs Fatigue life for *Densiphalt*® (Collop and Elliott, 1999)

In 2000 a research program was carried out by KOAC•WMD Apeldoorn to determine the engineering properties of *Densiphalt*® for Densit a/s (the full report can be seen in Appendix A). This research program consisted of the determination of stiffness and fatigue properties of *Densiphalt*® with specimens obtained from slabs previously manufactured by Densit a/s (Pelgröm, 2000). In this study the tests were undertaken using a four-point bending equipment to apply repetitive bending loads on beams with dimensions of 450 x 50 x 50 (mm).

The stiffness modulus was determined for three temperatures (0, 20 and 40 ºC) using a frequency sweep test (using 0.1, 0.5, 1.0, 4.9, 9.8, 19.5 and 29.3 Hz) and the results are presented in Figure 3.17.
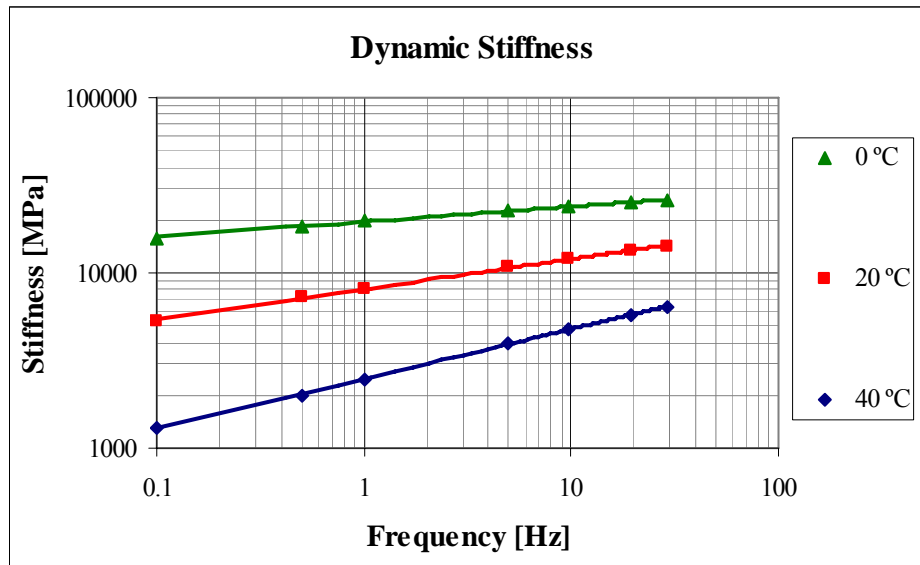
Figure 3.17 – Results for dynamic stiffness modulus of *Densiphalt*[®] determined by the frequency sweep tests (Pelgröm, 2000)

Four-point bending fatigue tests were performed at two temperatures (0 and 20 ºC) in controlled strain mode. At each temperature two strain levels were used (a lower strain level to obtain a fatigue life of about 10^6 load repetitions and a higher strain level to obtain a fatigue life of about 10^5 load repetitions). Three specimens were tested at each strain level. To determine the strain level two specimens were used in a pre-test (Pelgröm, 2000). The results from these tests are plotted in Figure 3.18.
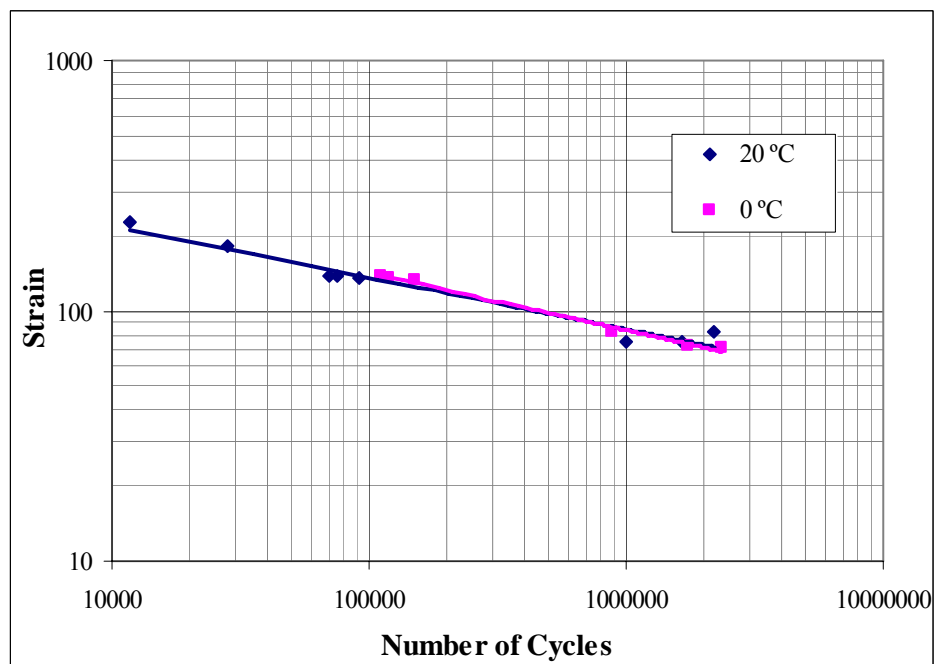
Figure 3.18 – Results of the fatigue tests (Adapted from Pelgröm, 2000)

More recently, van de Ven and Molenaar (2004) have studied the properties of a grouted macadam, which they refer as 'combi-layer'. In that study, the authors have carried out several tests to obtain the mechanical characterisation of the material. From the test results, stiffness master curves, indirect tensile strength and fatigue lines are reported. The uni-axial properties of the studied grouted macadam were also compared with the equivalent properties of asphalt concrete and cement concrete.

Based on the assumption that 25 percent of the volume of the final product consists of cement mortar, the authors expected a tensile strength of the grouted macadam of 1.25 MPa (25% of cement mortar tensile strength) at very high in-service temperature. In that situation, the contribution of the asphalt to the final strength may be neglected. According to this assumption, the mentioned values should be independent of the speed of loading, since the cement mortar would dominate the behaviour. To verify the assumption, indirect tensile tests were carried out at four different temperatures (0, 10, 20 and 30 °C) and the results showed that at 30 °C the strength is only 20 percent of the strength at 0 °C. According to the authors, this gives the impression that the temperature susceptibility is large, as in asphalt concrete mixtures. However the authors mentioned that care should be taken when analysing the results, since the loading strips may influence them.

Stiffness of the 'combi-layer' was measured with frequency sweep tests using a four-point bending equipment. Tests were performed in displacement control mode, using a displacement corresponding to a strain level of 50 με. A temperature range between 5 and 50 °C was used and stiffness values were obtained at 0.5, 1, 2, 4 and 8 Hz. Figure 3.19 shows a master curve produced with the results from the frequency sweep tests. According to the authors it highlights the temperature and loading speed dependence of the material. Hence, it points out the importance of using the right stiffness value for design calculations, when analysing a multi-layer pavement structure.

Fatigue tests were also carried out in displacement control mode by the same authors, using the same equipment, and the material seems to behave close to asphalt concrete mixtures, although the strain capacity of 'combi-layer' is generally lower than the strain capacity of asphalt concrete (Figure 3.20).
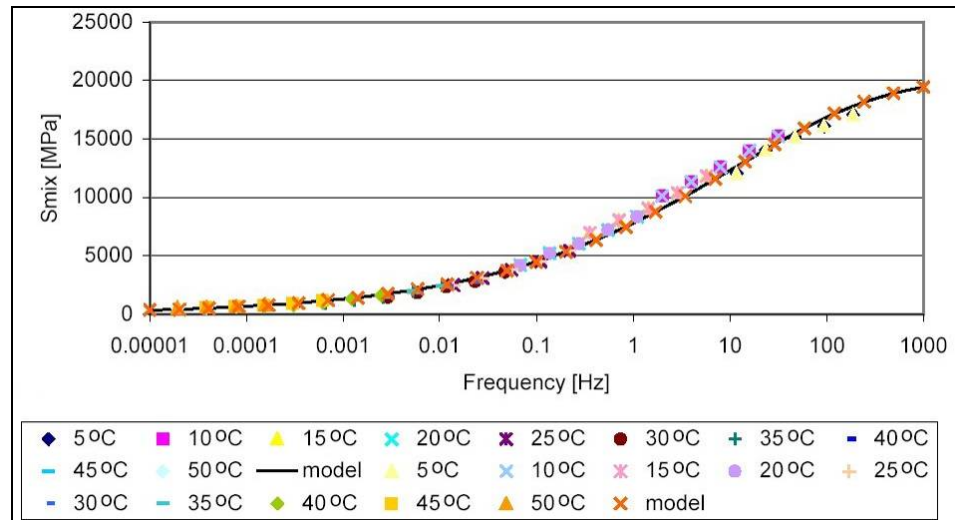
Figure 3.19 – Master curve for the stiffness of 'combi-layer' in a four-point bending test at 14 ºC (van de Ven and Molenaar, 2004)
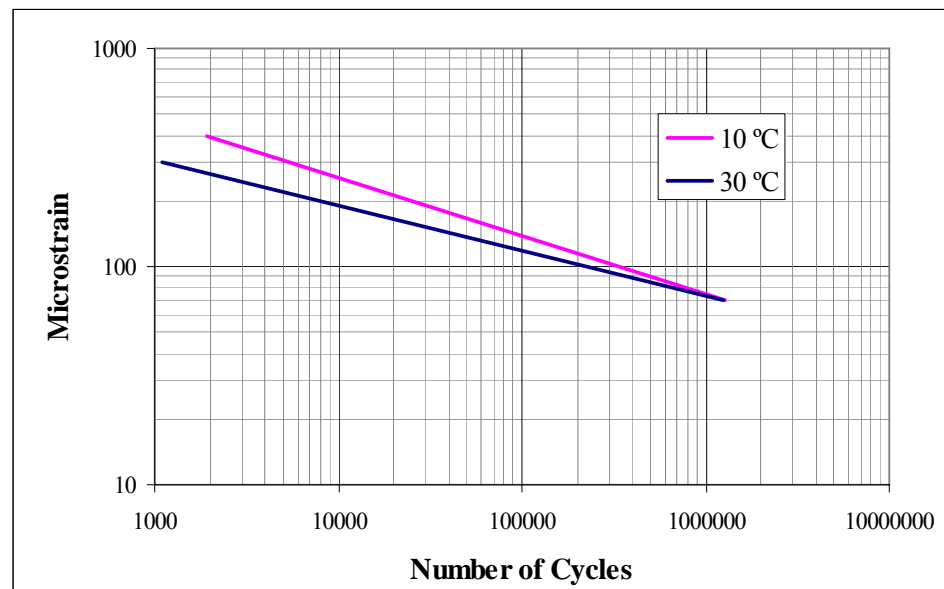
Figure 3.20 – Regression lines for fatigue of combi-layer at 8 Hz
(van de Ven and Molenaar, 2004)

From the previous figures, it seems that stiffness modulus is strongly affected by testing temperature and frequency. These are typical asphalt characteristics and therefore, it would appear that grouted macadams behave closer to asphalt materials than cementitious materials. However, in terms of fatigue resistance, the results show less consensus regarding the influence of testing conditions, namely temperature as can be observed in Figures 3.18 and 3.20. This issue will be discussed in more detail in Chapter 6, where results from a more comprehensive testing programme, regarding the influence of material and testing conditions in the mix design of grouted macadams, are presented.

3.4.2.2 Type of laboratory tests

The influence of the type of test used to determine the fundamental properties of a certain material is an important issue to consider when dealing with pavement design. Bituminous materials are often tested using different test methods, according to available equipment and the results are not necessarily the same from different tests. This appears to be also the case for grouted macadams. Setyawan (2003) has performed several fatigue tests, using two different test methods, an Indirect Tensile Fatigue Test and a Beam Bending Fatigue Test. In Figure 3.21 a reproduction of part of the results obtained by this author are plotted. The results show two different fatigue lines obtained for the same material, reinforcing the idea that one should be careful when choosing a fatigue line to simulate the fatigue performance of the material in pavement design.
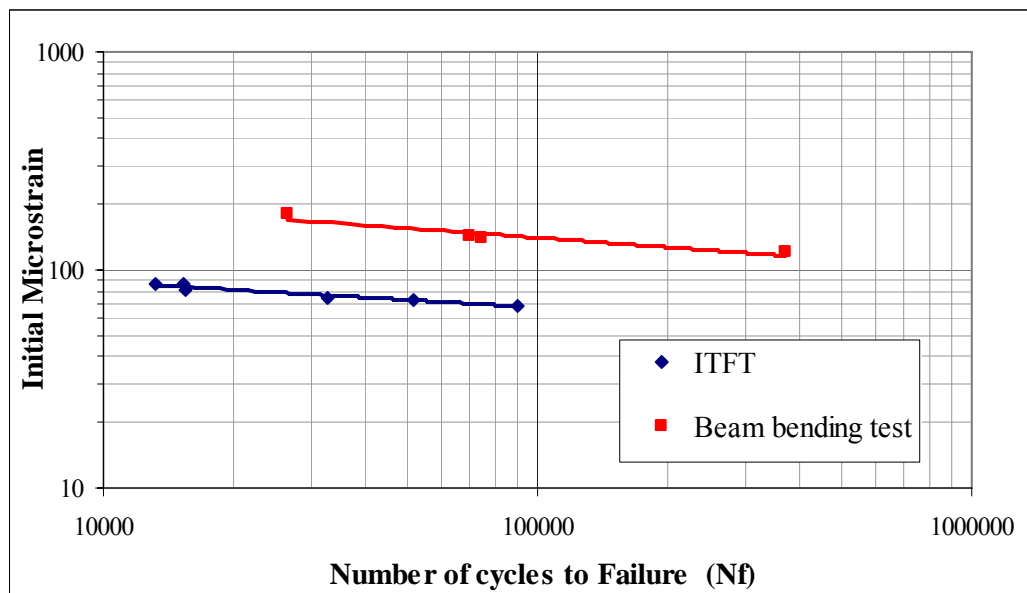
Figure 3.21 – Fatigue lines of one grouted macadam obtained from different test types (Data obtained from Setyawan, 2003)

3.5 Design of pavements incorporating grouted macadams

Even though this type of material has been used in pavements since the 1960's, there is lack of guidance available for designing pavements incorporating grouted macadams (Setyawan, 2003).

Guidance on the design of the grouted macadam mixture can be found in the literature (Boundy, 1979; Ahlrich and Anderton, 1991; Collop and Elliott, 1999; Anderton, 2000; Densit, 2000; Setyawan, 2003). However, little can be found regarding the design of pavements incorporating such material. Most pavement design methods currently used involve linear elastic theory and some assumptions regarding the composition of the materials used in each layer, e.g., homogeneity, isotropy, material continuity.

Collop and Elliott (1999) have carried out some design calculations for pavements with *Densiphalt*® using an analytical design approach. The analysis of the pavement structure was performed using a layered linear elastic model and calculations were made comparing a conventional HRA and *Densiphalt*® surface course materials. The main conclusions obtained from that study were that it would be possible to reduce the thickness of the base course by 10 to 20 mm when using *Densiphalt*® as an alternative to HRA in the surface course. However, the authors also emphasise that using such a simple model to calculate stress, strain and displacement in a layered elastic structure, it was not possible to simulate any tensile strains in the *Densiphalt*® layers, as it was in a compressive area in all cases. It would be necessary to carry out a more fundamental analysis to include additional factors (e.g., non-uniform tyre pressure) that may induce tensile stresses in the surface course.

Chapter 8 is dedicated to the discussion of this matter, where further details about design of pavements incorporating grouted macadams are given.

3.6 Summary

A group of proprietary grouted macadam mixtures have been presented in this chapter and the main properties of some of these mixtures have been discussed. However, it became evident from literature that a comprehensive mix and pavement design study of grouted macadam composites has not been carried out. Thus, in this investigation, such a study was performed (as presented in the following chapters), in order to develop a more complete characterisation of this type of mixture, to be used in the design of pavements incorporating grouted macadams.

4 DEVELOPMENT OF FOUR-POINT BENDING EQUIPMENT

4.1 Introduction

In a recent interlaboratory campaign organised by RILEM 182-PEB Technical committee "Performance testing and evaluation of bituminous materials", 11 different test methods, comprising uniaxial tension/compression, 2-, 3- and four-point bending and indirect tension tests, were utilised in order to investigate fatigue characteristics of a dense graded asphalt concrete mixture (Di Benedetto et al., 2003; Di Benedetto et al., 2004). In that study, it was concluded that fatigue lives are significantly affected by the test method. Amongst the test methods studied, the Indirect Tension Test showed the shortest life duration, which, according to the authors, is probably caused by significant accumulation of permanent deformation in addition to fatigue damage. It was also the only test to be carried out in load control, which usually means a shorter fatigue life. Load conditions and testing set-up, together with sample size, were pointed out as the main reasons for the differences in fatigue life obtained for different beam tests.

In order to study different alternatives to the standard mix design used by the project sponsors, and in order to better understand the fatigue properties of grouted macadams, a laboratory fatigue test, other than the more routine Indirect Tensile Fatigue Test (ITFT), was to be used. The objective was to select a test that simulates, in a more realistic way, the stress and strain conditions in a pavement layer. The test initially proposed comprised a load applied by a moving wheel on top of a grouted macadam beam, supported by a continuous rubber foundation. This test allows the beam to bend in a similar way to a pavement layer under moving traffic loads. However, as in the case of ITFT, it is difficult to separate the fatigue phenomenon from permanent deformation and the causes of specimen failure are not only restricted to fatigue. Therefore, other alternatives had to be considered.

4.2 Review of fatigue test equipment

Rao Tangella et al. (1990) carried out a research programme with the purpose of reviewing various fatigue test methods and recommending the most appropriate method for defining the fatigue response of asphalt-concrete mixtures. The evaluated test methods were classified into the following categories: simple flexure, supported flexure, direct axial, diametral, triaxial, fracture mechanics, and wheel-track tests. These methods were evaluated based on simplicity, ability to simulate field conditions, and applicability of the test results to design a pavement against fatigue cracking. In the study, the repeated flexure test received the highest ranking, followed by the direct tension and the diametral (indirect tension) repeated load tests, these being highly ranked due to their simplicity, lower cost and shorter testing time.

Taking the aforementioned into consideration and looking to the objectives of the present research study, it was decided to develop a new equipment, to study the fatigue response of grouted macadams, using the principle of simple flexure. Among the available methods, the four-point bending test (also known as third point flexure) was chosen, since the failure of the specimen in this type of test occurs in an area of uniform bending moment, which is not the case in a centre point flexure test. Four-point bending also avoids the need to glue the specimen to an end plate, as in the cantilever (two-point) bending test, which can delay the test set up.

Several pieces of equipment have been used worldwide to assess the fatigue characteristics of bituminous mixtures, using the simple flexure principle. Most of those recently developed (Tayebali et al., 1994$_a$; Pelgröm, 2000) comprise a four-point bending frame (Figure 4.1). In order to avoid internal stresses or strains in the specimens, imposed by restraints at the load or reaction points, such frames are normally manufactured with free rotation and translation at those points.

The results of any fatigue test are influenced by the mode of loading, which can be classified into two different test categories: controlled-stress (or load) and controlled-strain (or displacement). Failure (or the number of cycles to failure) in fatigue testing has been defined in various ways and sometimes arbitrarily, and the value cited depends on the mode of loading (Al-Khateeb and Shenoy, 2004).

In controlled-stress tests, some researchers have defined failure as the complete fracture of the specimen at the end of the test (Pell and Cooper, 1975; Tayebali et al., 1992). In order to protect the instrumentation (e.g., LVDTs) a practical limit was suggested by Rowe (1993), which defined failure at 90% reduction of initial stiffness, at which point the specimen displayed large cracks.
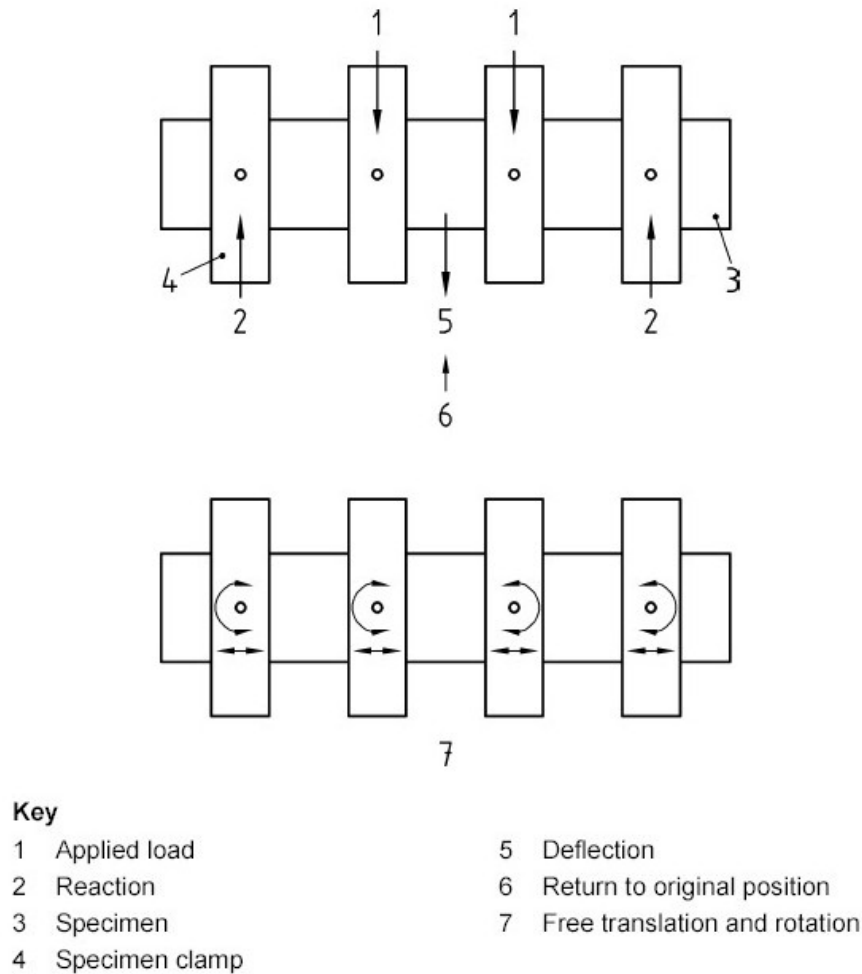
Figure 4.1 – Loading scheme of the specimens in the four-point bending test
BS EN 12697-24 (BSI, 2004$_d$)

Regarding controlled-strain tests, failure of the specimens is more difficult to define, since the stresses within the specimen decrease during the test, as the specimens gets progressively weaker due to the accumulation of damage, and total failure of the specimen is unlikely to occur. Several researchers have considered failure of the specimen when its stiffness value has reduced to half of the initial value (Tayebali et al., 1992; Tayebali et al., 1993; Di Benedetto et al., 2004).

Despite being the most common and widely used failure criterion, the 50% reduction in stiffness has more recently also been criticised by various researchers as being an arbitrary value that has no correspondence to any change in the properties of the material. Therefore, other failure criteria have been proposed. Van Dijk (1975) and Van Dijk and Visser (1977) have suggested that the dissipated energy approach allows results of different types of tests, carried out under different test conditions with several types of asphalt mixes, to be described by a single mix-specific relationship that relates the number of cycles to failure to the cumulative dissipated energy. Rowe (1993) suggested a new concept related to *crack initiation* instead of traditional failure of the specimen. In this concept, the number of cycles to failure is obtained by an energy ratio, based on the dissipated energy in each cycle of the test. Different energy ratios are suggested for strain or stress controlled tests. Ghuzlan and Carpenter (2000) used a failure criterion based on the change in dissipated energy (ΔDE) between two consecutive cycles. The failure is defined as the number of load cycles at which the change in this energy ratio begins to increase rapidly. Kim et al. (1997) introduced the 50% reduction in pseudo stiffness as a failure criterion for fatigue testing, which was assumed to be independent of the mode of loading. However, data in support of the 50% reduction in initial pseudo stiffness, in constant stress testing, were not shown. Al-Khateeb and Shenoy (2004) proposed a new failure criterion based only on the observation of raw data collected during a fatigue test. According to these authors failure is revealed by observing the distortion of the load-deformation hysteresis loop or the response waveform at the onset of the first crack appearance. The concept of fatigue failure for grouted macadams is further discussed in Chapter 6, where the results obtained from four-point bending fatigue tests, for several mixtures, are presented.

According to Rao Tangella et al. (1990) the controlled-stress mode of loading appears to represent the response of thick asphalt pavements to repetitive loading while the controlled-strain approach is suitable for thin pavements. Controlled-strain tests generally give greater fatigue life than controlled-stress tests, for the same mixture and similar initial conditions (stress/strain level).

A fatigue test carried out in controlled-stress can be expressed by a basic relationship between the number of cycles to failure and the stress level used in the test, as presented in Equation 4.1 (Pell and Taylor, 1969; Tayebali et al., 1994$_b$).

$$N_f = a\left(\frac{1}{\sigma_t}\right)^b$$
(4.1)

where: N_f = fatigue life;
        σ_t = applied tensile stress;
        a, b = constants determined from laboratory testing.

However, according to Rao Tangella et al. (1990), early fatigue research found that fatigue life of bituminous mixtures was often better correlated with tensile strains than with tensile stresses, and that the basic failure relationship could be characterized as in Equation 4.2. Pell and Taylor (1969) have also suggested a similar relationship for the estimation of fatigue in base courses.

$$N_f = c\left(\frac{1}{\varepsilon_t}\right)^d$$
(4.2)

where: N_f = fatigue life;
        ε_t = applied tensile strain[#];
        c, d = constants determined from laboratory testing.

In an attempt to account for differences sometimes observed in the fatigue relationship between life and strain, as loading frequency and temperature vary, a mixture stiffness term can be added to Equation 4.2 as shown in Equation 4.3 (Monismith et al., 1985).

$$N_f = c\left(\frac{1}{\varepsilon_t}\right)^d\left(\frac{1}{S_0}\right)^e$$
(4.3)

where: N_f = number of tensile strain, ε_t, applications to failure;
        S_0 = initial stiffness modulus of the asphalt mixture;
        c, d, e= experimentally determined coefficients.

[#] 'applied initial tensile strain', in load controlled tests.

Based on laboratory test data presented in the form of Equation 4.3, several models have been proposed to predict the fatigue lives of pavements (Finn et al. 1977; Shell 1978; Asphalt Institute 1981)[*]. To develop these models, laboratory results have been calibrated by applying shift factors, based on field observations, to provide reasonable estimates of the in-service life of a pavement considering the appearance of cracking due to repeated loads (Tayebali et al., 1994$_b$).

4.3 Design and manufacture of the equipment

Prior to manufacture of the equipment used in this study, several factors were taken into consideration in the design stage. Thus, according to laboratory constraints, in association with time and budget limitations, the equipment should:

- be used with existing axial testing machines;
- be simple to manufacture;
- be relatively economic;
- allow use with different materials and different specimen dimensions, subsequent to this project;
- allow easy test set-up.

In order to control costs and time spent in the production, the equipment was manufactured at the University of Nottingham, in the Civil Engineering School's workshop. Thus, standard pieces were chosen from catalogues, in order to obtain high precision and minimise the manufacture time.

The dimensions of the specimens to be tested dictated the dimensions of the frame. It was decided to use prismatic specimens (beams) sawn from slabs, which were produced in the laboratory using an existing roller compactor. The dimensions of the slabs obtained from this process were restricted to 305 mm (the maximum dimension of the square moulds used in the roller compactor). Therefore, the maximum dimension of the beam that could be used in the flexural test was established. The other dimensions of the beam (Figure 4.2) were selected as 50×50 (mm), since the thickness of the surface course with this type of material does not normally exceed 50 mm.

---

[*] See Tayebali et al., 1994$_b$

The four-point bending rig was then manufactured with 90 mm between each load and reaction point (270 mm total span) and it allows future use of beams with dimensions up to 70×65 (mm). This piece of equipment was not designed to allow horizontal movement at the loading and reaction points. However, due to the type of ball bearings chosen, a small amount of lateral movement was detected after construction of the equipment, which was taken into consideration in the calibration process. Lateral movement is necessary to prevent internal stresses developing in the specimen due to end restraints. Nonetheless, taking into consideration the expected vertical movement (with maximum amplitude of approximately 200 microns), it was calculated that the restraint of the associated horizontal movement at the outer clamps (which do not exceed 0.7 microns for the maximum vertical deformation) would not impose significant stresses in the specimen. Further details on this issue are given in Section 4.4, which details the equipment calibration protocol.

Figure 4.2 – Grouted macadam specimen to be used in the four-point bending test

Considering the dimensions of the specimen and its expected stiffness modulus (obtained from literature) the order of magnitude of the loads involved in this test was calculated, after which, each piece of the four-point bending frame was designed. The frame was made robust enough to prevent significant deformation of any of its parts under load, which would have invalidated the results obtained from the tests.

In order to connect the frame to the testing machine (Figure 4.3) used for this test, special pieces were designed and manufactured to fit the existing actuator and

reaction plate. The four-point bending rig was also designed taking into account the use of one LVDT, in order to measure the vertical movement at the neutral axis of the specimen and to control the test when using the controlled-strain mode of loading. Figure 4.4 shows the four-point bending assembly obtained from this design process.

Figure 4.3 – Testing machine to be used in the four-point bending tests
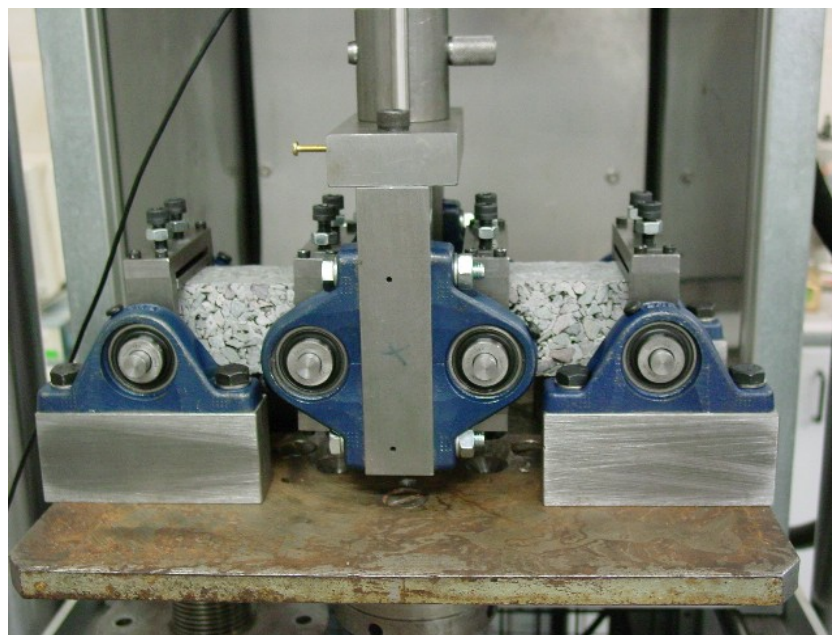
Figure 4.4 – Four-point bending frame

The servo-hydraulic testing machine (MAND) used in this project is able to apply loads up to 100 kN and it enables vertical compressive and tensile forces to be applied to a sample under static or cyclic conditions. For the present test, it was decided to use a sinusoidal loading pattern to avoid permanent deformation of the specimens under their own weight. The machine is fitted with a temperature-controlled cabinet with a range of temperatures between -5 and 40 °C, which allowed the fundamental properties of grouted macadams to be determined at different temperatures.

A *Rubicon* digital servo control system is used to operate the machine and perform the tests, during which, data is collected using general data acquisition software, also supplied by *Rubicon*, and stored in a computer. The software allows the test to be controlled by three different signals (load, actuator stroke and central LVDT) by continuously monitoring the specified signal, providing a feedback signal to the control system. The control system compares this feedback signal with the input command signal and the difference is amplified and fed to the servo-valve, which adjusts the oil flow to the actuator to reduce the difference between the input and output signals, such that the actuator responds precisely to the command signal (Osman, 2004).

4.4 Equipment calibration

Once the four-point bending frame had been manufactured, it was attached to the testing machine, in order to check the existence of any play (slack) within the system and, if so, identify the location and eliminate it, readjusting the frame. Any relative movement in the fixing points and/or in the attachment to the actuator would invalidate the results.

To assess the presence of any play in the system a stiff wooden beam (with the dimensions of a normal specimen) was used in preliminary tests using a sinusoidal loading pattern. Following these tests, it was necessary to carry out small modifications in the attachment of the frame to the machine actuator.

The next step was to calibrate the LVDT, using proper calibration equipment (Figure 4.5). The type of LVDT that was used had a very limited range of displacement measurement, thus providing better accuracy.
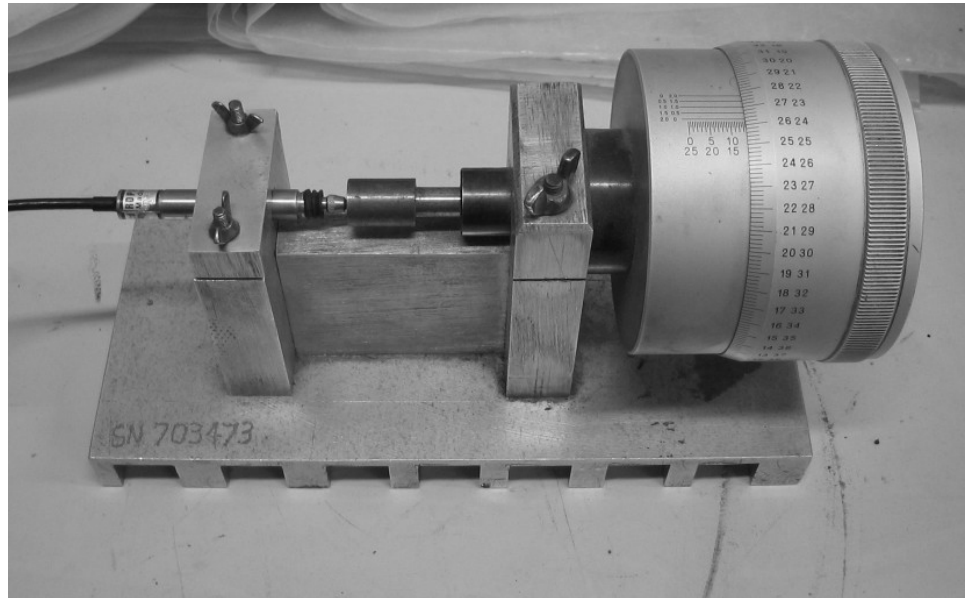
Figure 4.5 – LVDT calibrator

Preliminary tests, carried out using the wooden beam, were also used to establish the test procedure. It included setting-up the test, by placing the specimen into the frame, tightening the clamps, locating it in the correct position to start the test, and also controlling the test with the available *Rubicon* software associated with the testing machine.

From the preliminary tests it was established that the final test procedure should include a pre-test, performed in a short period and with a reduced strain or stress level (to avoid damaging the specimen), to determine the stiffness and phase angle of the material, followed by the fatigue test, carried out until specimen failure. Furthermore, during the preliminary tests it was detected that, for the required test frequency (10 Hz), the hydraulic pump associated with the testing machine was not capable of responding fast enough to allow the use of controlled-stress tests. During this type of test, the deflection at the centre of the beam increases, as it becomes weaker with the accumulation of damage under the load repetitions. However, the existence of a threshold value was observed for the maximum actuator movement amplitude at high frequencies, after which, the test would be controlled by the

displacement rather than by the load. Based on these limitations, it was decided to use exclusively controlled-strain (or displacement) tests.

Bending tests performed on a beam made from material with known stiffness modulus, in order to verify the results obtained from the tests, completed the calibration process. Thus, an aluminium beam was chosen, with a known stiffness modulus of 70 GPa. During this stage of the calibration process, a vertical movement was detected in the outer clamps, due to the type of bearings used. The outer bearings work as a kind of "kneecap", allowing some misalignment in the axis. The displacement of the central part of the beam was thus found to be over estimated as a result of the vertical movement of the outer clamps. To take this movement into consideration, two additional LVDTs were used to quantify the vertical movement of the outer clamps, which was then subtracted from the movement measured by the central LVDT, in order to obtain the correct vertical displacement of the central part of the beam.

In an ideal situation, the supports should have the freedom to move laterally, as mentioned earlier in Section 4.3. Using the LVDTs placed in the outer clamps, it was determined that the beam supporting points were free to move up to 6 microns (when applying the maximum strain level in the test). According to the previous calculations, the maximum extension of the beam under bending was estimated to be lower than 0.7 microns, which is well within the lateral freedom given by the supports. It was therefore determined that no major stresses would be induced into the specimens during the tests as a result of the restraint offered by the outer clamps.

4.5 Data acquisition system

Tests performed with the piece of equipment developed under this project were carried out using an existing testing machine as well as the software available for control of the test and data acquisition. Therefore, the precision of the results obtained in the tests was limited by the capabilities of the controlling and data acquisition software. Two types of test were carried out using this apparatus: a short duration test, where the Complex Modulus (Stiffness Modulus and Phase Angle) of

the material was determined (hereafter referred to as stiffness test), and a long duration test to determine the material Fatigue Life.

Different software was used for the data acquisition in the two types of tests. One that is able to collect several data points per cycle was used for the stiffness test, and a second one that collects only the peak values, obtained for all the electrical signals collected by the control system (e.g., load, stroke, LVDT readings), for each cycle, was used for fatigue tests. The number of datapoints collected from the first software enabled the determination of the phase lag (Figure 4.6) between load and displacement (characteristic of viscous materials), which is the basis of the phase angle calculation. Further details are given in the following section, where a description of the tests carried out using this equipment, is made.
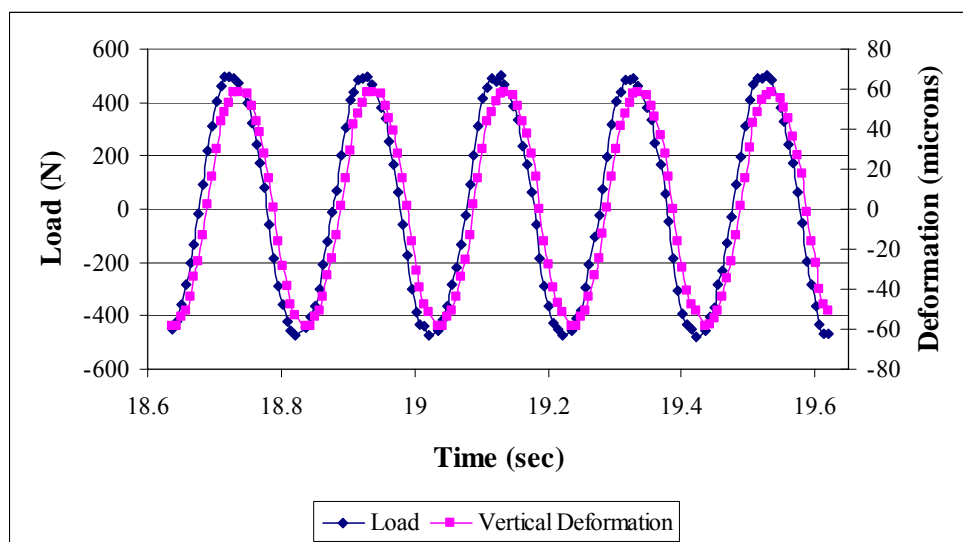
Figure 4.6 – Typical sinusoidal signals obtained from the stiffness tests

The second type of software was used with the purpose of collecting information about the change in the material properties (i.e., stiffness reduction) during the test, without excessively increasing the size of the data files. However, this software did not allow calculation of the phase angle to be made, since the peak values collected were associated with the corresponding cycle and not with time. Therefore, the failure criterion used for the fatigue test was established as the number of cycles obtained for 50% reduction of the initial stiffness. In order to guarantee that this point would be obtained from the data collected, the end of the test was established as the cycle when the initial load measured had dropped by 70% (approximately

equivalent to 70% reduction of the initial stiffness value, since the tests were carried out in controlled-displacement), after which the control system would automatically stop the test (Figure 4.7).
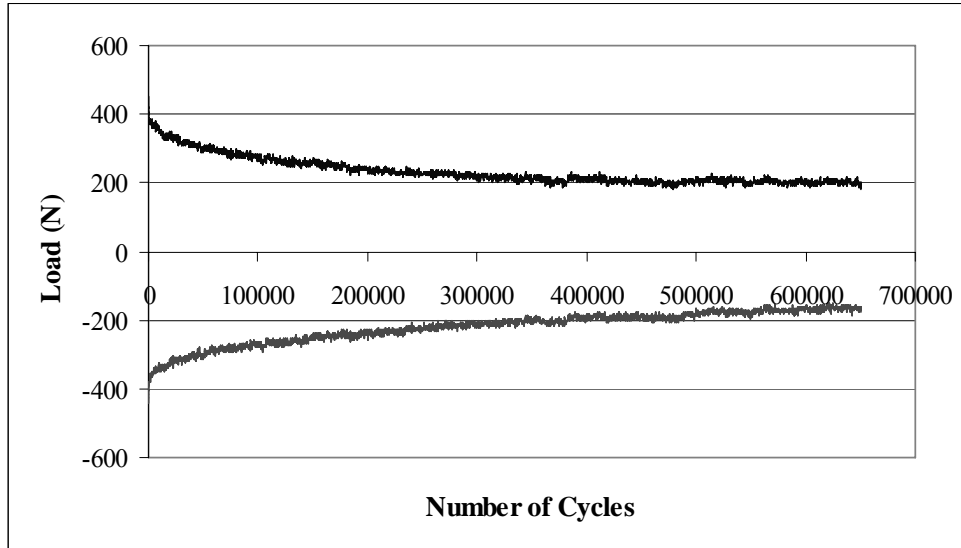
Figure 4.7 – Typical data collected from the four-point bending fatigue tests

4.6 Tests performed with the equipment

Having established the test procedure and mastered the data acquisition system, tests were carried out using the four-point bending apparatus. To perform the tests, it was necessary to establish the strain levels that were going to be used. Thus, for the stiffness test, a maximum strain amplitude of $50\,\mu\varepsilon$ was selected for which no damage in the specimen was to be expected. This value was established based on a preliminary series of fatigue tests carried out using a grouted macadam of standard mix design. In normal circumstances, fatigue tests are carried out using a certain number of specimens, which are tested at different strain (displacement) levels. The results obtained for each individual test (according to the specified failure criterion) are then plotted together to establish a fatigue line that represents the material behaviour under repetitive load applications.

Scatter in the results of fatigue tests is unavoidable (Di Benedetto et al., 2004) and it is important to test as many specimens of the same mixture as is practicable. Too few

specimens may not represent adequately the mixture behaviour and too many specimens would take too much effort and time to be tested, as well as a large amount of material. According to Ghuzlan and Carpenter (2000), at least four specimens must be tested to establish a representative fatigue curve. In the present study, five specimens were obtained from each slab produced in the laboratory. Therefore, it was decided to use five specimens per mixture for the stiffness and fatigue tests. In some cases, namely for the standard mixture, extra slabs were produced to make the fatigue results more representative. However, variability between specimens of different slabs (and sometimes between specimens of the same slab) cannot be avoided completely, even though the same procedure, equipment and technicians are used to produce them.

Four-point bending tests were carried out in strain (displacement) control and it was necessary to determine the deflection of the central part of the specimen equivalent to a specific strain level (maximum strain applied at the outer fibre of the beam), which was obtained based on Equations 4.4 and 4.5. According to Tayebali et al. (1994$_a$), for shear deformations to be neglected, the square of the height (h) to beam span (l) ratio must be much less than one ($(h/l)^2 \ll 1$). However, in the present study, both bending and shear deformation of the beam were considered, and the distance between each support was one third of the beam span (270 mm).

$$\sigma_t = \frac{P \cdot l}{b \cdot h^2} \qquad\qquad (4.4)$$

$$\varepsilon_t = \frac{108 \cdot \delta \cdot h}{23 \cdot l^2 + 36 \cdot h^2 \cdot (1+\nu)} \qquad\qquad (4.5)$$

where: σ_t = tensile stress (Pa);
      P = load amplitude applied on specimen (N) – *P/2* on each loading point;
      l = beam span (m);
      b = beam width (m);
      h = beam height (m);
      ε_t = applied tensile strain (m/m);
      δ = beam deflection at neutral axis (m);
      ν = Poisson's ratio.

Based on these relationships, the complex modulus, E (Pa) can be calculated for each cycle of the test, dividing the maximum stress by the maximum strain (Equation 4.6).

$$E = \frac{\sigma_0}{\varepsilon_0} \qquad\qquad (4.6)$$

A common way of presenting the complex modulus is by its modulus, $|E|$ in association with the phase lag between the stress and strain (phase angle, ϕ). In such circumstances, it is generally termed "Stiffness Modulus", which will be the term used for the remainder of this dissertation.

In the stiffness tests, 100 cycles were used to determine the stiffness modulus of the material, considered as the average of the values obtained for each cycle. The phase angle, ϕ (deg) was obtained based on the dissipated energy, which was computed, for each cycle, as the area within the stress-strain hysteresis loop. The phase angle was, therefore, obtained from the following relationship:

$$w_i = 0.25 \cdot \pi \cdot \varepsilon_i^2 \cdot E_i \cdot \sin(\phi_i) \qquad\qquad (4.7)$$

where: w_i = energy dissipated at cycle i;

ε_i = peak to peak strain at cycle i;

E_i = stiffness modulus at cycle i;

ϕ_i = phase angle between stress and strain at cycle i.

The available software was not designed specifically for this type of test. It does not allow a frequency sweep test to be carried out automatically to characterise the material. Since the test had to be started and stopped manually, two frequencies were selected for the stiffness determination tests; otherwise it would have been too time consuming. For each specimen, the testing procedure included a stiffness test at 5 Hz, followed by a similar test at 10 Hz and concluded with a fatigue test at the desired strain (displacement) level, also at 10 Hz. In order to guarantee that the specimens were not subjected to any damage between each test, the machine actuator was configured to operate under load control and the load level was kept equal to zero following each test.

As mentioned before, the test machine is equipped with a temperature-controlled cabinet, which allows the tests to be carried out at any temperature between -5 and 40 ℃. The main testing programme was carried out at 20 ℃, but some tests were also carried out a 0 and 5 ℃. Further details about the testing programme are presented in Chapter 6, which describes the mix design study.

4.7 Summary

In the UK, the Indirect Tensile Fatigue Test (ITFT) is routinely used to determine the fatigue life of bituminous materials. However, the test does not represent the actual flexure of a pavement layer, under a moving wheel. Therefore, a four-point bending apparatus have been developed, as presented in this chapter, in order to carry out a comprehensive mix design study of grouted macadam mixtures, based on their fundamental characteristics (i.e., complex modulus and fatigue life). This equipment also allows the fatigue life determination without the 'unwanted' effect of permanent deformation (which always occurs in the ITFT tests).

5 BASIC CHARACTERISATION OF THE MATERIALS

5.1 Introduction

As mentioned previously, the material studied in this research project can be generally classified as a grouted macadam. Part of the testing was carried out using a commercial grout, supplied by the project sponsors – Kajima Construction Europe (U.K.) Ltd, and therefore, the standard mixture mentioned several times in this dissertation could be named as *Densiphalt*®. It comprises an open-graded asphalt skeleton with 25 to 30% voids into which a cementitious grout is poured. This grout is formulated by adding water to a pre-processed cementitious powder (produced by Densit a/s from Denmark). Several variables were studied in the composition of the standard mixture and the results obtained from that study are presented in the following chapter. In the present chapter, characterisation of each component used in the production of grouted macadams in this research project is made, complemented with a basic characterisation of the standard mixture.

The standard mixture design that has been used in UK applications was characterised by Collop and Elliott (1999). In this research project, further investigations were made, regarding the mixture design, in order to assess the best properties of this semi-flexible material and also in order to verify the suitability of the material to be used in structural layers, as an alternative to the most popular present application, i.e. as a surface course. The mixture design used by Collop and Elliott (1999) was used in this study as a starting point, to establish the procedure to produce specimens and to determine some properties of the material that had not been studied previously.

In the following sections, the physical properties of aggregate and bitumen used in the open-graded asphalt mixture are presented, followed by the characterisation of the grout and its mixing and application procedure.

5.2 Aggregate

The present applications of grouted macadam are limited to surface courses of heavy-duty pavements, due to its good characteristics in terms of rutting and wearing, fuel and oil spillage resistance. Aggregates used in this type of layer should be sound, durable and with high abrasion resistance. The type of aggregate used should also be obtained from crushed rock and should be single sized, in order to achieve a very high voids content in the bituminous mixture.

In the present study, the aggregate type used was mainly granite, which was obtained from Bardon Hill Quarry. The gradation used in the standard mixture consisted of a 10 mm nominal single sized aggregate specified in the British Standard BS 63: Part 1 (BSI, 1987) and the grading limits were previously presented in Table 3.9. Table 5.1 shows the gradation of the 10 mm single sized aggregate used in the current project.

Table 5.1 – Gradation of the 10 mm single sized aggregate used

BS Sieve Size (mm)	Percentage passing
14	100
10	89.5
6.3	1.9
5.0	0.8
2.36	0.2

The reason for using a nominal single sized aggregate is related to the ease of procurement for field applications, which could be done directly from the quarry's screened stockpile.

The aggregate used in the present study had a gradation similar to that adopted by Setyawan (2003) which lies in between the two types of aggregate gradations specified by the *Densiphalt*® Handbook (Densit, 2000), which were shown earlier in Figure 3.3. At the beginning of the research project, an estimate of the necessary quantities of each single sized aggregate was made, after which, the aggregates needed for the entire project were obtained and their gradations and relative density values were determined. Table 5.2 and Figure 5.1 summarise those characteristics of the aggregate.

Table 5.2 – Gradation and Particle Density of the aggregate used in the project

Sieve size (mm)	Nominal Aggregate Size						
	28 mm	20 mm	14 mm	10 mm	6.3 mm	Dust	Filler*
	Percentage Passing						
37.5	100	100	100	100	100	100	100
28.0	95.8	100	100	100	100	100	100
20.0	23.7	99	100	100	100	100	100
14.0	1.8	5.2	89.9	100	100	100	100
10.0	0.6	0.7	22.2	89.5	100	100	100
6.3	0.5	0.3	3.1	1.9	60.4	100	100
5.0	0.5	0.1	2.6	0.8	43.8	100	100
3.35	0.5	0.1	2.1	0.4	7.9	97.2	100
2.36	0.5	0.1	2.1	0.2	1.6	87.3	100
1.18	0.5	0.1	1.8	0.1	0.5	57.5	100
0.6	0.5	0.1	1.7	0.1	0.2	39.2	100
0.3	0.5	0.1	1.6	0.1	0.1	25.4	100
0.212	0.5	0.1	1.5	0.1	0.0	20.4	100
0.15	0.5	0.1	1.4	0.1	0.0	16.9	99.82
0.075	0.4	0.0	1.1	0.1	0.0	11	96.81
Receiver	0.0	0.0	0.0	0.0	0.0	0.0	0.0
Particle Density on an oven-dried basis (Mg/m^3)	2.774	2.746	2.750	2.751	2.737	2.133	---
Particle Density on a saturated and surface-dried basis (Mg/m^3)	2.785	2.759	2.773	2.772	2.764	2.329	---
Apparent Particle Density (Mg/m^3)	2.805	2.783	2.812	2.811	2.814	2.654	---
Water Absorption (% of dry mass)	0.4	0.5	0.8	0.775	1.0	9.119	---

* Specific gravity of filler (determined according to BS 812-2 (BSI, 1995$_a$)): 2.74 Mg/m^3
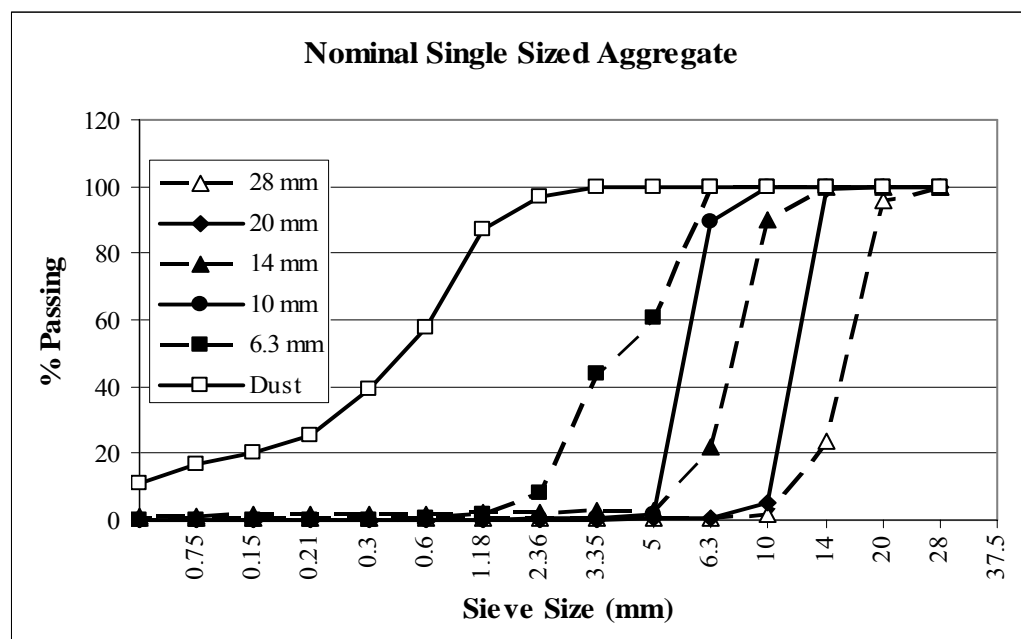
Figure 5.1 – Gradations of the nominal single sized aggregates

5.3 Bitumen

As in the case of the aggregate, the bitumen used in the standard mixture was of similar grade to the one used in the study carried out by Collop and Elliott (1999). Thus, a 160/220 pen straight-run Middle Eastern bitumen was used to manufacture the porous asphalt skeleton of most mixtures studied in the current project. At a later stage of the project, different grades of bitumen were also used, to assess the influence of the binder type on the fundamental properties of grouted macadams. Thus, a 40/60 pen straight-run bitumen and a Polymer Modified Bitumen (PMB), marketed as *Cariphalte DA* and supplied by Shell Bitumen UK, were used. The properties of the binders used are summarised in Table 5.3.

Table 5.3 – Penetration and Softening Point values of the bitumens used during the project

Bitumen grade	Penetration (dmm)	Softening Point (°C)
160/220	192	36.5
40/60	52	51.2
PMB*	110/150	≥ 70

* Cariphalte DA, manufactured using SBS type polymers. Values specified by Shell Bitumen UK.

5.4 Open-graded Asphalt

Production of the standard open-graded asphalt was based on the same mixture composition used by Collop and Elliot (1999), since it fits the limits specified in the *Densiphalt*® Handbook (Densit, 2000), as presented previously in Tables 3.2 and 3.3. The decision to use cellulose fibres in the mixture was made with the objective of increasing the thickness of the bitumen film, coating the aggregates, and also of increasing the stability of the porous asphalt skeleton, since a very soft binder grade was used.

The porous asphalt was produced in the laboratory using pre-batched constituents. Before starting mixing, aggregates and bitumen were kept in an oven at 140 °C for 4 hours. The hot aggregates were initially mixed with the fibres using a paddle mixer for 1 minute, in order to distribute the fibres within the aggregate matrix. The bitumen was then added and the material was mixed for 2½ minutes. After this

period, the bituminous mixture was mixed by hand to avoid the occurrence of any segregation and then mixed mechanically for a further 2½-minutes period. Finally, the hot mixture was placed back in the oven for 10-15 minutes to make sure it was at the correct compaction temperature.

Depending upon the type of specimen produced, the porous asphalt compaction process was carried out either with a roller compactor or a vibrating hammer. When using the roller compactor, slabs with a specified thickness and an area of 305×305 mm^2 were produced using square moulds. The thickness of the slabs was pre-set in the roller compactor and the necessary number of passes to achieve that thickness was applied. If the specimen to be produced had a specific shape that did not allow the use of the roller compactor, a vibrating hammer was used to compact the mixture into an appropriate mould (e.g. thermal cracking specimens). Once the compaction was finished, the mixture was left to cool down in the mould until the following day, when it was grouted.

In order to verify the specimen production procedure (i.e., the compaction of porous asphalt skeleton and resultant air voids content) two tests were used. In the first, the edges of a compaction mould were sealed with silicone prior to the compaction of the porous asphalt slab, after which, an 80 mm thick slab was produced and allowed to cool down. The voids were then filled with water up to the surface of the porous asphalt. The amount of water added was weighed and the equivalent volume of voids was calculated. The percentage voids content was obtained after measuring the dimensions of the slab to determine the total volume. The second test consisted of taking four cylindrical cores from the slab and calculating the air void content of each according to British Standard BS EN 12697-Part 6 (BSI, 2003). These procedures were repeated for another slab with 40 mm thickness and the results are presented in Table 5.4.

Table 5.4 – Air voids content of the porous asphalt skeleton

Slab thickness	Volume of voids (%)				
	Procedure 1	Procedure 2			
80 mm	28.5	27.8	28.5	27.9	28.9
		28.28 (avg)			
40 mm	29.8	28.9	28.3	28.0	28.7
		28.48 (avg)			

As can be seen in the previous table, the air voids content obtained for the porous asphalt skeleton, with these laboratory procedures, is situated within the limits (25 to 30%), specified by the *Densiphalt*® Handbook (Densit, 2000) which was selected to ensure full penetration of the voids with the grout. The variability among the results may be justified by the difficulty in accurately measuring the dimensions of specimens with such an open aggregate skeleton structure.

5.5 Cementitious Grout(s)

Viscosity of the grout is the most important property to be controlled in order to obtain full penetration of the voids in the asphalt skeleton and consequently good behaviour of the mixture after curing. On the one hand, if the mortar is not fluid enough, some voids at the bottom of the layer may not be filled, which will lead to early failure of the layer under traffic. On the other hand, if the grout has too much water, penetration will not be a problem but the overall strength of the mixture will be reduced and segregation of its cementitious components may take place.

To assess the best methodology of producing the grouted macadam samples in the laboratory, preliminary slabs were produced. Since the grouting of the mixture is carried out inside a mould, expulsion of the air from the asphalt skeleton cannot occur laterally, increasing the difficulty of the grouting process in the laboratory. The first slab was grouted without vibration, in keeping with the procedure normally carried out in the field, but full penetration was not achieved, as can be seen in Figure 5.2, which represents a specimen cored from the slab. Thus, a vibrating hammer was used thereafter to vibrate the mould and produce slabs and specimens with full penetration of the grout, as illustrated in Figure 5.3.

Figure 5.2 – Preliminary Ø150 mm specimen made for establishment of procedures

Figure 5.3 – Ø100 mm specimen obtained with full penetration of grout

The grout mixing process was prepared in the laboratory using a rotary mixer (type HOBART A-120 MIXER), with a wire whip attachment, running at 194 and 353 RPM, inside a stainless steel bowl. Based on recommendations given by the grout suppliers and after some preliminary tests, the adopted mixing procedure was as follows:

1. Dry mix powder for 1 min (low speed);
2. Add 2/3 of water and mix for 2 mins (low speed);
3. Add remaining 1/3 of water and mix for 5 mins (low speed);
4. Increase speed and mix for further 3 mins (high speed);
5. Clean bowl to release material adhering to the side;
6. Mix for 1 min to homogenize the grout (high speed);
7. Check run-out (flow) time in the *Densiphalt*® funnel.

The amount of water used in the grout may have to be slightly adjusted depending on the result of the run-out time obtained in the funnel (previously illustrated in Figure 3.9). However, according to the Densiphalt® Handbook (Densit, 2000), 16.2% of water by mass of powder may be used as a guideline. The run-out time, for one litre of grout, obtained for any batch of grout should have values between 12 and 16 sec (10 and 18 sec, respectively as the minimum and maximum allowed limits), as specified in the Handbook. Thus, if the grout is not fluid enough after mixing with 16.2% of water, some more water should be added to get the correct viscosity (measured by the run-out time). The experience obtained during this project showed that the amount of water is highly dependent on the storage conditions of the powder. Hence, different batches may also need different amounts of water. After preliminary

tests, 17.5% water by mass of powder was used as a guideline throughout the project, although the run-out time was always checked to guarantee homogeneity among the properties of different slabs and mixtures produced.

After mixing the grout, impregnation of the porous asphalt skeleton should be carried out immediately and within a period of 45 to 60 min, before the workability of the grout becomes too low. The grout should be kept moving, e.g., with slight rotation, to avoid segregation and to maintain the grout fluid. The grouted macadam is then left overnight, to allow hardening to take place, before removing it from the moulds.

Further mechanical tests were carried out on the grouts used in this project to better characterise them. Thus, starting from the main (commercial) grout used in this investigation, cubes and beams were cast to determine its compressive and flexural strength. The cubes' dimensions were $50 \times 50 \times 50$ mm, while the beams were 350 mm long, with a cross section of 50×50 mm, the dimensions being determined by the dimensions of the available moulds. The tests were carried out according to the standard BS EN 196-1:1995 (BSI, 1995$_b$). Compressive strength was obtained by measuring the maximum load applied to the specimen and dividing it by the cube's cross-sectional area. The load was increased smoothly at the rate of 2400 ± 200 N/s until fracture of the specimen. Flexural strength was determined by means of four-point bending tests where the load was increased smoothly at a rate of 50 ± 10 N/s until failure of the specimen. The maximum load was then used to calculate the maximum tensile stress at which the specimen broke, representing the flexural strength.

During the course of the present research project, in addition to the standard Densit$^{®}$ grout, two more grouts were used, in order to study the effect of grout type on the final properties of grouted macadams. The details on the use of the grouts are given in the following chapters, but the main objective was to verify to what extent a weaker grout would affect the properties of the final mixture. Therefore, a weaker grout supplied by the project sponsors and a "modified" grout were used. The composition of the modified grout is not known and the weaker grout was obtained by simply adding 25% silt to the commercial Densit$^{®}$ powder. The results of the tests carried out on the 3 types of grout are presented in Table 5.5 and graphically illustrated in Figures 5.4 and 5.5.

Table 5.5 – Compressive and flexural strength of the grouts used

Age (days)	Compressive strength (MPa)			Flexural strength (MPa)		
	Densit® grout	Weaker grout	Densit® modified grout	Densit® grout	Weaker grout	Densit® modified grout
1	43.8	10.5	26.0	--	--	--
4	67.7*	24.3	52.4	--	--	--
7	74.4	27.4	67.3	--	--	--
28	111.0	35.2	92.1**	12.0	7.4	9.9***

* value obtained at 3 days curing time
** value obtained at 33 days curing time
*** value obtained at 41 days curing time

Grout Comparison

$y = 19.502 \text{Ln}(x) + 43.127$
$R^2 = 0.9728$

$y = 19.059 \text{Ln}(x) + 26.939$
$R^2 = 0.9936$

$y = 7.3494 \text{Ln}(x) + 12.113$
$R^2 = 0.9708$

- Densit grout
- Modified Densit grout
- Weaker grout
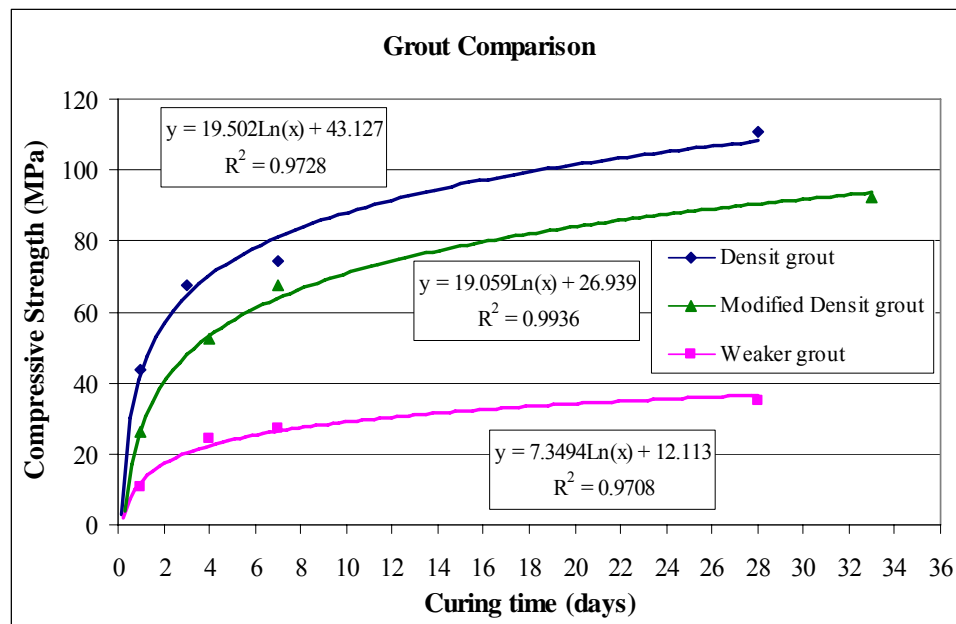
Figure 5.4 – Compressive strength values of the three grout types used
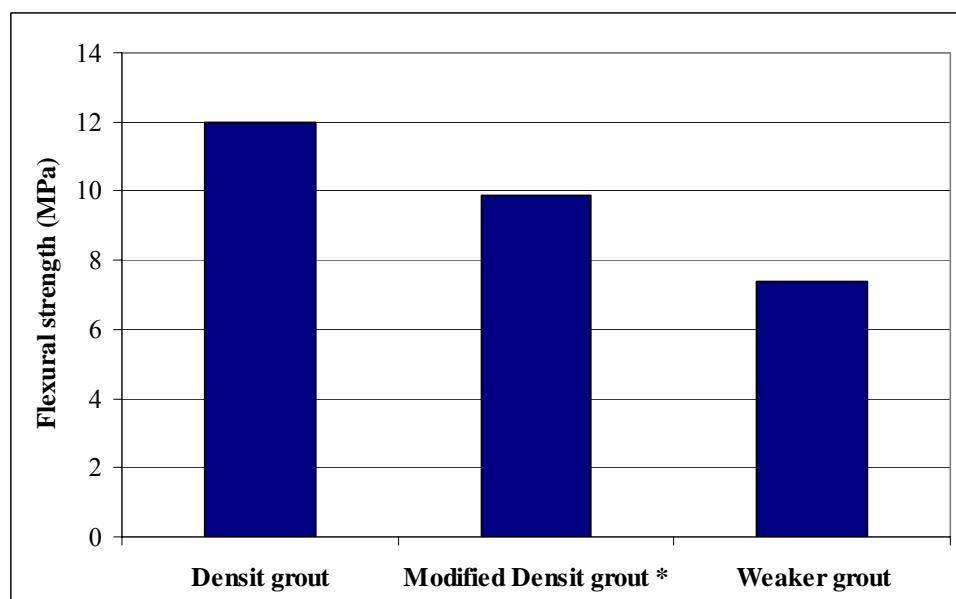
* result obtained at 41 days curing time

Figure 5.5 – Flexural strength of the grouts used at 28 days

Autogenous (drying) grout shrinkage is a property that may reduce the performance of grouted macadams, when occurring to a significant extent. It may lead to the appearance of micro-cracks within the material that, in specific circumstances, may result in the formation of macro-cracks and consequent failure of the material under traffic loading. It may also allow the ingress of water into the matrix of the asphalt and grout particles, reducing its internal stability, which may result in early failure of the material. In order to quantify the amount of shrinkage of the grouts used in the present project, extra beams (similar to the ones used for flexural strength determination) were cast and their length was monitored during the curing process. The results obtained are presented in Table 5.6 and Figure 5.6, representing the average values obtained for 3 beams cast from each grout type, except in the case of the weaker grout where, due to the limited amount of powder supplied by the project sponsors, only one beam was cast. During the curing process, the beams were stored in an unsealed condition (exposed to air) at room temperature (approx. 20 °C).

Table 5.6 – Drying shrinkage of the grouts investigated

Age (days)	Drying shrinkage (microstrain)		
	Densit$^®$ grout	Weaker grout	Densit$^®$ modified grout
1	2951	3878	3338
4	--	4534	4271
7	3141	4847	4775
28	3341	6045	5431
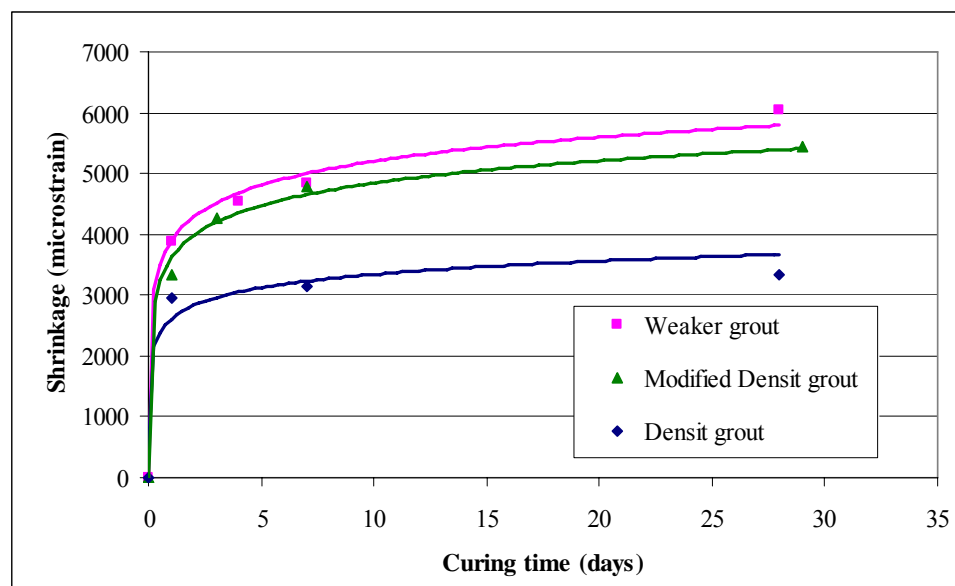
Figure 5.6 – Drying shrinkage of studied grouts

A series of four-point bending stiffness tests was also carried out on the Densit®
grout beams. The average values obtained are presented in Table 5.7 and in all cases
correspond to curing times longer than 28 days. The results obtained show the
independence of stiffness modulus from test frequency, which is a characteristic
property of elastic materials.

Table 5.7 – Stiffness modulus of the standard grout

Frequency (Hz)	Average Stiffness (MPa)
1	18872
2	18632
5	19123
10	19075
Average	18925

5.6 Grouted Macadam

As previously mentioned, a description of the main properties of the standard
mixture used in the current project is presented in this section. The results obtained
from tests carried out using different mixtures are presented in Chapter 6.

5.6.1 Coefficient of Thermal Expansion

Thermal properties of pavement materials are important in situations where they are
used in outdoor applications, being subjected to significant thermal cycles. A
decrease in the air temperature may induce internal stresses in the pavement layers
that may result in the appearance of thermal cracking. In order to better understand
how the studied grouted macadams perform under temperature variations, a series of
tests was carried out using both grout and grouted macadam specimens
(beams - 300 mm long) to determine their coefficient of thermal expansion. The
beams were subjected to a temperature cycle with an amplitude of approximately
44 °C (from -3 up to 40 and down to -4 °C). The extension of each beam was
measured using a 200 mm long dial gauge between 2 "demec" pips glued at the
surface of the beams. The results of these tests are presented in Table 5.8.

Table 5.8 – Coefficient of thermal expansion (α) obtained for the standard grouted macadam mixture and for the grout used

Temperature amplitude (°C)	Coefficient of thermal expansion, α (10^{-5}/°C)					
	Standard grouted macadam			Grout		
	Beam 1	Beam 2	Avg.	Beam 3	Beam 4	Avg.
-3 to 40	0.875	0.825	0.85	1.55	1.66	1.60
40 to -4	1.045	1.190	1.12	1.45	1.66	1.55
Average	0.96	1.01	0.98	1.50	1.66	1.58

The results obtained for the standard grouted macadam are in line with the results shown by Anderton (2000), being slightly lower than the 1.09 or 1.2×10^{-5}/°C presented for RMP, produced respectively with limestone and gravel aggregates. The higher values obtained for the grout beams highlight the importance of the bitumen in grouted macadams, reducing the expansion of the material as a whole, while each portion of grout expands at a higher rate, with an increase in the temperature. The existence of a small amount of voids, within the final structure of the grouted macadam mixture, may explain the difference on the values of the coefficient of thermal expansion obtained between the temperature increasing and decreasing stages. Since the bitumen penetration grade is very high, it becomes more fluid at temperatures in the region of those used during the test, which may have induced the bitumen to move and fill part of the small void in the mixture. This would have slowed the expansion of the whole mixture, resulting in a coefficient of thermal expansion lower than that obtained for contraction.

5.6.2 Early-age mechanical properties

One of the most important properties of grouted macadams, when compared with concrete, is the early gain in strength and the reduced time to achieve the final properties of the finished layer. It is well accepted that pavements comprising grouted macadams can be opened to traffic generally after 24 to 48 hours, while cementitious concrete pavements usually need 21 to 28 days.

In order to assess the properties of grouted macadams in the early stages of curing, a series of tests was carried out using cylindrical specimens made with the standard grouted macadam. The specimens were obtained by individually grouting each porous asphalt specimen that had previously been produced using a gyratory

compactor. Each specimen was sealed at the underside, with a plastic disc, and laterally, with a rubber membrane, to keep the grout inside the voids of the porous asphalt skeleton, while the grout cures. In order to simulate the damage imposed by traffic loads at early life, each specimen was loaded with a specific load using a Nottingham Asphalt Tester machine, in the Vacuum Repeated Load Axial Test (VRLAT). In this "damaging" test, a 50 kPa vacuum pressure was used to simulate the lateral confinement of the material in the field. Each specimen was loaded with 300 pulses at an axial stress of 400 kPa, after which it was left to rest for the remainder of the 7-day curing period. Each specimen was loaded at a different stage of curing, in order to study the effect of curing time on mechanical response prior to opening to traffic. Table 5.9 presents the curing times at which the specimens were loaded. After production, all the specimens were stored in a temperature-controlled cabinet at 20 ºC until the final test was performed, in an attempt to reduce the variability among the results.

Table 5.9 – Time elapsed before loading and corresponding vertical strain

Specimen	Time before loading (hours)	Vertical creep strain during loading (%)
1	6	2.2
2	7	2.8
3	8	3.4
4	9	1.3
5	10	2.0
6	12	1.5
7	15	1.0
8	18	0.8
9	21	0.8
10	24	0.7
11	38	0.7
12	48	0.9
13	86	0.8
14	120	0.7
15	168	0.5
16	*	--
17	*	--

* Undamaged specimens

From the above table it is possible to define the minimum curing time, before which a small number of heavy loads applied by the traffic definitely imposes some damage in the material, by means of permanent deformation. Despite some scatter, due to

material variability, the minimum time determined was of approximately 18 hours. After this time, a stabilisation can be observed in the level of permanent strain that resulted from the "damaging" test, which is graphically presented in Figure 5.7. The last two specimens presented in the table were not subjected to any damaging loads, in order to compare their properties with the properties of the damaged specimens after the 7-day curing period.
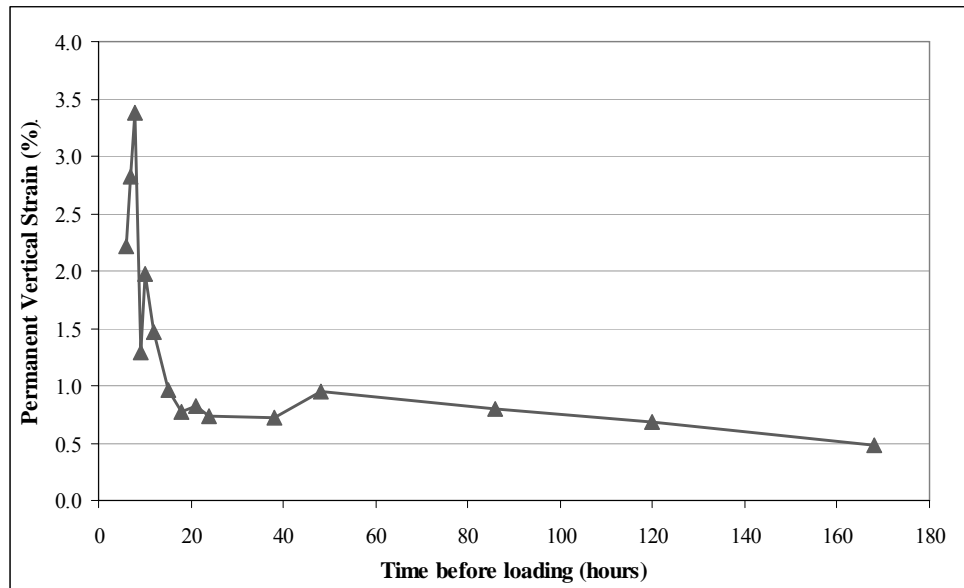
Figure 5.7 – Permanent vertical strain after loading at a range of curing times

An assessment of the damage sustained by the specimens that had undergone creep testing at early curing stages was completed by performing stiffness (ITSM) and fatigue (ITFT) tests on the specimens, after 7 days of curing and at 20 ºC. The results are shown in Table 5.10 and Figure 5.8. Only one stress level was used in the fatigue tests, since the objective was to evaluate the relative effect of curing time on the fatigue resistance of grouted macadams rather than to characterise the material fatigue life in detail. A stress level of 600 kPa was chosen in order to obtain a reasonable number of cycles to failure within a reasonable testing time, since the first ten specimens were produced within 24 hours and needed, therefore, to be tested with the minimum time interval possible between each.

The results obtained show that the first 24 hours of curing had an important role in the final properties of the grouted macadam, as these generally improve within this period of time. Therefore, it is reasonable to say that, as a safety measure, pavements

containing grouted macadams should not be opened to heavy traffic within 24 hours of grouting. The results obtained after that period must be interpreted carefully, since they were obtained based on individual specimens (produced individually) and present a high level of scatter, particularly in the fatigue tests, where a higher degree of scatter is normally expected.

Table 5.10 – Material properties obtained in the Early-life Tests at 20 ºC

Specimen	Time before creep loading (hours) (see table 5.9)	Stiffness at 7 days curing (MPa)	Fatigue life at 600 kPa (no. pulses)
1	6	6052	1150
2	7	7129	2325
3	8	6161	1813
4	9	6262	1145
5	10	5376	913
6	12	4762	2449
7	15	6203	4308
8	18	6807	3088
9	21	8691	6573
10	24	8186	5372
11	38	8045	5748
12	48	8306	824
13	86	6649	5835
14	120	7007	2319
15	168	6276	1414
16	*	8889	12640
17	*	8756	10853

* Undamaged specimens

The stiffness results obtained for the undamaged specimens were slightly higher than expected at 20 ºC (when compared with those presented in Table 5.11). This can be explained by the amount of extra grout in the specimens, as a result of an actual void content higher than designed, which was a consequence of the compaction method used. A gyratory compactor was used to compact each specimen individually, in order to obtain cylindrical specimens ready to grout and test using the Vacuum Repetitive Load Axial Test (VRLAT) protocol. However, it was observed that a mixture comprising such a single-sized aggregate gradation becomes harder to compact and all the specimens ended up with approximately 4% more voids than the design value (28%).

Fatigue results obtained with these tests may not have a very realistic meaning, especially the ones obtained after 24 hours curing. A possible explanation can be the high severity of the "damaging" load applied by the VRLAT tests, either by the stress value or by the number of load repetitions.
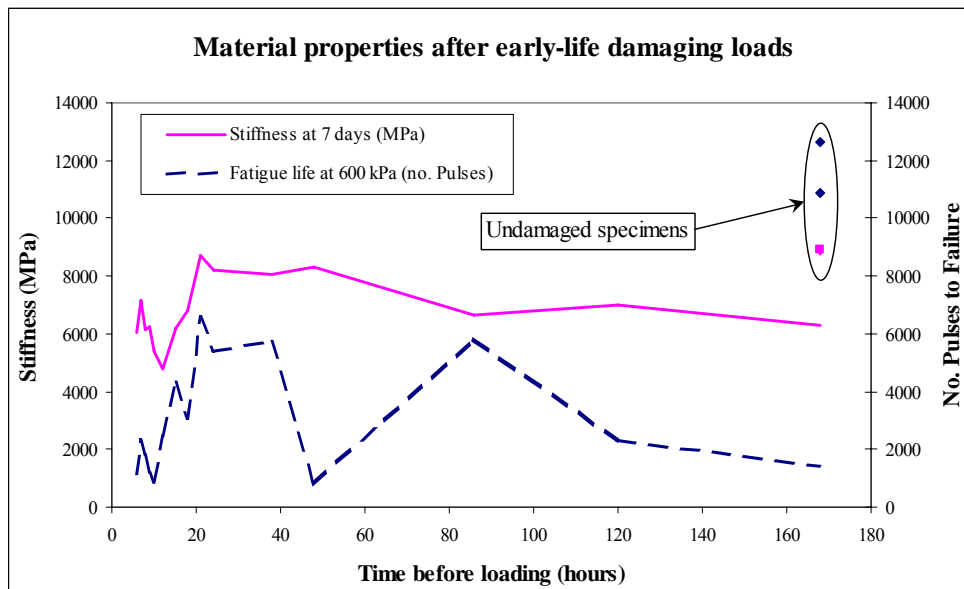
Figure 5.8 – Results obtained in the ITSM and ITFT tests at 7 days curing time following early-life damaging loads

A more comprehensive testing programme should be carried out if a very accurate determination of the effect of curing time in the final properties of grouted macadams is intended. However, this investigation has allowed the guidelines proposed by the grout suppliers, regarding the necessary curing time (24 h) before opening to traffic, to be confirmed.

5.6.3 Resistance to permanent deformation

As previously mentioned in Chapter 3, a series of Repeated Load Axial Tests (RLAT) was carried out by Collop and Elliott (1999), on a certain number of specimens, to determine the permanent deformation resistance of a grouted macadam similar to the standard mixture used in this investigation. According to the authors, the material displays very good permanent deformation resistance. The results shown in Figure 5.7, although having been obtained under more severe loading conditions,

confirm the tendency of the material to show minimal permanent deformation, as curing time increases. Therefore, it was decided not to perform any further tests on the studied mixtures, regarding resistance to permanent deformation, but to concentrate on the determination of the other fundamental properties of grouted macadams for the remainder of this investigation.

As part of the grouted macadam standard mix design characterisation, stiffness and fatigue tests were carried out using two types of tests: the indirect tension test (ITSM/ITFT) and the four-point bending test.

5.6.4 Indirect Tensile Stiffness Modulus (ITSM)

5.6.4.1 Effect of temperature

Regarding the stiffness modulus of the standard grouted macadam, a series of ITSM tests were carried out early in the present research project, not only to compare the results with the ones obtained from literature but also to complete the information about the material properties at different temperatures. The results are presented in Table 5.11 and Figure 5.9, which represent, for the present project, the average values obtained for 8, 10 and 7 tested specimens, respectively for the temperatures of 10, 20 and 40 °C.

Table 5.11 – Stiffness modulus of standard grouted macadam, from ITSM tests (124 ms rise time)

Temperature (ºC)	Stiffness modulus at 28 days (MPa)	
	Present project	Collop and Elliott (1999)
10	8506	12570
20	6699	7110
40	2288	2600

The difference between the results presented in Figure 5.9, especially for the temperature of 10 °C, can perhaps be explained by the different types of aggregate used in each investigation. However, a further reason could be suggested, namely the ageing of the binder throughout the testing programme. In their investigation, Collop and Elliott (1999) used the same 10 specimens to determine the stiffness modulus at

3 different ages and 5 different temperatures (0, 10, 20, 30 and 40 ºC). Therefore, the temperature cycles to which the specimens were subjected may have influenced the final properties of the binder used in the material (measured after 28 days), resulting in a higher stiffness modulus. In the present study, the specimens were tested only once, at 28 days and at the desired temperature. After the stiffness modulus determination, the specimens were used to determine the fatigue life at 10 and 20 ºC (described later in this section). It was decided not to carry out ITFT tests at 40 ºC, since at that temperature, the specimens would be more susceptible to deformation under repetitive load applications, which could invalidate the results in terms of fatigue performance.
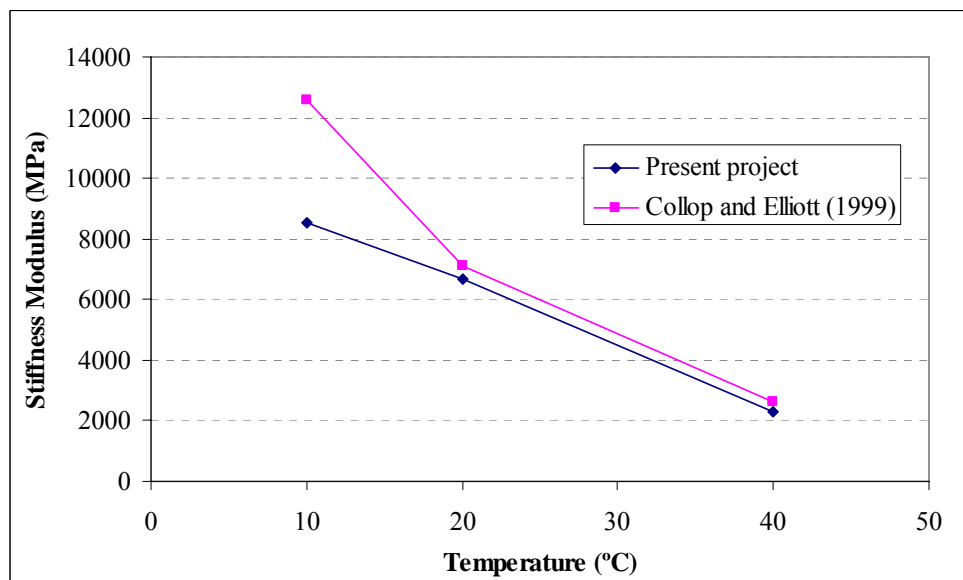
Figure 5.9 – Comparison of ITSM results between previous and present projects

The specimens left from the stiffness modulus determination (at 40 ºC) were used, 3 months later, to determine the stiffness modulus at 10 ºC, in order to verify the hypothesis previously mentioned. Hence, it was found that the specimens' stiffness modulus had increased when compared with the results obtained previously, for the same temperature. The average value obtained was 11545 MPa, which is significantly higher than the 8506 MPa previously obtained. The later results are much closer to the values presented by Collop and Elliott (1999), confirming the hypothesis suggested; even though the specimens were not subjected to the same conditions during the testing programme, some ageing/hardening of the binder occurred in both cases.

5.6.4.2 Effect of binder ageing

In order to assess the effect of binder ageing, four grouted macadam specimens (100 mm cores taken from a 2-year old slab) were then subjected to a "long term ageing" test protocol. After measuring the dimensions of the specimens, ITSM tests were carried out, at 20 ºC, to determine their stiffness modulus, before placing them in an oven, at 85 ºC, for 120 hours. According to Scholz (1995) this test simulates the ageing of the bitumen present in a dense-graded bituminous mixture, in service for 15 years or more. Therefore, the final properties (stiffness modulus) determined would correspond to the material characteristics at least 17 years after being constructed. 24 hours after taking the specimens from the oven, ITSM tests were carried out again, to assess the additional amount of ageing induced in the specimens, represented by the increase in the stiffness modulus of the specimens. The results are presented in Table 5.12 and plotted in Figure 5.10, where a comparison is also made with the values presented in Table 5.11 for results obtained in the present project at 20 ºC.

Table 5.12 – Effect of ageing on the stiffness modulus of grouted macadam

Specimen	Stiffness modulus (ITSM) at 20 ºC (MPa)	
	Before ageing	After ageing
1	8576	12466
2	7829	11882
3	9677	14366
4	10069	14343
Average	9038	13264
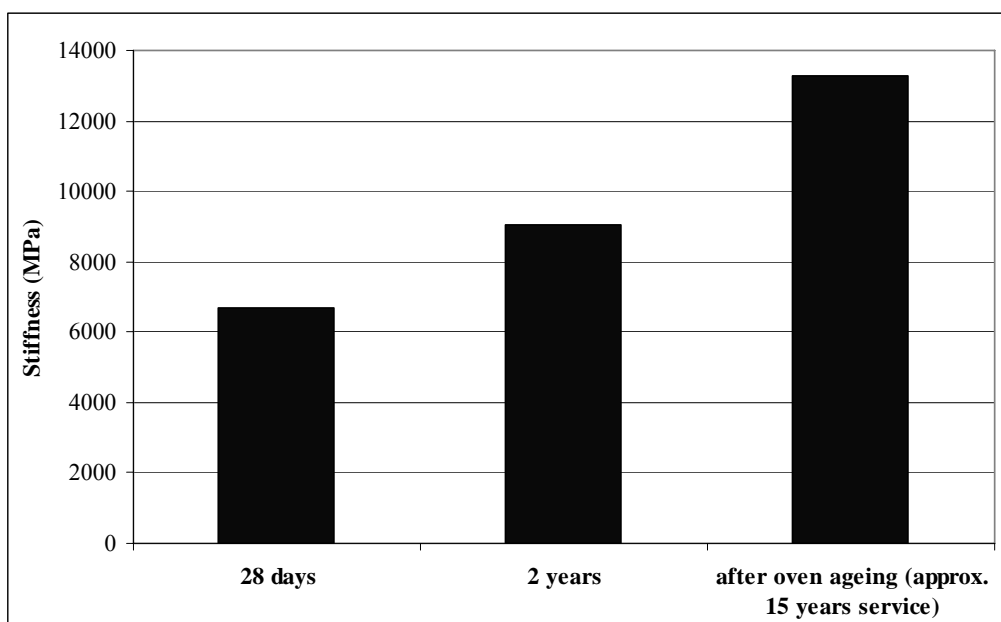
Figure 5.10 – Stiffness modulus of grouted macadam before and after ageing

5.6.4.3   Effect of testing strain level

Experience gathered during the present project also showed that if the strain level used in the ITSM tests is too high, some damage occurs in the specimen during each loading pulse, reducing the stiffness modulus value (which is calculated as the average of the values obtained from 5 consecutive pulses). Figure 5.11 represents a typical response of the studied grouted macadam, in a series of tests carried out to assess the influence of the horizontal strain level, used in the ITSM tests, on the results obtained. Four horizontal deformation levels were used in the ITSM tests for each specimen.

Starting from the standard 5 μm, the deformation was increased to 9 and 13 μm, finishing with a deformation of 3 μm. If no damage occurred during the test, the final result should be higher than the first, according to the material's tendency to increase in stiffness value with a decrease in the deformation (strain) level, due to its viscoelastic nature. However, as can be observed in Figure 5.11, the stiffness value obtained in the last test was lower than that obtained in the first. It is clear that some damage had been induced in the specimen even though only a few pulses of higher load/deformation were used during the test. The strain level plotted (obtained for each deformation level) was calculated based on the relationships specified in DD213 (BSI, 1993).
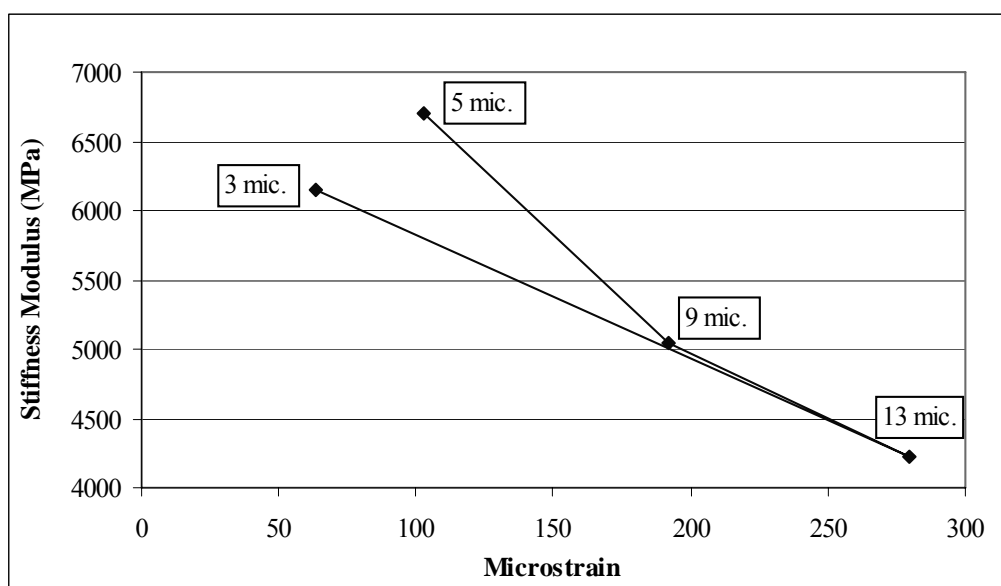
Figure 5.11 – Typical result obtained from ITSM tests for different strain levels

5.6.5 Four-point bending stiffness tests

Further tests were carried out using the four-point bending equipment described in Chapter 4, from which the stiffness modulus of the standard grouted macadam at 20 ºC was also determined. With this testing equipment, it was possible to calculate the stiffness modulus at different frequencies, as well as the corresponding phase angle, which improves the characterisation of viscoelastic materials. Table 5.13 summarises the average values obtained for the standard grouted macadam in this type of test.

Table 5.13 – Stiffness modulus and phase angle of standard grouted macadam at 0 and 20 ºC

Temperature (ºC)	Age (days)	Stiffness Modulus (MPa)		Phase Angle (deg)	
		5 Hz	10 Hz	5 Hz	10 Hz
0	28	17054	18077	5.3	4.3
20	7	6992	8074	16.2	13.3
	28	7416	8412	15.5	13.1

Although derived from a different test, the results shown are close to those obtained in the ITSM, especially those determined at a frequency of 5 Hz, which has a peak to peak load cycle time of (100 ms) that is closer to the rise time used in the ITSM (124 ms), when compared with the peak to peak time of the test carried out at 10 Hz (50 ms).

5.6.6 Indirect Tensile Fatigue Tests (ITFT)

Regarding the fatigue behaviour of the standard grouted macadam, ITFT and four-point bending tests were also carried out. The first type of test was carried out using the specimens previously tested for stiffness at 10 and 20 ºC, varying the stress level of the test for each specimen, in order to obtain the fatigue behaviour of the mixture over a wide region of stress/strain. The results are plotted together in Figure 5.12, for a better comparison, plotting the logarithm of initial strain against the logarithm of number of cycles to obtain a linear relationship between the variables.
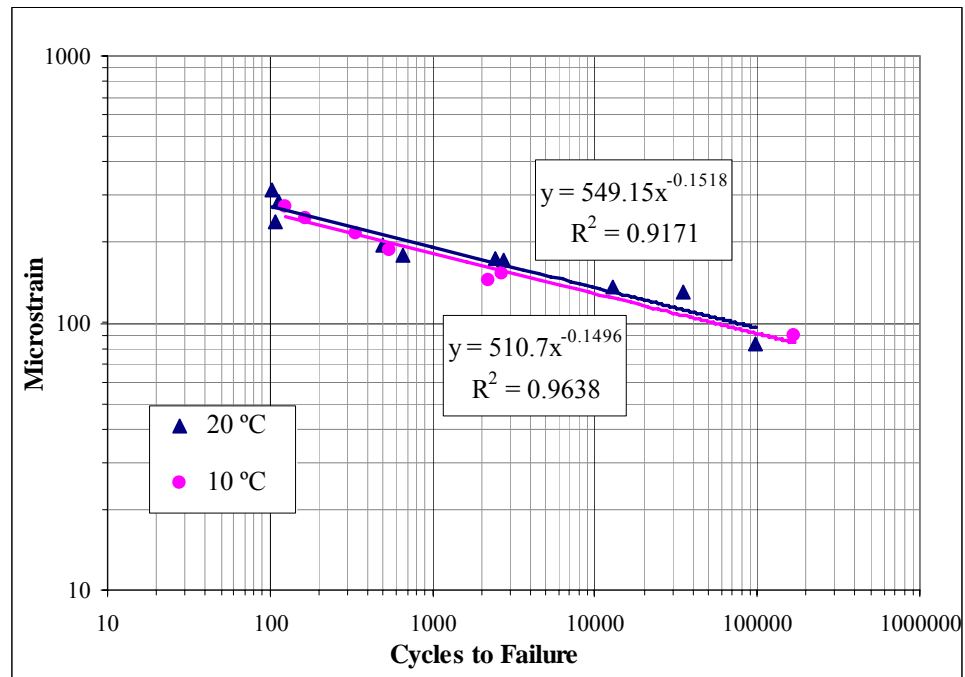
Figure 5.12 – Fatigue results obtained from ITFT tests at 10 and 20 ºC

As can be seen in this figure, the temperature variation seems to have little effect upon the fatigue life of grouted macadam using the indirect tension test, at least for a moderate temperature and within a limited range. The fatigue lines obtained for the two temperatures are very close to each other and could be plotted as one single line without significantly increasing the scatter among the results. According to Pell and Taylor (1969), the fatigue life of BS 594 (HRA) base course type mixes was primarily controlled by the magnitude of the tensile strain, the effects of temperature and speed of loading being accounted for by their effect on the stiffness of the mixture (i.e. moving up and down the same fatigue line).

Fatigue tests carried out on basic crushed rock base course mixes by Pell and Taylor (1969) showed that over the stress levels used, some non-linear behaviour was in evidence for the specimens tested at 0 and 10 °C, but for those tested at 20 and 30 °C, non linear behaviour was displayed over the whole range. This indicates that the slopes of the strain-life lines are dependent upon the amounts of non-linear behaviour displayed by the mix over the range of stress levels used. Based on the trends obtained (Pell and Taylor, 1969), it was suggested that the fatigue results should be considered in two parts, one in which linear behaviour holds over the range of stress levels used and the other where non-linear behaviour is displayed. For both cases the results were expressed in the form of $N = K(1/\varepsilon)^n$, where N represents the

number of load applications; K and n are coefficients determined experimentally and; ε is the amplitude of the applied tensile strain in the mix.

ITFT results obtained by Collop and Elliott (1999) at 40 ºC, presented in Chapter 3, are significantly different from those presented above (at 10 and 20 ºC). This is due to the type of bitumen used in the mixture (200 pen grade), which becomes very soft at temperatures above 30 ºC (non-linearity). Therefore, at 40 ºC (above the softening point) the bitumen is already in a fluid state and the results obtained in the ITFT tests may be strongly influenced by permanent deformation of the specimens under load repetitions. Naturally, in such state, the bitumen is more likely to flow than to crack due to its low viscosity, which can originate higher fatigue lives.

5.6.7 Four-point Bending Fatigue Tests

As previously mentioned, a series of four-point bending fatigue tests was also carried out to analyse the fatigue behaviour of the standard grouted macadam. This test represents more realistically the bending of a pavement layer under the application of traffic loads. Furthermore, it also prevents the accumulation of permanent deformation in the specimen during the test, when carried out in controlled-displacement (strain) mode of loading. Thus, 20 specimens of the standard grouted macadam were tested using this test method, at 2 different temperatures and 2 curing ages (10 specimens at 20 ºC and 7 days curing time; 5 specimens at 20 ºC and 28 days; and 5 specimens at 0 ºC and 28 days), after being tested for stiffness and phase angle. The fatigue tests were carried out at 10 Hz and the results are plotted in Figures 5.13 and 5.14, where the effects of temperature and curing time can be observed.

As in the case of ITFT tests, the influence of temperature on the fatigue properties of grouted macadams is minimal and could perhaps be neglected, since the lines obtained for 0 and 20 ºC are very close to each other (see Figure 5.13). However, it is also important to consider the limited range of temperatures involved in the tests, and that a bigger error in the fatigue life estimation is possible if the results are extrapolated to temperatures far from the ones investigated. The results obtained from the fatigue tests also highlight the similarity between the fatigue behaviour of

the standard grouted macadam at 7 and 28 days. As can be observed in Figure 5.14, the fatigue lines are practically coincident, which is due to the quick curing time of the grout used. Based on these results, it was decided to use 7 days curing time as the "standard" time for testing for the remainder of the present investigation.

4 PB fatigue results - effect of temperature

$y = 2508.9x^{-0.2478}$
$R^2 = 0.9942$

$y = 2574.9x^{-0.2382}$
$R^2 = 0.9936$

▲ 28 days, 20 ºC

◆ 28 days, 0 ºC
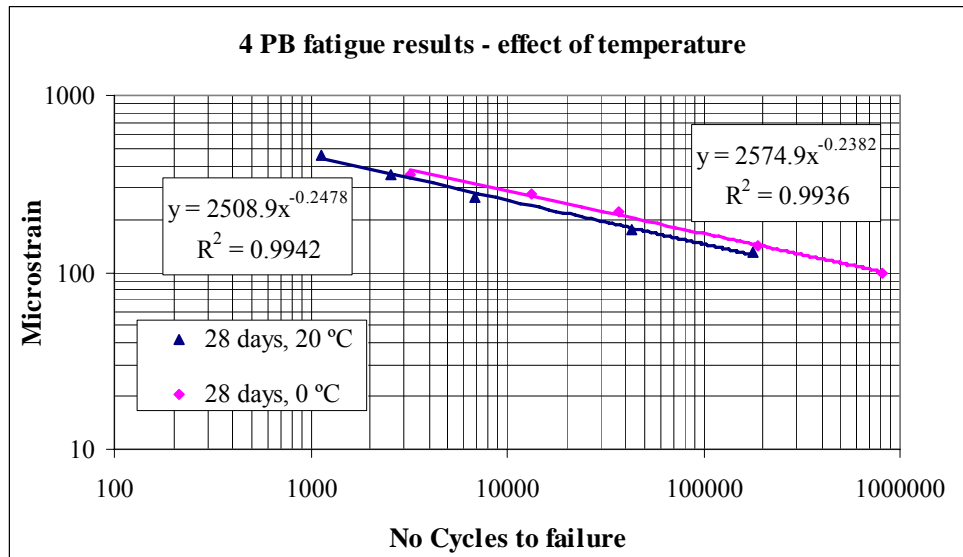
Figure 5.13 – Effect of temperature in the four-point bending fatigue life of the standard grouted macadam

4 PB fatigue results - effect of curing time

$y = 2452x^{-0.2426}$
$R^2 = 0.9673$

$y = 2508.9x^{-0.2478}$
$R^2 = 0.9942$

▲ 28 days, 20 ºC

■ 7 days, 20ºC
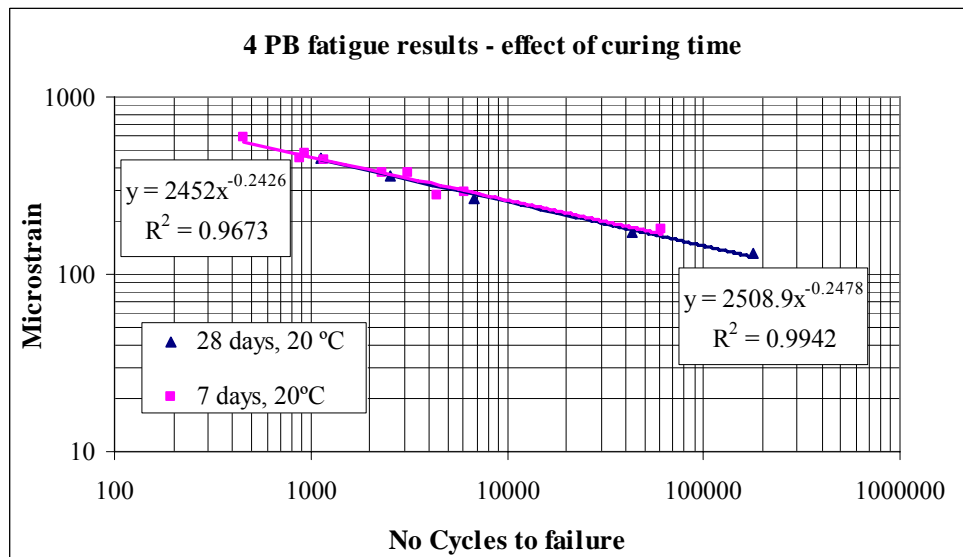
Figure 5.14 – Effect of grout curing time in the four-point bending fatigue life of the standard grouted macadam

Similar results, regarding the influence of temperature on the fatigue life of grouted macadams, were also presented by Pelgröm (2000), as mentioned in Chapter 3, reinforcing the idea that grouted macadams are less temperature susceptible than other bituminous mixtures in terms of fatigue.

5.7 Summary and Conclusions

In the present research project on grouted macadams, the main component of the asphalt skeleton was the granite aggregates, mostly single-sized and with the nominal size of 10 mm. The other asphalt mix component, i.e. bitumen, was chosen in most cases to be a 200 pen grade, as part of the standard mix design. Its basic properties, together with those of the other bitumen types used during this investigation (50 pen and PMB) were also presented in this chapter. With respect to the grouted macadams, the third and last component, i.e. the grout, was also discussed in the present chapter, where the three different grout types used in this project were described. However, only the standard grouted macadam mixture was characterised in this chapter. Different mix designs and variations from the standard are discussed in the following chapter.

The main properties of the standard mixture are therefore summarised in this section, together with the main conclusions, as follows:

- The coefficient of thermal expansion of the standard mixture was determined and the value obtained was on average $0.98 \times 10^{-5}/°C$, while the values obtained for the grout alone were on average $1.58 \times 10^{-5}/°C$.

- A study was carried out to determine the influence of traffic loading during the early stages of curing on the final properties of the standard mixture. It allowed the guidelines given by the grout suppliers, regarding the necessary curing time before opening to traffic (24 h), to be confirmed. It also highlighted that pavements with grouted macadam surface courses should never be opened to heavy traffic before 18 h of curing.

- The influence of temperature on the mechanical properties of grouted macadams is more significant in terms of stiffness modulus, where a decrease in temperature considerably increases the stiffness value. In terms of fatigue, little effect was observed on the behaviour of the mixture when the test temperature was kept below 20 °C. Only when temperature increases significantly (above the softening point of the bitumen) the fatigue line of the mixture is changed (increasing the fatigue life). This is due to the ability of the bitumen to withstand any induced damage, because of its fluid state.

- Ageing of bitumen seems to have a significant effect on the stiffness modulus of grouted macadams. In the tests carried out during the project, not only has long-term ageing shown an increase in stiffness of approx. 47%, but also a short/medium-term ageing (3 months, including temperature fluctuations have shown a 35% increase in the stiffness modulus in some grouted macadam specimens.

- The standard strain level used in the ITSM tests (corresponding to a horizontal deformation of 5μm under the load application) may induce some damage in the specimens, even though only a few pulses are applied.

- The four-point bending apparatus developed during this project allowed the calculation of the stiffness modulus and phase angle of the material at a range of frequencies, which was not possible with ITSM tests.

- The effect of curing time (medium/long-term) was also evaluated using 4-point bending tests, and it was determined that the mechanical properties of grouted macadams do not change significantly after 7 days of curing.

6 GROUTED MACADAMS MIX DESIGN STUDY

6.1 Introduction

Most of the work carried out in the past with grouted macadams in the UK has been made with a standard mix design, previously presented by Collop and Elliott (1999), which obtained mixed success. In order to better understand its behaviour and to be able to predict the life of pavements incorporating grouted macadams more accurately, a mix design study was carried out. This included the evaluation of the mechanical properties of several mixtures (including the standard mix design, as presented in the previous chapter), taking into consideration different variables and application fields. In this chapter, the results obtained for each mixture are presented and discussed, in respect of the effect that small changes in the components of grouted macadams may or may not have on the final properties of the mixture.

6.2 Variables considered in the study

Based on the standard mix design presented in Table 3.2, modifications were made to the proportions of the final asphalt mixture's components, and different grouts were also used to assess the effect of those variables.

The optimum binder content of the standard mixture was determined according to Equation 3.1. Taking the percentage of limestone filler into consideration, calculations were made and the result obtained was approx. 4.5%, which is not far from the value used in the standard mix design (4.1%). This amount of binder corresponds to a thick bitumen film around the aggregates. However, due to the type of binder used (very soft) and the open-graded aggregate structure, the binder is likely to drain. To prevent this binder drainage, cellulose fibres are used in the standard mixture, increasing the stability of the mixture during transportation and laying.

In order to assess the influence of slightly changing the binder content, simulating the variability on site, a grouted macadam mixture was produced in the laboratory with 3% binder (by mass of total asphalt mixture), maintaining the percentage of fibres. The effect of bitumen film thickness was also studied by producing a mixture with a low binder content (1.5% by mass of asphalt). In this case, fibres were not included, in order to improve the workability of the asphalt mixture, since the risk of binder drainage was negligible.

To investigate the influence of the type of binder used in grouted macadams, two mixtures were produced in the laboratory with, respectively, a 50 pen straight-run bitumen and a polymer modified bitumen (PMB) with the addition of Styrene-Butadiene-Styrene (SBS) thermoplastic elastomers, which were then tested using 4-point bending tests.

In applications where skid resistance is not an issue, the use of an aggregate type different from the one specified in the standard mix design of grouted macadams may not represent a handicap in terms of mixture performance. Hence, it may significantly reduce the cost of production, if a local aggregate can be chosen instead of a better quality aggregate that needs to be transported from a long distance to the working site. To assess the influence of the aggregate type in the mechanical properties of grouted macadams, a mixture with limestone was prepared, replacing the granite aggregate used in the standard mixture.

Regarding the aggregate size and grading, three alternatives to the standard mix design were studied: (i) a more continuous grading; (ii) a 14 mm single sized aggregate; (iii) a 20 mm single sized aggregate. In the first case, it was intended to verify if a more continuous aggregate grading (as presented by Anderton, 2000) would allow a full penetration of the voids by the grout and, in those circumstances, what its mechanical properties would be. Taking the voids structure into consideration, the aggregate grading was obtained by substituting 50% of the 10 mm single sized aggregate by 30% of 14 mm and 20% of 20 mm single sized aggregates. The option to add only bigger aggregate sizes was made in order to avoid blocking the connectivity between voids in the asphalt skeleton, which would compromise full penetration of the grout. The second alternative was used to assess the sensitivity of

grouted macadams to small changes in the voids structure/size. The last alternative was used to evaluate the possibility of using grouted macadams in pavement layers different from the surface course, and in greater thicknesses. This would be the case in a highway pavement rehabilitation, where a grouted macadam might be used as a base or binder course covered by a thin bituminous overlay, reducing the thickness of the existing pavement that would need to be replaced, due to the enhanced properties of grouted macadams. Gradations of each aggregate fraction used were presented in Table 5.2 and the alternatives analysed in this mix design study are presented in Figure 6.1. The grading specified by Anderton (2000) for RMP is also plotted in the same figure for comparison with the more continuous grading. Binder content of the mixtures with bigger aggregate sizes was adjusted to maintain the same binder film thickness as the standard mixture.
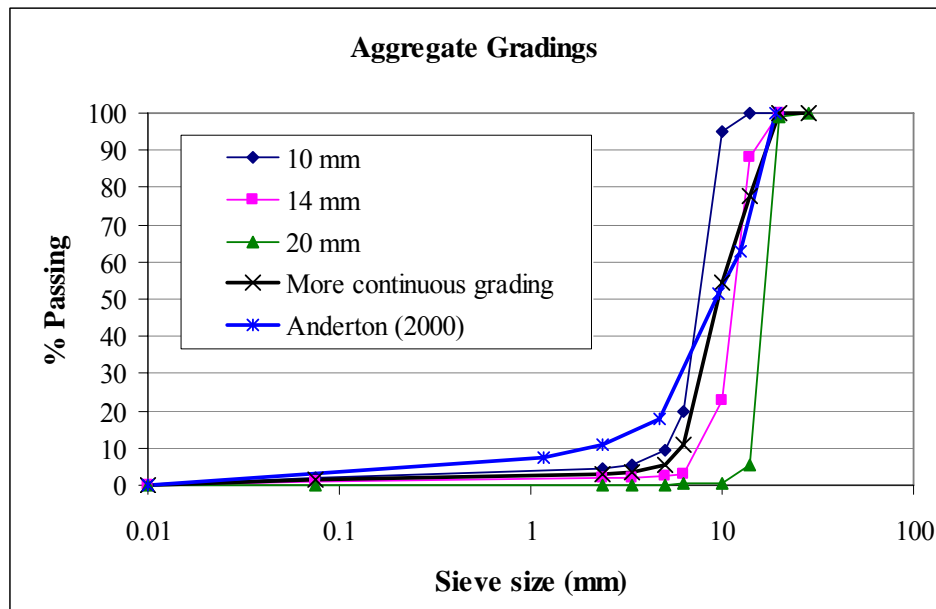
Figure 6.1 – Alternative aggregate gradings analysed in the mix design study

In order to complete the information regarding the influence of binder content and aggregate type/size on the properties of the final mixture, three more mixtures were prepared: (i) with 3% binder, using a 10 mm single sized limestone aggregate; (ii) with 4.1% binder, using a 14 mm single sized granite aggregate; (iii) with 4.1% binder, using a 20 mm single sized granite aggregate.

The influence of grout properties on the behaviour of grouted macadams was evaluated by the use of three different grouts, which were presented in Chapter 5: (i) the standard Densit$^{®}$ grout; (ii) a weak grout, supplied by the project sponsors;

(iii) a modified Densit® grout produced by adding 25% silt (by mass of total powder) to the standard grout.

6.3 Mechanical properties of studied grouted macadams

The laboratory programme established for this study includes stiffness and fatigue tests, carried out in the four-point bending testing apparatus, which comprise the main part of the mix design study. Thermal cracking tests were also performed for three grouted macadam mixtures (including the standard mixture, a mixture with 1.5% binder (by mass of asphalt) and also a mixture with a 50 pen binder). However, due to time limitations and difficult working conditions (tests carried out at -5 °C), the remaining variables were not considered. Results from all tests are presented in the next sub-sections (the detailed results for individual specimens are presented in the Appendices).

6.3.1 Stiffness modulus and phase angle

Following what was discussed in Chapter 5 for the standard mixture, stiffness modulus and phase angle of each studied mixture were determined at 5 and 10 Hz. The temperature chosen for this study was 20 °C, since the objective of this investigation was to establish a comparison between the mechanical properties of several mixtures. The comparison should therefore be made at a single temperature. The time at which tests were carried out was established to be 7 days after grouting, as explained in the previous chapter. Five specimens were used for the determination of the mechanical properties of the majority of mixtures studied, and the results presented in this section represent the average values obtained for those five specimens, unless otherwise specified.

6.3.1.1 Influence of binder content

Figures 6.2 and 6.3 represent the influence of binder content on the stiffness modulus and phase angle of grouted macadams. The results shown were obtained by changing

the binder content of the standard mix design (4.1% by mass of porous asphalt). In the case of 3% binder, the other components of the asphalt mixture were kept constant, simulating eventual on site variability of binder content in the mixture. On the other hand, the mixture with 1.5% binder was produced to assess the effect of significantly reducing the amount of bitumen used in the constitution of grouted macadams, which could represent cost savings.
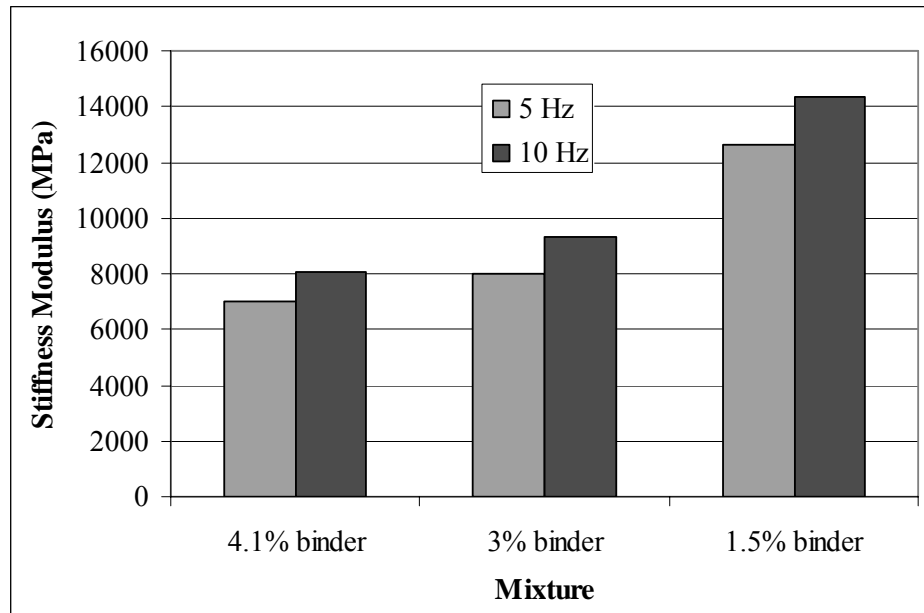
Figure 6.2 – Influence of binder content on the stiffness modulus of grouted macadams
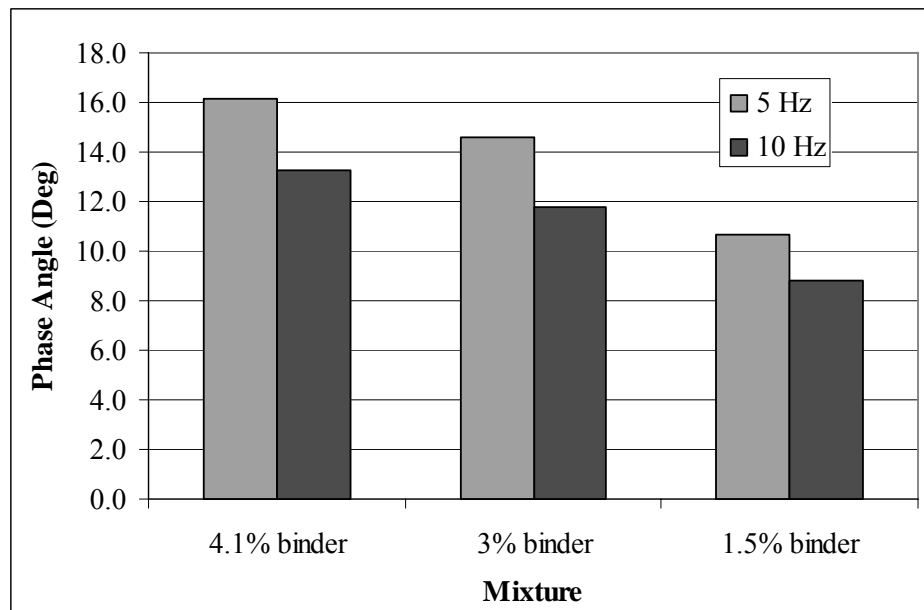
Figure 6.3 – Influence of binder content on the phase angle of grouted macadams

In terms of stiffness and phase angle, the reduction in binder content seems to improve the properties of the mixture, since the stiffness modulus increases and the phase angle decreases (the mixture becomes more elastic). However, these results cannot be analysed separately since, with the increase in stiffness, the mixture becomes more brittle, which may adversely affect other mechanical properties (fatigue and thermal cracking).

6.3.1.2   Influence of binder type

The use of a harder bitumen increases the stiffness modulus and reduces the phase angle of grouted macadams, in the same way as for traditional bituminous mixtures, as can be observed in Figures 6.4 and 6.5, where the standard mixture produced with 200 pen bitumen is compared with a mixture containing a 50 pen binder. On the other hand, the use of a polymer modified bitumen – PMB (SBS thermoplastic rubber) does not seem to have a significant effect on those properties. Its enhanced characteristics are more evident in the fatigue performance, which is discussed in the following section.

Figure 6.4 – Influence of binder type on the stiffness modulus of grouted macadams
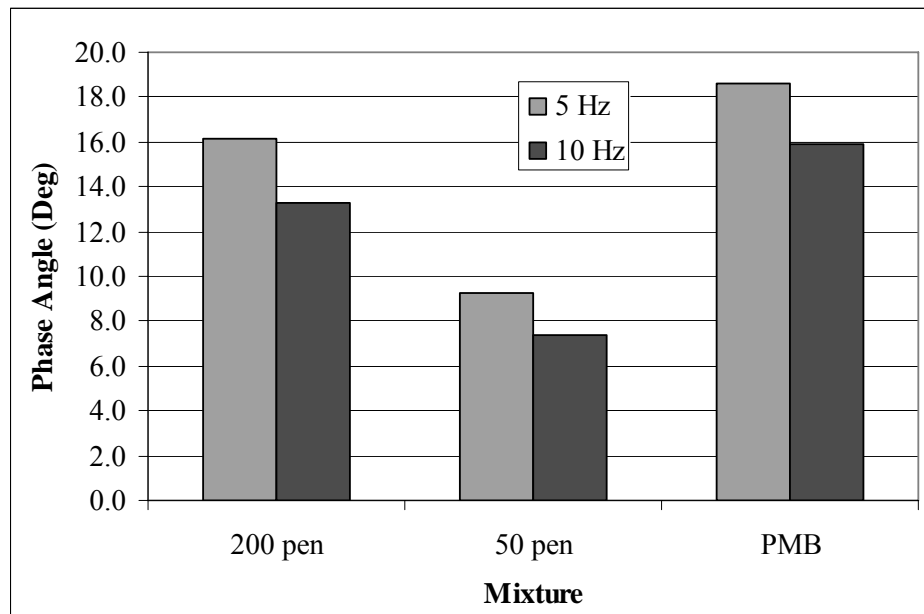
Figure 6.5 – Influence of binder type on the phase angle of grouted macadams

6.3.1.3   Influence of aggregate type

Although being a type of aggregate that is not usually used in surface course layers, due to its wearing characteristics, namely its low Polished Stone Value (PSV), limestone aggregate was investigated in this study. It could represent an alternative aggregate to other higher quality and more expensive aggregates, should grouted macadams be used in a different layer, e.g., a binder or base course, or in applications where skid resistance of the surface is not an issue. The results obtained for the standard mixture (produced with granite) and the alternative mixture are presented in Figures 6.6 and 6.7.

Purely with regard to the stiffness modulus, the studied grouted macadams incorporating limestone aggregate showed properties at least as good as the standard mixture (produced with granite). This could be used as valuable information in pavement design, resulting in reduced thickness for bound layers. However, only one source was used for each aggregate type and, therefore, it should not be generalised without further testing.

Figure 6.6 – Influence of aggregate type on the stiffness modulus of grouted macadams
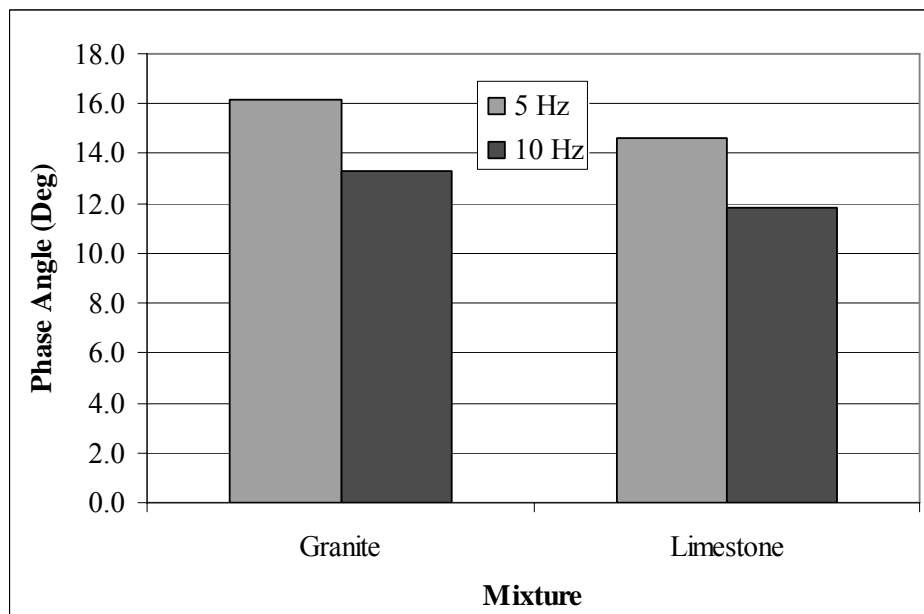
Figure 6.7 – Influence of aggregate type on the phase angle of grouted macadams

6.3.1.4   Influence of aggregate size/grading

Figures 6.8 and 6.9 represent the results obtained for three mixtures, alternatives to the standard mix design (with a 10 mm single sized aggregate). Therefore, two different aggregate sizes (14 mm and 20 mm) and a different aggregate grading (more continuous, comprising various aggregate sizes), from the same source as the

10 mm aggregate, were used to evaluate the effect of aggregate size/grading on the mechanical properties of grouted macadams.
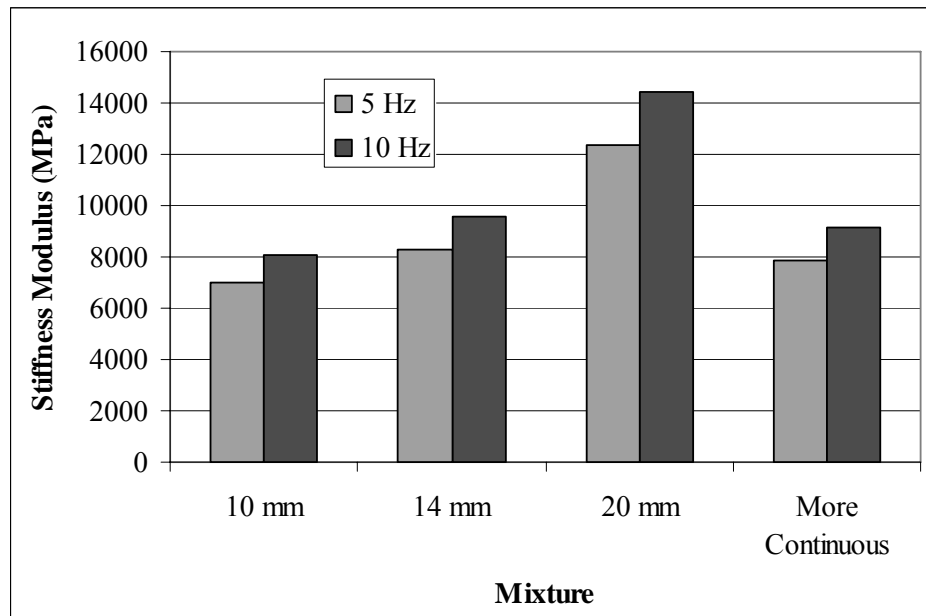
Figure 6.8 – Influence of aggregate size/grading on the stiffness modulus of grouted macadams
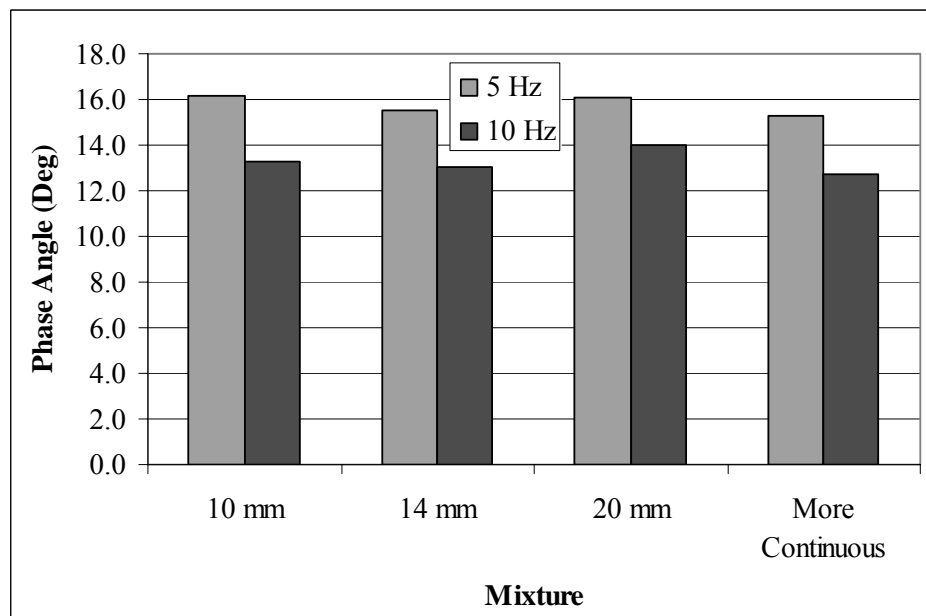
Figure 6.9 – Influence of aggregate size/grading on the phase angle of grouted macadams

The use of a bigger aggregate size implies a reduction in the binder content, in order to keep the bitumen film thickness constant, as a consequence of a reduced aggregate surface area. In this study, a binder content of 3% (by mass of total asphalt mixture)

was used for the 14 mm single sized aggregate while 2% binder was used in the case of the 20 mm aggregate. Thus, binder film thicknesses similar to that used in the standard mixture (with 4.1% binder) were obtained for the other mixtures. In the case of the more continuous aggregate grading, a binder content of 4% was used, since calculations according to Equation 3.1 gave a result equivalent to that obtained for the standard mixture, using the same equation.

The influence of bitumen film thickness can be identified by the phase angle of the mixtures, which is very similar for all mixtures presented in the figures above, confirming the binder film thickness calculations. On the other hand, stiffness moduli of the mixtures with bigger aggregate sizes are higher than that of the standard mixture, due to bigger voids created in the asphalt matrix, which were filled with grout, resulting in stiffer materials (approximately proportional to the aggregate size). The use of a more continuous grading did not result in a significant improvement in the stiffness modulus because the void sizes were not increased, due to a better aggregate packing (obtained by using different aggregate sizes).

6.3.1.5   Influence of grout properties

Figures 6.10 and 6.11 show the results obtained for mixtures produced with different grouts (corresponding to different grout properties, according to results presented in Chapter 5).

The type of grout used in the production of grouted macadams does not seem to significantly change the stiffness modulus and phase angle of the mixture, provided that full penetration of the mixture is achieved, as can be observed in Figures 6.10 and 6.11. Results obtained for the mixture with modified Densit$^{®}$ grout are slightly higher than the other mixtures. However, this can be explained by the different construction process used in the production of that mixture. The specimens were obtained from a slab, which was extracted from a half-scale pavement constructed in the laboratory. Binder ageing, before grouting and while waiting to be tested, may have increased the stiffness modulus of the mixture. The different compaction process (carried out manually with a small roller compactor) may also have led to a

slightly different void structure in the asphalt skeleton and a corresponding change in the final properties of the mixture.
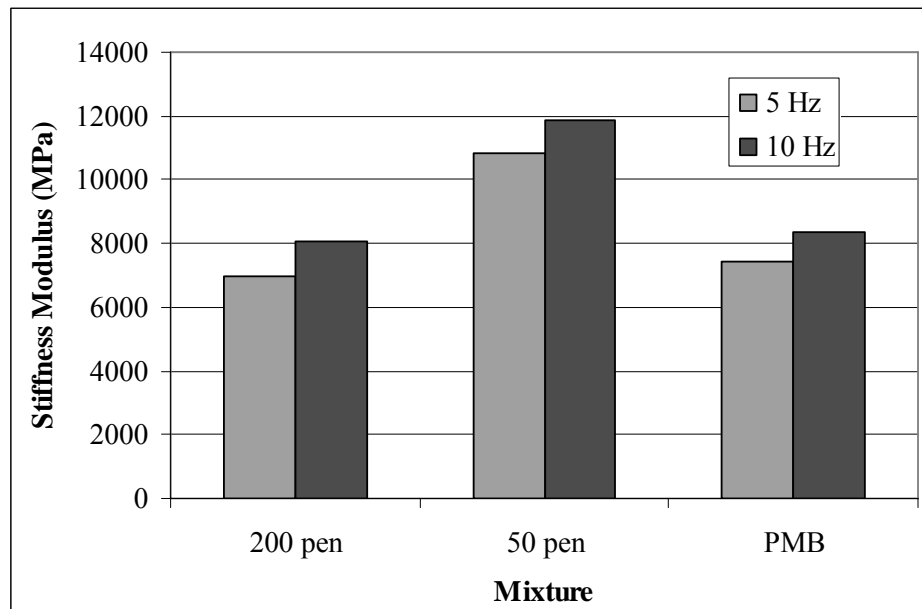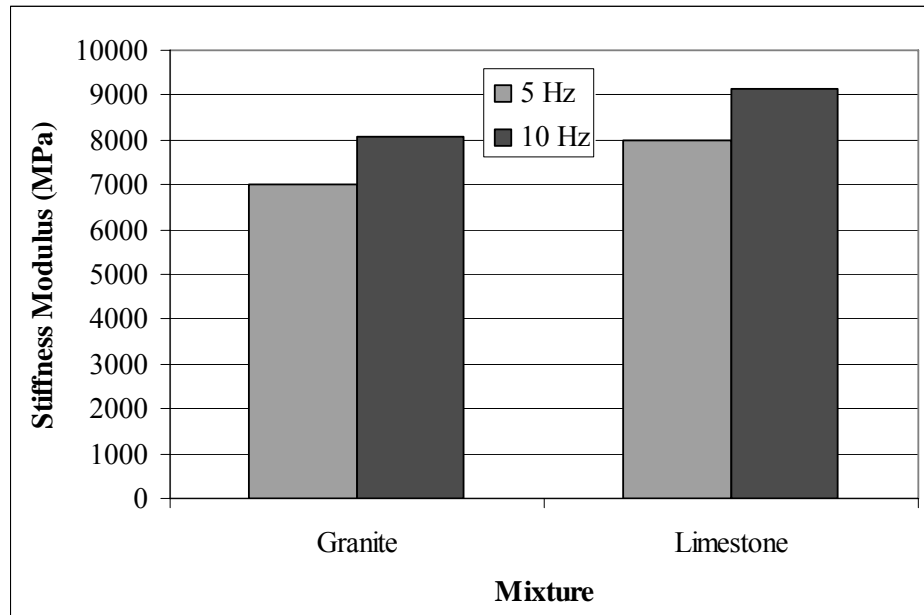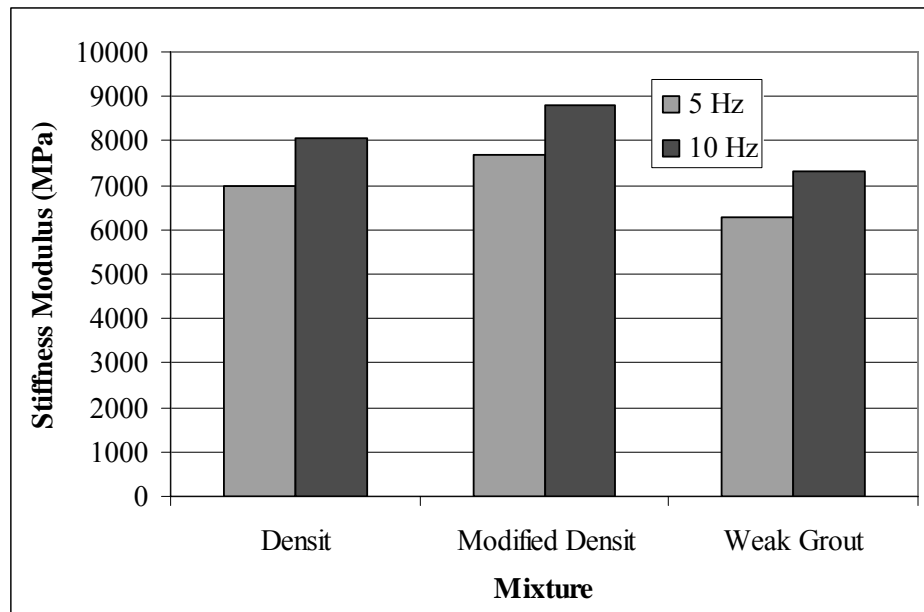

Figure 6.10 – Influence of grout type on the stiffness modulus of grouted macadams
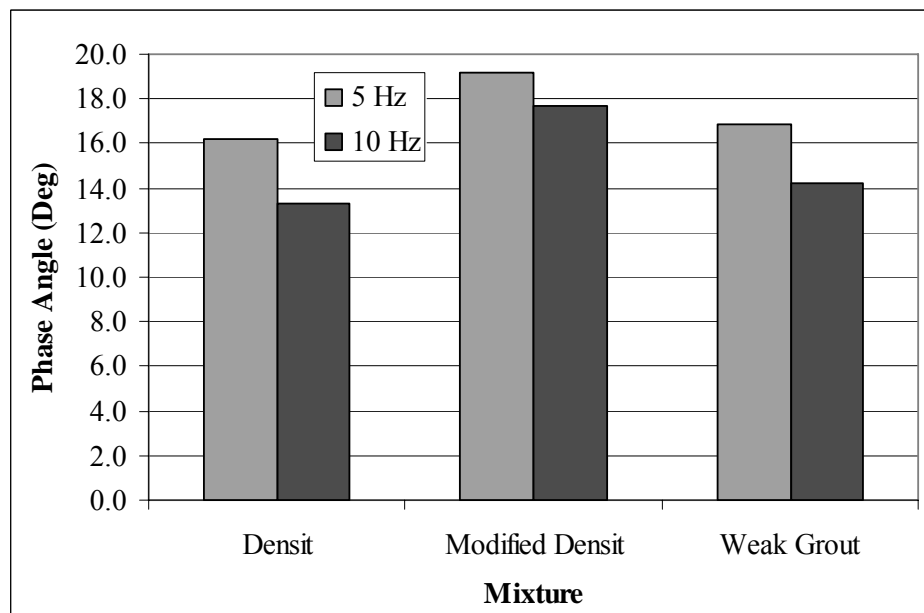
Figure 6.11 – Influence of grout type on the phase angle of grouted macadams

6.3.1.6 Influence of combined variables

As mentioned in the previous section, the mix design study was completed with the production of three extra mixtures, combining more than one variable (in comparison

to the standard mix design) in the same mixture. The results obtained for stiffness modulus and phase angle of those mixtures are presented in Figures 6.12 and 6.13.
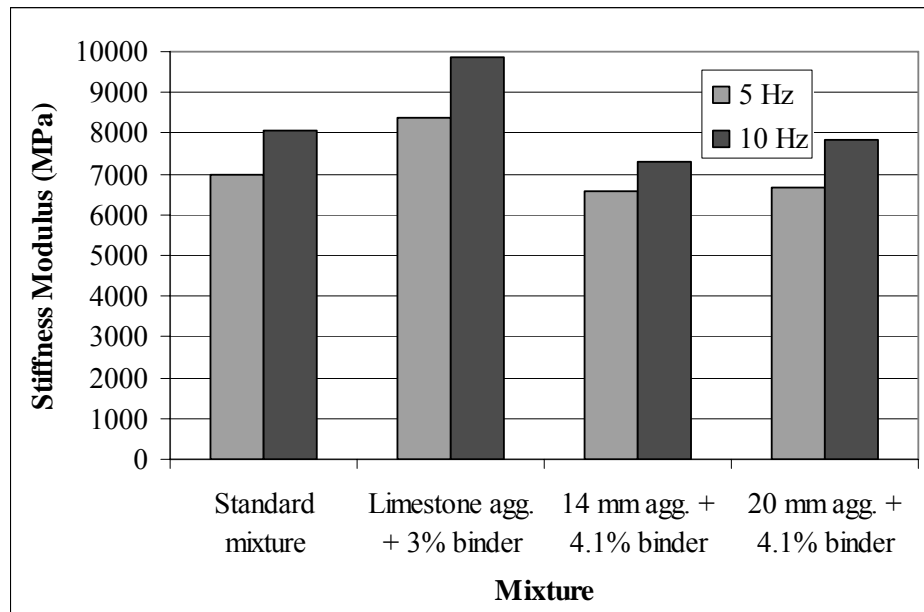
Figure 6.12 – Influence of combined variables on the stiffness modulus of grouted macadams
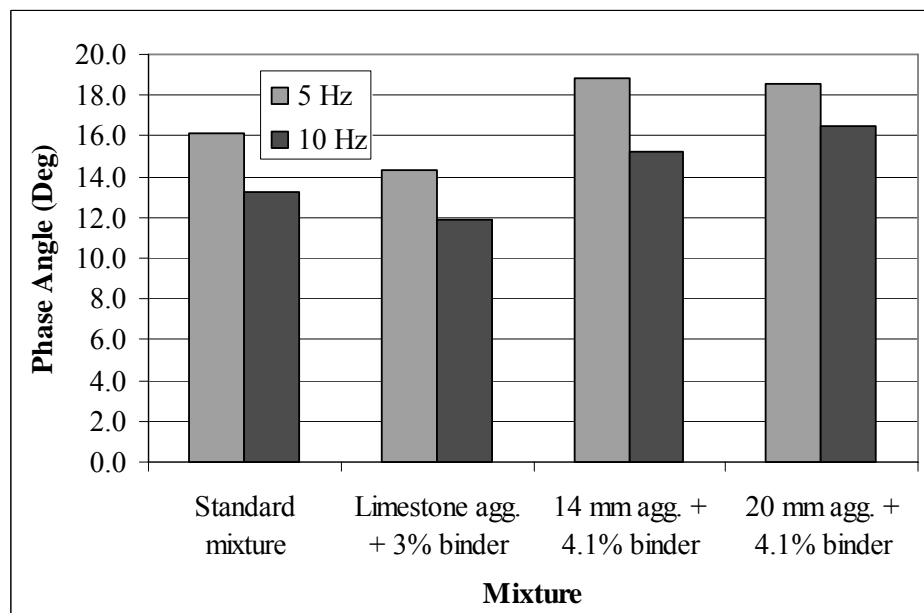
Figure 6.13 – Influence of combined variables on the phase angle of grouted macadams

From the figures above it is possible to observe that, in terms of stiffness modulus, there is no advantage in using bitumen film thicknesses higher than that of the standard mixture, as in the cases of the last two mixtures presented. However, this richness in bitumen may result in an improved fatigue life. Therefore, the analysis of

the influence of such variables is made after the fatigue results presented in Section 6.3.2.6. On the other hand, results obtained for the mixture produced with limestone aggregate and a reduced binder content (3% by mass of total asphalt) are in accordance with those presented for the same variables separately. Further analysis is made after presenting the fatigue results of each mixture. However, as a general remark, it could be said that the similar stiffness modulus obtained for the mixtures with 4.1% bitumen confirms that stiffness depends mostly on the volume of bitumen, which for grouted macadams means volume of the mineral aggregate, VMA (assuming that all the voids are filled with grout which may be seen as aggregates, after curing).

The phase angle of each mixture presented in the previous figures is mainly influenced by the binder film thickness of the mixture, higher for mixtures with bigger aggregate sizes, which correspond to the mixtures where bitumen content was kept constant (4.1%), regardless of the aggregate surface area.

6.3.2 Fatigue life

Fatigue resistance is one of the most important properties to be taken into consideration in order to predict the performance of grouted macadams, given that permanent deformation is not usually an issue. The results obtained in the four-point bending fatigue test, corresponding to the variables discussed in the previous section, are presented in this section. When appropriate, results are compared with those presented in Chapter 5, in order to give a better understanding of the influence of each studied variable.

6.3.2.1 Influence of binder content

Changing the binder content of grouted macadams, and consequently the binder film thickness, does not seem to have a substantial effect on the fatigue resistance of the mixtures, provided that aggregates are fully coated with bitumen. Figure 6.14

presents the results obtained from mixtures with the standard 4.1% binder content and with reduced binder contents (3 and 1.5%, by mass of asphalt mixture).
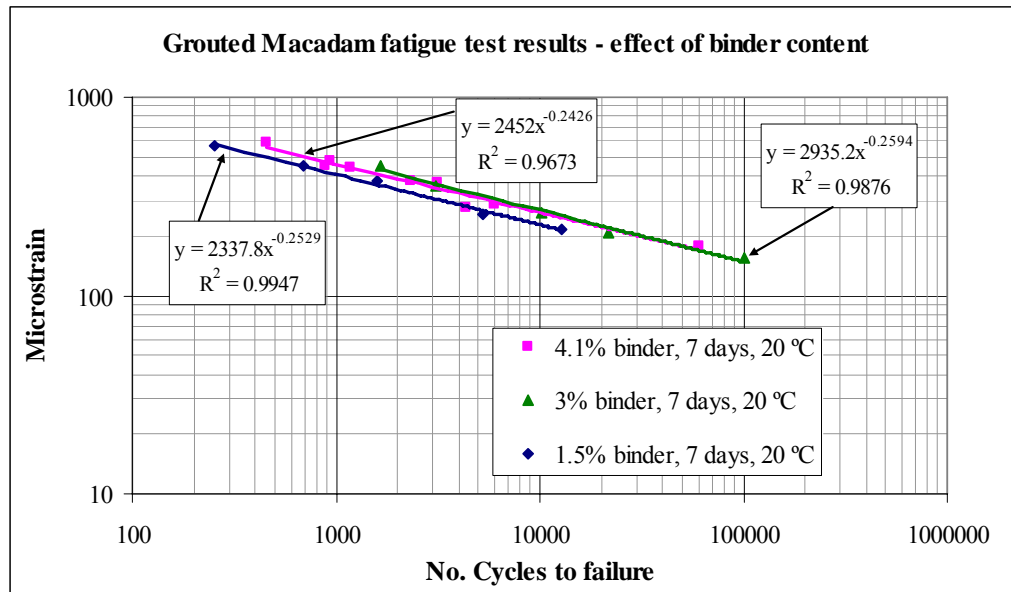
Figure 6.14 – Influence of binder content on the fatigue life of grouted macadams

The results show a lower fatigue life for the mixture with 1.5% binder (perhaps at the limit for aggregate coating, as visually observed), which was produced without cellulose fibres. However, the difference is not marked and between the other two mixtures it is almost insignificant. This suggests that fatigue performance of grouted macadams is more dependent on the length that a crack has to travel, rather than on the binder film thickness. The structure of the three mixtures studied is very similar, since the aggregate is the same, resulting in equivalent crack lengths, and similar fatigue lives.

The approach to crack propagation in a grouted macadam is different from that in a bituminous mixture. In the first case, assuming that the aggregate is sound, the crack has to propagate through the bitumen film surrounding the aggregates and the grout, only going through the grout at the weak spots (thin connections between voids in the asphalt skeleton, subsequently filled with grout). Therefore, the length of a crack is increased when compared with the case of a bituminous mixture, where a crack can propagate through the mastic (bitumen with small aggregate particles), filling the spaces between bigger aggregates. Figures 6.15 and 6.16 schematically represent the position of a crack on a beam comprising respectively a grouted macadam and a bituminous macadam mixture.
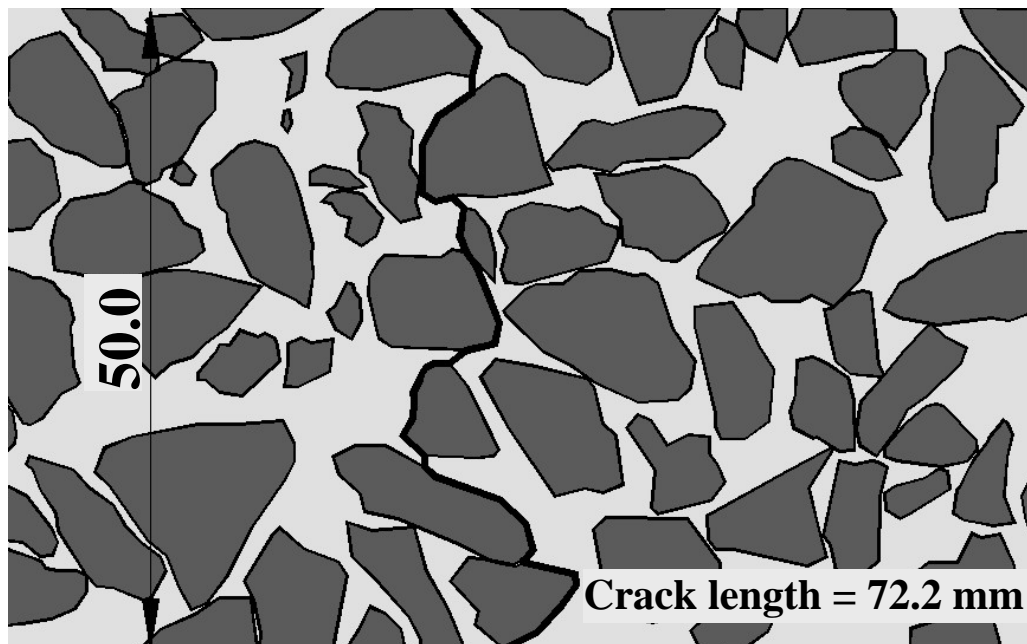
Figure 6.15 – Possible position of a crack in a grouted macadam beam
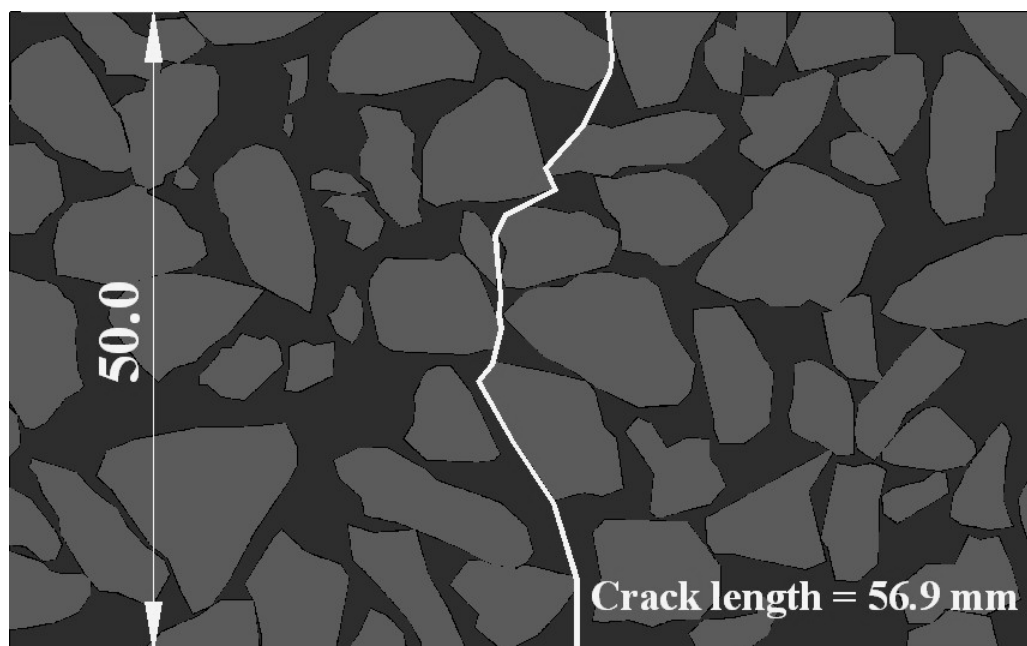
Figure 6.16 – Possible position of a crack in a bituminous macadam beam

In the examples presented in the previous figures, the crack in the grouted macadam beam is approximately 27% longer than the crack in the bituminous macadam beam. The increased length and the more acute angles lead to the need for more stress (or more load applications) to cause fracture, which can be seen as one of the reasons for an extended fatigue life of grouted macadams for lower strain levels, compared with bituminous mixtures, as exemplified in Figure 3.16.

6.3.2.2   Influence of binder type

Restricting the analysis to grouted macadams, in a situation where the structure of the mixture is maintained, the properties of the binder should have a significant influence on the behaviour of the material. Figure 6.17 represents the fatigue results obtained for three mixtures produced with three different binder types: (i) 200 pen, used in the standard mixture; (ii) 50 pen, commonly used in the highway industry; (iii) Cariphalte DA, a polymer modified bitumen (PMB) with enhanced fatigue properties, supplied by Shell Bitumen UK Ltd.
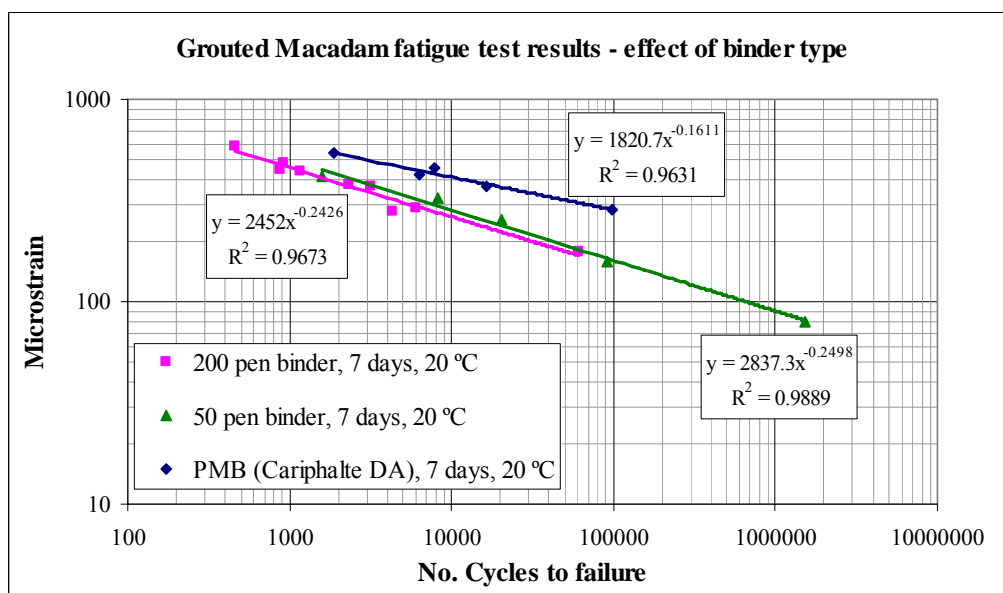
Figure 6.17 – Influence of binder type on the fatigue life of grouted macadams

Results from the figure above confirm the extended fatigue life obtained by using a polymer modified bitumen. If the initial costs of such a mixture may be higher than those of a mixture with normal bitumen, its long term performance can make its use feasible. On the other hand, and from the fatigue life point of view, a grouted macadam produced with a harder straight-run bitumen seems to have similar performance to that of a mixture produced with a binder as soft as the 200 pen bitumen used in the standard mixture. Thus, in applications where stiffness modulus and fatigue life are the most important properties, it may be more advantageous to choose a harder binder (resulting in stiffer mixtures, which implies reduced layer thicknesses in pavement design). However, if the horizontal movements of the layers underneath (due to thermal contraction) take on significant proportions, the use of a

softer binder may be recommended. Further details are given in the Section 6.3.3, regarding thermal cracking of grouted macadams.

6.3.2.3   Influence of aggregate type

If the use of limestone aggregate in the composition of grouted macadams results in slightly increased stiffness modulus, the same seems to happen in terms of extended fatigue life, as can be observed in Figure 6.18. However, the difference is minimal and, for surface applications of the mixture, the wearing properties of each aggregate may influence the choice of granite as the aggregate for grouted macadam surface courses. Nonetheless, as previously discussed, the use of limestone aggregate in grouted macadams to be applied in layers different from the surface course may be beneficial, both in terms of cost (allowing a local aggregate to be used in locations where there is no granite available), and in terms of mechanical properties (increased stiffness modulus and equivalent fatigue life).
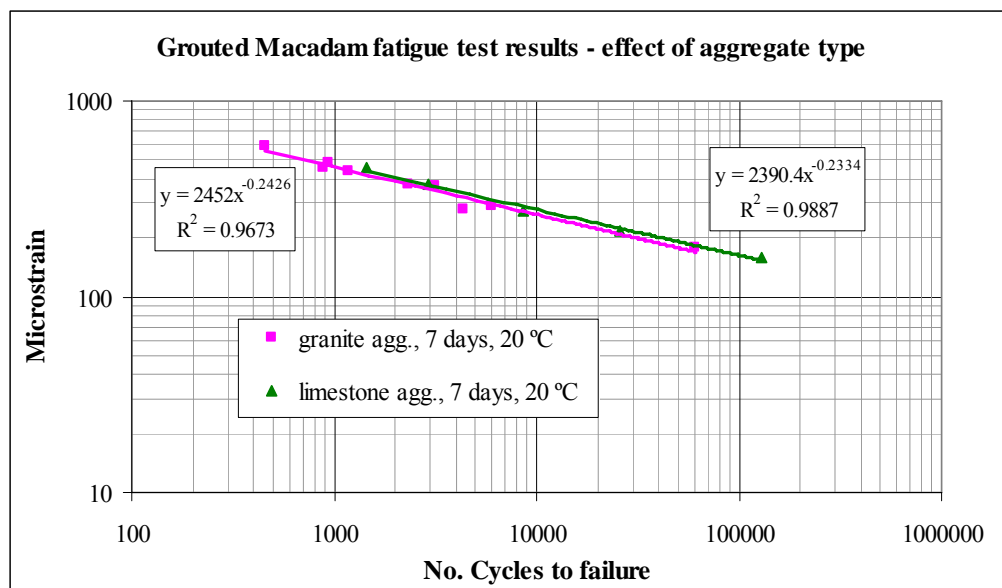
Figure 6.18 – Influence of aggregate type on the fatigue life of grouted macadams

6.3.2.4   Influence of aggregate size/grading

The results obtained from the fatigue tests, carried out to analyse the influence of aggregate size or grading on the corresponding performance of the mixture, are presented in Figure 6.19.
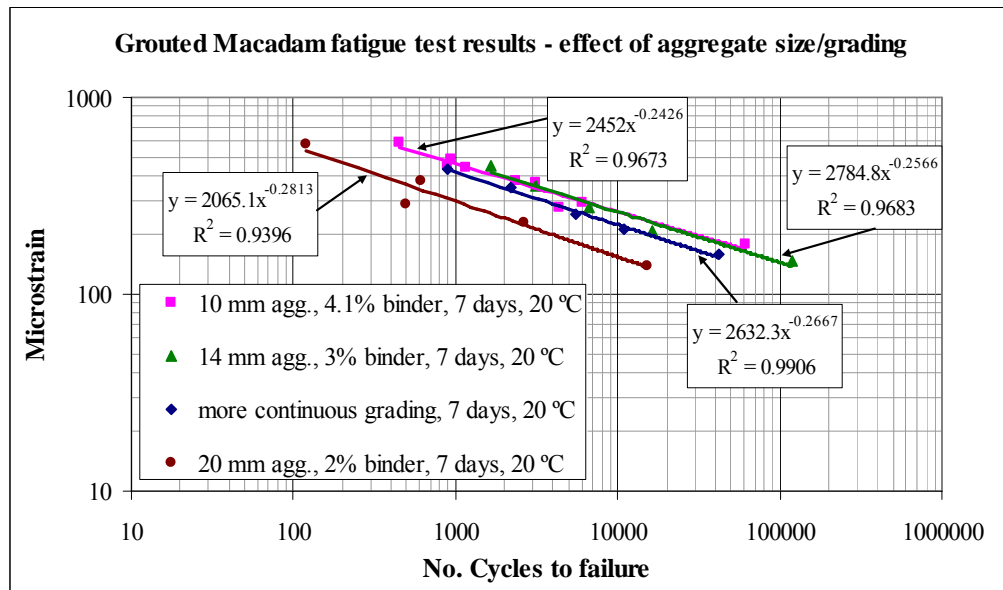
Figure 6.19 – Influence of aggregate size/grading on the fatigue life of grouted macadams

The use of a 14 mm single sized aggregate seems to have little effect on the fatigue properties of grouted macadams compared with the use of the standard 10 mm single sized aggregate. Thus, it may be more convenient to use the first in situations where a (slightly) stiffer material may induce savings in material costs, by reducing the thickness of the layers. However, the results obtained for a coarser aggregate (e.g. 20 mm single sized) may not properly represent its actual fatigue life. The ratio between the dimensions of the specimens and the maximum aggregate size is just above 2.0, which may not be appropriate for fatigue tests. Any slightly weak area due to variation in particle packing will dramatically reduce the fatigue life of the specimen. Due to its considerably increased stiffness modulus (1.78 times the stiffness modulus of the standard mixture), further tests should be carried out using bigger specimens to assess the actual fatigue life of this mixture. The mixture produced with a more continuous grading shows an intermediate fatigue performance, with a fatigue life slightly less than those obtained with 10 mm and 14 mm single sized aggregates.

6.3.2.5 Influence of grout properties

Although not a comprehensive grout investigation, three grouts were used in the mix design study, in order to assess the influence of grout properties on the mechanical

characteristics of grouted macadams. Properties of the grouts were presented in Chapter 5, and Figure 6.20 represents the fatigue lines obtained, for the mixtures produced with those grouts, from four-point bending fatigue tests.

Grouted Macadam fatigue test results - effect of grout

$y = 11001x^{-0.4392}$
$R^2 = 0.9735$

$y = 2452x^{-0.2426}$
$R^2 = 0.9673$

$y = 3185.4x^{-0.2987}$
$R^2 = 0.9686$

- ■ Densit grout (20 ℃)
- ▲ Modified Densit grout (20 ℃)
- ◆ Weak grout (20 ℃)

Microstrain

No. Cycles to failure
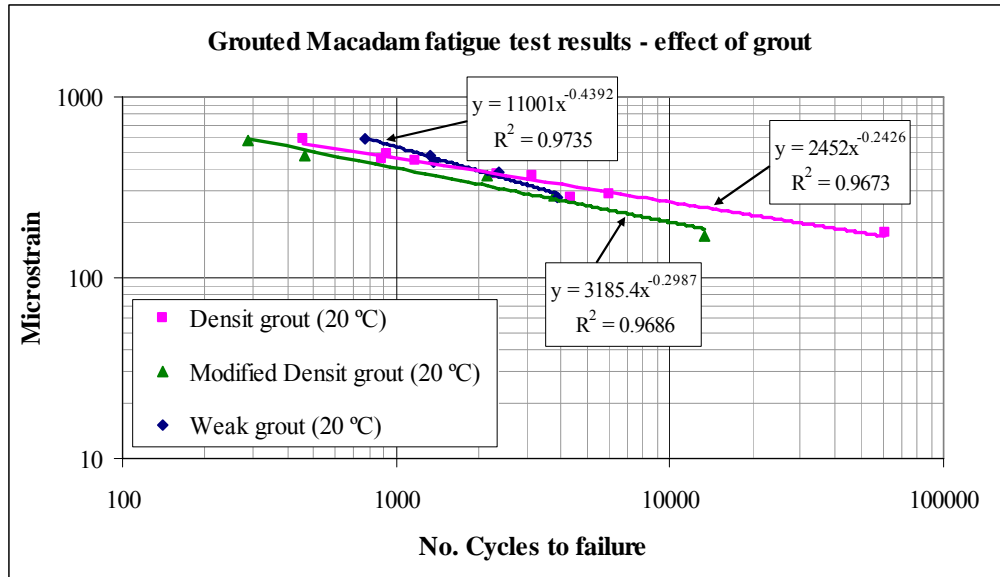
Figure 6.20 – Influence of grout strength on the fatigue life of grouted macadams

Grout strength, and particularly grout shrinkage, are characteristics that can have some influence on the fatigue performance of grouted macadams, as can be observed in the figure above. The best results were obtained for the standard mixture, characterised by a flatter fatigue line, while the mixture with the modified grout shows a slightly lower fatigue performance. The weak grout used in this study presented the highest fatigue life for high strain levels but, due to its steeper line, is the one with the shortest life in the low strain range (the range normally accepted for pavement design). The reason why shrinkage is the characteristic with more influence in fatigue life of grouted macadams is related to the structure of the mixture. As shown in Figure 6.15, the crack tends to propagate through the bitumen film (between the aggregate and the grout). If the grout presents high shrinkage values, each 'particle' of grout, filling the asphalt voids, reduces its size, creating a kind of 'network' of voids between the asphalt and the grout itself. Furthermore, each 'link' of grout between bigger voids in the asphalt skeleton is a good candidate for a micro-crack within the continuous hydrated paste (grout). These micro-cracks and the 'network of voids' affect the fatigue life of grouted macadams by reducing the resistance to crack propagation, resulting in some micro-cracks evolving more easily into macro-cracks.

6.3.2.6   Influence of combined variables

The analysis of grouted macadams' fatigue performance was completed by producing three more mixtures. In those mixtures, some of the variables evaluated in the previous sections were combined and the results were compared with those of the standard mixture, as presented in Figure 6.21.
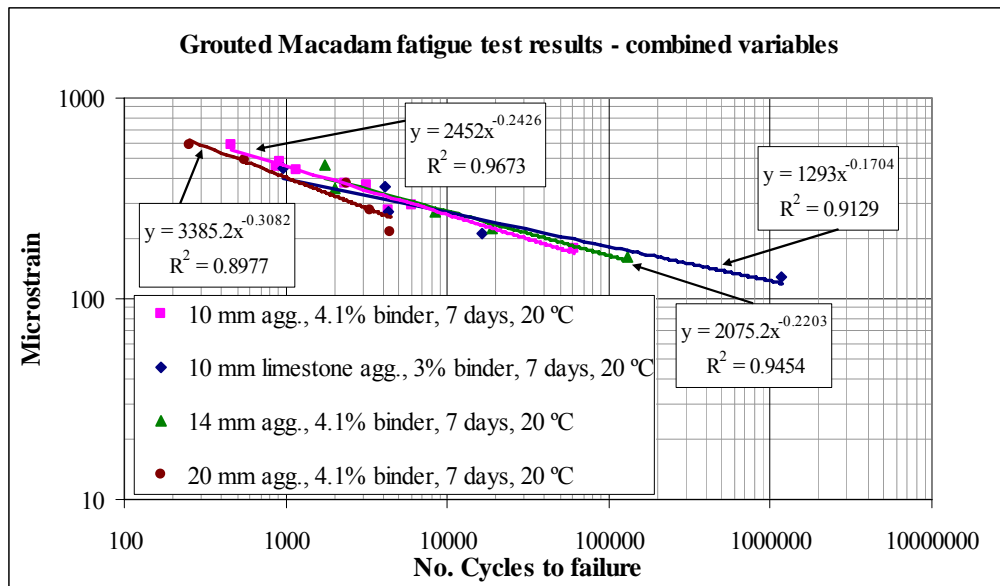
Figure 6.21 – Influence of combined variables on the fatigue life of grouted macadams

Following previous discussion about the use of limestone aggregate in grouted macadams, the figure above confirms the slightly longer fatigue life of the mixture with that aggregate type, now with a lower binder content (3% by mass of asphalt), which is an even stiffer mixture (better for pavement design). The increased binder film thickness used in the mixture with the 20 mm single sized aggregate (resulting from keeping the binder content of the standard mixture) has improved the fatigue life of that mixture compared with the one presented in Figure 6.19, comprising the same aggregate, but it remains nonetheless the mixture with the lowest fatigue life. The ratio between the specimens' dimensions and the maximum aggregate size may be the reason for the shorter fatigue life of this mixture.

Although resulting in small changes in the fatigue life of the mixture, small changes to the proportions of each component in the mix design do not affect significantly the

overall behaviour of grouted macadams. This is very clear in Figure 6.22, where most of the mixtures evaluated in this mix design study are plotted together in one fatigue line and the results are highly correlated, as indicated by the high correlation coefficient (R^2).
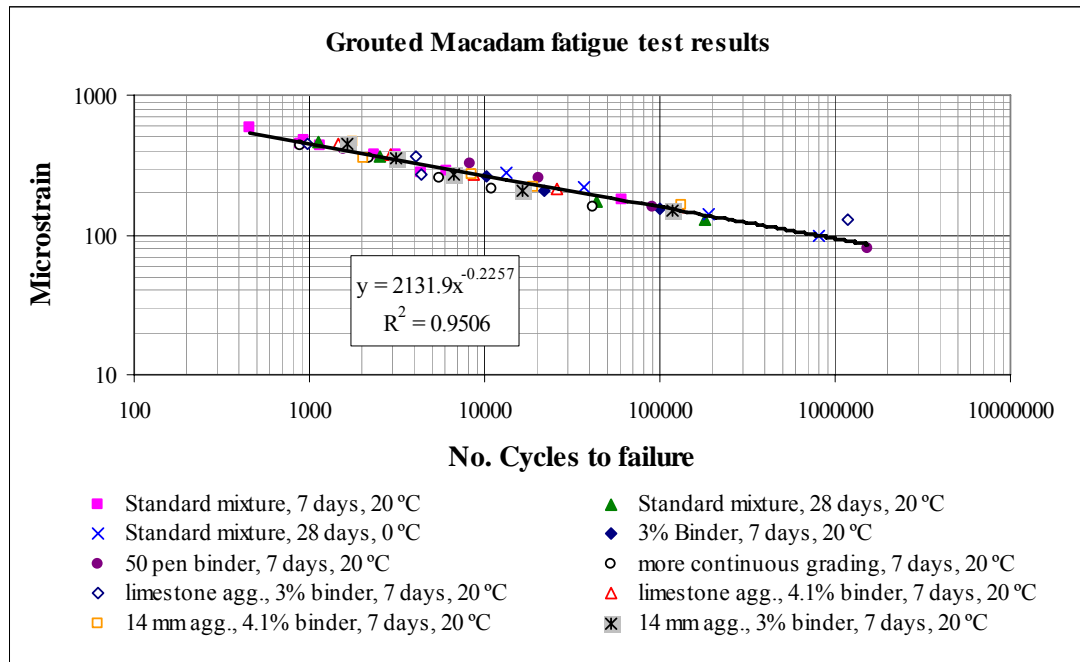
Figure 6.22 – Correlation between several grouted macadam fatigue lines

The mixtures that did not follow the same trend closely are: (i) the mixtures produced with 20 mm single sized aggregates; (ii) the mixture produced with 1.5% binder (by mass of asphalt); (ii) the mixture produced with PMB; (iv) the mixtures produced with different grouts. Depending upon the final application of grouted macadams, the use of any of these types of mixture may be allowed, provided that laboratory tests are carried out to determine their mechanical properties.

On the other hand, recipes may be created for grouted macadams following the standard mix design, allowing some variability in the proportions of each component (within defined ranges), without compromising the performance of the mixture in terms of stiffness modulus and fatigue life.

In applications where the pavement is subjected to high temperature ranges, especially when grouted macadams are used on top of cement bound materials, attention should be paid to the thermal properties of the mixture. In order to assess the susceptibility of grouted macadams to cracking, due to horizontal movements

originated by thermal cycles, a series of tests was carried out, as presented in the following section.

6.3.3 Resistance to thermally induced cracking

Thermally induced cracks in the surface course of a pavement are often in reality reflective cracking due to the appearance at the surface of the naturally occurring thermal cracks in a cement bound base (Kazarnovsky et al., 2000), although in some locations they can just occur in the asphalt without any cemented base. Daily temperature variations impose tensile stresses in the cementitious base due to the expansion and contraction of the material. These stresses create transverse cracks in the base, with a natural spacing that depends on the properties of material and on the thickness of the layer (Ellis et al., 1997), although nowadays they are often induced at 3 m spacing. The cracks will then propagate through the overlying layer.

A study of thermally induced cracks is essential in the case of grouted macadams, both because of the presence of cementitious materials in its constitution, and because of its normal application as a surface course of pavements that may have cement bound layers as a base. Thus, several tests have been undertaken during this project to determine the resistance of grouted macadams to thermally induced cracking. The tests have been carried out using a piece of equipment previously developed at the University of Nottingham (Brown et al., 2001). This equipment is schematically illustrated in Figure 6.23 and simulates the opening and closing movement of a crack in the base, caused by temperature variations.
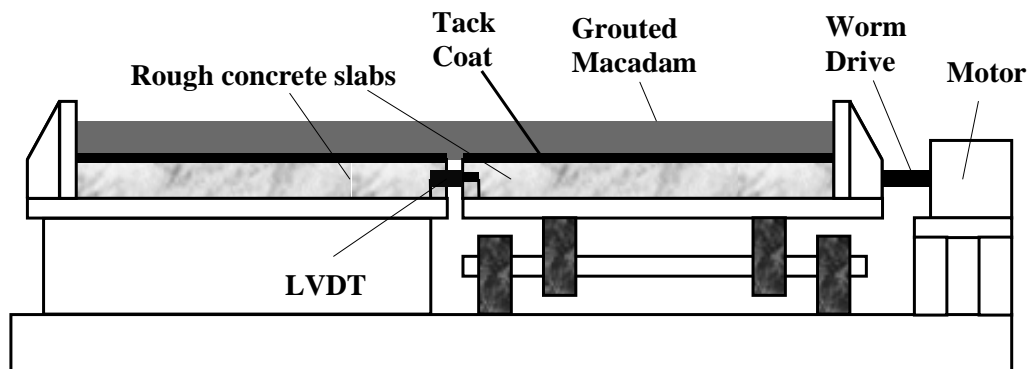
Figure 6.23 – The thermal cracking simulation apparatus

The equipment comprises a horizontal 2.0 m long by 0.2 m wide frame, made in two halves, one being fixed and the other moving horizontally. Two concrete slabs are bolted on top of each half of the frame to simulate the discontinuous (cracked) base over which the overlay is applied. An electric motor, connected to the mobile half by a worm drive, controls the opening and closing of the gap between the two slabs with a certain opening rate, which can be lower than 0.1 mm per hour, if necessary. It is a very slow movement during which tensile stresses are imposed on the overlying specimen, just above the joint. When these stresses exceed the tensile strength of the material, a crack will initiate at the bottom of the specimen, propagating towards the surface and leading to failure. The equipment is kept in a temperature-controlled room (usually at -5 °C) to simulate low night-time temperature. At this temperature, the material shows a more brittle behaviour and the stresses induced by the contraction of the concrete base achieve their highest values. A computer program that calculates the opening rate, for a specific amplitude and duration of the cycle, controls the movement of the motor using the feedback from a LVDT situated between the two halves. The strain level at the surface is determined using a 'Demec' dial gauge to measure the movement between 'Demec' pips glued to the specimen with a specific distance between them (according to the dimensions of the 'Demec' gauge).

An equipment with the same working principle has been used in Belgium (Visscher and Vanelstraete, 2003) to study the reflection cracking of bituminous overlays with reinforcing interface systems on top of concrete slabs. According to these researchers, the thermal cracking test is a powerful tool in studying different interface systems, as a qualitative analysis, but due to the complex and heterogeneous structure of the bituminous mixtures, the quantitative results of one single test on a specific system should always be considered with caution.

In the present study, two types of specimen were produced in order to determine the resistance to thermally induced cracking of grouted macadams, respectively, detached from and bonded to the jointed concrete base.

In the first case, necked specimens (Figure 6.24) were produced to determine the strain level imposed in the specimen at crack initiation and failure. The specimens

were manufactured with a smaller section in the central part to control the area where the crack would develop. Production of specimens took place in a purpose-designed mould (Figure 6.25) into which the porous asphalt was compacted and grouted. After production, each specimen was placed in the equipment (without the concrete slabs) and glued to the end plates. A polythene film was used between the specimen and the horizontal frame to reduce friction and avoid other stresses being induced in the specimen.
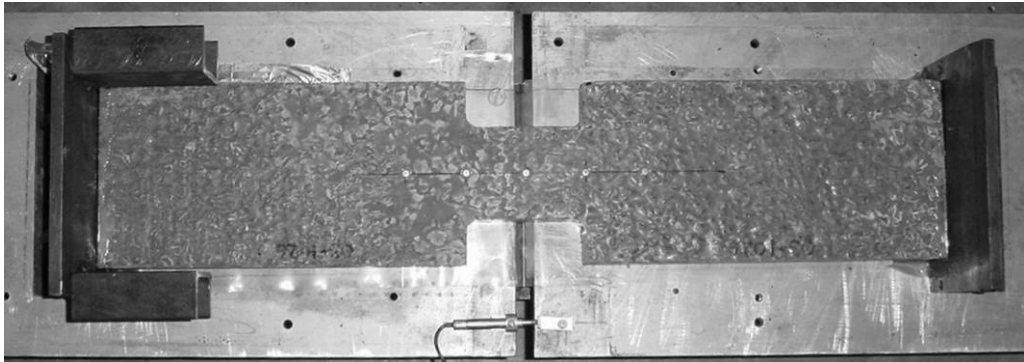
Figure 6.24 – Specimen used to determine the resistance of grouted macadams to thermally induced cracking

Figure 6.25 – Mould used to manufacture thermal cracking specimens

After calibrating the equipment, a preliminary test was carried out to check the procedures and establish a standard methodology, in order to guarantee repeatability amongst tests, which were carried out seven days after grouting. The maximum horizontal movement imposed on the specimens was 1 mm, over a period of time of 8 hours. This amplitude and period of time do not follow any standard in particular, being mostly related with limitations on the opening times of the building where the tests were carried out. Nonetheless, the relative behaviour of each variable in the mixture was identified, since those testing conditions were kept constant for all tests.

Figure 6.26 shows one specimen at the end of the test, including an indication of the strain measurements taken between Demec pips. Three grouted macadam mixtures were evaluated using this testing methodology, as discussed previously, and the results are summarised in Table 6.1 and graphically illustrated in Figure 6.27.
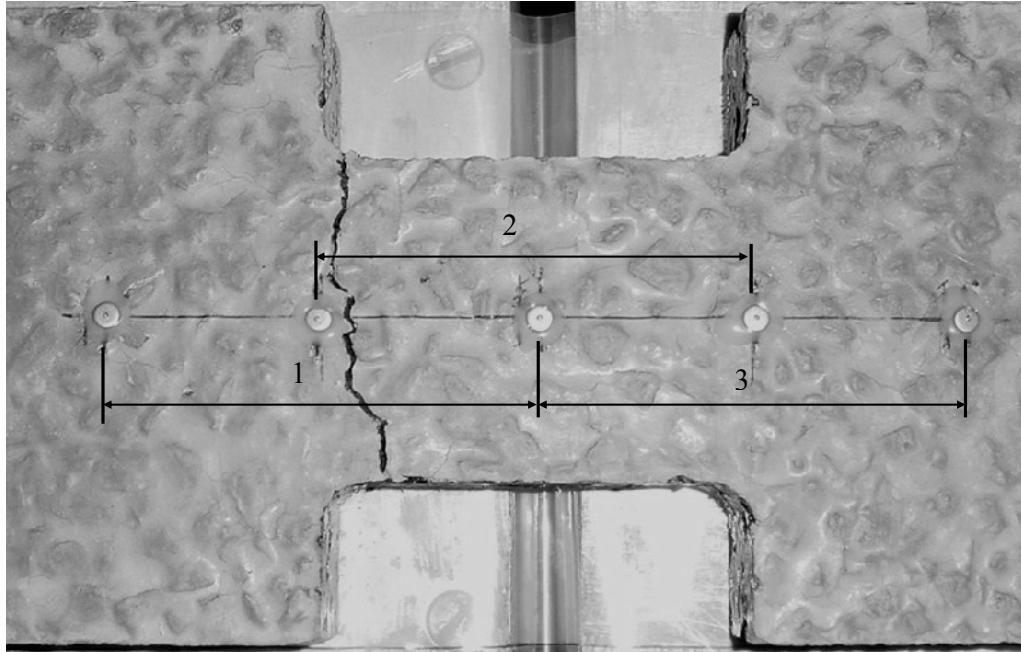
Figure 6.26 – Thermal cracking specimen at the end of the test

Table 6.1 – Maximum tensile strain at failure in thermal cracking tests

Mixture	Tensile strain at failure ($\times 10^{-6}$)
Standard	3768
50 pen binder	1267
1.5% binder	1028

The results presented in the table above represent an average of the three values measured at the surface of the specimen, as illustrated in Figure 6.26, when the specimen failed. Failure was defined as the moment when one of the readings stopped increasing (or even decreased), as a consequence of a crack occurring in a region out of range of that measurement. Figure 6.27 illustrates the failure point of the mixtures studied, while the determination of surface strain at failure is exemplified in Figure 6.28, for the mixture with 50 pen binder.

According to the results presented above, the standard grouted macadam used in this project showed a resistance to thermally induced cracking comparable to a

20 mm DBM using a 50 pen bitumen, as obtained by Collop et al. (2001), since the strain level obtained for surface crack initiation was approximately 3500 microstrain. It also highlights the importance of binder type and binder film thickness in the resistance of grouted macadams to thermally induced cracks. The mixtures with 50 pen binder and 1.5% binder showed results of approximately 1/3 of the standard mixture's strain at failure.
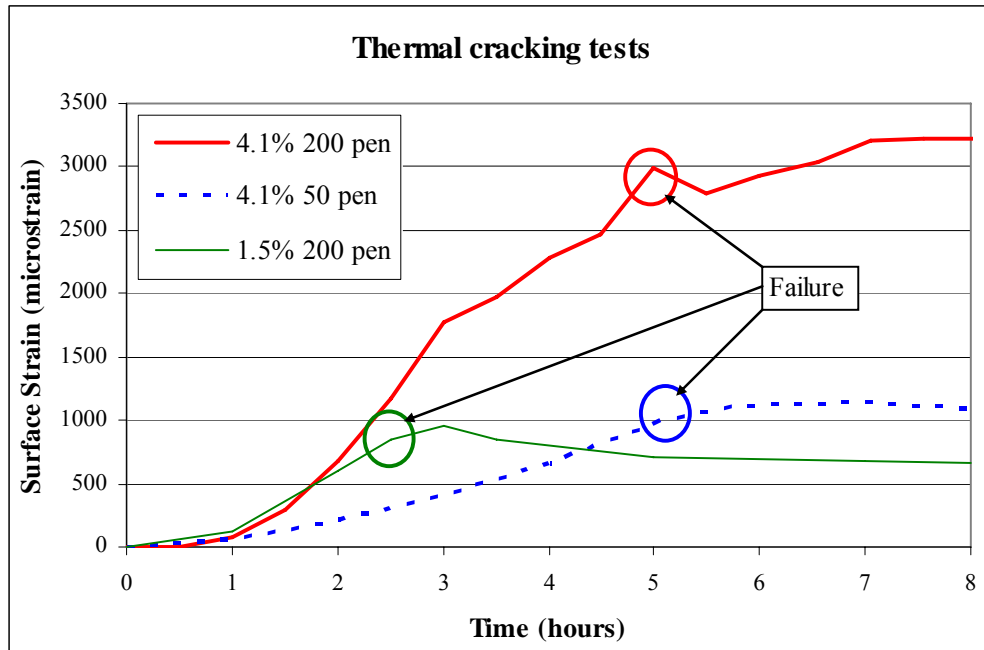
Figure 6.27 – Definition of failure of grouted macadams in thermal cracking tests
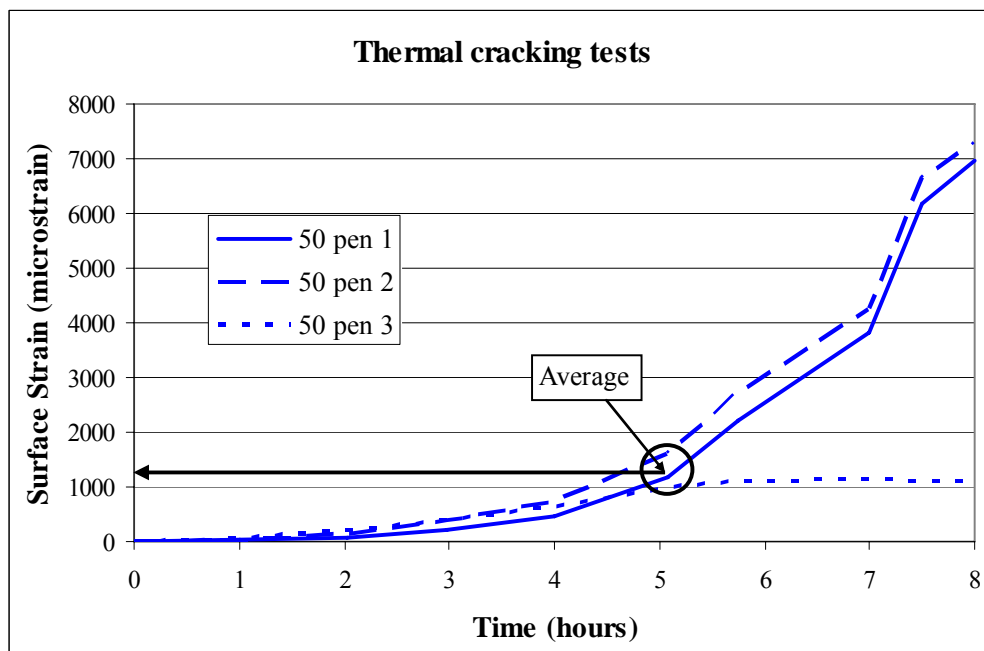
Figure 6.28 – Determination of surface strain at failure of grouted macadams, in thermal cracking tests

Although the results may be susceptible to some variability, which was not assessed due to the small number of specimens tested, the standard mixture has allowed the tensile strain of the specimen to increase up to 3 times the amount obtained in the other mixtures before failure and, at the same time, the corresponding stress value, calculated according to the stiffness modulus of each mixture (presented in Section 6.3.1), was also 2 times higher than the values obtained with the stiffer mixtures. This is a clear indication of the extended thermal cracking resistance of grouted macadams produced with the standard mix design.

A complementary study was carried out with the thermal cracking apparatus, in order to assess the influence of including a grid reinforcement between the base (using rough concrete slabs) and the surface course (standard grouted macadam mixture) in the resistance of the surface course to thermally induced cracks. In this investigation, two tests were undertaken, one unreinforced and the other reinforced with a fibreglass grid known as Glasgrid®, with a tensile strength of 100 kN/m (based on strength of each strand - 12.5 mm × 12.5 mm grid size). Tack coat was applied between the concrete slabs and the porous asphalt, prior to compaction, in order to bond the grouted macadam specimen to the base and study the reflection of the crack (or joint between concrete slabs) through the overlay.

In this test, the specimens were produced directly in the testing rig, on top of the concrete slabs, using specially designed side parts to be able to compact and grout the porous asphalt layer. Once the production of a specimen was finished, the sides and the ends were removed. The ends were then fixed back with an epoxy glue to each end of the specimen and bolted to the rig to simulate the effect of a continuous pavement.

The adopted test procedure was to use several cycles, each with a crack opening period of 8 hours, the first cycle being carried out with a crack opening of 1.0 mm and this amplitude being increased for each subsequent cycle, until failure of the specimen had occurred. Failure was taken as the occurrence of a severe full depth crack. The tests were carried out in consecutive days, performing one cycle per day.

The measurements carried out during the tests, at regular intervals, were the strain on the upper surface and sides of the specimen. The upper surface was instrumented with a line of Demec pips, at 100 mm intervals, between which the strain

measurements were taken, while the side strain was measured in only one location at each side, immediately above the discontinuity in the concrete base.

The results obtained from the two tests are presented in Figures 6.29 and 6.30, as the strain measured at the surface of the specimens. These figures illustrate well how the strain is distributed when a reinforcing grid is used between a cracked base and a grouted macadam overlay.
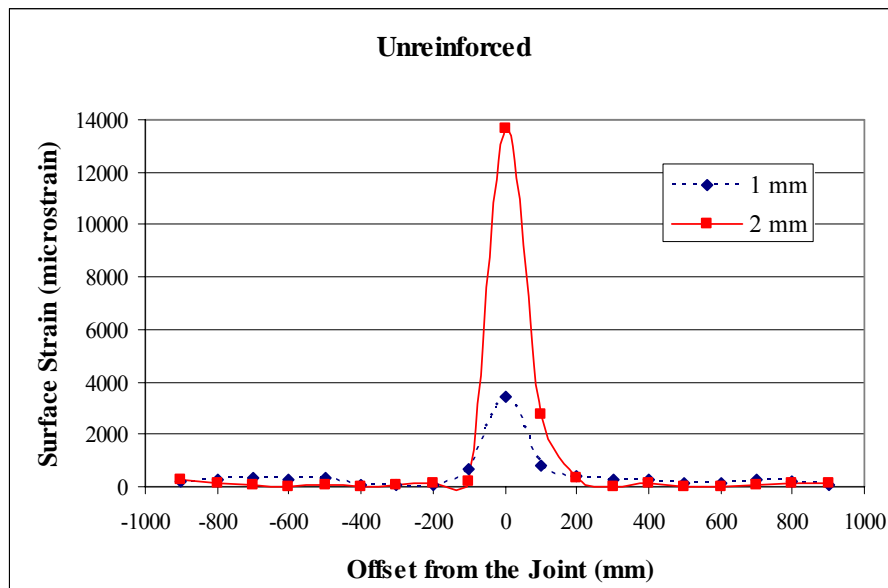
Figure 6.29 – Surface strain distribution in thermal cracking tests of Grouted macadams (unreinforced)
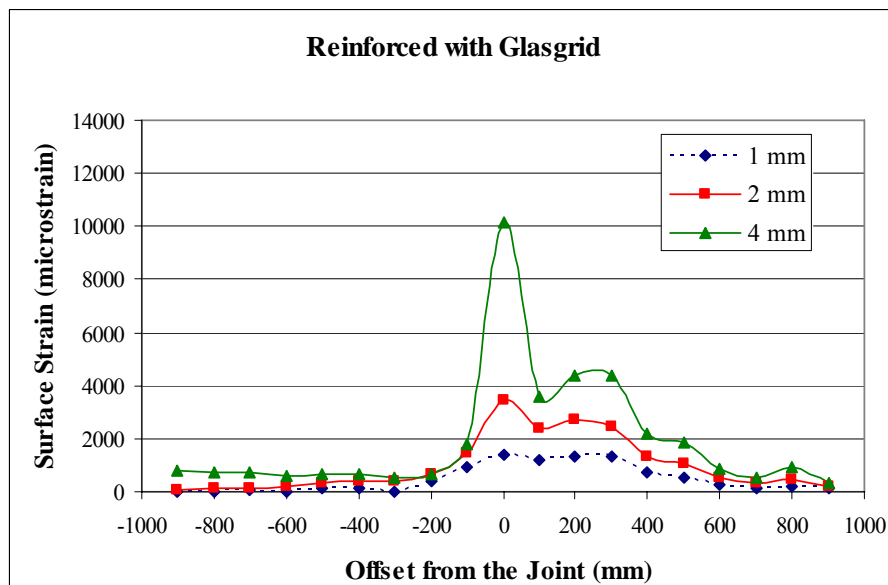
Figure 6.30 – Surface strain distribution in thermal cracking tests of Grouted macadams (Glasgrid® reinforced)

During the tests visual observations were carried out in order to determine the development of cracking and the failure of the specimens. The specimens were painted white to help identify the appearance of cracks. Figures 6.31 and 6.32 show visual observations taken at the end of both tests. It can be seen that, in the case of the Glasgrid® reinforced specimen, the cracking pattern is composed of several thin cracks while, in the case of the unreinforced specimen, the crack in the base propagated through the Grouted macadam as one major wide crack. The reinforced specimen showed a resistance to thermally induced cracking in the order of two times that of the unreinforced specimen, since it could withstand a movement of the crack underneath (4 mm), two times bigger than the unreinforced specimen (2 mm), before failure.
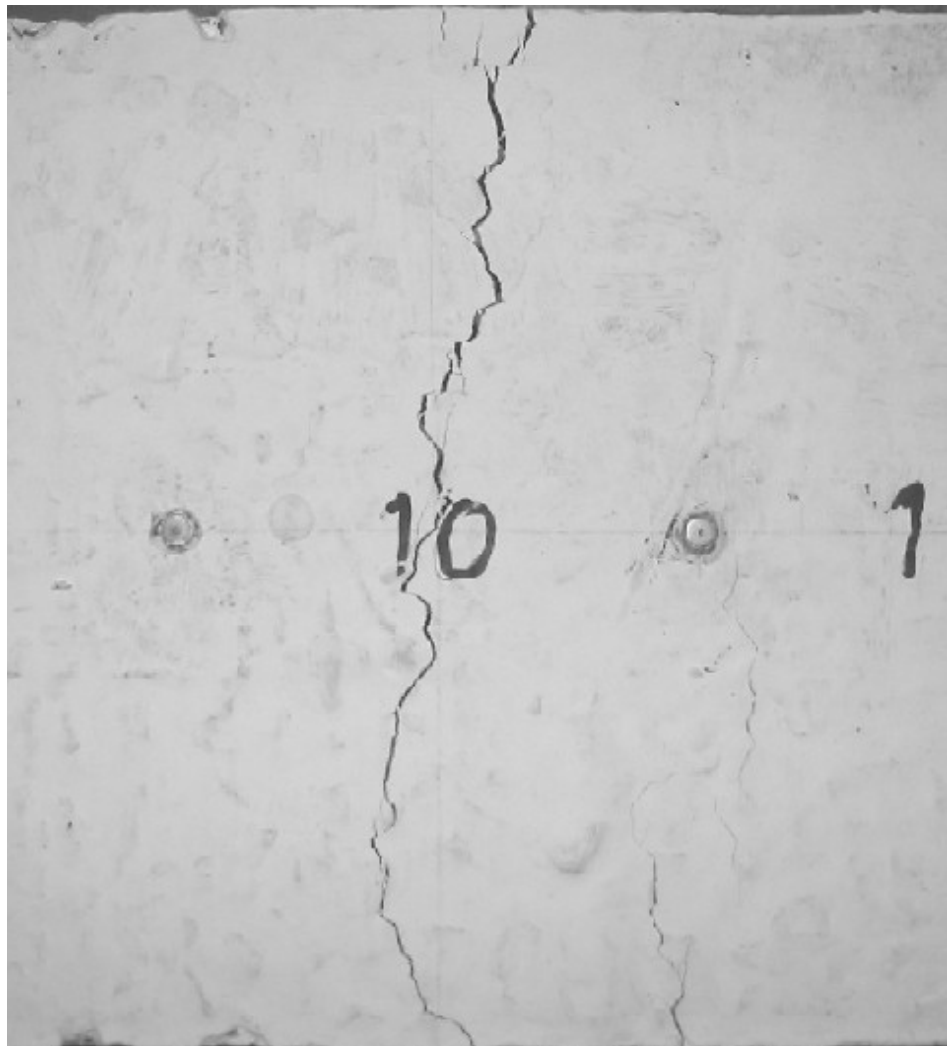
Figure 6.31 – Cracking pattern at the surface of the unreinforced specimen at the end of the test (after 2 mm)

Figure 6.32 – Cracking pattern at the surface of the Glasgrid® reinforced specimen at the end of the test (after 4 mm)

The highest strain is expected to occur at the base of the grouted macadam layer, just above the joint between the concrete slabs. This is also the strain that may be related to the failure of the specimen. In Figure 6.33, a comparison between the maximum strains measured at the surface and on the sides of the specimen is made. It can be seen that, for the unreinforced specimen, the maximum strain at failure occurs, as expected, at the base. However, for the Glasgrid® reinforced specimen, the highest value of strain at failure was measured at the surface. This can be explained by the ability of the grid to spread the strain or by the phenomenon of de-bonding between the concrete slabs and the Grouted macadam specimen, due to the axial strength of the grid.

In Figure 6.33, it can also be observed that the failure occurs, for both specimens, at a strain level close to 10000 microstrain. Comparing this value with the results

obtained by Brown et al. (2001), with the same equipment, for unreinforced 100 pen DBM material (approximately 6000 microstrain), it can be understood that the standard grouted macadam mixture used in this project can perform at least as well as the previously studied asphalt, when bonded to a cracked base, with regard to the resistance to reflective cracking.
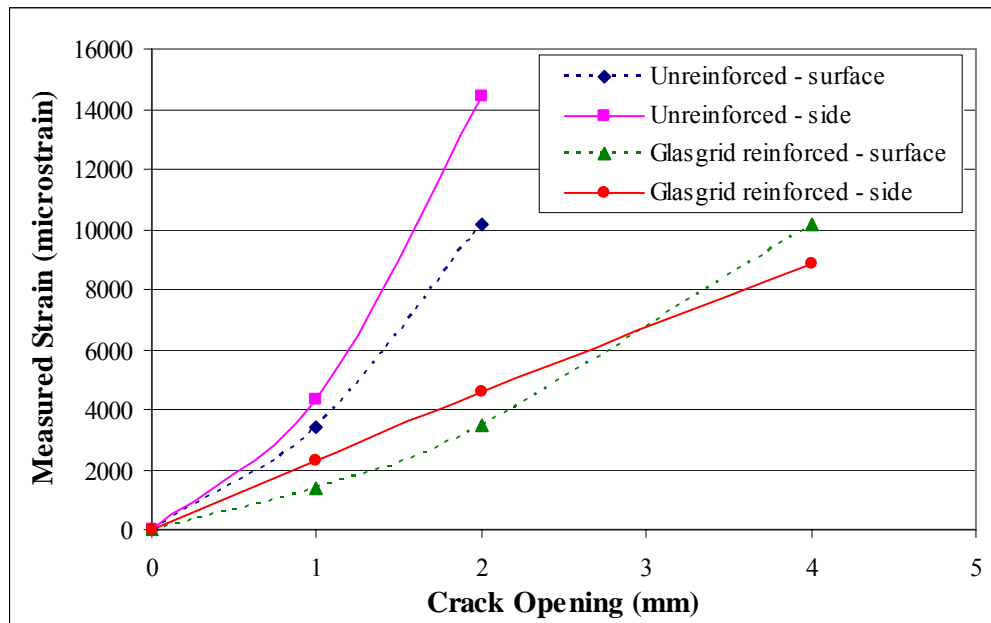
Figure 6.33 – Strain evolution until failure of specimen in thermal cracking tests

6.4 Summary and Conclusions

The results presented in this Chapter are the outcome of a mix design study, carried out to assess the influence of several variables on the mechanical properties of grouted macadams. The study was based on a standard mixture that has been used in the UK for the past few years. The influence of variability in the composition of the mixture was assessed, and significantly different mix designs were evaluated, in order to increase the application field of grouted macadams. In this study, the mechanical properties evaluated included the stiffness modulus and the resistance of grouted macadams to fatigue cracking and to thermally induced cracking (normally in the form of reflective cracking, in pavements with cementitious base layers). The assessment of the resistance to permanent deformation was not carried out, since results previously obtained by other researchers, namely Collop and Elliott (1999) show that grouted macadams are not susceptible to deformation.

In summary, the standard mix design incorporates a 10 mm single sized granite aggregate and a 200 pen straight-run bitumen (4.1% by mass of asphalt), with the addition of 4% limestone filler and 0.15% of cellulose fibres, to produce the porous asphalt skeleton into which, a commercial grout (prepared by adding water to a Densit® cementitious powder) is poured.

The variables used in this mix design study included: (i) different binder contents (1.5% and 3% by mass of asphalt); (ii) different binder types (a 50 pen straight-run bitumen and a polymer modified binder with the incorporation of SBS rubber elastomers); (iii) a different aggregate type (limestone); (iv) different aggregate sizes and grading (a 14 mm single sized aggregate, a 20 mm single sized aggregate, and a more continuous aggregate grading); (v) combinations of some of the previous variables.

The main conclusions to be highlighted from this investigation are summarised as follows:

- A small reduction in the binder content does not affect the stiffness and fatigue performance of grouted macadams, as observed in the results obtained for the mixture with 3% binder (by mass of asphalt). However, mixtures with very low binder content (notably the 1.5% binder mixture studied) present reduced fatigue performance even though showing an increased stiffness modulus. The resistance to thermally induced cracking is also affected by the thin binder film thickness obtained with such mixtures.

- Different grades of straight-run bitumens have limited influence on the fatigue life of grouted macadams; nonetheless, harder binders produce stiffer mixtures. This may suggest the use of harder binders rather than softer binders where fatigue life and stiffness modulus are the most important properties. However, the resistance to thermally induced cracking is compromised with the use of hard bitumens. On the other hand, polymer modified binders (like the SBS thermoplastic rubber modified bitumen used in this study) significantly increase the fatigue life without compromising the stiffness modulus of the final mixture.

- Despite having a low polished stone value (PSV), limestone seems to be a good alternative to granite (or other high quality aggregate) in applications where the

skid resistance of the pavement is not an issue or in layers different from the surface course, where grouted macadams are normally used. In the tests carried out with limestone substituting granite, the mixtures performed as well as (or even better than) the standard mixture, both in terms of stiffness modulus and fatigue life.

- Stiffness is mostly related to the volume of bitumen used in grouted macadams, increasing with the reduction of the bitumen volume. However, the aggregate size may also have some influence on the mixture stiffness. The use of a 14 mm single sized aggregate did not have a significant influence on the fatigue life of the mixture, but in pavement design, the use of that aggregate size may result in cost savings, due to its higher stiffness modulus, reducing the thickness of the bound layers in the pavement.

- The properties of the grout used in grouted macadams have limited influence on the stiffness modulus of the final mixture. However, the same cannot be said regarding the fatigue life, since grout strength and particularly grout shrinkage have a significant effect on the performance of the mixture. Both alternative grouts showed higher shrinkage values than the standard grout resulting in lower fatigue lives for the mixtures with those grouts.

- Small variations to the standard mix design do not have a significant effect on the fatigue performance of the final mixture. Hence, it is possible to establish a fatigue line incorporating data from most of the mixtures studied with a high correlation coefficient (R^2=0.95). The exceptions to this rule are the mixtures with 20 mm single sized aggregate, the mixture with low binder content (1.5%) and the mixtures with different grouts, all with lower fatigue performances, and the mixture with PMB binder that showed an enhanced fatigue performance, compared with the standard mix design. However, care should be taken regarding the use of the 20 mm aggregate fatigue results, since the dimensions of the specimens used in the tests may not be big enough to properly represent the actual fatigue life of such a mixture.

- Mixtures with soft binders and thick bitumen film present the best resistance to thermally induced cracking (the standard mixture showed a tensile strain level three times higher than the other mixtures, before failure of the specimen, and can be compared with a 20 mm DBM mixture using a 50 pen binder, in terms

of thermal cracking resistance). This property can be further improved by using a grid reinforcement between the cracked pavement base and the grouted macadam surface course. The results obtained for a specimen with Glasgrid[®] reinforcement showed thermal cracking resistance two times higher than that obtained for an unreinforced specimen bonded to concrete slabs with tack coat. Nonetheless, in these tests, the unreinforced grouted macadam showed similar results to an unreinforced 100 pen DBM mixture (obtained by Brown et al., 2001).

7 DETERIORATION OF HALF-SCALE PAVEMENT UNDER TRAFFIC LOADS

7.1 Introduction

Following the conclusion of the mix design study, a half-scale pavement was constructed in the laboratory to be trafficked using the Pavement Test Facility (PTF) located at the University of Nottingham. The objective of this investigation was to evaluate the performance of some of the mixtures studied, both in terms of mix design and use of reinforcement.

Due to limitations regarding the maximum wheel load that the equipment was able to apply, the pavement structure was designed in such a way that failure of the surface course should occur within a reasonable number of load applications. This concern was taken into account during the design of the pavement, since the time to complete the test was also limited, due to demand for the equipment. The final results showed that the bearing capacity of the unbound layers was overestimated, resulting in premature failure, which highlights the importance of the supporting layers when using grouted macadam in pavement construction.

7.2 Pavement Test Facility (PTF)

The main part of the Pavement Test Facility is a piece of equipment developed at the University of Nottingham a few decades ago (Brown and Brodrick, 1981). However, the hydraulics were reconditioned in 2001 (Figure 7.1), when it was relocated into the new Pavement Research Building, as part of the laboratory of the Nottingham Centre for Pavement Engineering. Figure 7.2 represents a schematic of the PTF with indication of the main components. The movement of the wheel is controlled by a hydraulic motor which pulls the steel rope (attached to both sides of the carriage housing the wheel) in both directions.

The test is carried out at an approximate velocity of 4 km/h and the maximum load that can safely be applied to the pavement at that speed is 12 kN (for lower speeds the load can go up to 15 kN). The maximum velocity achievable by the equipment is 8 km/h but, in those circumstances, the load becomes unsteady, especially if the surface of the pavement presents some unevenness. According to the type of tyre used in the test (Figure 7.3), the stress applied at the surface of the pavement (in the current project, 630 kPa at 12 kN) can be similar to that applied by a tyre of a normal heavy goods vehicle. However, the total load applied to the pavement is still significantly lower than that applied by a real vehicle wheel/axle. Therefore, the thickness of each layer must be scaled down, in order to obtain some measurable results within a reasonable number of load applications (wheel passes).
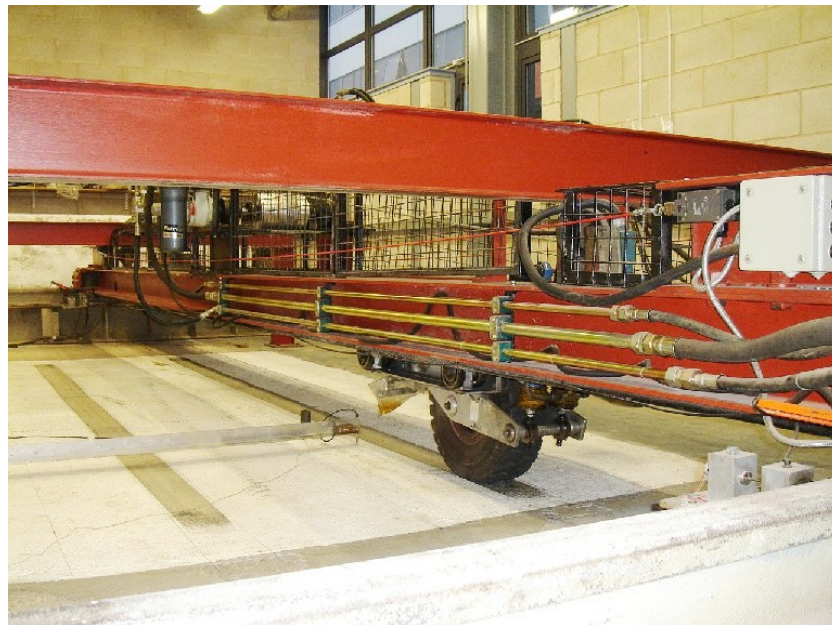
Figure 7.1 – General view of the Pavement Test Facility (PTF)
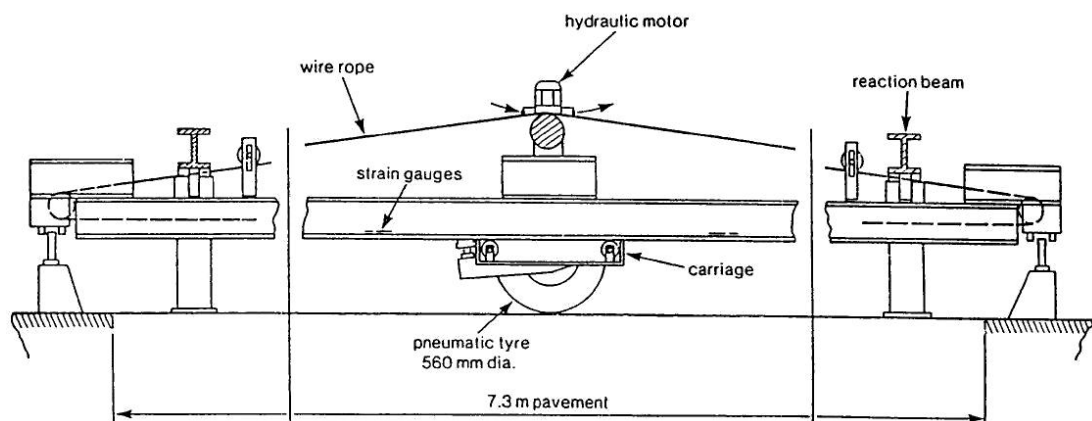
Figure 7.2 – Side view of the Pavement Test Facility (Brown and Brodrick, 1981)

The test pit is 1.5 m deep, 7.0 m long and 2.4 m wide. However, the length of the pavement that the wheel can traverse is just 5.0 m. Furthermore, only the central 4.0 m can be trafficked at constant speed, since the last 0.5 m of each end is used to decelerate, halt and accelerate. In those end 0.5 m sections, the load is also reduced to half with the objective of facilitating the reversal operation.
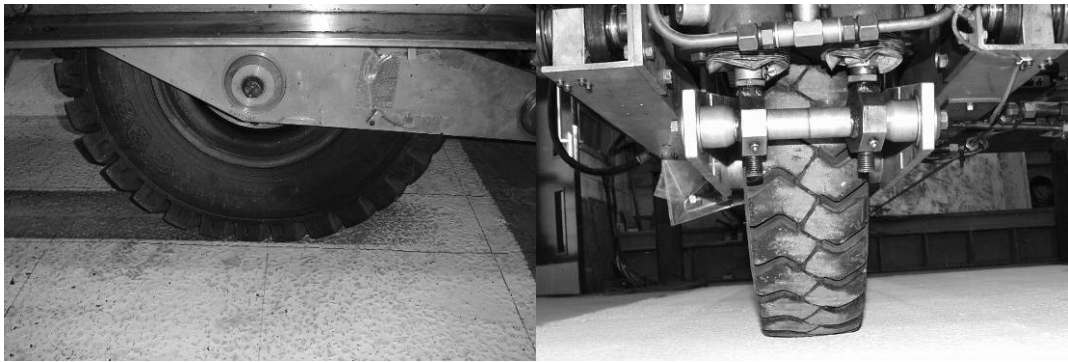
Figure 7.3 – Detail of the wheel/tyre used in the PTF

The instrumentation available, to monitor the degradation of the pavement's performance, includes strain gauges and load cells that can be imbedded in the pavement during construction. The surface deflection of the pavement can be measured by an external LVDT attached to a horizontal arm, which is fixed outside the pavement area (so that it is not influenced by the deflection bowl). All the signals can be connected to a data acquisition system and analysed afterwards. The electrical signals obtained from each device must be calibrated in order to convert them to the desired unit. The PTF operates at room temperature or up to 35 °C in the upper layer, which is achieved using infra-red heaters. However, it is not possible to refrigerate the room or the pavement and, therefore, the temperature tends to increase slightly during prolonged trafficking (with the heat produced by the hydraulic pump operating the PTF).

7.3 Variables included in the study

In this study, a direct comparison was established between five mixtures applied in the surface course, including the standard mix design that has been extensively tested up to the present point in this investigation. Thus, based on the results of the mix design study, three alternative mixtures were chosen to assess their performance in a

real (or half-scale) pavement situation. The last section was constructed using a standard grouted macadam mixture under-laid by Glasgrid® reinforcement (fibreglass grid, with 12.5 mm × 12.5 mm grid size, and a tensile strength of 100 kN/m), to evaluate the influence of the reinforcement on the performance of the material under traffic loading.

The test was set to be carried out in two wheel tracks, allowing the use of parallel sections in the surface course. Therefore, the surface of the pavement was divided into four longitudinal sections (2 sections per track) and one transverse section common to both tracks, which was used to assess eventual differential behaviour of the layers underneath each track. The layout of the pavement surface can be observed in Figure 7.4.
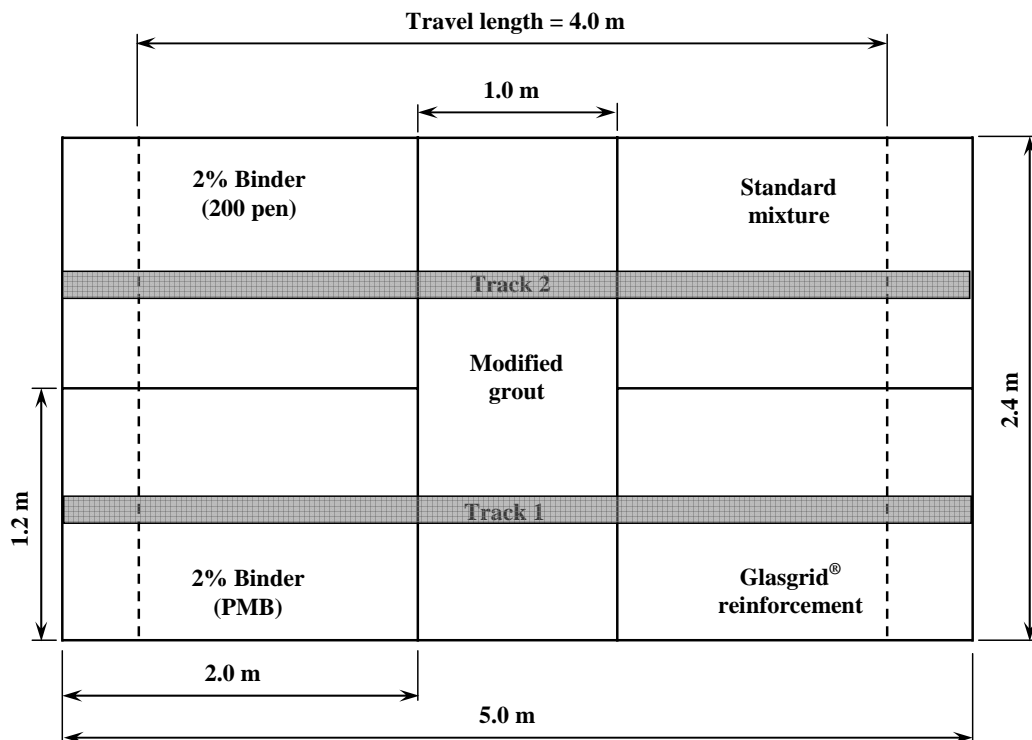
Figure 7.4 – Final layout of pavement sections

The choice of the variables to use in this test was made according to the fatigue results obtained in the mix design study and taking into consideration eventual cost savings by using cheaper materials or smaller quantities of the most expensive components. Therefore, a mixture comprising the polymer modified binder was used in this study, but a reduced binder content was chosen, in order to assess whether in such circumstances, the mixture would perform at least as well as the standard

mixture. To assess the effect of binder content, a mixture with a reduced binder content (the same binder content as the PMB mixture) was also used. The last of the five sections (central transverse section) was constructed with a mixture comprising a standard asphalt skeleton, but with a modified grout type of a lower compressive strength.

The reduced binder content used in two of the five sections was determined taking into consideration two requirements: (i) complete coating of the aggregates with bitumen; (ii) reasonable workability of the asphalt mixture in order to keep its voids content close to the specified range (25 to 30%). In order to assess those characteristics, a series of 6 Marshall compacted specimens was produced for the PMB mixture, each with a different binder content (ranging from 1.5 up to 4.0%). The dimensions and weight of each specimen were determined to calculate its density and voids content and a visual observation was undertaken to assess the level of uncoated aggregates. Results of this investigation are presented in Table 7.1. Regarding the aggregate coating, all binder contents resulted in specimens with good aggregate coating, except that with 1.5% binder, where some aggregates were not completely coated by the bitumen.

Table 7.1 – Voids content obtained for different binder contents

Binder content (%)	Density	Voids content (%)
1.5	1811	32.5
2.0	1822	31.6
2.5	1811	31.4
3.0	1833	30.0
3.5	1836	29.4
4.0	1879	27.1

Based on the results presented above it was decided to use 2% bitumen (by mass of asphalt mixture) in the sections with reduced binder content. Since these mixtures were produced in the laboratory, and due to the limited capacity of the mixer, mixing had to be divided into several batches to generate enough asphalt for the test sections. Furthermore, since these mixtures did not contain any cellulose fibres, a binder drainage test (Schellenberg method) was carried out on both the 2% binder mixtures, according to the Draft prEN 12697-45:2002 (BSI, 2002[a]). This was carried out in

order to assess if these mixtures were susceptible to binder drainage during the period of time between production and compaction, because after each individual asphalt batch was produced, it was placed back in an oven set at the compaction temperature until all the batches required for any one section were produced. The results obtained from the tests showed a mean drained material quantity of less than 0.1% for both mixtures, which corresponds to good behaviour of the mixtures against binder drainage. Thus, the choice of 2% binder did not present any inconvenience for the production, application and compaction of the mixtures, while contributing to a better understanding of the influence of using a reduced binder content, on the performance of the mixtures, under traffic loading.

Construction of the pavement demanded a considerable amount of grout, which was supplied by the project sponsors. However, one of the pavement sections was to be constructed with a different grout (with a lower compressive strength). Due to problems with the delivery of such a grout by the project sponsors, a specific investigation was carried out to obtain a weaker grout based on the powder of the standard material. In a first stage, several batches of grout were produced using different water contents (above the normal value), and cubes were cast from each batch. Twenty four hours after grouting the cubes were stripped from the moulds and segregation between the components of the grout was identified. This fact necessitated that a different approach should be used. In order to avoid segregation, a very fine material, silt (passing the 300 µm sieve size), was added to the cementitious powder and the water content was adjusted to produce grouts with workability equivalent to the standard grout. Three different silt contents (10, 30 and 50%, by mass of powder) were used to determine the compressive strength of the resultant grouts. Based on the test results at one-day curing time, the amount of silt, to be used as part of the modified grout, was determined by interpolation at 25%. The objective was to obtain a grout with a compressive strength equivalent to the average of the compressive strength of the other two grouts discussed in Section 5.5. Time restrictions prevented the use of the results obtained (later) for the compressive strength at 28-days curing time (which showed values higher than expected, as presented in Figure 5.4). Nonetheless, the modified grout obtained showed a noticeably lower compressive strength, compared with the standard grout.

7.4 Pavement construction

Prior to the construction of the pavement, calculations were made using a pavement design program previously developed at the University of Nottingham (Thom, 2000), in order to establish a pavement structure that would undertake some (quantifiable) degradation within a reasonable number of load applications (or period of time), due to the limited time available for the test. Taking that into consideration, it was decided to use a layer of concrete blocks (pavers), underneath the surface course, which would act as a cracked concrete (or cement bound) layer, creating a net of pre-defined regularly spaced reflective cracks. In theory, those cracks should propagate into the new surface layer (in the present case, grouted macadam), allowing the appearance of cracking on the surface, and subsequent degradation, to be monitored. The concrete blocks should be placed on top of a thin laying course of sand, which would be constructed on top of the granular material.

Based on the available information, material properties were estimated and introduced into the above-mentioned design program, which allows the inclusion of a reinforcing grid (one of the sections would be constructed with grid reinforcement). Two calculations were carried out for both reinforced and unreinforced situations, in order to design the thickness of the surface course corresponding to a fatigue life of approximately 50000 wheel passes (for the unreinforced section). The calculations resulted in a 35 mm thick surface layer, which should have a fatigue life of approximately 60000 passes. The results were based on the fatigue results of the standard grouted macadam mixture, obtained in the initial stage of the project using the Indirect Tensile Fatigue Test (the type of test for which the program was developed).

The subgrade (980 mm of clay) and type-1 granular sub-base (280 mm) used in the pavement construction were left inside the pit from a previous project. In order to characterise the existing foundation, a hole was opened through the sub-base, in one of the test pit corners, and a sample of the subgrade was extracted. This sample was then used to carry out a California Bearing Ratio (CBR) test and to determine the Plasticity Index (following liquid limit and plastic limit determinations). The CBR test was performed on two faces of a specimen placed inside a CBR mould,

according to the Asphalt Institute (1989) and the results showed an average CBR of 0.9% (very low), which indicates a subgrade with a very low bearing capacity. The Plasticity Index determination was based on BS1377:1990 Part 2 Classification Tests and the result obtained was 16% (LL=36; PL=20), representing a clay of intermediate plasticity. The water content of the subgrade was also determined, using four specimens extracted from the sample mentioned above, and the average result was 22.9%.

On top of the existing sub-base, an extra layer of granular material (135 mm thick) was applied over which 20 mm of sand was used as a laying course for the concrete blocks. Although the original plan was to complete the thickness of the granular material with type-1 sub-base material, a different granular material was used (a mixture of sand and gravel obtained from a local supplier). The decision was made based on the equipment available in the laboratory for compaction (a vibratory rammer/tamper), which would not have had the capability to properly compact a type-1 granular material. Therefore, the new granular material was applied in three thin layers (of less than 50 mm) and compacted manually, as illustrated in Figure 7.5, in order to achieve the maximum density.

Figure 7.5 – Compaction of PTF granular material

In order to monitor the degradation of the pavement bearing capacity, half of the middle section was instrumented. Three load cells were used to measure the stresses developed at approximately 200 mm depth (within the granular material layer) and three strain gauges were located at the underside and upper surface of the grouted

macadam layer. The position of the load cells was established in order to assess the distribution of the load under the wheel track and in the immediate area. Thus, two of the load cells were located under the track respectively under a concrete block and under the joint between two blocks. The third cell was placed under a block of a row adjacent to that under the wheel track. Figure 7.6 represents a simulation of the location of each load cell under the concrete blocks.

On top of each load cell a small amount of fine sand was placed in order to separate them from any large aggregate particles that could change the results obtained by concentrating the stresses at a single point. The remaining part of the granular material was then applied and compacted following the procedure described above. Following compaction, a thin layer of sand was applied to work as a laying course for the concrete blocks, which were put in place afterwards. The blocks were aligned longitudinally from the middle of the pit, and transversely from one of the joints separating the different sections. This procedure allowed the correct application of the blocks with respect to the position of the load cells, as described above.
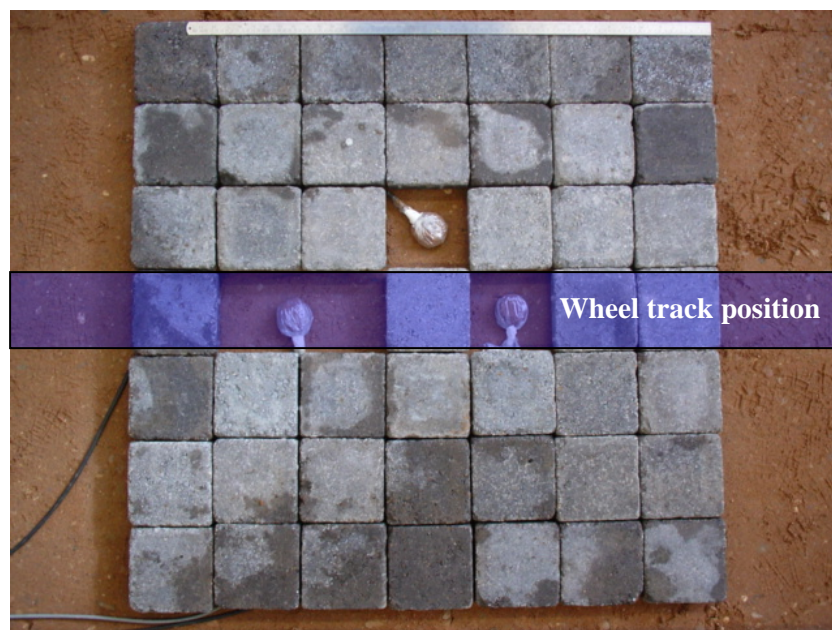
Figure 7.6 – Location of load cells in the granular material and their position relative to the concrete blocks

The German Dynamic Plate (GDP) and Dynamic Cone Penetrometer (DCP) tests were carried out on top of the sand, to estimate the bearing capacity of the pavement and the corresponding contribution of each layer. However, those tests were only performed after most of the concrete blocks were put into place, in order to increase

the stress level in the granular layers, due to the weight of the blocks, and to obtain more realistic values for the material properties. It is known that stiffness modulus of granular materials increases with the stress level. Thus, a few squares were left open in the layer of concrete blocks, along the wheel track positions, where the dynamic plate was placed to perform the tests (Figure 7.7). The DCP tests were also carried out in five of those locations (close to each corner and in the middle of the pit) slightly further away from the wheel tracks, as can be observed in Figure 7.8, to minimise the disruption of the wheel load distribution.
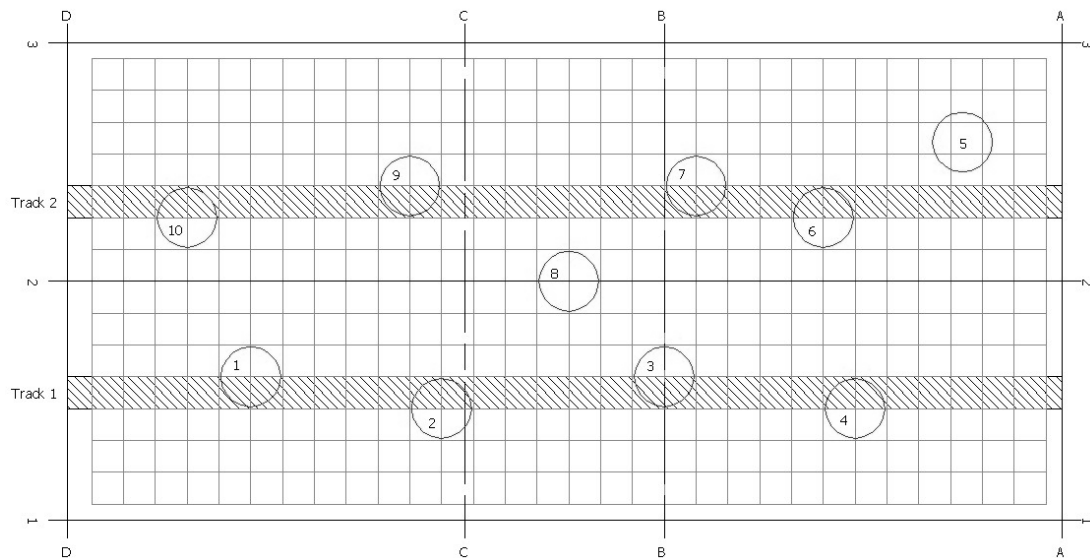
Figure 7.7 – Positions of the GDP tests

The DCP incorporates an 8 kg weight dropping through a height of 575 mm and a 60° cone having a diameter of 20 mm. The results of the DCP tests are presented in Figure 7.9, where it is possible to identify the boundaries (interfaces) between the different pavement layers, detected by a change in the penetration rate, and the corresponding thickness of each layer. In this figure it can also be observed that the major contribution from the granular layers to the bearing capacity of the pavement is given by the type-1 sub-base material. This 'improved' performance is partially due to the use of two geogrids in the sub-base layer, respectively located at the bottom and middle of the layer, which were already in place, left from the previous project. The geogrids were used as a subgrade improvement, due to its very low bearing capacity, as can be assessed by the CBR value below 1%. The central part of the pit shows the best performance, as can be seen in Figure 7.9 from the shallower slope of the line corresponding to position 8, probably due to a better compaction of the sub-base layer.

Figure 7.8 – Dynamic Cone Penetrometer test
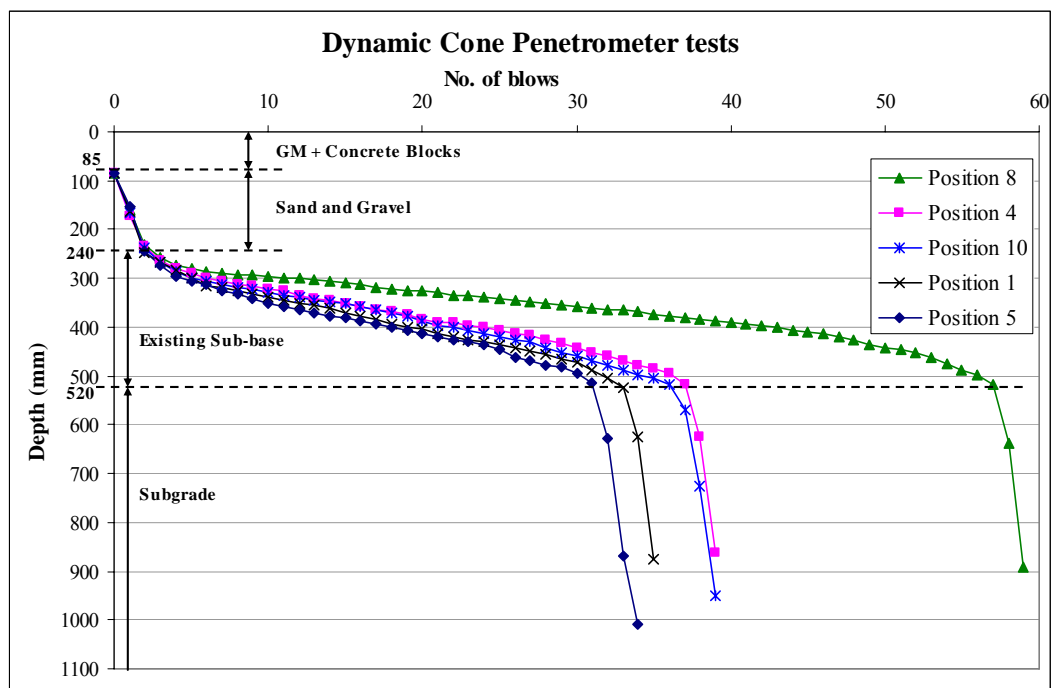
Figure 7.9 – Dynamic Cone Penetrometer (DCP) test results

The German Dynamic Plate (Figure 7.10) is usually used to determine the stiffness of pavement foundations, but can be used for granular materials in general. This equipment works in a similar way to the Falling Weight Deflectometer (FWD), but on a smaller scale, with a smaller mass involved and with only one geophone in the centre of the load. The plate must be adequately seated on top of the granular material and its stability examined by one to three drops of the loading mass as appropriate. Three additional drops of the loading mass are then applied. The result of the test is obtained by averaging the readings taken from the last three drops. The response of the material to the application of the load, measured by the surface deflection under the whole 300 mm diameter plate, is converted into an overall stiffness of the pavement underneath.

Figure 7.10 – German Dynamic Plate (GDP)

Ideally, a FWD test should always be performed, but on small sites like the PTF pavement, it becomes impractical. Based on Scott Wilson Pavement Engineering's large experience of performance testing on unbound foundation layers, a relationship between the results of both equipments (GDP and FWD) has been established, although a high level of scatter can be observed amongst the GDP results (Thom, 2003[b]). Equation 7.1 represents the correlation between the results of both types of equipment:

$$E_{GDP} = \frac{E_{FWD}}{\left(1 + E_{FWD}\big/150\right)} \tag{7.1}$$

Where E_{GDP} and E_{FWD} denote Stiffness derived respectively from the GDP and FWD equipment.

The results obtained with the GDP equipment are presented in Table 7.2, where the equivalent values of FWD stiffness, calculated from Equation 7.1, are also presented. One of the results (corresponding to position 5) was obtained without any concrete block around the equipment (as can be seen in Figure 7.10). It is clear from the result of position 5 that the overburden of the concrete blocks significantly changes the stiffness value of the granular material. Therefore, the result obtained for that position should not be considered as representative of the granular material stiffness.

Table 7.2 – GDP test results and equivalent FWD values

Position	E_{GDP} (MPa)	E_{FWD} (MPa)
1	43	60.3
2	49	72.8
3	43	60.3
4	44	62.3
5	36	47.4
6	42	58.3
7	46	66.3
8	49	72.8
9	47	68.4
10	44	62.3
Average	44.3	63.1
Std. Dev.	3.8	7.5
Disregarding values from Position 5		
Average	45.2	64.9
Std. Dev.	2.6	5.5

Once the characterisation of the granular material was finished, the layer of concrete blocks was completed and the joints filled with sand, in order to prevent any grout penetration to the layers underneath. The surface of the blocks was then cleaned from any dust or sand and tack coat was applied prior to the construction of each pavement section. The tack coat was used with two objectives: (i) to act as a sealant in the joints of the concrete blocks; (ii) to bind the surface course to the base. In order to guarantee a uniform distribution of the tack coat over the surface of the blocks, the application was carried out using a paint roll (Figure 7.11), controlling the rate of application by weighing the amount applied for the surface area of each section.

Figure 7.11 – Tack coat application in the first section

The porous asphalt mixture used in the construction of each section was produced in the laboratory, and compacted with a small roller compactor as illustrated in Figure 7.12. Due to the limited capacity of the mixer and ovens, needed to warm up the aggregates and bitumen prior to mixing, and to maintain all mixture batches at an adequate temperature, up to the time of application, only one section was constructed per day. After the mixture had time to cool down, the wooden pieces, used to contain laterally the mixture within the section area, were removed and the surface of the adjacent section was prepared to receive the bituminous mixture on the following day. In the case of the reinforced section, after the application and setting of the tack coat, a Glasgrid® reinforcement was placed on top of the concrete blocks

(Figure 7.13). The grid would subsequently be surrounded by the grout of the surface course and would then become an integral part of the surface layer.

Figure 7.12 – Compaction of porous asphalt in the first section

Figure 7.13 – Application of Glasgrid® reinforcement in the second section

The application of the porous asphalt in the other sections was made in a similar way as described for the first section. However, the central section was only applied after grouting all the other four sections, in order to prevent the two different grouts from mixing near the section joints. The same grout (standard Densit® powder) was used for the first four sections, which were grouted in a single operation on either side of the middle section, as illustrated in Figures 7.14 and 7.15.

Figure 7.14 – Application of the grout on the first two contiguous sections

Figure 7.15 – Application of the grout on the third and fourth sections

Prior to the application of the bituminous mixture in the last (middle) section, two strain gauges were placed on top of the concrete blocks (Figure 7.16), in order to

measure the strains induced in the surface course by the wheel loading. As in the case of the reinforcing grid, so the strain gauges would also be surrounded by the grout of the surface course. A third strain gauge was placed at the surface of the pavement, in the same section, after the compaction of the porous asphalt and before grouting, as illustrated in Figure 7.17. Two strain gauges (at the top and bottom of the surface course) were located in the wheel path, above a joint in the concrete blocks, and the third was placed adjacent to the wheel path and in the transverse direction.

Figure 7.16 – Pavement construction prior to the application of the porous asphalt in the last section

Figure 7.17 – Strain gauge located in the wheel path at the surface of the pavement

Once the grout from the last section had set, the level of the surface was monitored at several locations, which had also been used to monitor the level of the concrete blocks, in order to determine the thickness of the grouted macadam layer actually laid. Calculations made based on these readings gave the results presented in Table 7.3.

Table 7.3 – Average thickness of each section of the surface course

Section	Average thickness (mm)
Std. grouted macadam section	39
Reinforced section	39
Weak grout section (middle)	38
2% binder section	40
2% PMB section	42

The results presented in the table above should be analysed bearing in mind that the operations of laying and spreading the porous asphalt of each section were carried out manually, since it was not feasible to do it with a paver machine. Also the compaction was carried out with a light roller compactor as shown in Figure 7.12. Furthermore, the sections with reduced binder content showed an increased difficulty in the compaction operation, since the hot bitumen acts as a lubricant between the aggregate stones, and if the binder film thickness is reduced a higher degree of friction between the aggregates will result in less compaction of the material. Hence, the final thickness of the last two sections is slightly higher than the other sections, especially that of the polymer modified binder, which presents a higher viscosity due to its modified structure. The increased thickness of the layers (in excess of the designed 35 mm) resulted in slightly stiffer materials due to the volume of voids later filled with grout (a higher volume of grout and lower volume of bitumen results in a stiffer grouted macadam).

Once the pavement had been finished, the whole surface was painted white, so that the appearance of cracking and its development could be visually followed. Some auxiliary lines were drawn at the surface in order to help identifying the position and length of the cracks. The wheel was then positioned on the first track (the one passing over the instrumented section) ready for the start of the test.

7.5 Performance of the pavement during the test

The test was started after the grout of the last section had cured for 7 days. Ideally, all the sections should have been grouted at the same time, so that the performance of the different sections could be directly compared but, as previously explained, this was not possible. However, the fatigue tests carried out using the four-point bending equipment showed that after 7 days the curing time had little effect on the properties of grouted macadams. Thus, it was decided to start the test after 7 days, due to time limitations on performing the test, which had to be carried out in two wheel tracks.

The performance of the pavement was assessed in two ways: (i) visual observation, mapping the appearance and propagation of cracks; (ii) data acquisition from the LVDT, strain gauges and pressure cells installed in the pavement. The former was carried out once a day, at the end of trafficking, after stopping the wheel. The latter was performed several times a day (with a minimum of three recordings), in order to be able to follow the degradation of the pavement bearing capacity. In Figure 7.18 an example is given of the data acquired from the instrumentation, for one cycle, representing the initial condition of the pavement (after just 10 wheel passes). The test was performed only during daytime and both the pavement and the equipment were left to rest during the night. Regarding the pavement, these rest periods can be seen as a realistic way of simulating what happens in a real pavement. As far as the machine rest is concerned, this was to avoid overheating some of the mechanical parts, resulting in premature wearing and unnecessary maintenance/repairs in order to keep it running.

The data files obtained from the data acquisition system had to be converted into the variables that were being analysed, since all the signals recorded could only be plotted as time (sec.) against voltage (within the range of $\pm$ 5 volts). Therefore, calibration factors were applied to each signal in order to obtain the corresponding value in the desired units. Figure 7.19 represents the results obtained for the surface strain and deflection obtained at the beginning of the test. In that figure, the time has also been converted into travel distance of the wheel, according to its velocity.
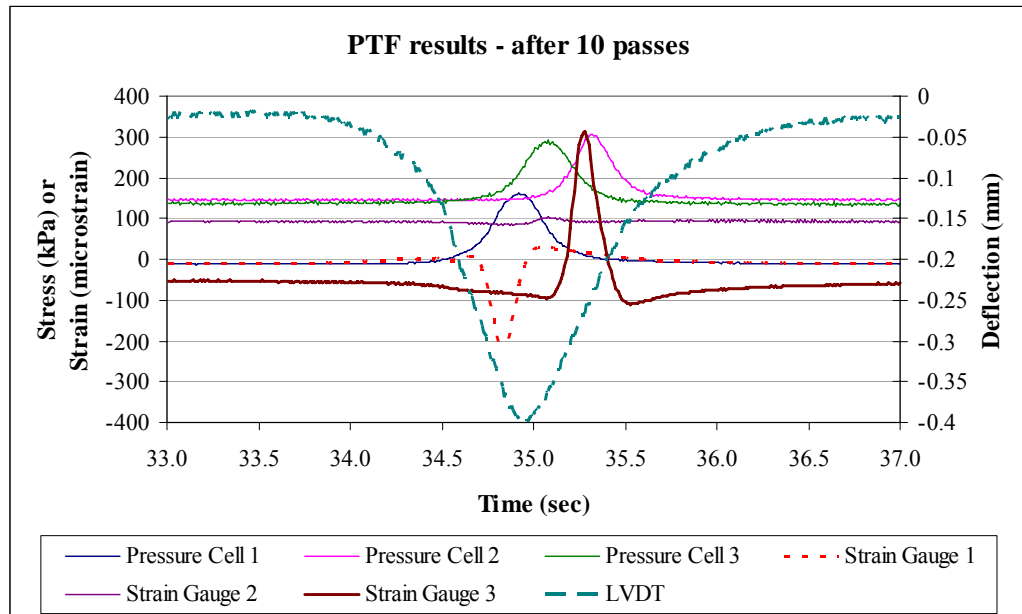
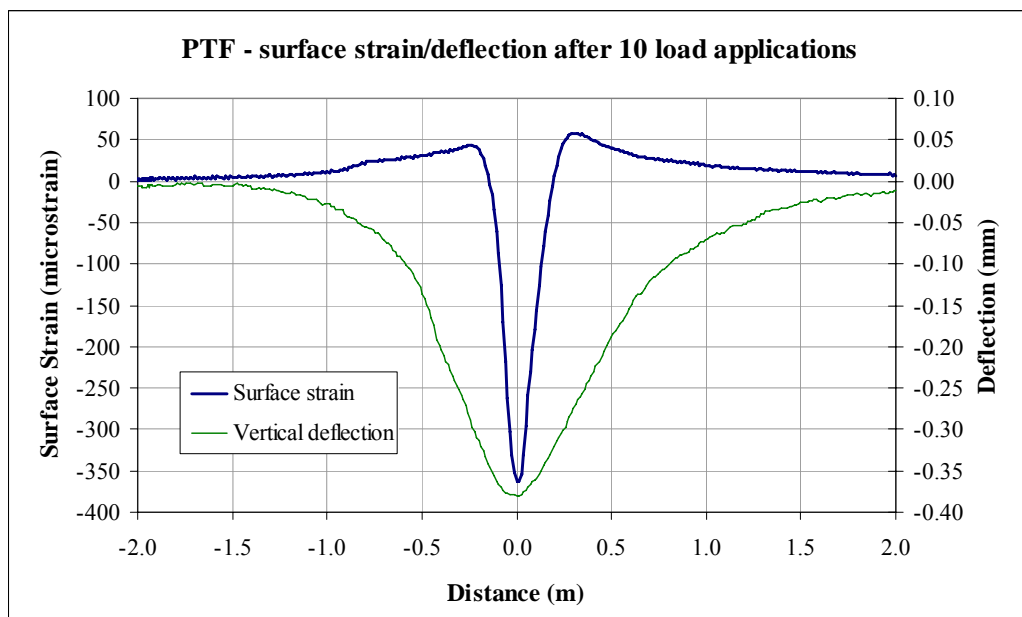Figure 7.18 – Converted signals from the instrumentation for one wheel pass

Figure 7.19 – Surface strain and deflection at the beginning of the test

Visual observations identified cracks across the joint between sections within a few 10´s of cycles, and gradually propagating along the construction joint. Even though care was taken to properly apply tack coat on the vertical interfaces between sections, it was not possible to avoid the formation of a discontinuity in those positions. This fact influenced the performance of the pavement, since the load could not be transferred to the next section and distributed over a bigger area, contributing to a premature failure of the pavement. This therefore highlighted the importance of the construction joints in the performance of grouted macadams. Feedback from the

project sponsors also confirmed some premature pavement failures in construction joints or day joints (when grouting operation has to be interrupted).

After the first day of testing (with 3127 cycles completed on track1), cracking was visible along the construction joints between the middle and the outer sections (active cracks – the vertical movement could be felt by placing the finger on top of the joint when the wheel was passing) and along the construction joint between the sections with the standard mixture, reinforced and unreinforced (in this case, only inactive fine cracking was visible). No cracking was visible along the construction joint between the sections with reduced binder content, which may be associated with their higher stiffness and thickness, resulting in better load distribution.

Apart from the construction joints, cracking was also visible parallel to the wheel path, positioned at approximately 160 mm from the edge of the tyre (coinciding with a longitudinal joint between concrete blocks). These cracks started near the construction joints between the middle section and the outer sections, propagating firstly to the middle section and to the other sections afterwards, as illustrated in Figure 7.20. The main reason for the appearance of such cracks is associated with lack of support from the layers underneath. The pavement was designed not to be too strong, but it seems that it's bearing capacity ended up being overestimated, especially with regard to the subgrade. At the end of the first day of testing, permanent deformation in the middle section, under the wheel, had already reached 6.9 mm. Hence, the position of the longitudinal cracks was also close to the rut inflection point, where the tensile strains are higher at the surface (similar to what can be observed in Figure 7.19), contributing to a quicker crack propagation.

Hairline cracking was also visible throughout the middle section, as can be observed in Figure 7.21 by the lines highlighted in orange, after the first day of testing. This type of cracking was not visible in any other section, which indicates a different behaviour of the material produced with the modified Densit® grout. The cause for the widely spread hairline cracking is the higher autogenous (drying) shrinkage of the modified grout (as previously presented in Table 5.6 and Figure 5.6).
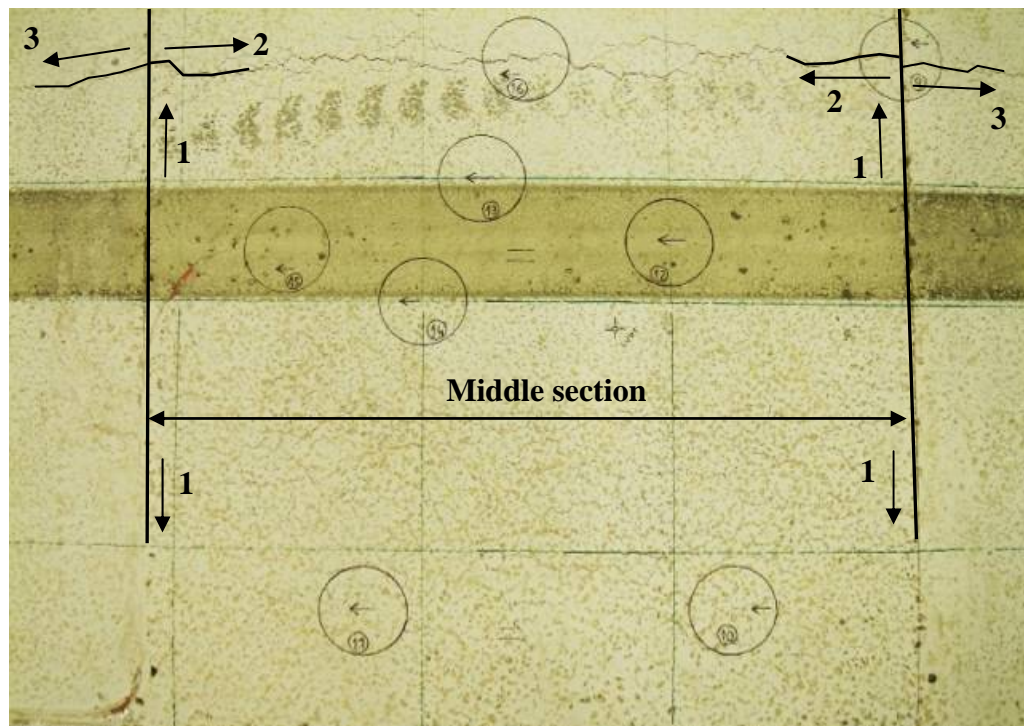
Figure 7.20 – Appearance and propagation of the first cracks in the PTF pavement
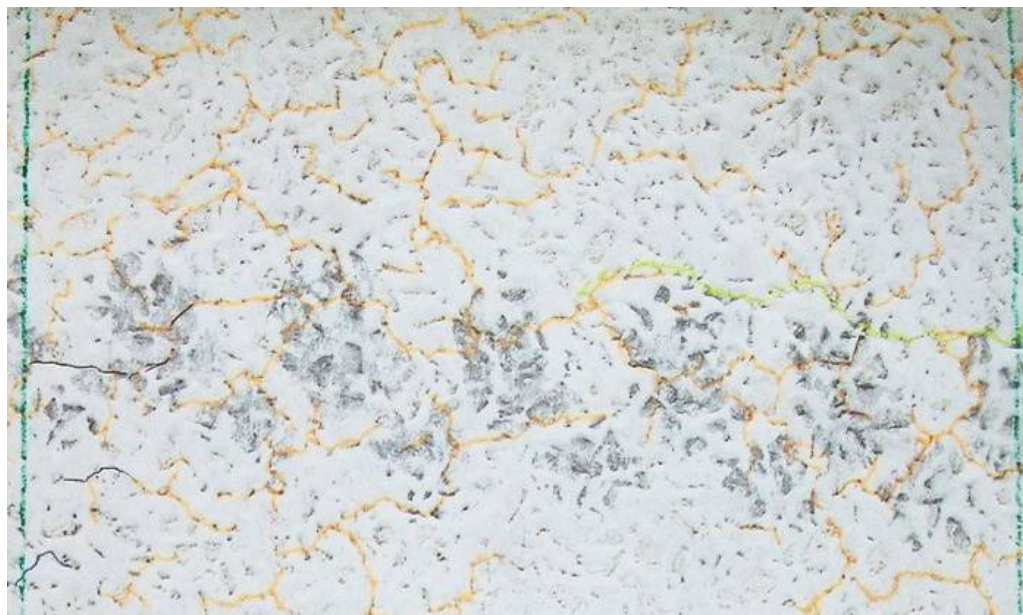

Figure 7.21 – Hairline cracking in the middle section due to autogenous shrinkage

The first track was trafficked up to 20000 cycles (wheel passes) and the degradation of the pavement was followed by measuring the recoverable deformation (deflection) several times a day and the permanent deformation daily (at the end of the day). Originally, only the deflection of the instrumented section (middle section) was measured, to complete the information for the same part of the pavement. However, after the formation of the construction joint cracks, the results no longer represented

the 'normal' pavement deflection. Therefore, after 15000 cycles, surface deflection was also measured on the other sections, moving the LVDT device each time a reading had to be taken. Crack propagation was also manually recorded on paper and highlighted on the pavement with a different colour, in order to differentiate the contribution of each day's cycles.

At the end of the test in the first track, the main cracking pattern resulted from the slow propagation of the cracks that appeared on the first day. The section with the worst performance was the middle section, with lower thickness, less stiff grouted macadam and a smaller area over which to distribute the wheel load, after the discontinuities at the construction joints were formed. Between the other two sections, the one with 2% polymer modified binder showed slightly better performance (lower amount of cracking) than the reinforced section constructed with standard grouted macadam. It should be emphasised that all main cracks occurred in locations where the tensile strains, imposed by permanent deformation (structural rutting), were close to their maximum values, and there was neither evidence of fatigue cracking nor reflective cracking from the concrete blocks, under the wheel path, at the end of the test. The reinforcing grid was not efficient in preventing the cracking at the surface (its location at the bottom of the layer did not contribute to a better performance of the material, since the maximum strains were situated at the surface). It would have been more effective in preventing thermal cracking (horizontal movements at the bottom of the layer, rather than vertical deformation).

Since surface cracking was exclusively derived from permanent deformation of the subgrade, and no sign of fatigue cracking was visible, it was decided to stop the test in track 1, after 20000 cycles, and move the wheel to track 2, in order to assess the performance of the mixture in the middle section on both tracks (establishing a direct comparison of the performance of both sides), and to carry out the test on the remaining two mixtures. At that stage, parts of the construction joint between the middle section and the un-trafficked sections were already cracked, as a consequence of the traffic in the first track. Hairline cracking was also visible in most of the middle section area.

The degradation of the sections under the second wheel track happened in a similar manner to that of the sections under the first track. The rate of crack propagation and permanent deformation was slower though. By the time the test was started in track 2, the middle section (comprising the modified grout) had already achieved a higher level of strength (curing of cementitious part), as compared with that at the beginning of the test in track 1, and therefore, the wheel load was distributed more efficiently and the rate of permanent deformation was reduced. Nonetheless, the position and propagation of the main cracks were observed in similar locations to those of track 1.

At 20000 wheel passes on both tracks, a comparison was made of the relative performance of each section/mixture. The modified grout section showed the worst performance, especially the part under track 1, both in terms of cracking and structural rutting. Amongst the other sections, the 2% PMB section seemed to be the one with best performance, both in terms of permanent deformation (Figure 7. 22) and also amount of visible cracking.
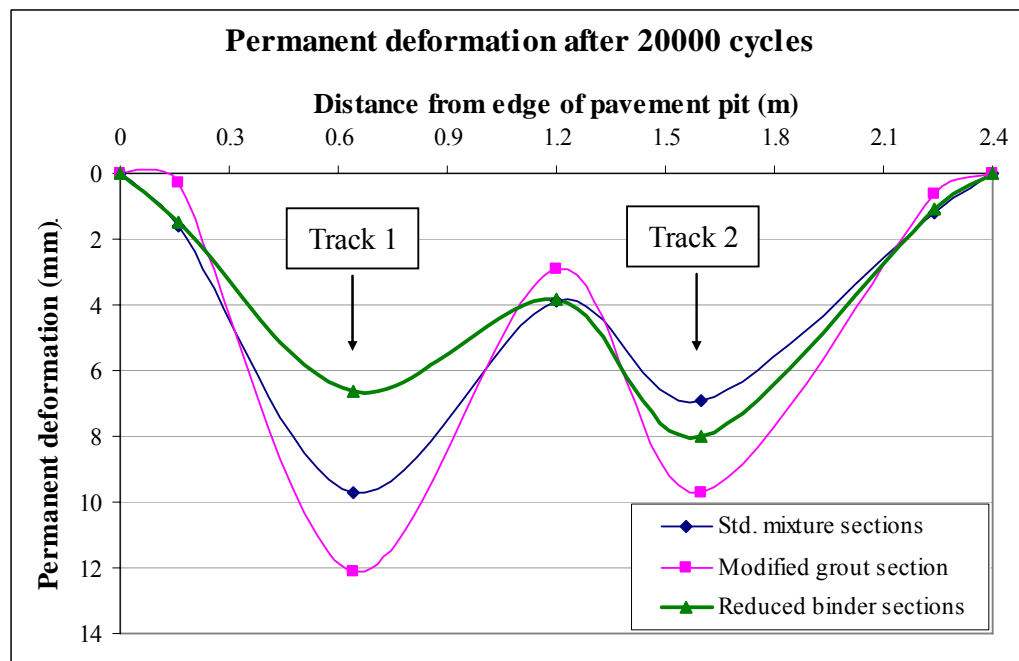

Figure 7.22 – Permanent deformation measured at the surface of the pavement, transversely to the wheel tracks, after 20000 wheel passes

At this stage some very fine (mostly transverse) cracks were visible on the second wheel path, especially on the standard mixture section, which could be either fatigue

or reflective cracking. Therefore, it was decided to continue running the test on that track in order to evaluate the possible degradation of such cracks. A further 20000 cycles were applied and the degradation of the above-mentioned cracks was reassessed. Visual observations confirmed the presence of the same cracks and a few others, but no apparent degradation (opening or propagation) was visible. The test was then extended for an additional 20000 cycles (i.e., 60000 cycles in total), after which a complete assessment of the pavement condition was carried out. The main cracks were still those formed by structural rutting, parallel to the wheel tracks, as schematically illustrated in Figure 7.23.

Figure 7.23 – Main cracks observed at the pavement surface at the end of the test

The thickness of the lines used in the figure above represent the severity of the cracks (a thicker line representing a wider crack). At this stage, the cracks observed on the second wheel path were still very fine and closed cracks and the deformation rate had also decreased, as can be deduced from Figure 7.24 which shows the evolution of permanent deformation in the middle section. Therefore, it was decided to terminate the test and to extract some specimens from each section, away from and in the wheel path, in an attempt to assess the damage induced by the traffic on the material close to the wheel tracks. Further details about the testing programme are given in the following section.

The origin of the observed deformation was confirmed while deconstructing the pavement. As can be observed in Figures 7.25 and 7.26, the deformation of the surface course is negligible and the subgrade was mainly responsible for the pavement rutting.
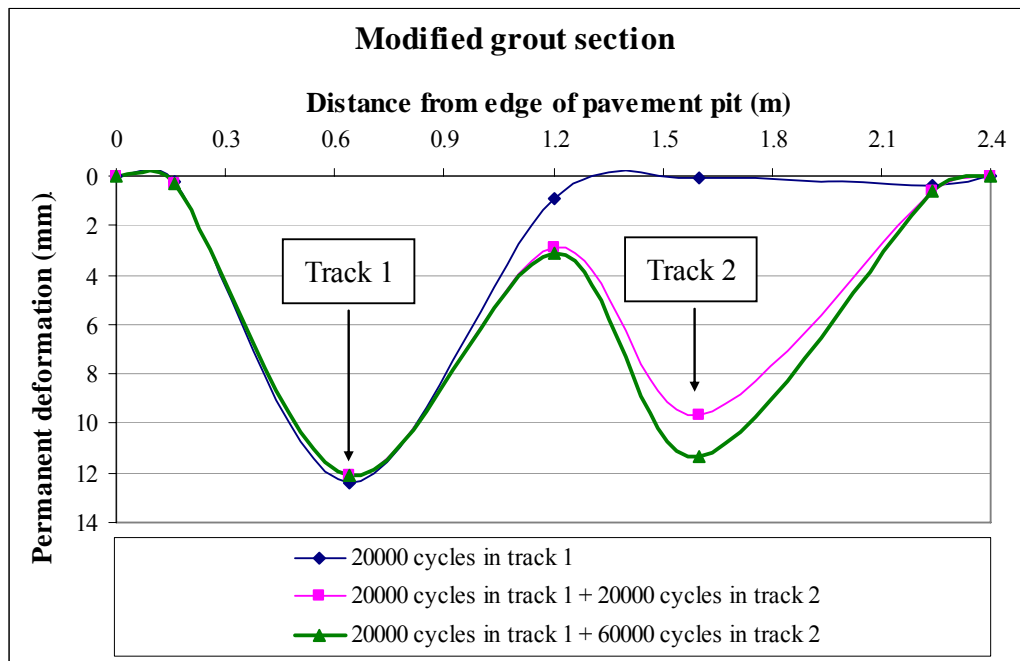
Figure 7.24 – Permanent deformation measured at the surface of the middle section, transversely to the wheel tracks

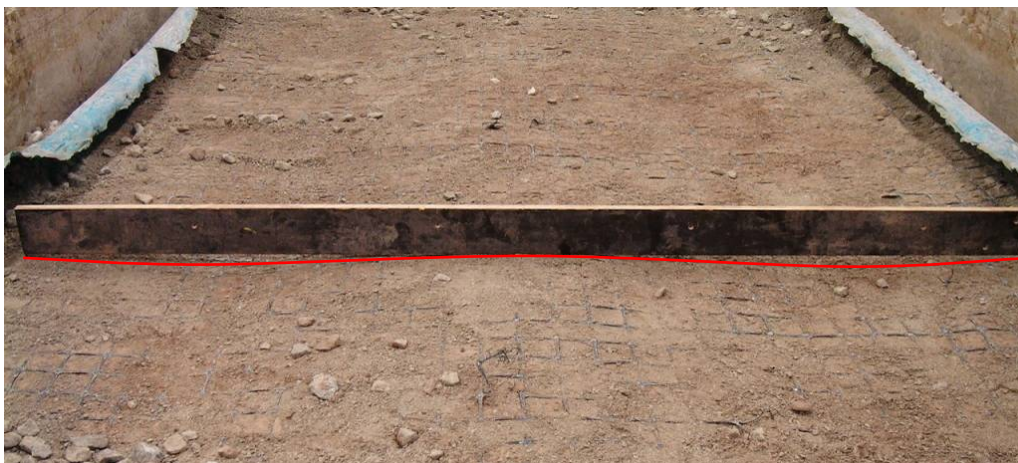Figure 7.25 – Negligible deformation within the surface course

Figure 7.26 – Permanent deformation observed at the top of the subgrade

7.6 Laboratory testing programme carried out on specimens extracted from the surface course

A series of laboratory tests was carried out on cores extracted from the surface course of all five sections of the PTF pavement (Figure 7.27). Two different types of specimen were used in this investigation: 'undamaged' specimens extracted from areas away from the wheel tracks, where no apparent damage had occurred (no visible cracking); specimens from the loaded areas (wheel tracks) where some fine cracks, possibly due to fatigue or reflective cracking, could be observed. The objective was to determine whether the specimens obtained from the loaded ('damaged') areas had undergone any degradation, when compared with the specimens from the 'undamaged' areas.
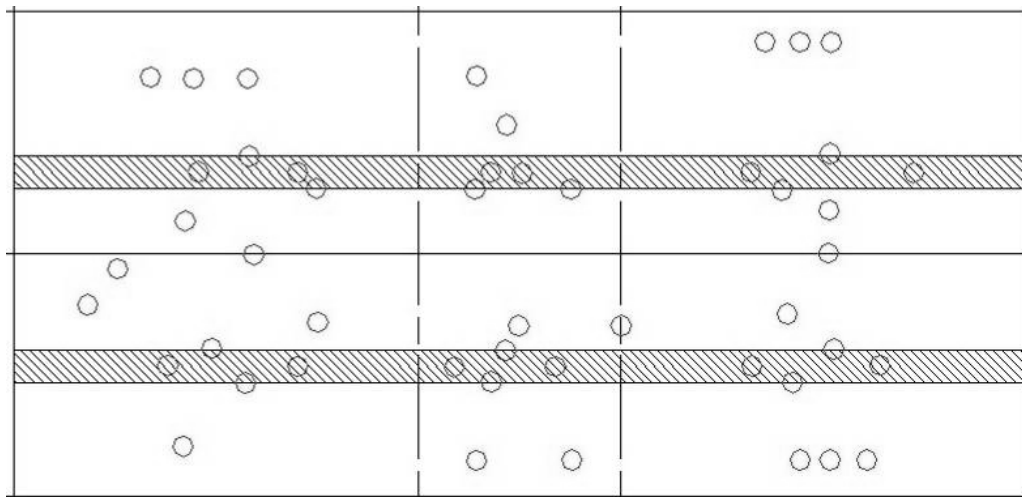

Figure 7.27 – Positions of the cores extracted from the surface course

Prior to coring, an arrow was painted on each core location indicating the direction of wheel tracking. The bottom of each irregular specimen was trimmed off, in order to obtain a flat surface and constant thickness. ITSM tests were then carried out on the specimens and their stiffness was determined. A horizontal deformation of 3 μm (instead of the standard 5 μm) was used to prevent damage to the specimens. ITFT tests were also carried out following the ITSM tests to assess if the residual fatigue life of the 'damaged' specimens was significantly affected in comparison with that of the 'undamaged' specimens. In all ITSM and subsequent ITFT tests, the specimens were positioned in the NAT so that the direction of trafficking was in line with the loading strips. Figure 7.28 represents the average results obtained for the ITSM tests carried out on specimens from each section.
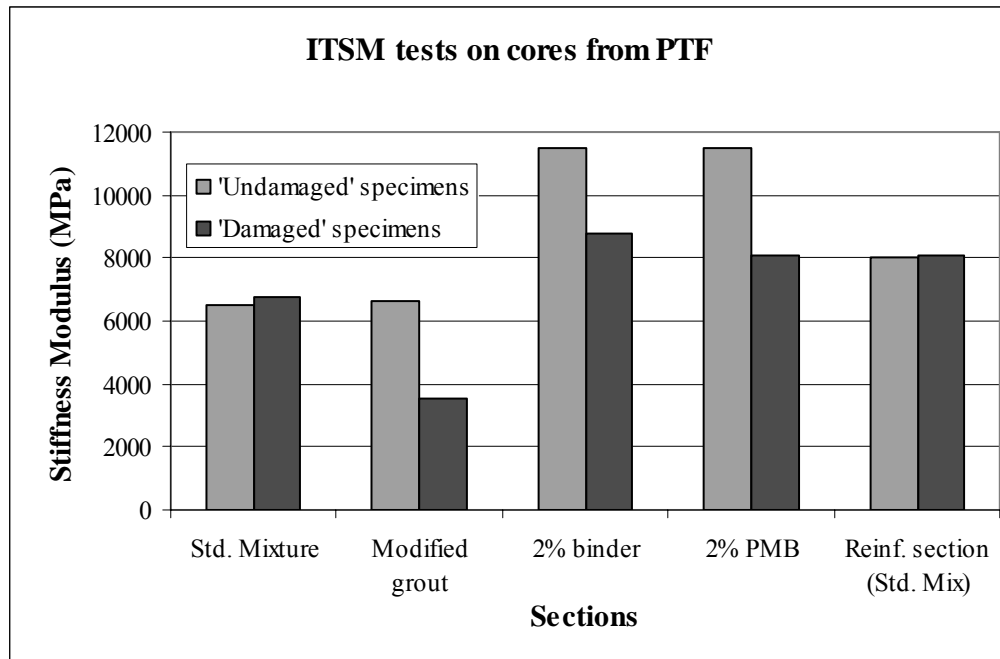
Figure 7.28 – Average ITSM test results obtained on cores extracted from PTF

Apparently, no damage was induced in the standard mixture, used in two of the five sections of the PTF (reinforced and unreinforced), while the stiffness modulus of the other mixtures was affected by the load applications. However, the damage seemed to occur at the beginning of the test, as the results obtained for 20000 cycles and 60000 cycles were nearly the same. For instance, the specimens from the middle section were extracted from both wheel tracks (each with a different number of loading cycles) and their stiffness modulus was approximately the same (3689 MPa for track 1 and 3510 MPa for track 2, on average). The stiffness reduction observed for the 2% binder section is also lower than that of the 2% PMB section, even though the former section was loaded 3 times more than the latter. In addition to this evidence, the performance of both sections against permanent deformation showed a different trend, with the 2% binder section presenting a higher deformation than the 2% PMB section, after 20000 cycles on both tracks (as illustrated in Figure 7.22). As previously stated, the degradation rate was much slower on track 2 after 20000 wheel passes.

Visual observation of the cores extracted from cracked areas of the surface confirmed the results shown above. None of the cracks observed had travelled through the entire thickness of the layer, an example being given in Figures 7.29 and 7.30, respectively representing a core extracted from the middle section and the

resulting hole in the pavement. In these figures, the open crack visible at the surface did not propagate much towards the bottom of the layer, stopping even before the middle of the 40 mm thick layer (approx.).

Figure 7.29 – Core extracted from PTF middle section

Figure 7.30 – Hole in PTF as a result of extracting a core from the surface course

In an attempt to better understand the influence of the load applications on the properties of the different mixtures, ITFT tests were carried out on the same specimens used for the ITSM tests. This would allow an estimation of the residual life of each mixture relative to the 'undamaged' specimens' fatigue life. Although the number of specimens obtained from each section is not very significant, their fatigue life can be plotted as a conventional fatigue line, as exemplified for the specimens extracted from both sections comprising the standard grouted macadam mixture (Figure 7.31). In this figure it is possible to observe that no apparent damage was induced in the specimens as a result of the load applications. The fatigue life obtained for the 'damaged' specimens is situated above the fatigue line obtained for the 'undamaged' specimens.
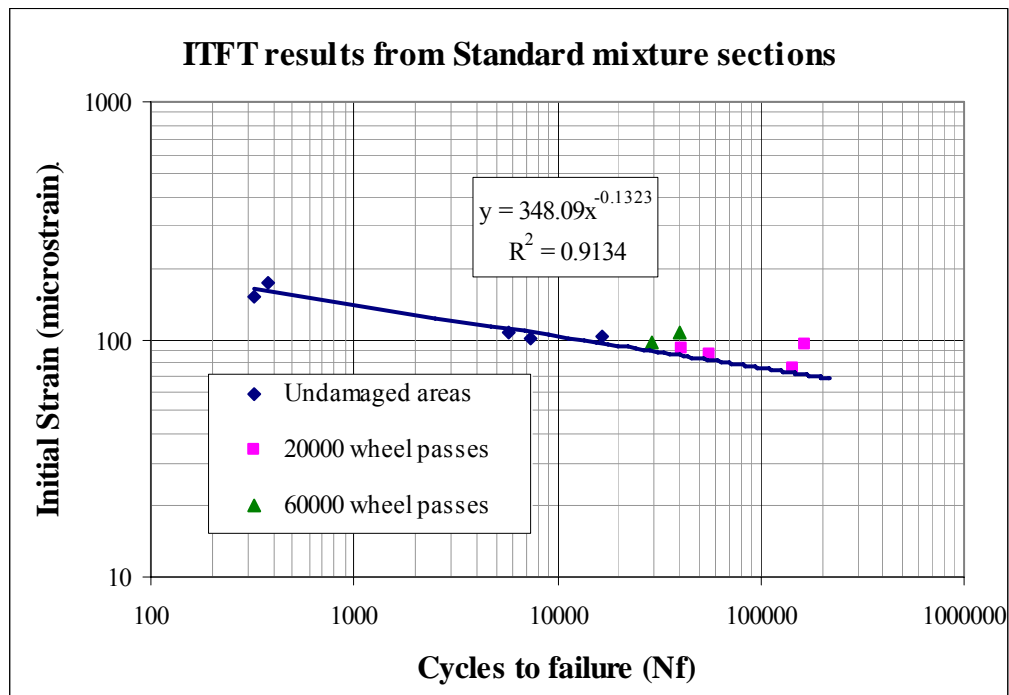

Figure 7.31 – ITFT results obtained from cores extracted from standard mixture sections

Similar trends were obtained for the other mixtures and the results are summarised in Figures 7.32 and 7.33, respectively, for the specimens extracted from 'damaged' and 'undamaged' areas. The amount of scatter in these results is significant, both due to the different materials analysed and the reduced number of specimens tested. Nonetheless, it can be observed that the fatigue life of the specimens was, in general,

not affected by the traffic. For an easier comparative analysis of the results, both fatigue lines are plotted together in Figure 7.34.
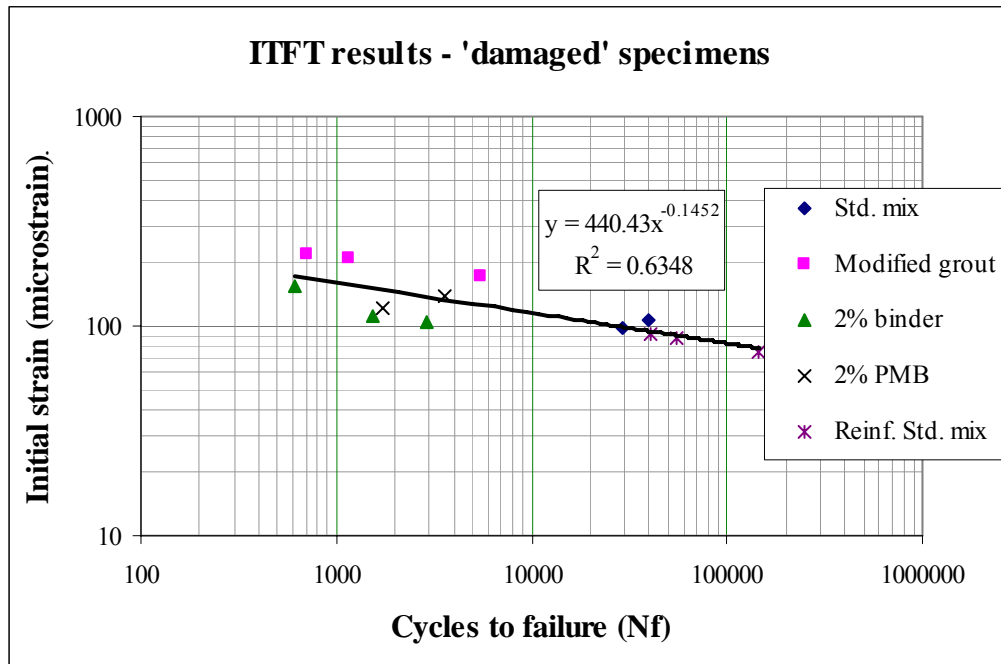

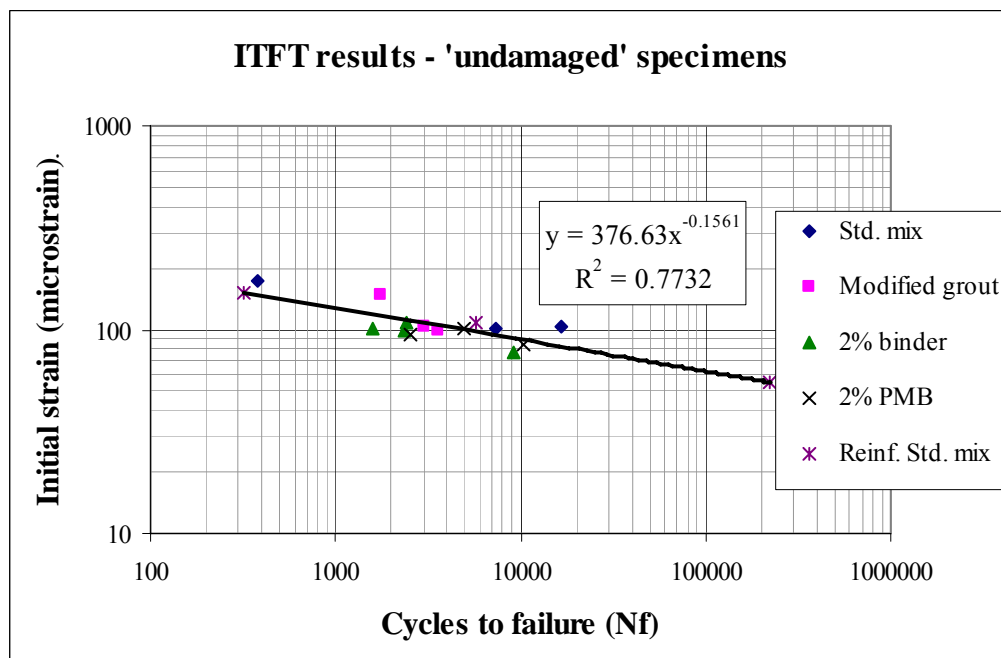Figure 7.32 – Fatigue results of 'damaged' specimens

Figure 7.33 – Fatigue results of 'undamaged' specimens

The influence of load applications on the performance of the mixtures was more perceptible in terms of a significant reduction in the stiffness of non-standard mixtures. This implies a reduction in the pavement bearing capacity, which may

result in a premature failure of the layers underneath leading to the appearance of surface cracking due to structural rutting, observed in this investigation. However, the grouted macadam mixtures did perform well in terms of fatigue cracking. Even the specimens extracted from the wheel path, containing some fine cracks, did not show any signs of a reduced fatigue life in the ITFT tests.
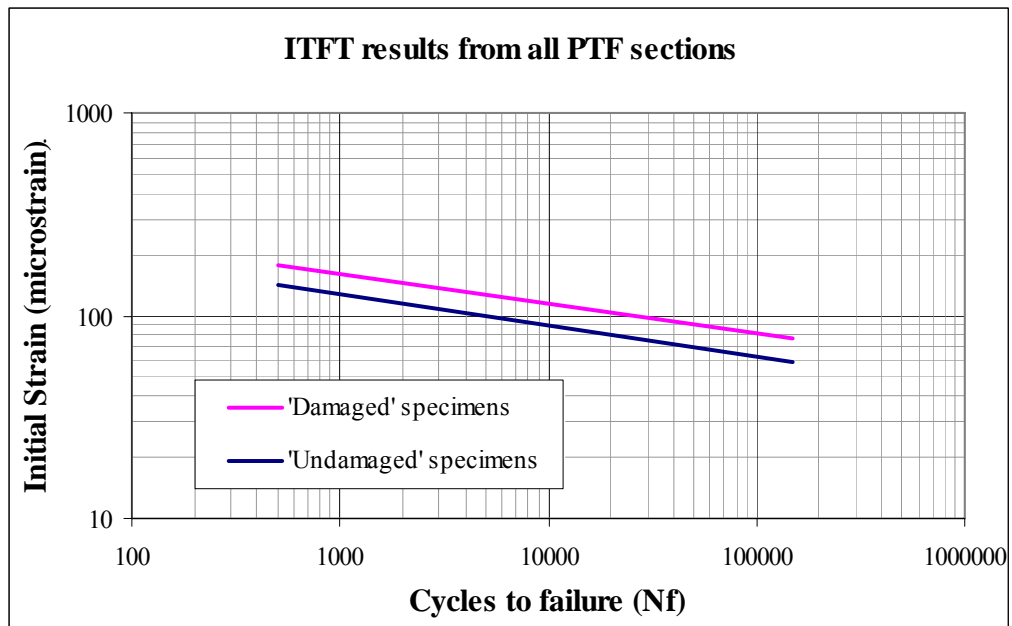

Figure 7.34 – Comparison between fatigue lines of 'damaged' and 'undamaged' specimens

Five slabs were also extracted from 'undamaged' areas of the surface course (one from each section), which were then cut into beams and tested in the four-point bend testing apparatus (using displacement control). From each slab, 5 beams were obtained and these tests allowed a more comprehensive characterisation of the mixtures in terms of stiffness, phase angle and fatigue life. Figures 7.35 and 7.36 represent the average stiffness and phase angle results obtained for those five specimens. The rank of each mixture, according to their stiffness, is comparable to that obtained from the ITSM tests, using the 'undamaged' cores. However, the absolute values obtained with the four-point bending tests are slightly higher than those from the ITSM. The variability of the results and the number of specimens used for each test type suggest that the four-point bending results may be more representative of the actual stiffness of each mixture.
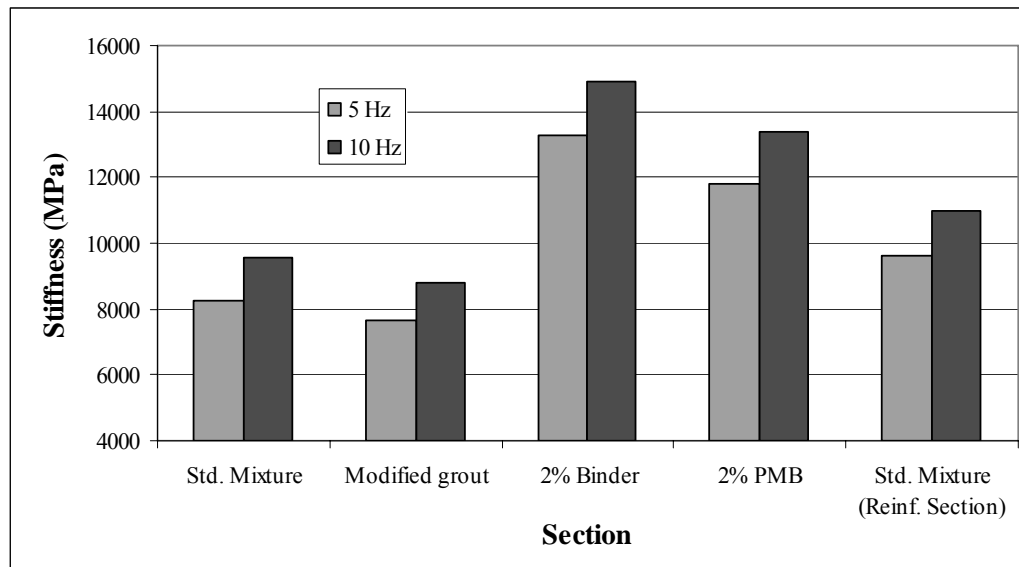
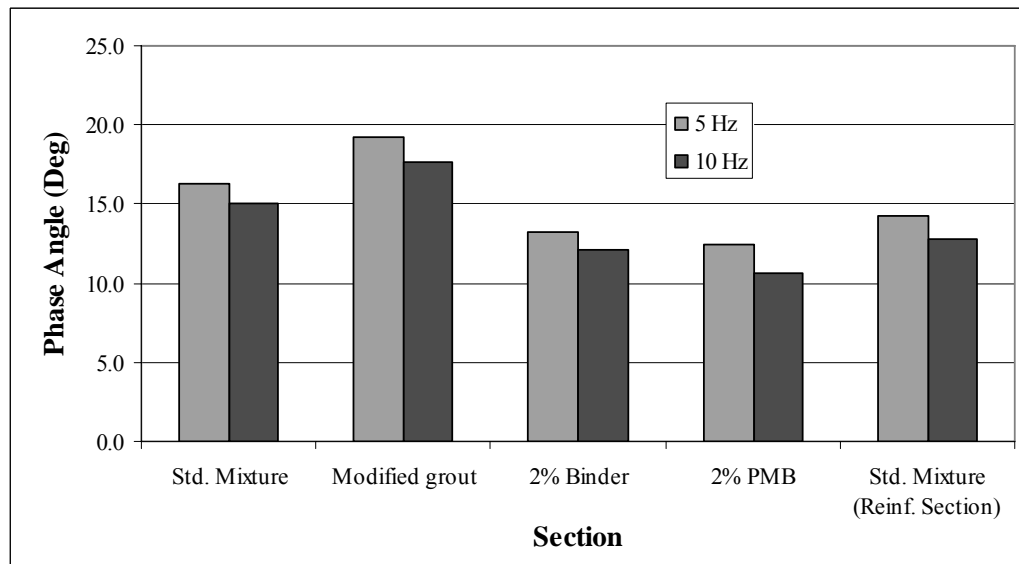Figure 7.35 – Stiffness modulus of each PTF mixture

Figure 7.36 – Phase angle of each PTF mixture

As in the mix design study, fatigue tests were carried out on the same specimens. The results of the standard mixture sections are plotted in Figure 7.37, which shows very similar fatigue lines for both sections. Thus, in Figure 7.38, the results from both standard mixture sections are plotted as part of the same fatigue line, in comparison with the other mixtures. The mixture with 2% PMB is the one with best fatigue performance, as expected from the results obtained in the mix design study, due to the modified nature of the binder. The modified grout mixture has a steeper fatigue line, showing a lower fatigue performance at low strain levels. Due to a thinner

bitumen film thickness, the 2% binder (200 pen) mixture presents the worst fatigue line, although not by much.
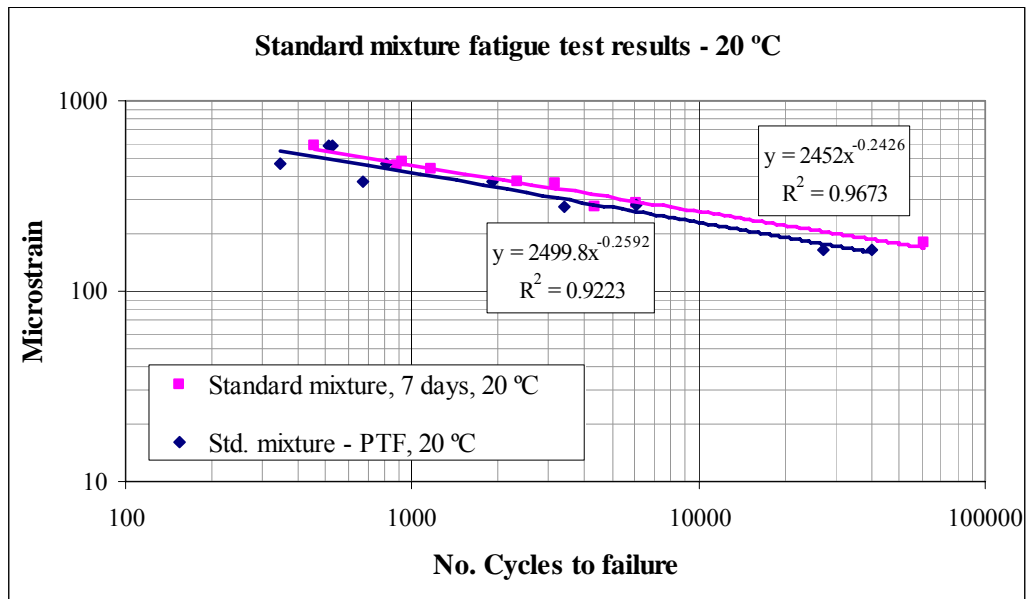

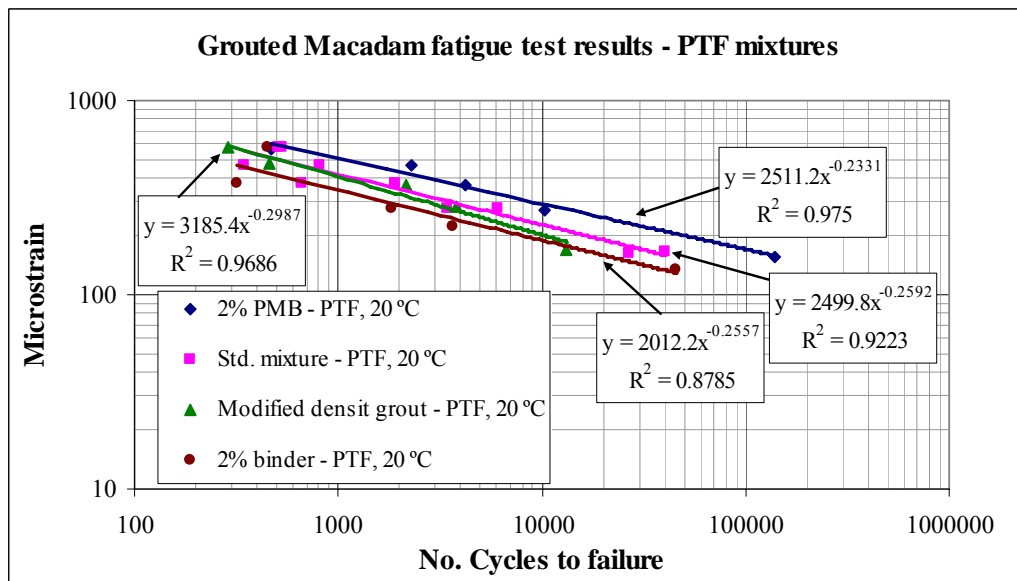Figure 7.37 – Four-point bending fatigue results of each PTF standard mixture

Figure 7.38 – Four-point bending fatigue results of each PTF mixture

Assuming that no damage has been induced in the specimens used for this investigation, the mixture used in the instrumented section (modified grout) should have reached failure after approximately 11000 load applications, based on the initial strain measurements at the bottom of the layer (approx. 200 µε) as shown in Figure 7.18 (Strain Gauge 1). However, the results obtained from the ITFT tests showed that the specimens extracted from the wheel path (after being subjected to

60000 wheel loads) had a residual fatigue life comparable to the 'undamaged' specimens. Although some error may be associated with the instrumentation readings, and some assumptions have to be made in the calculations, namely regarding the type of loading (strain controlled four-point bending tests, compared to a stress controlled situation in the PTF), these results highlight the particular fatigue behaviour of grouted macadams, that they seem to maintain their fatigue performance even after some damage (stiffness reduction) has been induced. Based on such facts, a different approach to fatigue performance of grouted macadams was considered and is discussed in the following chapter, regarding the design of pavements incorporating grouted macadams.

7.7 Summary and Conclusions

The present chapter is concerned with the construction in the laboratory of a half-scale pavement incorporating grouted macadam as the surface course, which was monitored in order to follow the appearance of cracking and its degradation, as well as the evolution of permanent deformation, while being loaded in the Nottingham Pavement Test Facility (PTF). The design of the pavement was influenced by the limited time available to run the test and the limited load that could be applied by the wheel in the PTF.

The variables included in the study were chosen mainly based on the results obtained from the mix design study (discussed in the previous chapter). The dimensions of the pavement pit allowed the use of five different sections in the surface course: one made with the standard mixture used as a reference; three sections comprising three alternative mixtures and; a fifth section with a standard mixture applied over a reinforcing grid (Glasgrid®). Regarding the three alternative mixtures, two sections were constructed with a reduced binder content (2% by mass of asphalt) using two different binders (a 200 pen straight-run bitumen and a polymer modified bitumen) and the last section was constructed with a modified Densit® grout. Two wheel tracks were used to apply the loads on all sections (4 longitudinal and 1 transverse, relative to the wheel track direction).

Complementary tests were carried out to assess the viability of the alternative mixtures, namely regarding the composition and strength of the modified grout, the binder drainage and voids content (density) of the mixtures with reduced binder content (produced without fibres). Some adjustments had to be made to the grout composition prior to pavement construction. Also the existing granular materials were characterised by some laboratory and 'in situ' tests. The subgrade CBR and Plasticity Index were determined, which showed a clay with intermediate plasticity and low bearing capacity (CBR below 1%). DCP and GDP tests were also carried out on top of the sub-base in order to characterise the whole granular part of the pavement structure.

Pressure cells and strain gauges were installed in one section of the pavement, in order to follow the degradation of the pavement performance. However, the instrumentation proved to be of limited use due to premature failure of the section where it was installed.

Some inevitable unevenness and thickness variation of the surface course was identified after construction, due to manual spreading of mixture and compaction with a light roller compactor. Nonetheless, full penetration of the grout was obtained in all pavement sections, as proved from the cores extracted from the surface course.

The first cracks appeared within a few 10's of cycles, across the construction joints between sections, gradually propagating along the joints, which highlight the importance of construction joints for the proper performance of the pavement. After a discontinuity had been created between the various sections, the load distribution was limited to the area of each individual section, increasing the stress level on the layers underneath. Due to a smaller area in the middle section, the increased stresses induced in the subgrade led to structural rutting, followed by the appearance of surface cracking parallel to the wheel track, due to the excessive permanent deformation.

Hairline cracking was observed in the modified grout section which did not influence significantly the performance of the mixture (except that the stiffness modulus may have been affected). Nonetheless, this emphasizes the importance of properly

characterising a cementitious grout prior to including it in a grouted macadam mixture, in order to predict its behaviour on site.

Very little fatigue cracking was observed in the wheel paths after 20000 cycles had been applied on each track. Additional traffic was carried out on the 2nd track in order to evaluate the degradation of the pavement, which was stopped after an extra 40000 wheel passes had been applied, due to a reduced degradation rate.

A set of laboratory tests (ITSM, ITFT, four-point bending tests) was carried out on specimens extracted from the surface course of each section, in order to evaluate possible damage to the mixtures in areas under the wheel path, i.e., areas in direct contact with the traffic loads, in comparison with 'undamaged' areas away from the wheel tracks. The main conclusions drawn from this set of laboratory tests are summarised as follows:

- No apparent damage was observed on the standard mixture's stiffness modulus (ITSM) obtained from specimens extracted from the loaded areas;
- Most of the damage observed in the other sections seemed to occur at the beginning of the PTF test (ITSM test results and permanent deformation after 20000 cycles are close to those after 60000 cycles);
- Limited crack propagation was identified on cores extracted from areas with wide surface cracks (the cracks travelled less than half the thickness of the layer);
- The fatigue performance of loaded or 'damaged' cores (from ITFT tests) was apparently not affected by traffic loads, although some care must be taken when analysing these results due to the limited number of specimens tested for each section;
- The four-point bending tests allowed a more comprehensive characterisation of the mixtures, whose results are in line with what was expected after the mix design study.

As a main conclusion from this study, the importance of the bearing capacity of the layers underneath a grouted macadam layer must be highlighted. A good overall performance of grouted macadam surface courses depends on the behaviour of the

supporting layers. Also the different fatigue performance of grouted macadams (when compared with conventional asphalts) was noted in the laboratory tests carried out, as evidenced by the residual fatigue life of the 'damaged' specimens being equivalent to that of the 'undamaged' specimens.

8 DEVELOPMENT OF DESIGN METHOD FOR PAVEMENTS INCORPORATING GROUTED MACADAM

8.1 Introduction

Grouted macadam has traditionally been used as a specialist surfacing, taking advantage of its excellent resistance to both deformation and fuel spillage. However, the evidence from tests carried out in this project is that it has potential for use as a more significant part of the structure of the pavement. Therefore, in this chapter, both grouted macadam surface courses and base courses are considered for pavement design.

The main issue regarding fatigue is developing a meaningful relationship between the results of laboratory tests and field performance. During the last few decades, performance models have been developed for flexible pavements with reasonable results. However, such models do not exist for pavements incorporating grouted macadams. In the present investigation, a shift factor has been determined to establish the link between the laboratory fatigue tests and the field performance of grouted macadams, based on the influence of rest periods on the mixture fatigue life. Several design charts have been developed for pavements incorporating both surface and base courses comprising grouted macadam. For a better understanding of the extended life of this type of material, traditional bituminous mixtures were used in the same calculations for a direct comparison.

An iterative approach was used, in addition to the traditional design method, in order to study the degradation of pavements incorporating grouted macadam during their lifetime, based on fatigue performance. In this analysis, typical stiffness reduction curves, obtained from fatigue tests, were used to simulate the degradation of the mixture with load repetitions.

8.2 Design principles considered

Across England, the mean annual temperature at low altitudes varies from about 8.5 °C to 11 °C (Met Office, 2005). However, pavement design is traditionally carried out at a reference temperature of 20 °C (Highways Agency, 2001, 2005). In the present project, stiffness and fatigue tests were carried out at 20 °C, from which the fatigue life equations were obtained. Nonetheless, results presented in Chapter 5 have shown that fatigue life of grouted macadams is not susceptible to temperature variations between 0 and 20 °C. Therefore, temperature has more influence on the value of stiffness used for design, which depends also on the loading frequency. According to the Highways Agency (2005), pavement design should be carried out at a reference condition of 20 °C and 5 Hz. ITSM and four-point bending tests carried out at 5 Hz, under this project, have shown similar stiffness results, for the same temperature. Increasing the frequency in four-point bending tests resulted in increased stiffness modulus values.

The value of stiffness chosen for pavement design in this study was obtained from tests carried out at 10 Hz, since the fatigue lines used then correspond to the same frequency. Thus, 8000 MPa (which is a conservative value) has been used in the calculations. Nonetheless, this may be assumed as an adequate value to use in pavement design, since similar values were also obtained in ITSM tests (corresponding to a frequency of approx. 5 Hz) carried out at 20 °C, on 2-year old specimens.

In this investigation, four pavement foundation classes were considered (Figure 8.1), as suggested by Nunn (2004), on top of which, one or two new layers would be applied. The design characteristics to be used for each foundation are shown in Table 8.1. Some of the results obtained from this study are based on pavement response calculations carried out using a multilayer linear elastic analysis computer program – BISAR 3.0 (Shell International, 1998), for each considered variable (foundation class and overlying materials).
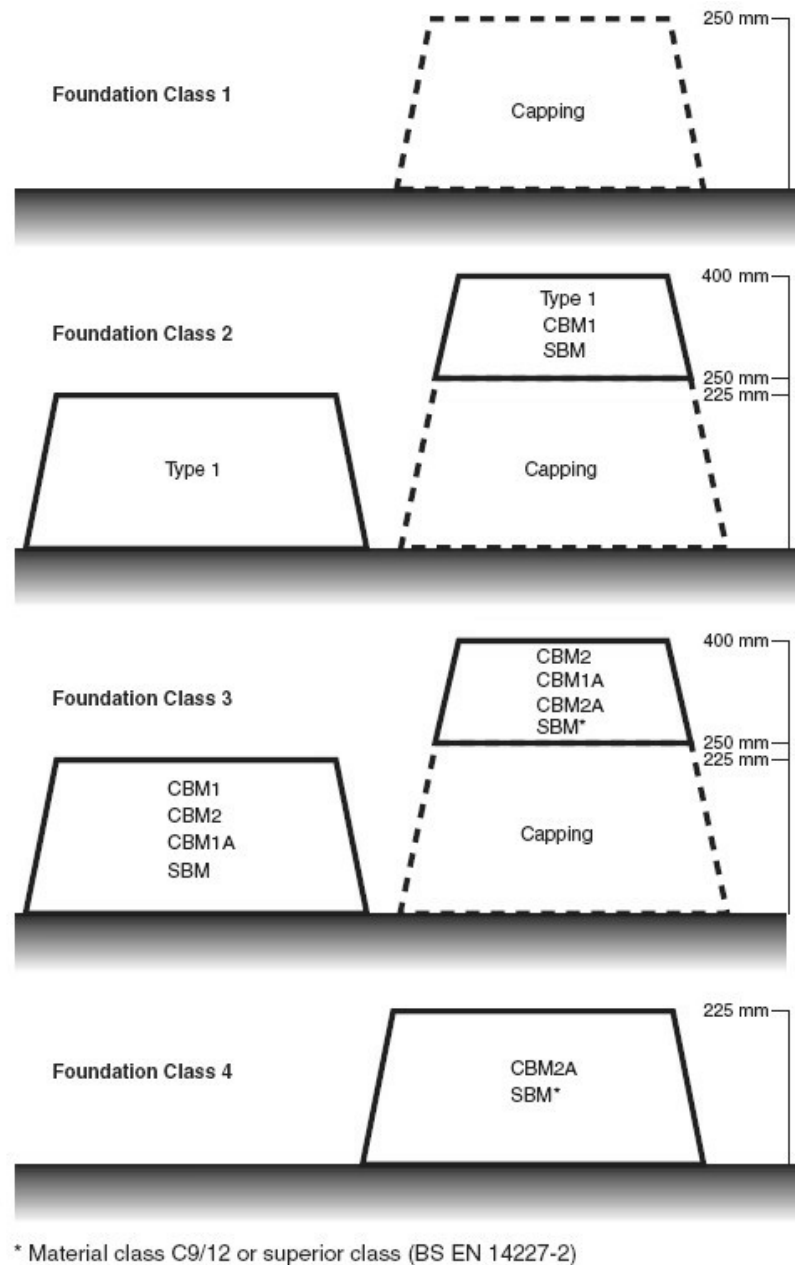
Figure 8.1 – Example designs for foundation classes 1 to 4 on 5% CBR subgrade
(Nunn, 2004)

Table 8.1 – Design characteristics of pavement foundations

Foundation Class	Stiffness (MPa)	Poisson's Ratio
1	50	0.35
2	100	0.35
3	200	0.35
4	400	0.35

The grouted macadam layer was used in the calculations in two different positions, either as a surface course or as a base/binder course. A DBM50 base course and an

HRA or SMA surface course were considered as comparative materials to the grouted macadam, respectively as base or surface course. Their mechanical properties are summarised in Table 8.2, according to the values specified in the new HD26/05 (Draft 4) (Highways Agency, 2005).

Table 8.2 – Mechanical properties of considered materials

Material	Stiffness (MPa)	Poisson's Ratio
Grouted Macadam	8000	0.25
DBM50	5400	0.35
HRA or SMA	3100	0.35

The results presented in the next section, relative to fatigue life of grouted macadam, were obtained by laboratory fatigue tests, from which, a fatigue line equation was determined. However, in order to establish a comparison with the fatigue performance of conventional bituminous materials, specified by Powell et al. (1984) and later by Nunn (2004), a shift factor had to be determined, since the fatigue criterion used by those researchers is relative to field performance. Further details are given in the next section.

8.3 Conventional design methods applied to pavements incorporating grouted macadam

8.3.1 Relationship between laboratory results and field performance

A major difficulty with fatigue testing is developing a meaningful relationship between the results of laboratory tests and field performance. Laboratory tests usually use sinusoidal loading and fixed strain or stress during one test, while in practice, the mode of loading is randomly distributed, including rest periods and lateral distribution of loads. Temperature variations in the asphalt layer and healing effects, due to intermittent loading, also influence the field performance of asphalts. For these effects correction factors (known as shift factors) should be applied. However, determination of the correct shift factor is fairly complicated, since it depends on the type of test, mode of loading, testing temperature and type of mixture (Shell, 1978; Rao Tangella et al., 1990).

Shift factors of 2-10 (Shell, 1978) or 20 (Brown et al., 1985) have been suggested to take into account the influence of rest periods. Additional factors of 2.5 (Shell, 1978) or 1.1 (Brown et al., 1985) have also been used to simulate the lateral distribution of loads, while the fatigue life associated with the crack propagation phase has been considered by a shift factor of 20 (Brown et al., 1985) or by the use of controlled-strain bending tests, instead of controlled-stress tests, which have been found to correlate well with the failure stage in wheel tracking tests on asphalt slabs (Shell, 1978). Therefore, ultimate shift factors of 10-20 (Shell, 1978) or 440 (Brown et al., 1985) have been suggested. Rao Tangella et al. (1990) mentioned values of 100 and 20 for shift factors, considering high loading rate sinusoidal bending tests carried out, respectively, with and without rest periods. Khweir and Fordyce (2003) have obtained a shift factor of 77, which was the result of superposition of ITFT data onto the fatigue line reported by TRRL LR1132 (Powell et al., 1984). Ekdahl and Nilsson (2005) have compared the fatigue criterion specified by the Swedish design code ATB Road with laboratory test results of different mixtures (using Indirect Tensile Fatigue Tests). According to these authors, a methodology based on ITFT tests developed by the Swedish National Road and Research Institute, to study the fatigue properties of mixtures to apply in pavement design, gave results that correlated well to field performance when a shift factor close to 10 was used. However, Ekdahl and Nilsson (2005) have suggested that, according to their recent study, the shift factor of 10 is not large enough and that a shift factor of 42.4 would be more appropriate, highlighting for example the positive effects of using polymer modified binders in the fatigue life of bituminous mixtures.

Based on the diversity of shift factors mentioned above, and on the concerns relative to the application of a specific shift factor to results obtained under different testing conditions, an attempt was made to determine the shift factor appropriate to the testing conditions used in this investigation. This would allow the use, in pavement design, of the grouted macadam fatigue lines determined under the present project. Therefore, a laboratory testing programme was established, using four-point bending tests, where different loading patterns were used during each test, as illustrated in Figure 8.2. This study focussed mainly on the effect of rest periods on the fatigue life of the standard grouted macadam mixture. Thus, five different loading patterns were used: (i) a continuous sinusoidal load; (ii) two sinusoidal loading cycles followed by

a rest period, with duration equivalent to one cycle; (iii) one loading cycle followed by a rest period of equivalent duration; (iv) one loading cycle followed by a rest period with duration equivalent to two cycles and; (v) 1000 loading cycles followed by an equivalent rest period.
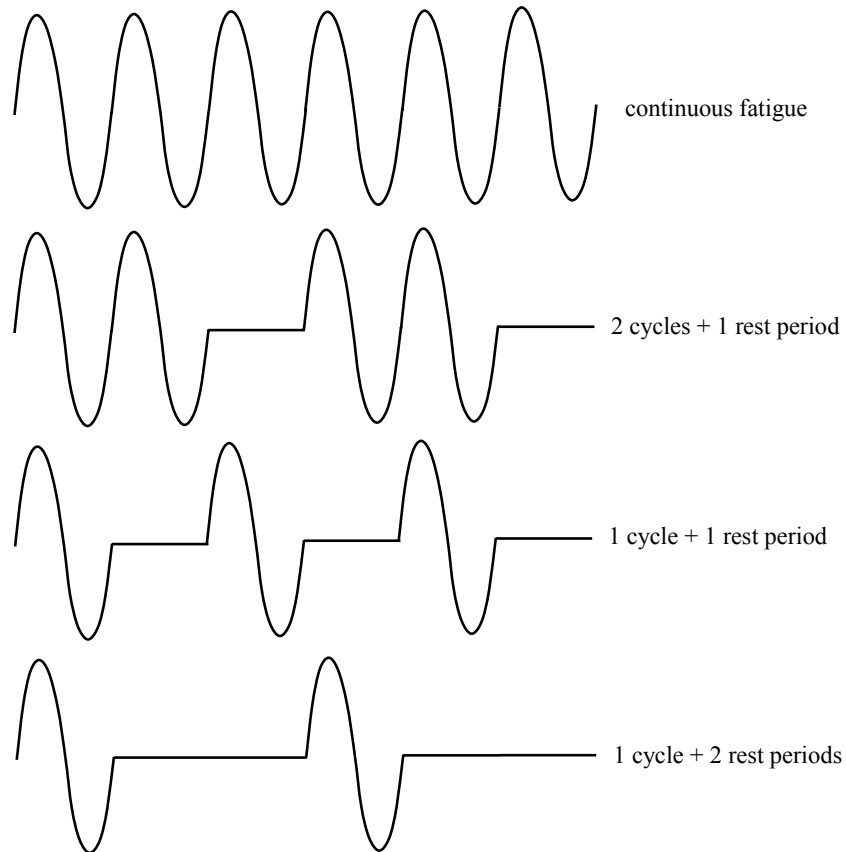
continuous fatigue

2 cycles + 1 rest period

1 cycle + 1 rest period

1 cycle + 2 rest periods

Figure 8.2 – Modes of loading used to determine the influence of rest periods on the fatigue life of grouted macadams

Due to limitations of the equipment in controlling the actuator with an intermittent loading pattern (rest periods between loading cycles), the maximum frequency that could be used was 5 Hz. Therefore, all tests were carried out at this frequency. The results obtained according to the modes of loading shown in Figure 8.2 are presented in Figure 8.3, where the extended fatigue life obtained by the inclusion of rest periods in fatigue tests is clear, increasing with the duration of the rest periods. Tests were stopped after the stiffness modulus of the mixture had dropped below half of its initial value. This value (50% of initial stiffness) would be used as the failure criterion, similar to what was used in the mix design study. The test becomes more time consuming when rest periods are included, especially when the duration of rest periods is longer than the loading time, and this was actually the reason why the longest rest period used was just two times the loading time.
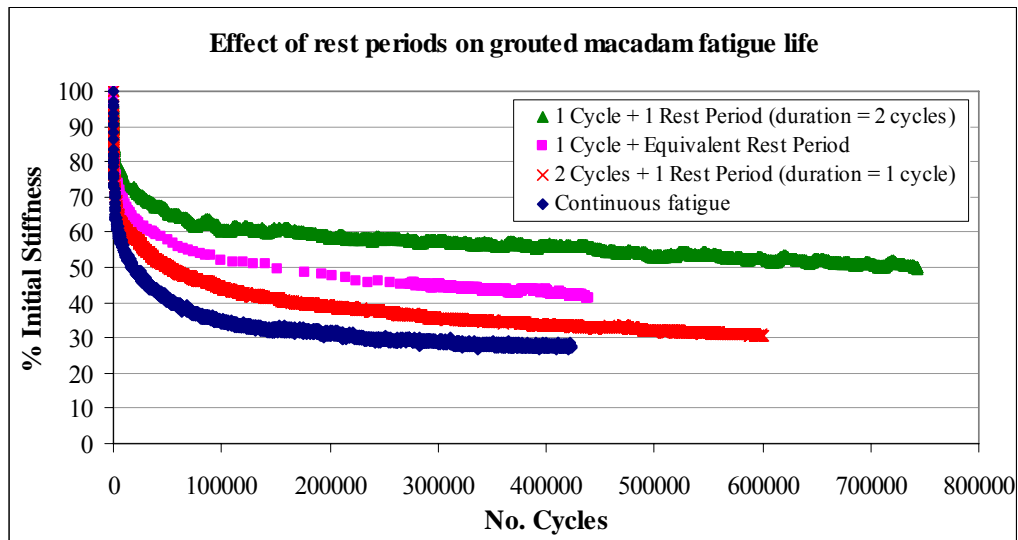
Figure 8.3 – Influence of rest periods duration on grouted macadam fatigue life

A fifth result was obtained using a different loading pattern, not represented in Figure 8.2, which comprised 1000 consecutive loading cycles followed by an equivalent rest period. The results of this test are presented in Figure 8.4, where each data-point represents the stiffness of the mixture at the end of each series of 1000 loading cycles. The maximum number of loading cycles plotted in this figure was reduced to 60000 cycles to get a clearer idea of the influence of rest period duration on the fatigue life.

In order to analyse the results of these tests from a field performance perspective, some assumptions have to be made. Thus, a pavement design life of 20 years was used assuming a heavily trafficked highway (design traffic of 150 million standard axles), with 6000 commercial vehicles per day (assuming a wear factor of 3.5 standard axles per vehicle). If these commercial vehicles were distributed over a period of 12 hours, the frequency would be approximately 1 commercial vehicle every 7.2 seconds (or 1 axle every 2 sec.). On the other hand, the frequency used in the laboratory tests (5 Hz) would correspond to a 'loading' time of 0.7 sec (3.5 axles/5 Hz) per vehicle. Assuming an average vehicle length of 12.5 m, the vehicle speed would be 17.86 m/s (approximately 40 miles/h). A rest period of 6.5 sec would be expected after each 0.7 sec of commercial vehicle loading (7.2 sec in total per vehicle). This corresponds to a rest period 9 times longer than the loading period.
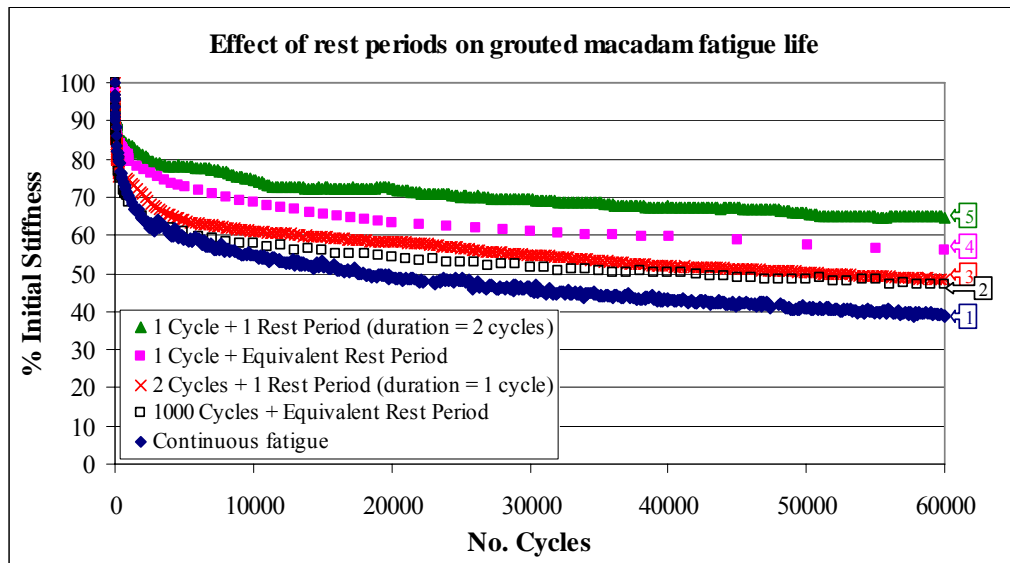
Figure 8.4 – Influence of rest periods on the fatigue life of grouted macadams

Taking into account only the rest periods to define a shift factor (which is very conservative, according to the results of other researchers), and based on the results presented above, the shift factor corresponding to each of the studied loading conditions was obtained as the ratio between the fatigue life (number of cycles up to 50% stiffness reduction) of each test and the fatigue life of the continuous fatigue test. The results are summarised in Table 8.3.

Table 8.3 – Shift factor obtained for each fatigue line

Mode of loading	No. of cycles	Shift factor
Continuous fatigue (1)	17739	1.0
1000 cycles + equiv. rest period (2)	40980	2.3
2 cycles + 1 rest period (3)	50823	2.9
1 cycle + 1 rest period (4)	140050	7.9
1 cycle + 2 rest periods (5)	734395	41.4

In accordance with the calculations discussed above, the shift factor obtained from line 5 (41.4) would be a very conservative value, since the rest period used in the laboratory tests is 4.5 times shorter than the rest period between each commercial vehicle calculated above. However, each commercial vehicle actually represents the concentration of 3.5 axle loads. As can be observed from lines 2, 3 and 4, the application of consecutive loads between rest periods decreases the fatigue life. Therefore, the extended life expected from the longer rest periods (9 times the loading period instead of 2 times, as for line 5) was ignored, taking the value of 41 as an adequate value for the shift factor (considering exclusively the effect of the rest

periods). The ultimate value used in the present investigation was 45, which includes an extra factor of 1.1 for the lateral load distribution as suggested by Brown et al. (1985). The final value also concurs with that suggested by Ekdahl and Nilsson (2005). Nonetheless, the final shift factor (45) is still considered a conservative value, due to the particular behaviour of grouted macadams, in terms of crack propagation.

In the case of low volume roads or distribution centres/warehouses, a higher value should be used for the shift factor, as the duration of the rest periods is significantly higher. However, it is not sensible to suggest a different value based on the available results. A new set of tests should be carried out, using longer rest periods, but that was not possible during the current project.

8.3.2 Design of pavements with grouted macadam surface courses

8.3.2.1   Influence of permanent deformation of the support

Permanent deformation of the support (structural rutting) can be one of the main causes of failure in grouted macadam surface courses, as could be observed in the previous chapter, in the half-scale pavement. Progressive settlement of the foundation generates a pair of moments in the surface course, which will induce permanent tensile strains in the material, as illustrated in Figure 8.5.
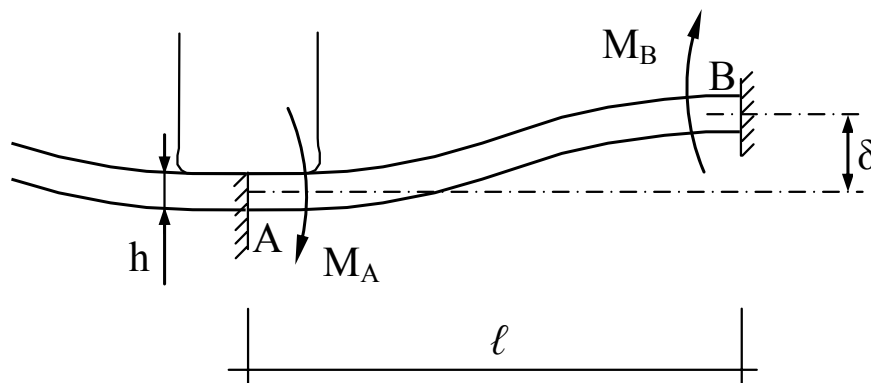
Figure 8.5 – Schematic representation of the internal moments induced by permanent deformation of the support

When the rut depth (δ) and width (2ℓ) assume significant figures, the maximum tensile strains induced, respectively, at the underside (position A - below the load), and at the surface (position B - at the end of the affected area) of the layer, may exceed the values that the mixture is capable of withstanding. Figure 8.6 represents the maximum tensile strains induced in a grouted macadam surface course, applied directly on top of the foundation, according to several hypotheses of rut depth and width (half of total rut width, to be more precise). Assuming that Figure 8.5 represents a simplification of the real situation, where some other factors intervene, it gives a rough approximation to the actual values involved. The results presented in Figure 8.6 were obtained according to Equations 8.1, 8.2, 8.3 and 8.4.

$$M_A = M_B = M_{max} = \frac{6EI\delta}{\ell^2} \qquad (8.1)$$

$$\sigma = E \cdot \varepsilon \qquad (8.2)$$

$$\sigma_{max} = \frac{M_{max}}{I} \cdot y \qquad (8.3)$$

Substituting Equations 8.1 and 8.2 into Equation 8.3, the maximum tensile strain is determined as follows:

$$\varepsilon_{max} = \frac{3 \cdot \delta \cdot h}{\ell^2} \qquad (8.4)$$

where:
M = Bending moment;
E = Stiffness Modulus;
I = Moment of Inertia;
δ = Rut depth;
ℓ = Half of rut width;
σ = Tensile stress;
ε = Tensile strain;
y = $h/2$
h = Layer thickness.

As a reference, the maximum strain values determined by the thermal cracking tests (presented in Chapter 6) can be used to define failure of the surface course, in this case imposed by permanent deformation of the support. Thus, taking the approximate value of 3000 $\mu\varepsilon$ as the maximum allowable tensile strain, it is possible to determine the maximum rut depth that the mixture can withstand, as a function of the rut width.

Taking the PTF pavement as an example, the maximum rut depth that the standard grouted macadam mixture could withstand, according to the measured rut width ($\ell = 0.56$ m, after the first day of testing on track 1), would be approximately 7.8 mm, as illustrated in Figure 8.7. The rut depth measured at the end of the day in the wheel path, on the middle section, was of approximately 9.0 mm. This explains why the first cracks appeared during the first day. It should be highlighted that when the load is applied, the value of the tensile strain under the wheel increases significantly (as a result of the recoverable deformation). This means that the allowable rut depth has to be reduced, according to the value of recoverable tensile strain generated by the wheel load, in order to ensure adequate performance.
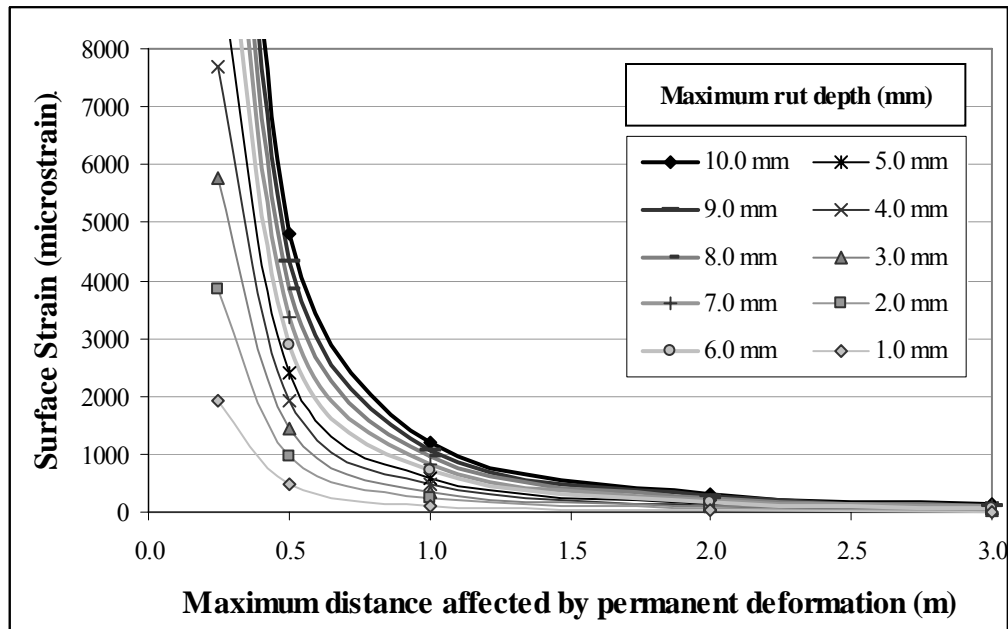
Figure 8.6 – Maximum tensile strains induced in grouted macadam surface courses as a function of rut depth and width

Even though permanent deformation of the support is an important issue to take into account, when designing a pavement with a grouted macadam surface course, this should not be the cause of failure in most situations, provided that the foundation is properly constructed. Therefore, fatigue and thermal cracking are the most important aspects to control. In the next section, the design of pavements incorporating grouted macadam surface courses is discussed, regarding the appearance of surface originated cracking.
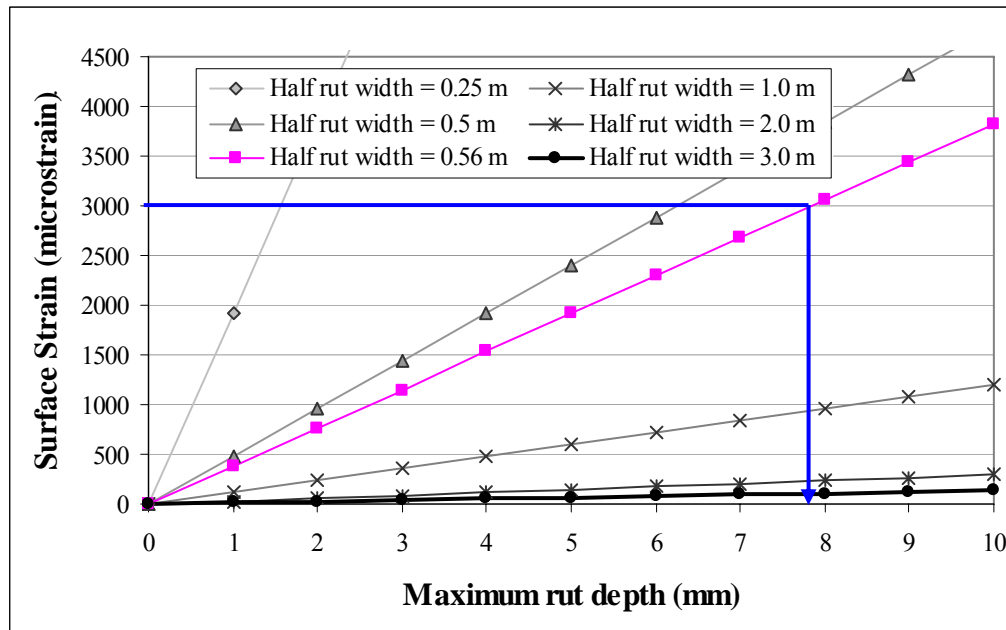
Figure 8.7 – Allowable rut depth of grouted macadam surface course used in PTF,
according to the rut width measured after one day of testing

8.3.2.2   Influence of surface originated cracking (top-down cracking)

As previously stated, four pavement foundations were used in a multilayer linear elastic analysis, to study the response of each structure to the application of a standard wheel load (40 kN). In this case, a conventional bituminous base (DBM50) was used on top of the foundation, over which a 40 mm thick surface course was applied (comprising either a conventional (HRA or SMA) or a Grouted Macadam mixture). The response of the pavement was analysed from two perspectives: failure of the base by fatigue (maximum strain at the bottom of the layer); failure of the surface course by fatigue (surface originated cracking). The latter is a result of tensile strains developed under the side of the tyre, near the pavement surface, which assume significant values in pavements with thick bound layers. In order to determine the maximum strain, a mesh of points was created, as illustrated in Figure 8.8, since its location can change slightly with changes in base thickness.
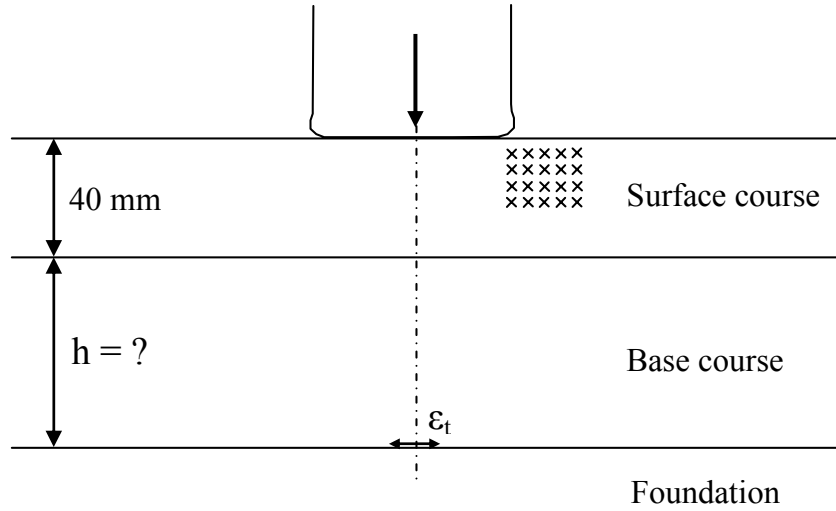
Figure 8.8 – Typical pavement structure used in BISAR to determine the critical tensile strains induced by a standard wheel load

Several iterations were made for each surface course, consecutively increasing the thickness of the bituminous base, and determining the expected fatigue life of both base and surface course, according to the tensile strains obtained. The fatigue life calculations of the grouted macadam layer were made according to the laboratory results obtained during the present project, and multiplying by the shift factor mentioned above (end of section 8.3.1), which resulted in Equation 8.5. On the other hand, the fatigue life of bituminous mixtures was calculated according to the fatigue criterion specified by Powell et al. (1984) and Nunn (2004), which represents the field performance of asphalt mixtures (Equation 8.6).

$$N = 2.7 \times 10^{-9} \cdot \varepsilon_t^{-3.9718} \tag{8.5}$$

$$N = 4.169 \times 10^{-10} \cdot \varepsilon_t^{-4.16} \tag{8.6}$$

where:
  N = Number of equivalent standard axle loads (ESALs);
  ε_t = Tensile strain induced at either surface or underside of bound layers.

The results of this study are presented in the following figures, on a comparative basis, in terms of the material used in the surface course. Thus, Figures 8.9 and 8.10 represent the design of the base and the influence of its thickness on the appearance of surface cracking.

Design of base (50 pen DBM)
under 40 mm HRA or SMA
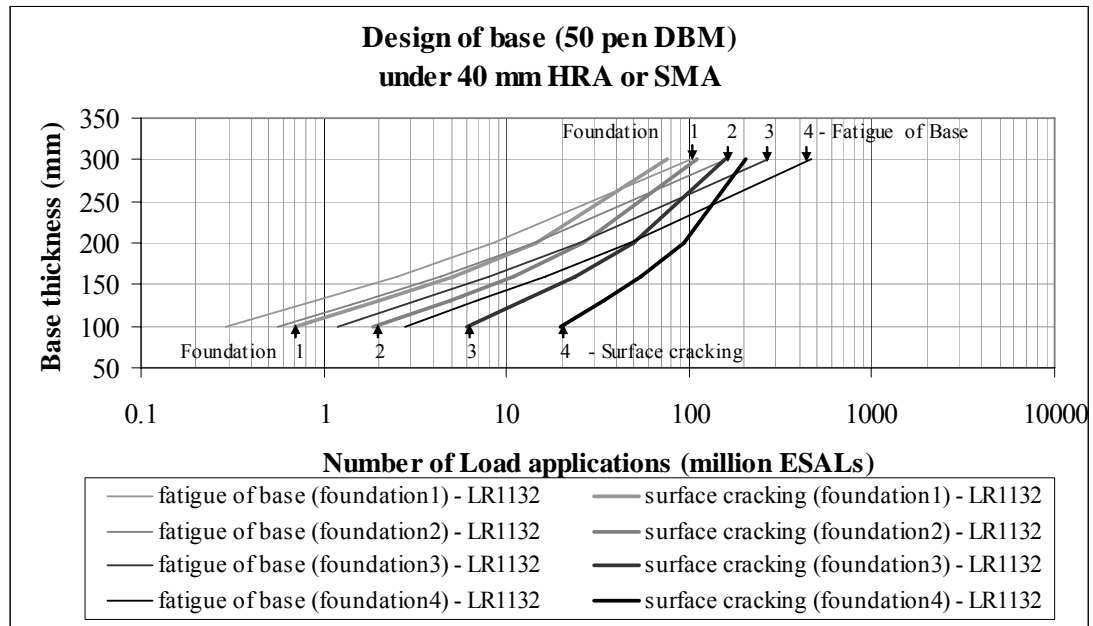
Figure 8.9 – Design of base under a 40 mm HRA or SMA surface course, taking into account the traditional fatigue criterion and the appearance of surface cracking

Design of base (50 pen DBM)
under 40 mm grouted macadam
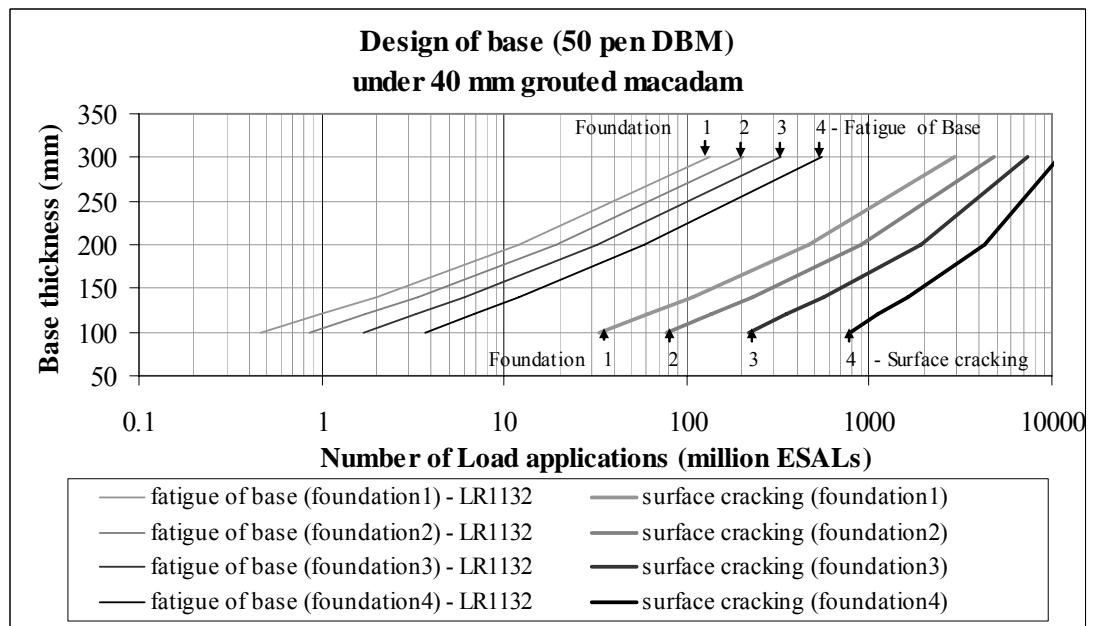
Figure 8.10 – Design of base under a 40 mm Grouted Macadam surface course, taking into account the traditional fatigue criterion and the appearance of surface cracking

From the above figures, it can be observed that for thicker pavement bases, when a bituminous surface course (HRA or SMA) is used, the critical failure criterion is the fatigue of the surface course. The same does not apply if a grouted macadam surface course is used instead, due to lower values of strain occurring at the surface, as a consequence of its higher stiffness, and due to the extended fatigue life of the mixture itself.

In Figures 8.11 and 8.12, a comparison is made between the results obtained for both types of surface course used, and their influence on the design of the base thickness is presented. Regarding pavement design, the benefits of using a grouted macadam surfacing are evident from the analysis of these figures, although more significantly in terms of fatigue cracking originated at the surface than in terms of fatigue of the bituminous base. Nonetheless, a longer fatigue life can be expected from pavements incorporating grouted macadam surface courses.
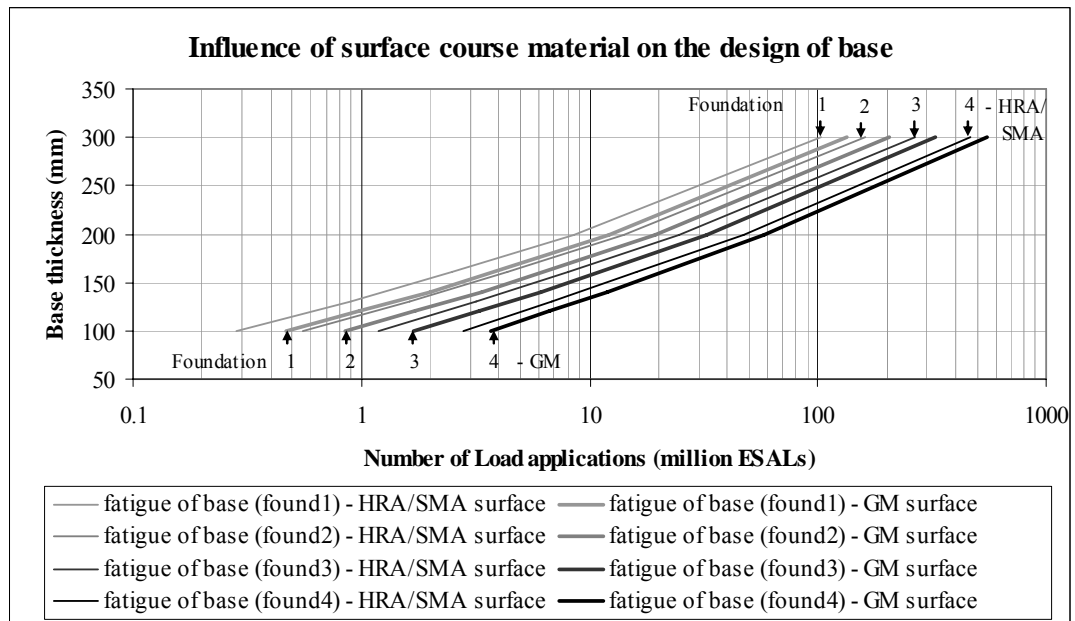
Figure 8.11 – Influence of the type of surface course on the design of the base, considering the traditional fatigue criterion (at the underside of the base)
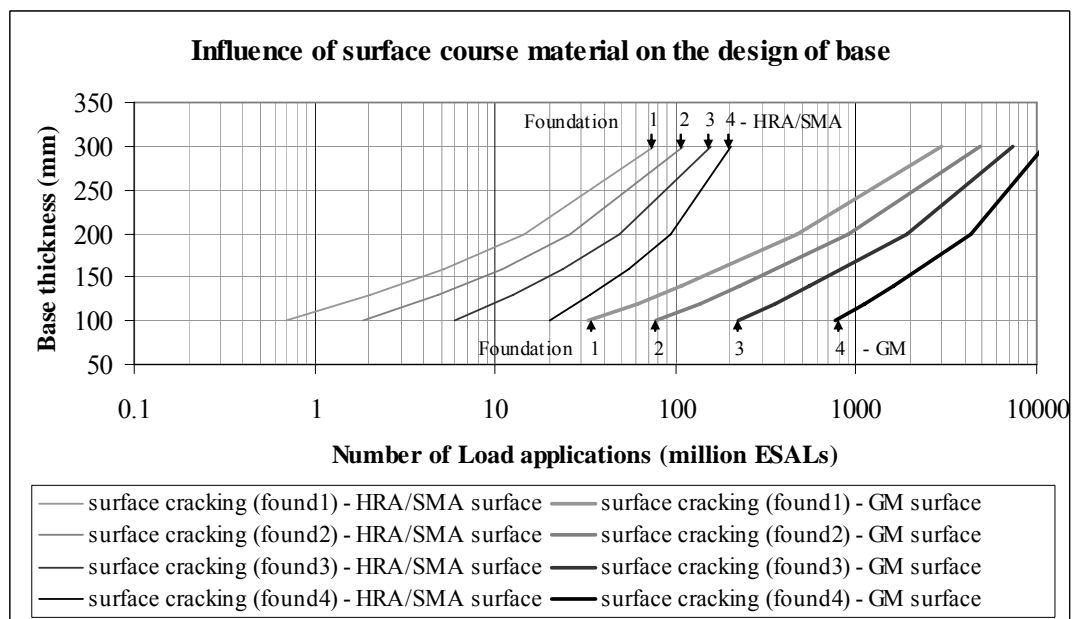
Figure 8.12 – Influence of the type of surface course on the design of the base, considering fatigue of the surface course (surface cracking)

8.3.3 Design of pavements with grouted macadam base courses

A methodology similar to that described in the previous section was used to study the design of pavements incorporating grouted macadam base courses. In this case, the material used in the surface course was a traditional HRA or SMA mixture. The results are shown in Figures 8.13 and 8.14, respectively for the standard grouted macadam mixture and for a stiffer grouted macadam (e.g., resulting from a reduced binder content), with a Stiffness Modulus of 12000 MPa, as those presented in Chapter 6, the mix design study.
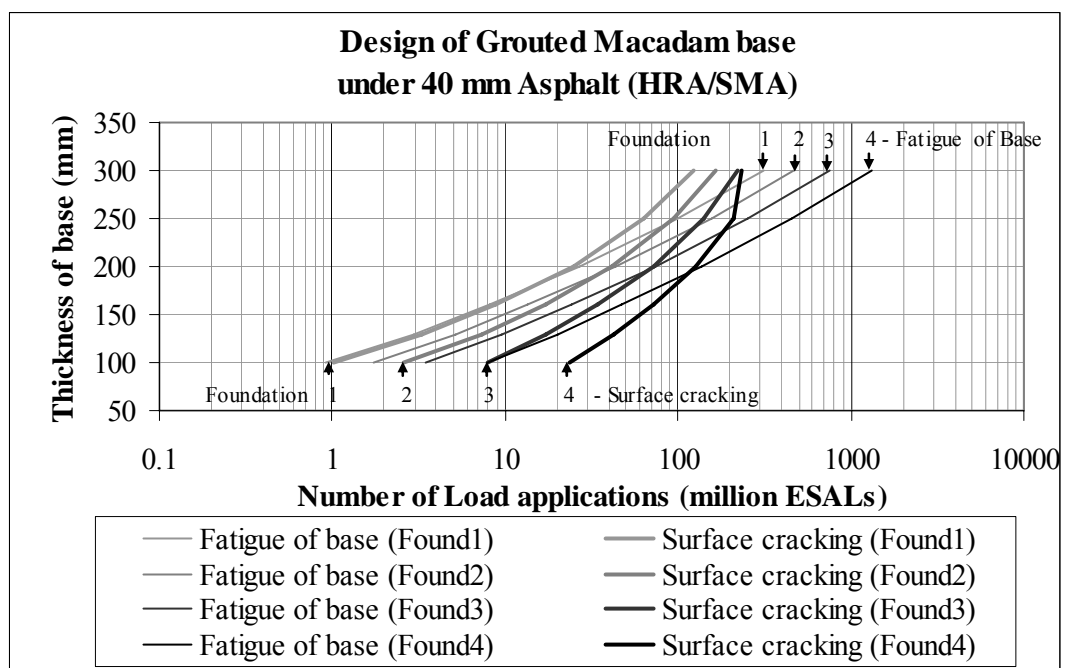
Figure 8.13 – Design of a standard grouted macadam base course under a 40 mm HRA or SMA mixture, considering fatigue of base and surface cracking

As can be observed from Figure 8.13, surface cracking (fatigue of the bituminous surface course) is the critical design criterion for pavements with bases thicker than 200 mm. In the case of a stiffer grouted macadam, particularly for pavements with less stiff foundations, surface originated cracking can be even more critical, as can be observed in Figure 8.14. For the case of Foundation Class 1 (50 MPa), the thickness of the base is always governed by fatigue of the surface course, while for the other foundation classes the critical criterion can be either (surface cracking, for pavements with bases above 150 mm thick). Nonetheless, an extended fatigue life can be observed for pavements incorporating grouted macadam base courses, and this is most evident for stiffer grouted macadam bases.

A comparison with the results obtained for pavements with bituminous base courses (from section 8.3.1) is made in Figures 8.15 and 8.16, using the standard grouted macadam mixture. Again, pavements incorporating grouted macadam mixtures show extended fatigue life, which could even be longer if a stiffer grouted macadam mixture was used.
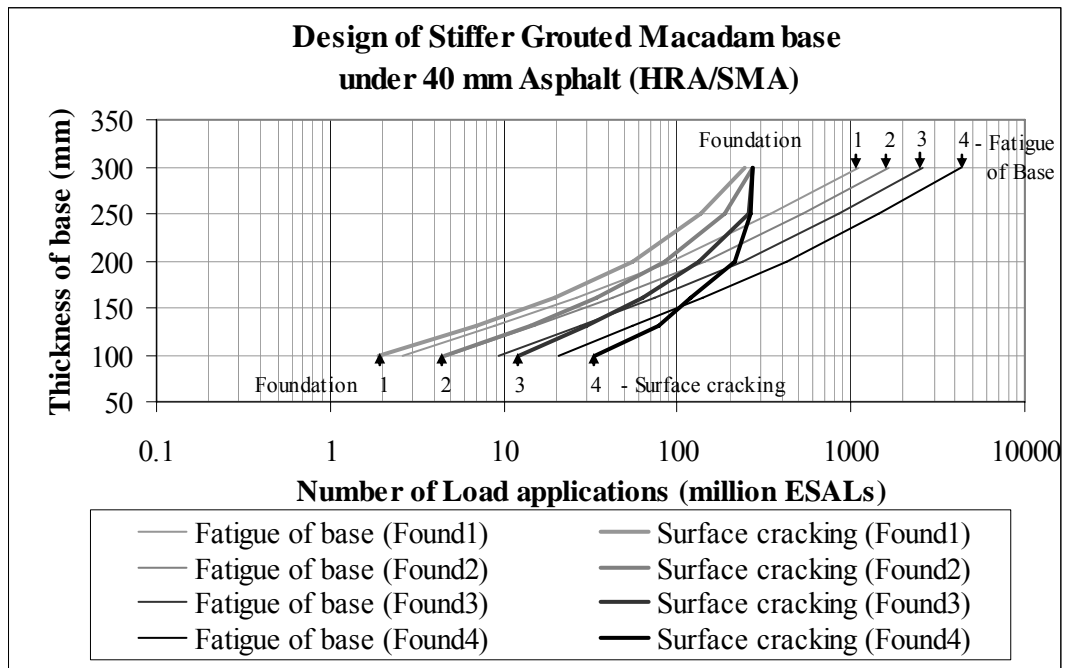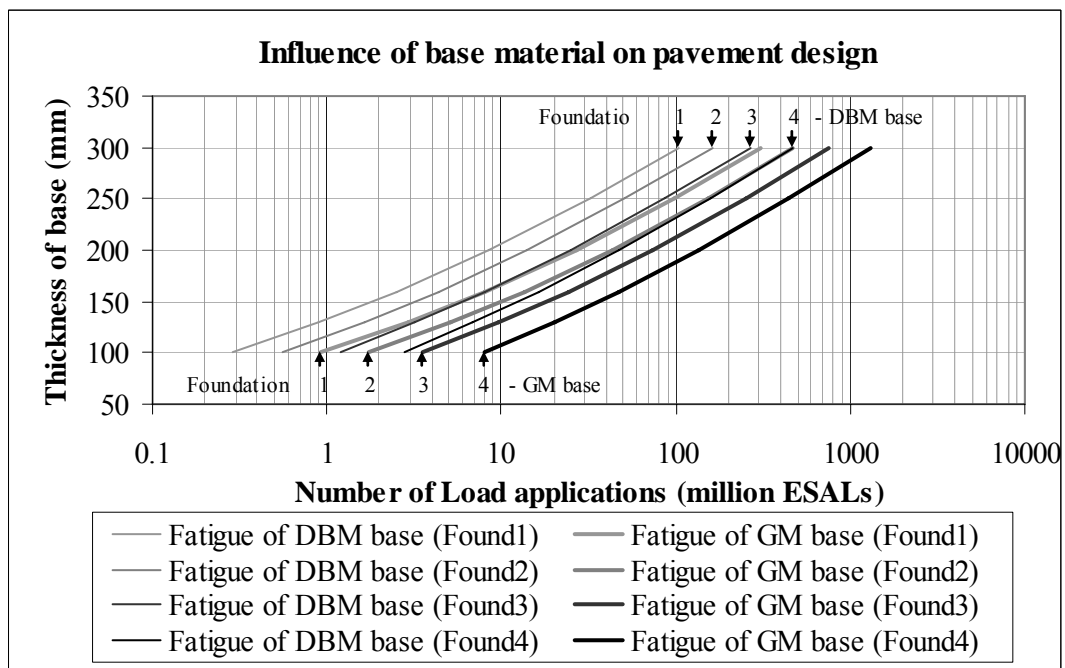

Figure 8.14 – Design of a stiffer grouted macadam base course under a 40 mm HRA or SMA mixture, considering fatigue of base and surface cracking

Figure 8.15 – Influence of material type on the fatigue life of the base

One issue that may arise from this pavement design study is the feasibility of constructing grouted macadam layers thicker than 200 mm. Contec (2005) claim they have achieved 210 mm (Figure 8.17), but full grout penetration may become more difficult to obtain in such thick layers. Thus, the application of consecutive layers may be necessary, in order to obtain pavements with up to 300 mm thick base courses (e.g., 150 + 150 mm).
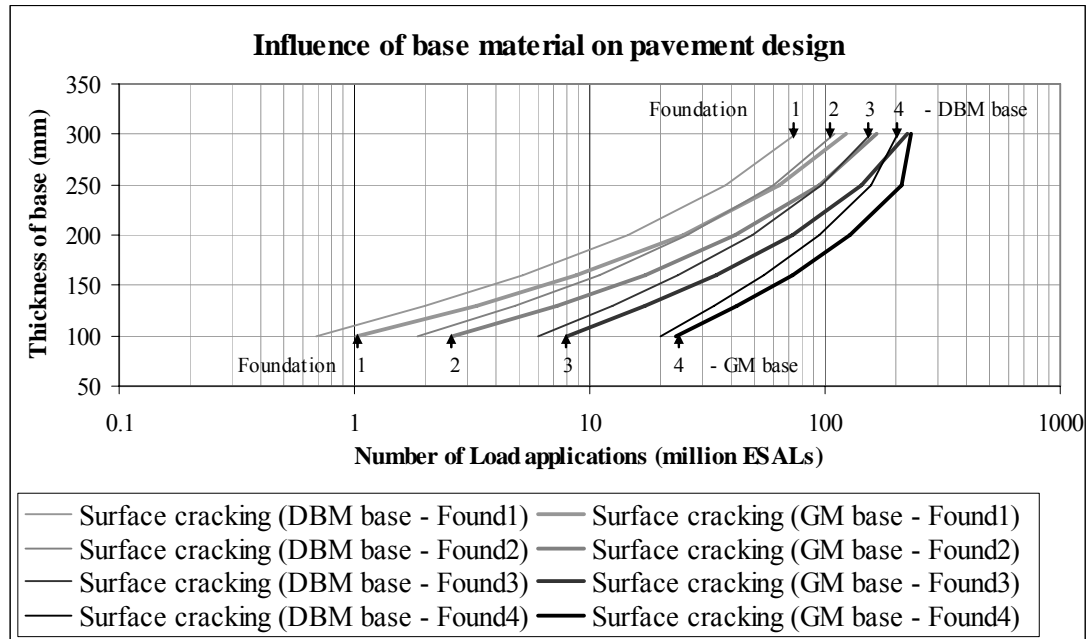
Figure 8.16 – Influence of base material on the fatigue of the surface course
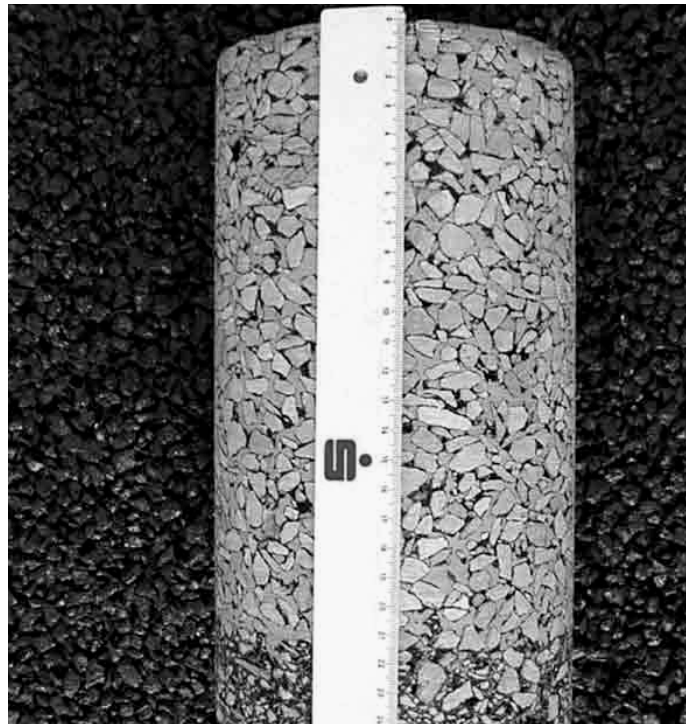
Figure 8.17 – Core extracted from a thick grouted macadam layer (Contec, 2005)

8.4 Assessment of pavement design method based on fatigue performance

In the previous sections, fatigue life was determined according to the traditional failure criterion (50% reduction on the initial stiffness, for controlled-strain tests). However, from the analysis of the stiffness reduction curves of controlled-strain fatigue tests, it was possible to observe that grouted macadam curves have a particular shape, flatter than normal asphalts. Therefore, an investigation was carried out with the objective of assessing the extended fatigue life of grouted macadams, if material behaviour beyond the traditional 50% stiffness reduction point was considered. In this study, an iterative approach was used, in order to simulate the degradation (stiffness reduction) of the mixture with time (number of load applications). The number of load applications was determined according to the fatigue life obtained from laboratory tests, without taking into account any shift factor to establish the actual number of standard axles, in a real pavement situation.

8.4.1 Laboratory testing programme

In order to compare the fatigue performance of grouted macadams with traditional bituminous materials, laboratory tests should be carried out on a bituminous mixture using the same testing equipment.

As previously stated, most of the laboratory tests carried out under this investigation (on grouted macadams) were performed using a four-point bending equipment developed during the present project. The limitations of the equipment, presented in Chapter 4, included the restraint of lateral movement in the beam supports (minimised by the type of bearings used in the construction of the equipment), and the need to regularly tighten the screws in the clamps (when testing asphalt specimens) because of creep under repeated loading. Since the operation of tightening had to be carried out manually, this would influence the test results in the sense that the temperature would oscillate every time the door of the temperature conditioning cabinet was opened to tighten the screws. That is not the case when testing grouted macadams, since they are not susceptible to permanent deformation and the screws did not need to be tightened.

A different type of testing machine was, therefore, used for the purpose of comparing fatigue performance of grouted macadams and bituminous mixtures. Amongst the testing machines available in the laboratory at the University of Nottingham, a trapezoidal cantilever testing machine (also known as two-point bending machine) was chosen in preference to the Nottingham Asphalt Tester (NAT), also available in the laboratory, which performs Indirect Tensile Fatigue Tests (ITFT). The two-point bending test is one of those specified in the European Standards for fatigue testing of bituminous materials, EN 12697-24 (BSI, 2004$_d$), and it represents more realistically than the ITFT the bending of a pavement layer. The same equipment type has been widely used to study the fatigue performance of asphalt mixtures by other researchers (Rowe, 1993; Breysse et al., 2003; Bodin et al., 2003; Breysse et al,. 2004).

A series of tests was carried out on laboratory prepared specimens to determine the fatigue performance of the standard grouted macadam mixture and a Dense Bitumen Macadam produced with a 50 pen binder (DBM 50). The trapezoidal specimens were extracted from slabs prepared using the same procedure that had been used when producing beams for the mix design study. Naturally, the thicknesses of the slabs were adjusted to be able to produce a representative number of specimens from each slab. Figure 8.18 schematically represents a trapezoidal specimen used in the tests. The temperature used in these tests was the same used for the mix design study (20 °C). Tests were carried out in displacement (strain) control at 10 Hz, the same as the tests performed in the mix design study, using four-point bending equipment.

Strain controlled tests are normally stopped after the Stiffness modulus of the specimen has been reduced to half of its initial value. However, observations made on the shape of the stiffness reduction curve of grouted macadams (Figure 8.19), using the four-point bending testing apparatus, suggested a fatigue performance different from that of conventional bituminous mixtures, presented in Figure 8.20 (Rowe, 1993; Kim et al., 2003; Lundstrom et al., 2004). Therefore, in the present study, tests were carried out further and stopped only when the stiffness modulus had reduced to 10% of its initial value. This allowed an assessment of mixtures' full performance during the tests.
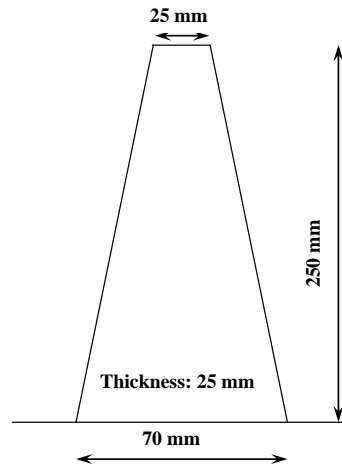
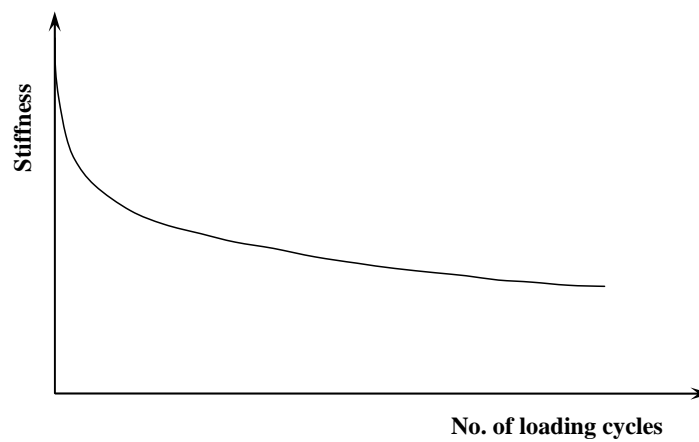Figure 8.18 – Dimensions of trapezoidal specimen used in two-point bending tests

Figure 8.19 – Typical trend of four-point bending strain-controlled fatigue tests on grouted macadams
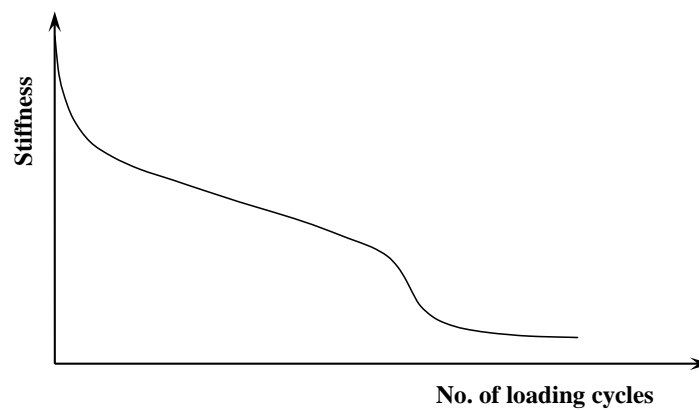

Figure 8.20 – Typical trend of strain-controlled fatigue tests (Rowe, 1993; Kim et al., 2003; Lundstrom et al., 2004)

8.4.2 Fatigue test results

The two-point bending fatigue test results obtained in this study for the standard grouted macadam mixture can be compared with those obtained under the mix

design study, using the four-point bending test apparatus. As can be seen in Figure 8.21, the fatigue lines obtained for both types of test, using the same failure criterion (50% stiffness reduction) are very close to each other and could be considered as one common trend line.

The results obtained for two-point bending tests show a higher amount of scatter when compared with four-point bending test results. The reason for that may be related to the specimen dimensions, since the thickness of trapezoidal specimens (25 mm) is just above two times the nominal aggregate size used in the mixture (10 mm), in contrast to the beam specimens used in four-point bending tests, where the dimensions of the specimens are five times the nominal aggregate size. Therefore, in the trapezoidal specimens, a chance of disturbance (concentration of voids, bitumen or fibres) within the mixture's structure is more likely to influence the fatigue life of the specimen than in the case of the beams (50×50 mm cross-section).

Grouted Macadams Fatigue Tests

$y = 2535.3x^{-0.2477}$
$R^2 = 0.9838$

$y = 2648.6x^{-0.2631}$
$R^2 = 0.8925$

■ Std Mixture - 4PB

♦ Std Mixture - 2PB

Microstrain

No. of cycles
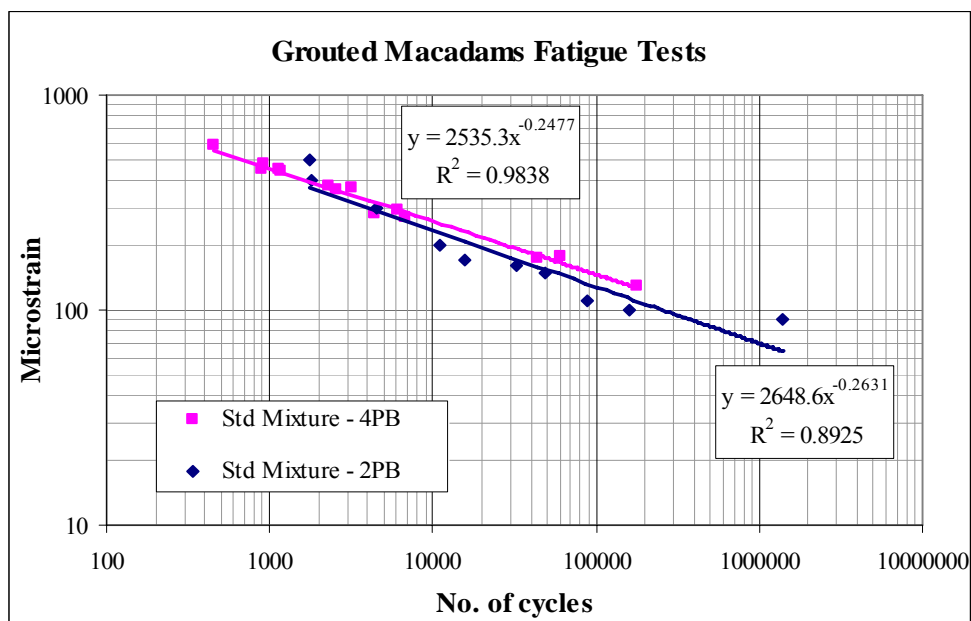
Figure 8.21 – Two-point and four-point bending fatigue test results obtained for the standard grouted macadam mixture

Two-point bending fatigue tests were also carried out on a DBM50 mixture in order to establish a comparison of both mixtures' behaviour. The results are presented in Figure 8.22, together with the fatigue line of the standard grouted macadam mixture (individual results are presented in Appendix E).
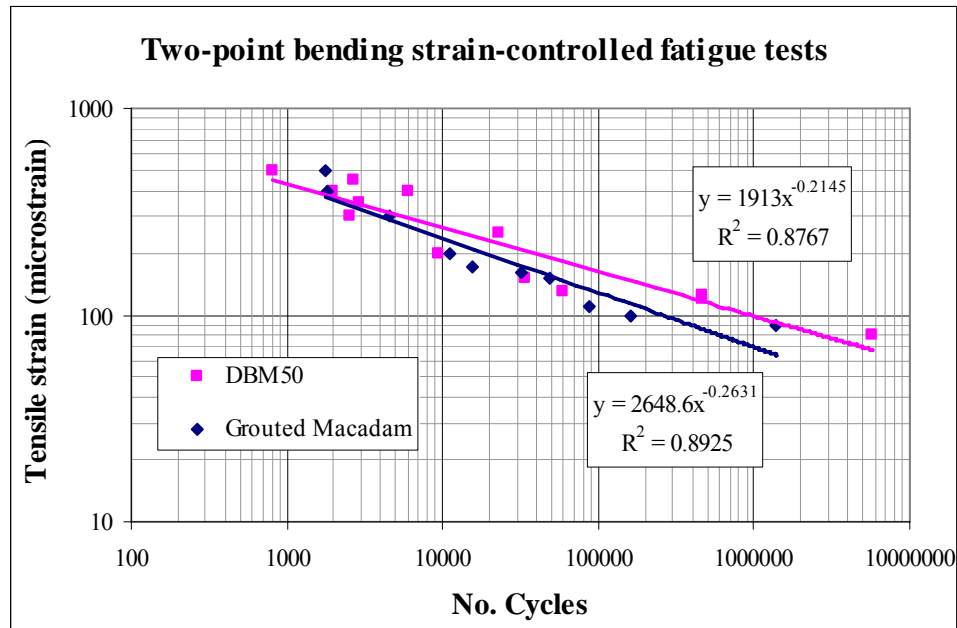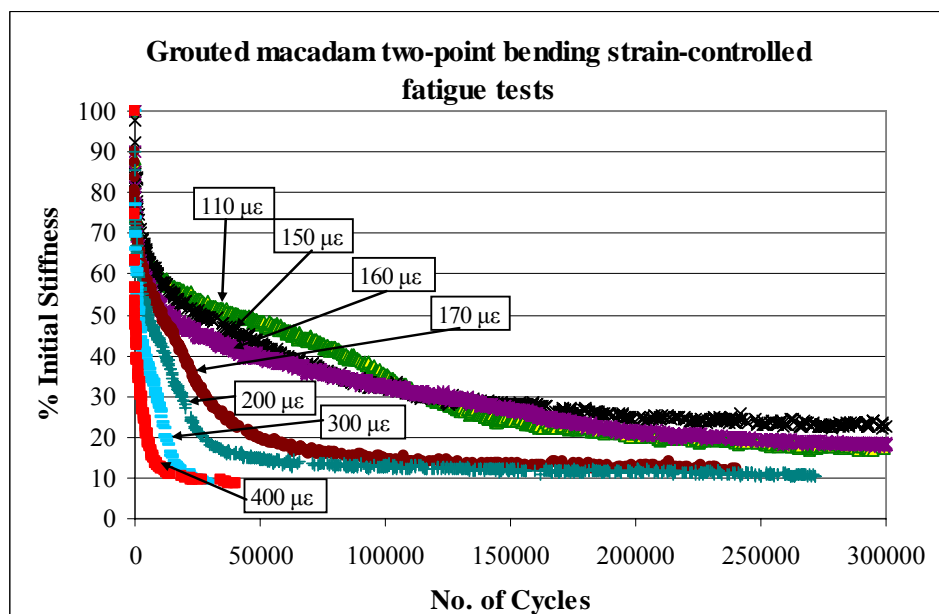
Figure 8.22 – Two-point bending fatigue test results obtained for the standard grouted macadam and a DBM50 mixture

Fatigue test results are generally plotted as a function of the strain level used in tests. Therefore, lower strain levels usually result in extended fatigue lives, as illustrated in the figure above, according to the failure criterion used. Figures 8.23 and 8.24 represent some stiffness reduction curves of the standard grouted macadam and the DBM mixtures used in this investigation. The strain level used in each individual test influences the stiffness reduction rate, where higher strains usually result in higher stiffness reduction rates at 'failure' (50% stiffness reduction).
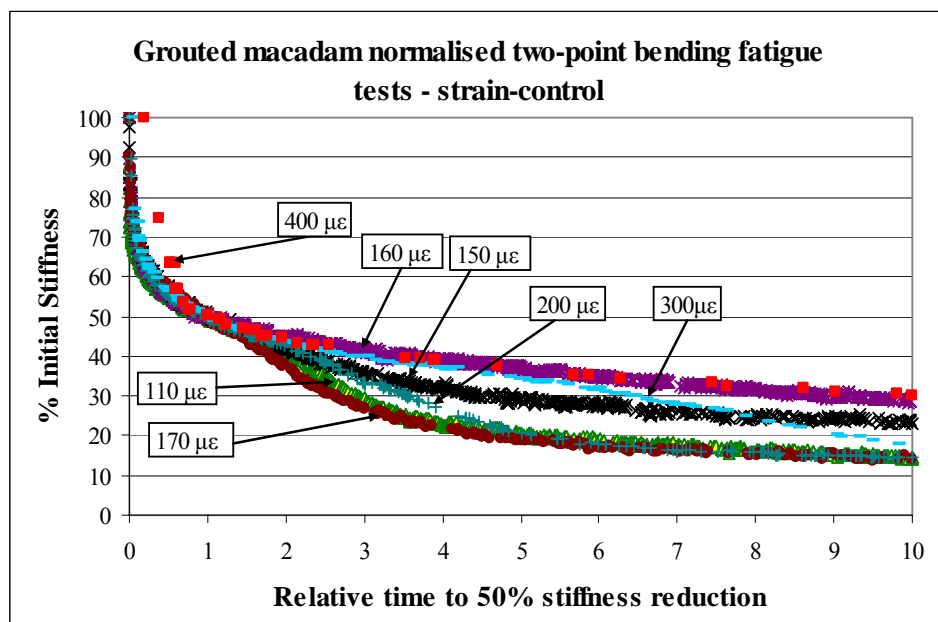

Figure 8.23 – Two-point bending fatigue test results obtained for the standard grouted macadam mixture
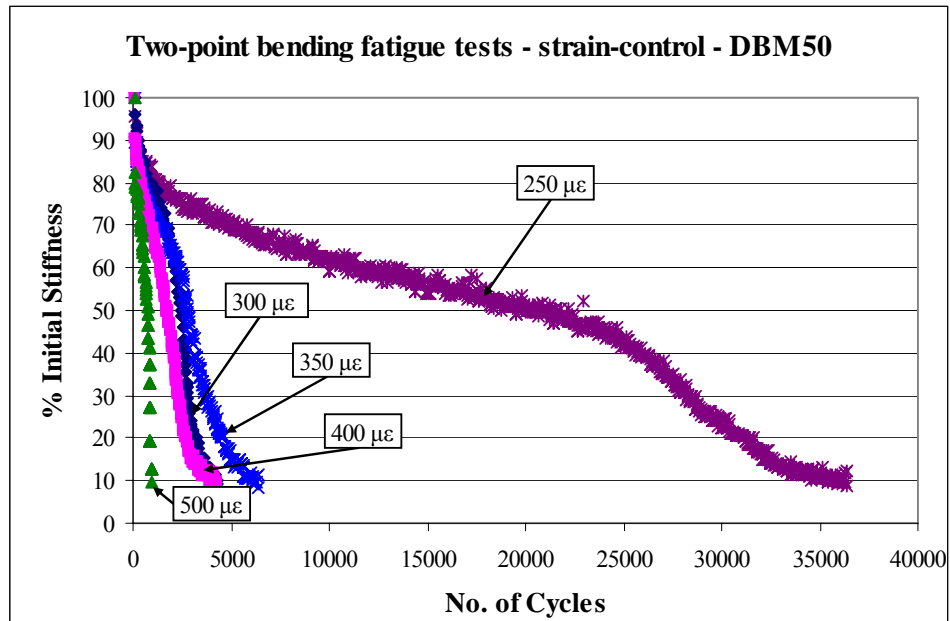
Figure 8.24 – Two-point bending fatigue test results obtained for the DBM50 mixture

In order to be able to analyse the results without the strain level dependency, they were normalised in relation to the number of cycles necessary to reach 'failure'. Thus, the relative time was obtained, for each data point, by dividing the number of cycles by the number of cycles corresponding to half of the initial stiffness value. This can be observed in Figures 8.25 and 8.26, respectively for the grouted macadam and the DBM 50 mixtures.

Figure 8.25 – Normalised two-point bending fatigue test results obtained for the standard grouted macadam mixture
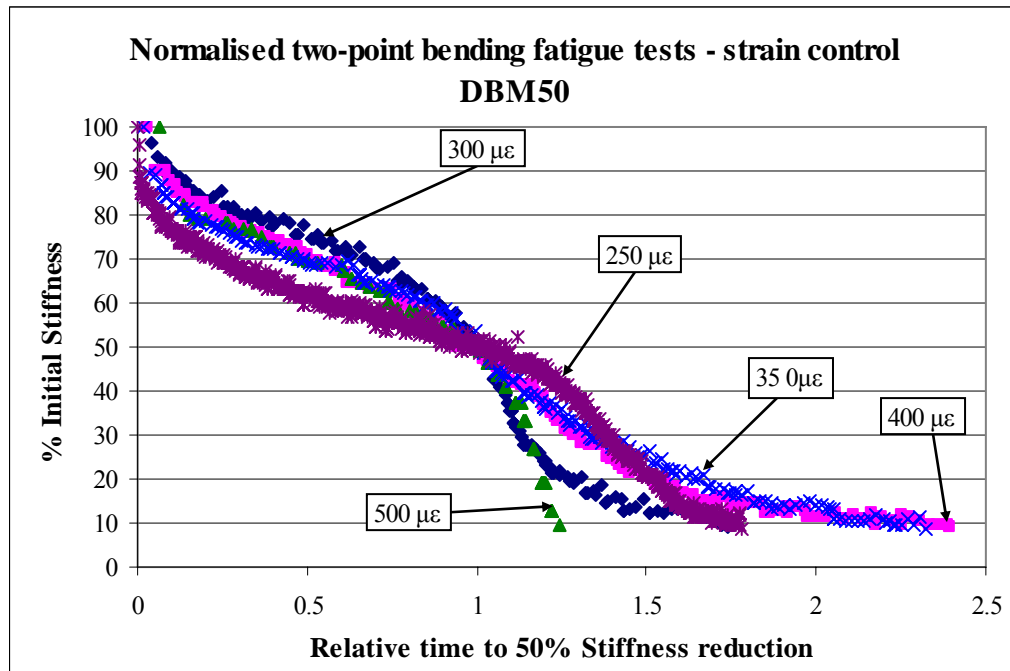
Figure 8.26 – Normalised two-point bending fatigue test results obtained for the
DBM50 mixture

Even though some scatter exists in these figures, especially at relative times greater
than 1.0, it is possible to observe the different trend followed by each type of
material, i.e., grouted macadam and asphalt (DBM 50). The rate of stiffness
reduction after approximately 50% of the initial value is dramatically different for
the two types of material. While the rate increases rapidly in the case of asphalt
materials, this does not happen in the case of grouted macadams, where the rate tends
to decrease with time (number of cycles). This suggests that grouted macadams will
continue to perform well, even after the established 'failure point', which is not the
case for asphalt materials. The results obtained were then averaged in order to best fit
a trend line to them and define equations that could be used in the design method
presented in the following section.

Figures 8.27 and 8.28 show the trends obtained for both materials. Data from the
models obtained for both material types, showing very good agreement with the
original data, are plotted together in Figure 8.29 for a direct comparison. In this
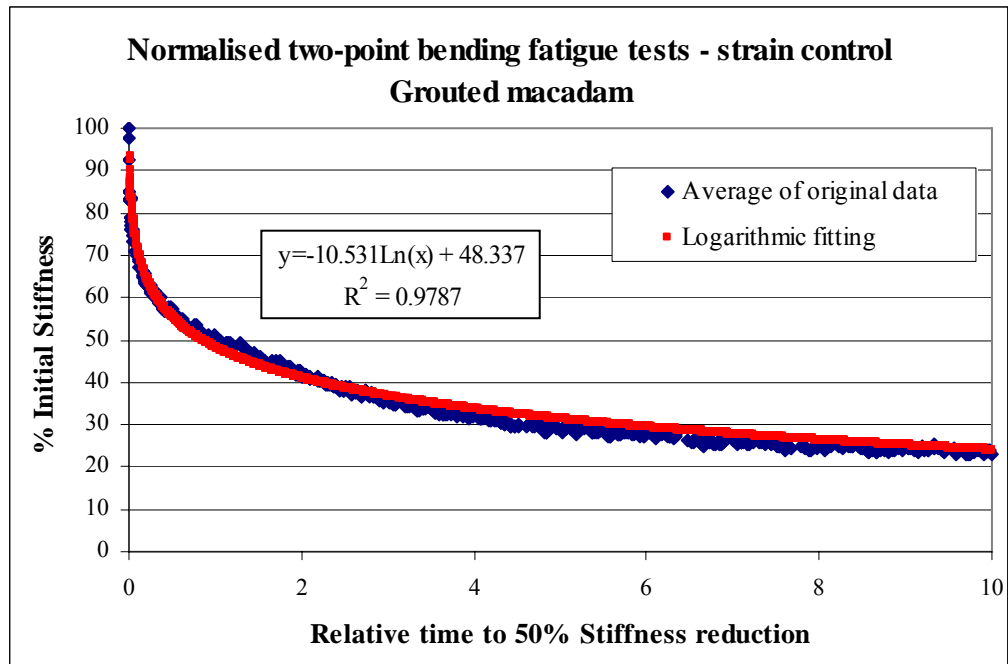figure, the different behaviour of the two materials becomes even more evident.

Figure 8.27 – Normalised standard grouted macadam fatigue test results (2PB)
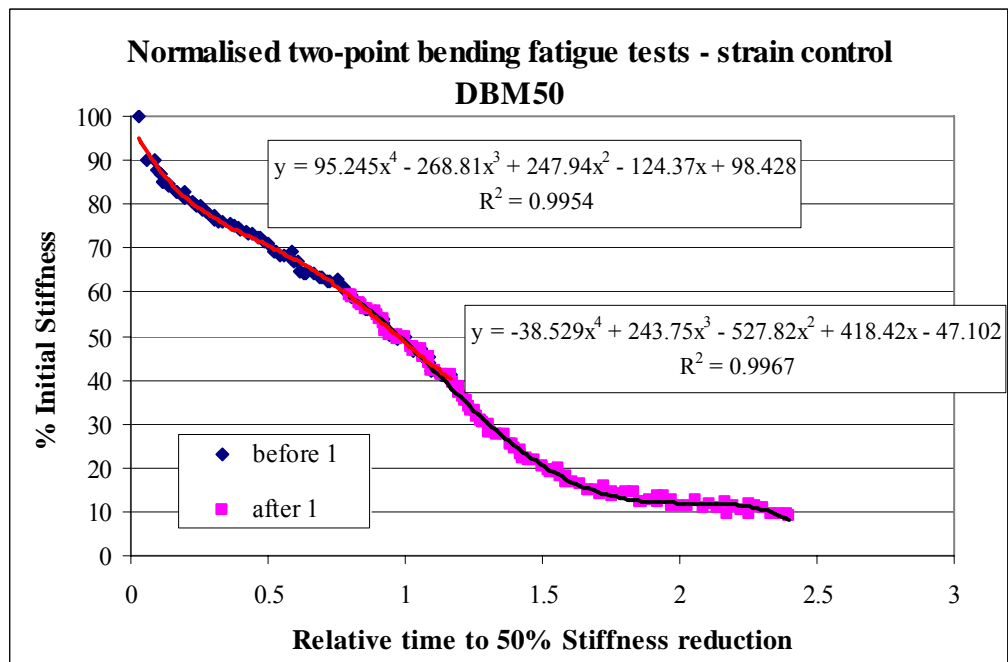

Figure 8.28 – Normalised DBM50 fatigue test results (2PB)

The different fatigue performance shown has a significant influence on the design of pavements, according to the new approach discussed in the following section, where an iterative process is used to simulate the stiffness reduction of the materials in the pavement. The cumulative number of cycles is calculated relative to the fatigue life obtained using the conventional failure criterion, as presented in Figure 8.22.
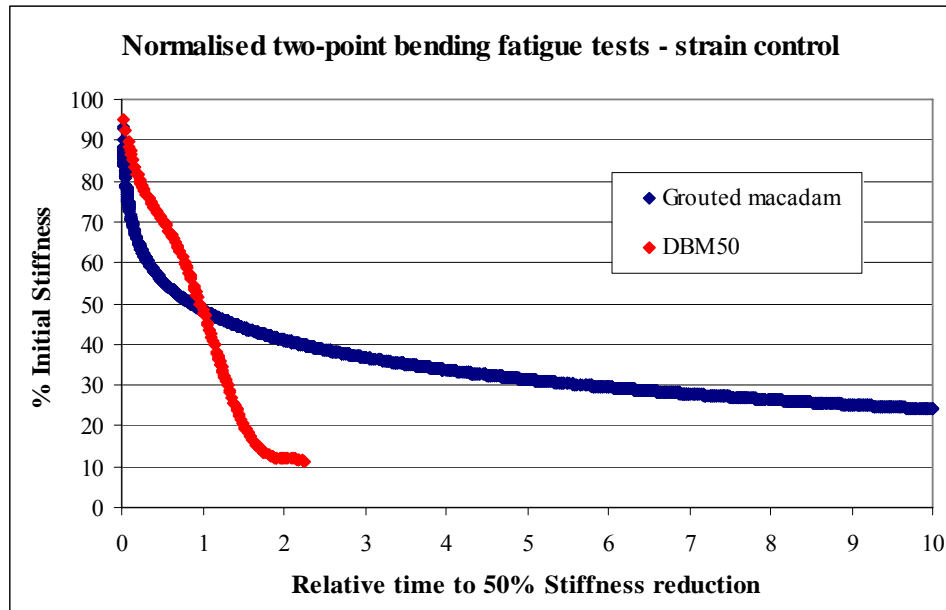
Figure 8.29 – Comparison between grouted macadam and DBM50 normalised data

8.4.3 Pavement design based on fatigue performance

In order to analyse the fatigue performance of both materials as they get weaker, by accumulation of damage, an iterative approach was used. In this methodology, four pavement structures were used in a multi-layer linear elastic analysis computer program – BISAR 3.0 (Shell International, 1998) to study the response of each pavement to the application of a standard load (40 kN). Similar to what was presented in Sections 8.3.1 and 8.3.2, four foundation classes were used, over which a 40 mm grouted macadam or DBM50 surface course would be applied directly. The pavement response was calculated for several levels of 'degradation', represented by several levels of stiffness reduction in the bound material layer (either grouted macadam or DBM).

Fatigue life of bituminous materials is traditionally defined by the number of load applications that the materials can be subjected to before failure, at a particular stress or strain level. In pavement design the strain criterion is normally used, and the maximum permissible strain is established by means of laboratory tests where the fatigue line of the material is determined. The thicknesses of the pavement layers are increased until the strain criterion is satisfied. In such calculations, the degradation of the material properties is not taken into account, as the strain is considered constant throughout the pavement life.

However, in reality such an assumption is not correct. As the material properties, namely stiffness, decrease the strain levels imposed in the pavement increase, resulting in a gradually lower resistance of the mixture to fatigue. In order to take this fact into consideration, an iterative process was used, whereby, for each pavement structure studied, the strain level was determined for several levels of degradation (stiffness reduction).

Since the rate of stiffness reduction changes during a fatigue test (reducing with time or number of load applications) different stiffness intervals were used, in order to follow the stiffness reduction curve more closely. Thus, at the beginning of the test, short intervals were obtained for the relative time, according to the interval of stiffness considered (Figure 8.30 represents the example obtained for the grouted macadam mixture. The same concept was used for the DBM 50 mixture). Within each interval, the average stiffness value was used as the input value for the determination of the strain level in the pavement, which was assumed constant during the interval.
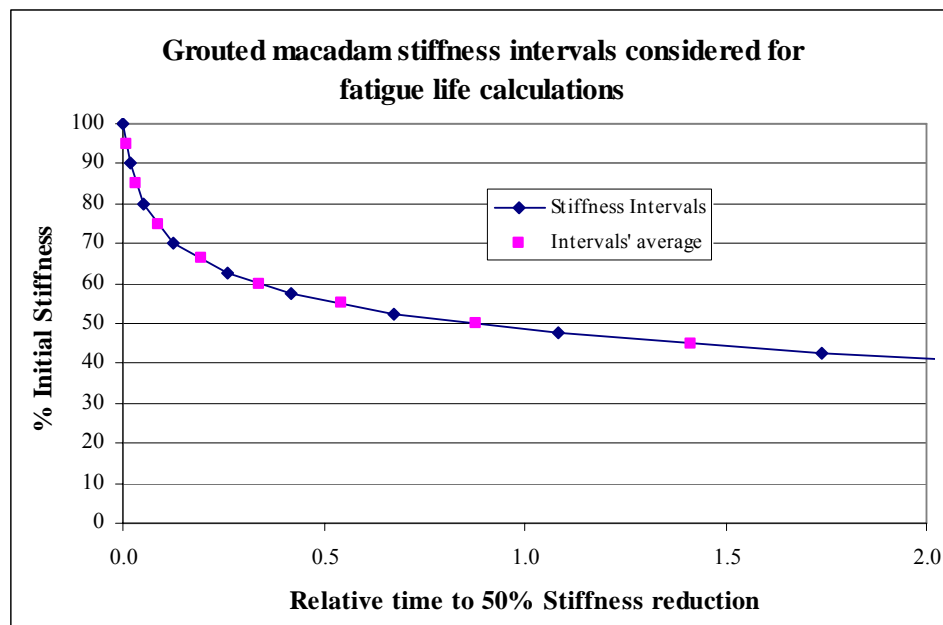

Figure 8.30 – Stiffness intervals used for the calculation of grouted macadam's cumulative fatigue life

For each strain level, the corresponding fatigue life was estimated (based on the traditional fatigue line of each mixture, i.e., assuming constant strain until failure). However, since failure is not obtained during each intermediate interval, but only a

portion of the fatigue life is consumed, the cumulative fatigue life is calculated by adding the life consumed during each interval (also known as the "Miner's Law"), as schematically illustrated in Figure 8.31.
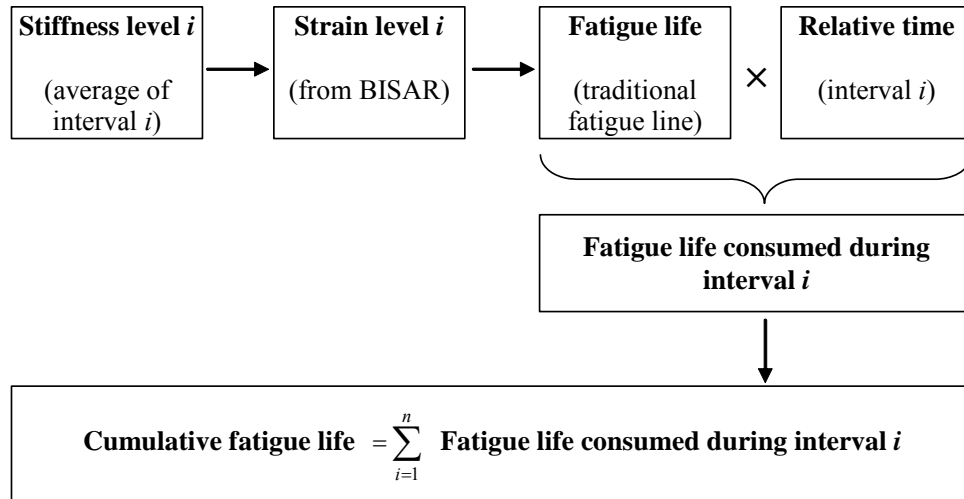

Figure 8.31 – Cumulative fatigue life calculations

According to the new approach, the fatigue life of any material, calculated until 50% stiffness reduction (which is the traditional failure criterion), gives lower results than if a normal estimation is made based on the corresponding fatigue line. This happens because the new approach takes the continuously decreasing stiffness into consideration. As a reminder, the number of load applications was determined according to the fatigue life obtained from laboratory tests, without taking any shift factor into account to establish the actual number of standard axles in a real pavement situation. An example is given in Figure 8.32 for the two studied materials, according to the foundation type used in the calculations. It is clear that the normal fatigue calculations overestimate the life of the mixtures.

Although the pavement structures used in this study may not be totally realistic, due to the high strain levels induced in the surface course, an increased fatigue life of grouted macadam can be observed regardless of the approach used for fatigue life estimation. However, the difference in extended life of grouted macadams reduces with the increase in bearing capacity of the foundation, since the influence of the surface course becomes less influential on the overall behaviour of the pavement, as the strains are reduced (Figure 8.33).
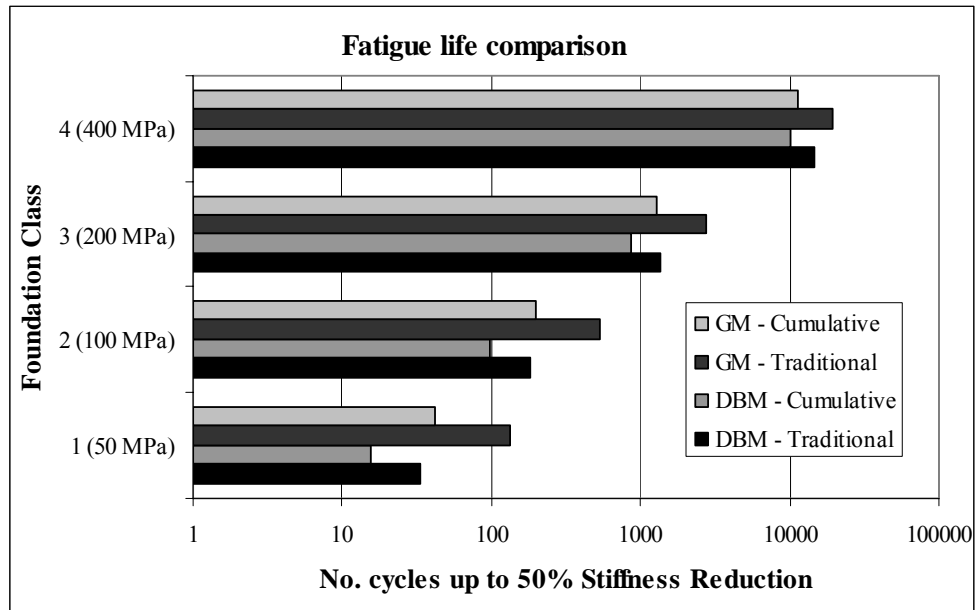
Figure 8.32 – Traditional and cumulative fatigue life of grouted macadam and DBM
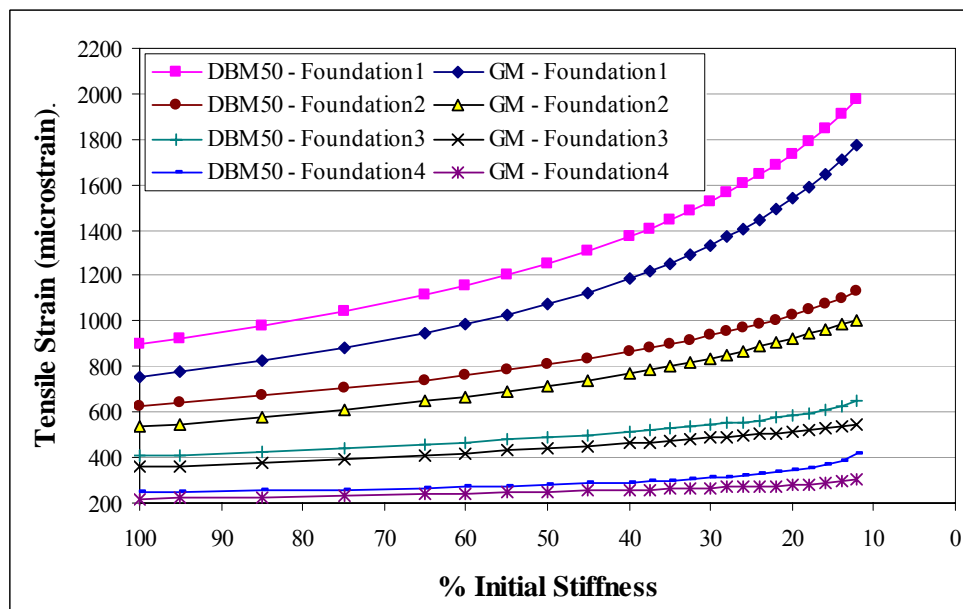

Figure 8.33 – Tensile strain obtained on the underside of the surface course of each pavement structure

The traditional failure criterion used in fatigue tests may not represent the true fatigue life of grouted macadams due to the particular behaviour presented by this type of material. In fact, the main advantage of grouted macadams is most noticed after the stiffness modulus of the mixture has achieved 50% reduction of its initial value. The new iterative approach to fatigue life highlights the extended fatigue life of grouted macadam surface courses, compared with conventional asphalt mixtures (such as DBM50). Figure 8.34 presents the cumulative number of cycles obtained for each pavement with different foundation classes, taking into account the degradation

of each mixture, while Figure 8.35 represents the development of the tensile strain on the underside of the surface course with the cumulative number of load applications.
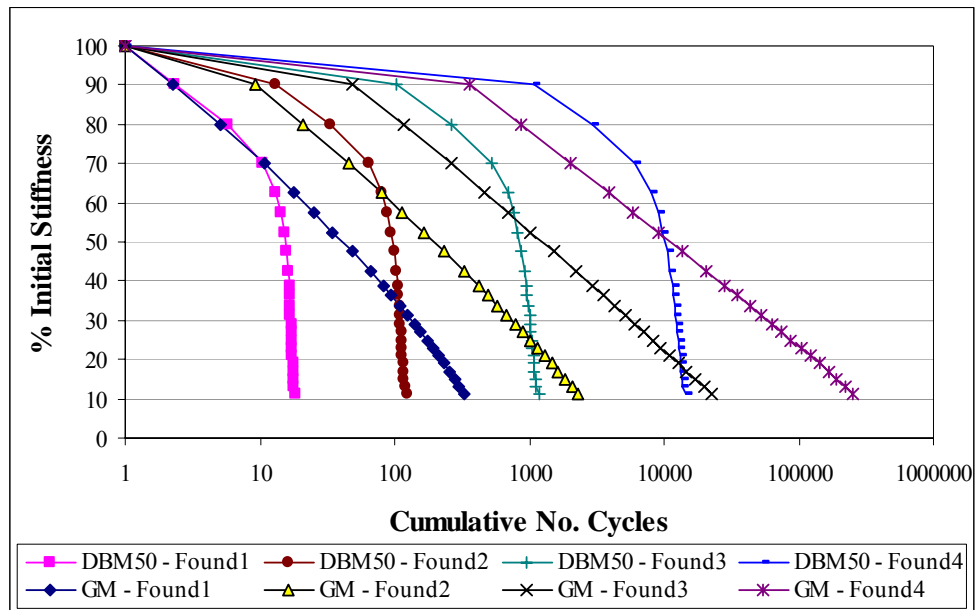

Figure 8.34 – Cumulative fatigue life of grouted macadam and DBM including degradation of the mixtures

In the figure above the different behaviour of the two types of mixture is evident. After a stiffness reduction of approximately 40 to 50%, the DBM50 mixture has little life left, while the grouted macadam mixture continues to lose stiffness approximately according to the logarithm of the cumulative number of cycles.
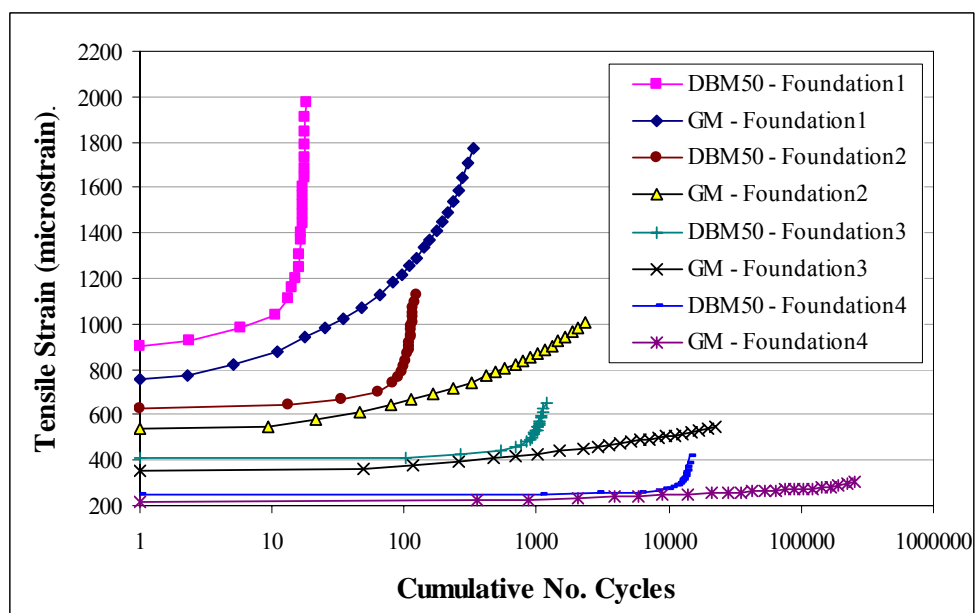

Figure 8.35 – Tensile strain developed under the surface course with the cumulative number of cycles for each studied pavement structure

8.5 Summary and Conclusions

Pavement design has generally been made based on laboratory test results, to which shift factors are usually applied to establish the relationship between the laboratory results and the material field performance. In the last few decades, fatigue life models have been developed and validated for bituminous mixtures, using feedback information gathered in the field. However, such models have not been tested to assess their suitability to be applied to grouted macadam mixtures. Therefore, a comparative analysis was carried out between results obtained for both grouted macadam and conventional asphalt mixtures, in order to verify the accuracy of such models in the design of pavements incorporating grouted macadam mixtures.

In the present investigation, two different approaches were used: a traditional methodology, where fatigue life is determined, converting laboratory test results into field performance by the application of shift factors; an iterative approach, where the response of the pavement was determined for several levels of degradation. For the former, a grouted macadam shift factor was determined, based on the effect of rest periods on the fatigue life of the mixture. The latter was carried out on a comparative basis, using a traditional DBM50 mixture as a reference for each pavement structure. The reason for this type of analysis was that a different stiffness reduction trend was observed during grouted macadam fatigue tests. In this study, fatigue tests were carried out beyond the traditional failure criterion (50% of initial stiffness), where grouted macadam showed a behaviour notably different from a conventional asphalt.

Throughout this chapter, four pavement foundation classes were used, as suggested by Nunn (2004) for a more versatile approach to pavement design. The stiffness modulus of the foundations ranged from 50 to 400 MPa, while a single Poisson's ratio of 0.35 was used. Traditional mixtures (HRA, SMA and DBM50) were also used to compare with grouted macadam, respectively in surface and base courses.

According to what was discussed above, a shift factor of 45 was determined for grouted macadam mixtures, which should be multiplied by the fatigue life obtained in the laboratory, in order to predict the actual pavement fatigue life more realistically. The shift factor suggested is still considered a conservative value, since

it does not include results from tests with very long rest periods between each load application. Binder ageing was also not considered in the determination of the shift factor. This may increase the stiffness modulus of the mixture, reducing the tensile strains, and may, indirectly, extend the fatigue life of the pavement.

Grouted macadams have traditionally been considered as rut resistant surfacings. However, their performance depends on the bearing capacity of the supporting layers. A simplified methodology was used to assess the influence of structural rutting on the appearance of surface cracking, leading to pavement failure. The maximum tensile strain, determined in thermal cracking tests (discussed in Chapter 6), was used to define failure of the standard grouted macadam mixture. Several values of structural rut depth and width of the permanent deformation bowl (rut width) were used to determine the maximum tensile strain induced in the mixture. An example was given for the pavement constructed in the PTF.

The influence of surface originated cracking on pavement design was also assessed. This type of failure may be significant in pavements with thick bound layers. In this study, 40 mm thick HRA/SMA and Grouted Macadam surface courses were used on top of a DBM50 base, the thickness of which was determined according to the traditional fatigue failure criterion (on the underside of the base) and according to the development of surface tensile strains that may result in fatigue cracking. Design charts have been developed to determine the base thickness, assuming both types of surface course. In these charts, extended fatigue lives can be obtained for pavements incorporating grouted macadam surface course, if the same base thickness is used, in comparison with HRA or SMA surface courses. Alternatively, a lower base thickness is necessary to obtain the same fatigue life.

A different application of grouted macadam, as a base course, was also investigated in this chapter. Design charts have been developed for two types of grouted macadam: the standard mixture and; a stiffer mixture (12000 MPa). Both mixtures have shown better performance than traditional DBM50 mixtures, with reduced base thickness or extended fatigue life resulting from the stiffer grouted macadam mixture, as expected. A particular issue that should be highlighted is the dominance of surface cracking above a certain base thickness (200 mm and 150 mm,

respectively, for the standard and the stiffer grouted macadam mixtures). Thus, only the surface layer would need to be subjected to future maintenance operations.

Even though extended fatigue life was obtained in all calculations made in the present chapter, for pavements incorporating grouted macadam the main advantage of such a type of mixture may be neglected by assuming the traditional failure criterion (50% of the initial stiffness, for strain-controlled fatigue tests) to define the fatigue life of this type of mixture. As demonstrated in Section 8.4, the particular behaviour of grouted macadam after the traditional failure point has been achieved, may extend the life of such a mixture even further. The iterative approach used in this investigation clearly indicates the lower damage growth rate of grouted macadam under fatigue. According to this property, grouted macadam could, in theory, have an indeterminate fatigue life, provided that the support is properly prepared.

9 CONCLUSIONS AND RECOMMENDATIONS

In this chapter, a summary of the main issues discussed in each previous chapter is presented, with particular attention paid to the main conclusions obtained from the present project. Some recommendations for future research are also suggested at the end of the chapter.

A review of the main types of pavement used in road construction and the principal design methods was made in Chapter 2. For each type of pavement (flexible, rigid and semi-rigid), the main properties and usual forms of distress were discussed. A brief introduction was made to semi-flexible pavements, with reference to Chapter 3 for further details. UK current practice in terms of pavement design was also discussed in Chapter 2, where the evolution of the concept of pavement design was presented. An attempt to establish a European Design Method, involving experts from twenty European countries, was described. The so called 'fundamental design method' would use a mechanistic approach, where material analytical models would be used to predict the performance of the pavement under specified traffic and climatic conditions. However, it was recognised that this goal is still to be achieved and that the design methods in regular use are either analytically based or empirical.

Chapter 3 reviewed the appearance and development of semi-flexible materials, i.e., grouted macadams, identifying the main application fields and discussing results obtained by other researchers in the past. Although limited literature is available about grouted macadams, the constitution and properties of the main types of mixture used in the past were described in this chapter. The influence of testing conditions on the final properties of the mixtures was also discussed. It is generally accepted that grouted macadams behave closer to asphalt than to concrete, although showing some characteristics of both types of material. This chapter, as well as the previous one, provided useful background information that was used as a starting point for the present research project, namely regarding the standard mix design and the methods used for pavement design.

The development of a four-point bending equipment was described in Chapter 4. This equipment was used as an alternative to the Nottingham Asphalt Tester (NAT) and the 'wheel on beam' test equipment, both available in the Nottingham Centre for Pavement Engineering laboratory. A four-point bending test equipment has several advantages, namely: (i) more realistic simulation of the bending of a pavement layer (compared with the NAT); (ii) elimination of specimen permanent deformation during the test, if used in displacement-control mode; (iii) possibility of determining the phase angle and stiffness modulus of the mixture at different frequencies. Due to technical and economic restrictions, the equipment was manufactured at the University of Nottingham, in the Civil Engineering School's workshop. The four-point bending rig was assembled and attached to an existing servo-hydraulic testing machine. Tests were carried out inside a temperature controlled cabinet (possible temperatures ranging from -5 to 40 °C). Before starting the series of tests, the equipment was calibrated using a specimen with known stiffness modulus. Although having limited capabilities, the controlling and data acquisition software of the machine allowed the performance of stiffness and fatigue tests at 5 and 10 Hz for different temperatures.

Properties of the materials used during this research project were presented in Chapter 5. Thus, after a general characterisation of the aggregates, bitumens and grouts used in this investigation, a comprehensive characterisation of the 'standard' grouted macadam mixture used in the project was presented. This included the study of the coefficient of thermal expansion, the early-age mechanical properties, the stiffness modulus and the fatigue life of the mixture. For the latter two, the influence of temperature, binder ageing, testing strain level, frequency and test type on the properties of the mixture were taken into account. The main properties and conclusions are summarised as follows:

- The coefficient of thermal expansion of the standard grouted macadam mixture was determined to be on average 0.98×10^{-5}/°C.
- Pavements with grouted macadam surface courses should never be opened to heavy traffic before 18 h of curing, according to the study carried out to determine the influence of traffic loading during the early stages of curing on the final properties of the standard mixture. This confirmed the guidelines

given by the grout suppliers, regarding the necessary curing time before opening to traffic (24 h).

- The influence of temperature on the mechanical properties of grouted macadams is significant in terms of stiffness modulus. In terms of fatigue, little effect was observed on the behaviour of the mixture when the test temperature was kept below 20 ºC. Only for temperatures above the softening point of the bitumen, were significant changes observed in the fatigue line of the mixture (increasing the fatigue life).

- Ageing of bitumen seems to have a significant effect on the stiffness modulus of grouted macadams. In the tests carried out during the project, not only has long-term ageing shown an increase in stiffness of approx. 47%, but also a short/medium-term ageing (3 months, including temperature fluctuations have shown a 35% increase in the stiffness modulus in some grouted macadam specimens.

- The mechanical properties of grouted macadams do not change significantly beyond 7 days of curing, as determined using 4-point bending tests.

Chapter 6 presented the results of the mix design study carried out during this project to optimise the composition of grouted macadam mixtures. Several variables were considered in this study (including small variations to the standard mix design and significantly different mixtures), and included: (i) different binder contents (1.5% and 3% by mass of asphalt); (ii) different binder types (a 50 pen straight-run bitumen and a polymer modified binder with the incorporation of SBS rubber elastomers); (iii) a different aggregate type (limestone); (iv) different aggregate sizes and grading (a 14 mm single sized aggregate, a 20 mm single sized aggregate, and a more continuous aggregate grading); (v) combinations of some of the previous variables. The main conclusions to be highlighted from this investigation are summarised as follows:

- Stiffness is mostly related to the volume of bitumen used in grouted macadams, increasing with a reduction of the bitumen volume.

- Fatigue performance of grouted macadams is not affected by small variations in the binder content. However, very low binder contents noticeably reduce fatigue performance of grouted macadams even though an increased stiffness

modulus should also be expected. The resistance to thermally induced cracking is also affected by the thin binder film thickness obtained with such mixtures.

- The use of harder straight-run bitumen seems to have limited influence on the fatigue life of grouted macadams, while increasing the stiffness modulus of the mixtures. However, the resistance to thermally induced cracking is compromised with the use of hard bitumens. On the other hand, polymer modified binders (like the SBS thermoplastic rubber modified bitumen used in this study) significantly increase the fatigue life without compromising the stiffness modulus of the final mixture.

- Despite having a low polished stone value (PSV), limestone seems to be a good alternative to granite (or other high quality aggregate) in applications where the skid resistance of the pavement is not an issue.

- The properties of the grout used in grouted macadams have limited influence on the stiffness modulus of the final mixture. However, the same cannot be said regarding the fatigue life, since grout strength and particularly grout shrinkage have a significant effect on the performance of the mixture. Higher shrinkage values resulted in shorter fatigue life.

- Small variations to the standard mix design did not have a significant effect on the fatigue performance of the final mixture. Hence, it was possible to establish a fatigue line incorporating data from most of the studied mixtures with a high correlation coefficient ($R^2 = 0.95$). The exceptions to this rule are the mixtures with 20 mm single sized aggregate, low binder content (1.5%), and lower strength grouts (with shorter fatigue lives), and the PMB mixtures (with extended fatigue lives).

- Mixtures with soft binders and thick bitumen films presented the best resistance to thermally induced cracking (the standard mixture showed a tensile strain level three times higher than the other mixtures, before failure of the specimen, and can be compared with a 20 mm DBM mixture using a 50 pen binder, in terms of thermal cracking resistance).

- The use a grid reinforcement between a cracked pavement base and the grouted macadam surface course can significantly increase the resistance of the mixture to thermally induced cracking. The results obtained for a specimen with Glasgrid® reinforcement showed thermal cracking resistance (maximum

movement of the layer underneath, before failure) two times higher than that obtained for an unreinforced specimen bonded to concrete slabs with tack coat. Nonetheless, in these tests, the unreinforced grouted macadam showed similar results to an unreinforced 100 pen DBM mixture (obtained by Brown et al., 2001).

The deterioration of a half-scale pavement constructed in the laboratory was discussed in Chapter 7. The main objective of this investigation was to follow the appearance and degradation of cracks on grouted macadam surface courses under traffic loading, while assessing the performance of some of the mixtures used in the mix design study (including the use of reinforcement). Five different sections were used in the surface course: one made with the standard mixture (used as a reference); three sections comprising three alternative mixtures (2% of a 200 pen binder; 2% of a PMB binder; a modified grout) and; a fifth section with a standard mixture applied over a reinforcing grid (Glasgrid®). The design of the pavement was influenced by the limited time available to run the test and the limited load that could be applied by the wheel in the PTF. The main conclusions to be drawn from this study are summarised below:

- The construction joints play an important role in the performance of pavements incorporating grouted macadams. The joints between sections were the first places showing signs of failure under the application of the wheel loads.

- In an attempt to accelerate the pavement degradation rate, the bearing capacity of the granular layers was overestimated, resulting in structural rutting, which led to the appearance of surface cracking parallel to the wheel path due to excessive permanent deformation. This highlights the importance of the support in the performance of pavements with grouted macadam surface courses.

- Hairline cracking observed in the modified grout section (due to grout shrinkage) did not seem to significantly influence the performance of the mixture (except with regard to the reduction of stiffness modulus). Nonetheless, this emphasizes the importance of properly characterising a cementitious grout prior to the inclusion in a grouted macadam mixture, in order to predict its behaviour on site.

- Very little fatigue cracking was observed in the wheel paths after 20000 cycles had been applied on each of the two tracks used. Additional trafficking was carried out on the 2nd track in order to evaluate the degradation of the pavement, which was stopped after an extra 40000 wheel passes had been applied, due to a reduced degradation rate.

A set of laboratory tests (ITSM, ITFT, four-point bending tests), carried out on specimens extracted from the surface course of each section, was also presented in Chapter 7. This study was performed in order to evaluate possible damage undergone by the mixtures, in areas under the wheel path, i.e., areas in direct contact with the traffic loads, in comparison with 'undamaged' areas away from the wheel tracks. The main conclusions drawn from this set of laboratory tests are summarised as follows:

- No apparent damage was observed on the standard mixture's stiffness modulus obtained from specimens extracted from the loaded areas.

- Most of the damage observed in the other sections seemed to occur at the beginning of the PTF test.

- Limited crack propagation was identified on cores extracted from areas with wide surface cracks.

- The fatigue performance of loaded or 'damaged' cores was apparently not affected by traffic loads, although some care must be taken when analysing these results due to the limited number of specimens tested for each section.

- The four-point bending tests allowed a more comprehensive characterisation of the mixtures, whose results are in line with what was expected after the mix design study.

Finally, in Chapter 8, the design of pavements incorporating grouted macadams is discussed. Two approaches were used in this investigation: (i) a traditional design method, for which a shift factor was determined, to establish the relationship between laboratory fatigue results and field performance; (ii) an iterative approach, where the response of the pavement was determined for several levels of degradation of the grouted macadam mixture. For both design methods, four pavement foundation classes were considered, whose stiffness modulus ranged from 50 to 400 MPa, while a single Poisson's ratio of 0.35 was used for all foundations.

Traditional mixtures (HRA, SMA and DBM50) were also used in comparison with grouted macadam, respectively in surface and base courses. The main findings and conclusions obtained in this chapter are presented below:

- A shift factor of 45 was determined for grouted macadam mixtures (to be used with the traditional design method), which should be multiplied by the fatigue life obtained in the laboratory, in order to predict the actual pavement fatigue life more realistically.

- A simplified methodology was used to assess the influence of structural rutting on the appearance of surface cracking. Several values of structural rut depth and width of the permanent deformation bowl (rut width) were used to determine the maximum tensile strain induced in the mixture.

- The influence of surface originated cracking on pavement design was also considered in the traditional design approach. In this study, 40mm thick HRA/SMA and Grouted Macadam surface courses were used on top of a DBM50 base. Design charts have been developed to determine the base thickness, assuming both types of surface course. In these charts, extended fatigue lives can be obtained for pavements incorporating grouted macadam surface course, if the same base thickness is used, in comparison with HRA or SMA surface courses. Alternatively, a lower base thickness is necessary to obtain the same fatigue life.

- The use of grouted macadam as a base course (overlaid by a traditional asphalt layer) was also investigated in this chapter. Design charts have been developed for two types of grouted macadam: the standard mixture and a stiffer mixture. Both mixtures have shown better performance than traditional DBM50 mixtures. A particular issue that should be highlighted is the dominance of surface cracking above a certain base thickness (200 mm and 150 mm, respectively, for the standard and the stiffer grouted macadam mixtures).

- The main advantage of using grouted macadams may be overlooked, by assuming the traditional failure criterion (50% of the initial stiffness, for strain-controlled fatigue tests) to define the fatigue life of this type of mixture. The particular behaviour of grouted macadam after the traditional failure point has been achieved, may extend its life even further. The iterative approach used in this investigation clearly indicates the lower damage growth rate of grouted

macadam under fatigue. According to this property, grouted macadam could, in theory, have an indeterminate fatigue life, provided that the support is properly prepared.

Although this project has contributed to a better understanding of the behaviour of grouted macadams, it is still possible to carry out further investigations. Therefore, the following recommendations are suggested for future research:

- Numerical modelling of the structure of this type of mixture could be performed (on a micro scale), in order to establish the role of each component of the mixture according to the particular behaviour shown in fatigue tests.

- A more comprehensive set of fatigue tests including rest periods should also be carried out, in order to confirm the shift factor value determined for the standard grouted macadam mixture. Other mixtures could also be included in the study, should the shift factor be generalised to other grouted macadam compositions (e.g., mixtures comprising modified binders).

- The failure criterion used for fatigue tests should also be further investigated, since the traditional criterion used for bituminous mixtures seems to be unsuccessful in representing failure of grouted macadam mixtures, according to the results obtained in this project.

- Full-scale trials should be used, under real traffic loading, to assess the performance of both surface and base courses comprising grouted macadams.

- The use of industrial waste materials and by-products either as aggregate or filler substitutes, or as grout constituents should be investigated. This would allow a clear reduction of the costs of grouted macadams, while reducing the environmental impact originated by the waste materials.

- Further investigation could be carried out regarding the grout composition (which was not studied in the present project), in order to optimise the grout strength that is really necessary for such an application. Economic issues should also be taken into consideration in this study.

- An economics oriented study should be carried out to determine the actual costs of grouted macadam mixtures, in order to provide supporting data to pavement engineers when deciding which mixture to use in a specific application.

- Finally, modifications to the construction technique currently used in the production of grouted macadams could be further investigated for the rehabilitation of pavements comprising porous asphalt surface courses. Instead of removing the porous asphalt layers, a grout could be used to fill the voids of the mixture, turning it into a type of grouted macadam, over which a new layer of porous asphalt (or other mixture) could be applied. In such a scenario, the grout type (cementitious or other) and constitution would have to be investigated, in order to optimise its workability, since the void content of conventional porous asphalts is lower than that used in the present study and some of the voids may be obstructed by dust and/or dirt.

REFERENCES

Ahlrich, R. C. and Anderton, G. L., (1991). *Evaluation of Resin-Modified Paving Process*. Transportation Research Record 1317: 32-41. Washington, D.C.

Al-Khateeb, G. and Shenoy, A., (2004). *A Distinctive Fatigue Failure Criterion*. Journal of the Association of Asphalt Paving Technologists, Vol. 73, pp. 585-622.

AMADEUS, (2000). *Advanced Models for Analytical Design of European Pavement Structures*. European Commission. Brussels.

Anderton, G. L., (1996). *User's Guide: Resin Modified Pavement*. U.S. Army Engineer Waterways Experiment Station. Vicksburg.

Anderton, G. L., (2000). *Engineering Properties of Resin Modified Pavement (RMP) for Mechanistic Design*. ERDC/GL TR-00-2. U.S. Army Corps of Engineers. Vicksburg.

Asphalt Institute, (1989). *The Asphalt Handbook.* Manual Series No. 4 (MS-4), pp. 422-427.

BACMI, (1992). *Bituminous Mixes and Flexible Pavements – An Introduction.* British Aggregate Construction Materials Industries. London.

Bodin, D., De La Roche, C., Piau, J. M., Pijaudier-Cabot, G., (2003). *Prediction of the Intrinsic Damage during Bituminous Mixes Fatigue Tests*. 6th RILEM Symposium on Performance Testing and Evaluation of Bituminous Materials. Zurich.

Boundy, R., (1979). *Development of a Resin/Cement grouted coated Macadam Surfacing Material*. M. Phil. thesis. University of Nottingham. Nottingham.

Breysse, D., De La Roche, C., Domec, V., Chauvin, J. J., (2003). *Influence of Rest Time on Recovery and Damage during Fatigue Tests on Bituminous Composites*. 6th RILEM Symposium on Performance Testing and Evaluation of Bituminous Materials. Zurich.

Breysse, D., Domec, V., Yotte, S., De La Roche, C., (2004). *Better Assessment of Bituminous Materials Lifetime Accounting for the Rest Periods*. 5th RILEM International Conference on "Cracking in Pavements". Limoges.

British Board of Agrement (BBA), (1994). *Hardicrete Heavy Duty Surfacing.* Agrement Certificate No 88/1969. Watford.

British Board of Agrement (BBA), (1996). *Worthycim Heavy Duty Paving.* Agrement Certificate 87/1900. Watford.

Brown, S. F. and Brodrick, V. B., (1981). *Nottingham pavement test facility*. Transportation Research Record 810. pp. 67-72.

Brown, S. F. and Brunton, J. M., (1985). *An Introduction to the Analytical Design of Bituminous Pavements*. University of Nottingham. Nottingham.

Brown, S. F., Brunton, J. M. and Stock, A. F., (1985). *The Analytical Design of Bituminous Pavements*. Proc. Institution of Civil Engineers, Part 2, Vol.79, pp. 1-31.

Brown, S. F., Thom, N. H., Sanders, P. J., (2001). *A study of grid reinforced asphalt to combat reflection cracking*. Journal of the Association of Asphalt Paving Technologists, Vol. 70, pp. 543-570.

BSI, (1987). *British Standard 63: Part 1: 1987: Road Aggregates - Specification for single-sized aggregate for general purposes*. British Standard Institution. London.

BSI, (1990). *British Standard 1377: Part 2: 1990: Methods of test for Soils for civil engineering purposes – Classification tests*. British Standard Institution. London.

BSI, (1993). *British Standard Draft for Development DD 213 - Method for Determination of the indirect tensile stiffness modulus of bituminous mixtures*. British Standard Institution. London.

BSI, (1995$_a$). *British Standard BS 812: Part 2: 1995: Testing aggregates – Methods of determination of density*. British Standard Institution. London.

BSI, (1995$_b$). *British Standard BS EN 196: Part 1: 1995: Methods of Testing cement – Determination of strength*. British Standard Institution. London.

BSI, (2002). *British Standard Draft for Development DD AFB – Method for Determination of the fatigue characteristics of bituminous mixtures using indirect tensile fatigue*. British Standard Institution. London.

BSI, (2002$_a$). *Draft EN 12697-45 Bituminous mixtures - Test methods for hot mix asphalt - Part 45: Binder drainage – Schellenberg method*. British Standard Institution. London.

BSI, (2003). *British Standard BS EN 12697: Part 6: 2003: Bituminous mixtures - Test methods for hot mix asphalt – Determination of bulk density of bituminous specimens*. British Standard Institution. London.

BSI, (2004). *British Standard BS EN 14227: Part 1: 2004: Hydraulically bound mixtures – Specifications – Cement bound granular mixtures*. British Standard Institution. London.

BSI, (2004$_a$). *British Standard BS EN 14227: Part 2: 2004: Hydraulically bound mixtures – Specifications – Slag bound mixtures*. British Standard Institution. London.

BSI, (2004$_b$). *British Standard BS EN 14227: Part 3: 2004: Hydraulically bound mixtures – Specifications – Fly ash bound mixtures*. British Standard Institution. London.

BSI, (2004$_c$). *British Standard BS EN 14227: Part 5: 2004: Hydraulically bound mixtures – Specifications – Hydraulic road binder bound mixtures*. British Standard Institution. London.

BSI, (2004$_d$). *British Standard BS EN 12697: Part 24: 2004: Bituminous mixtures - Test methods for hot mix asphalt – Resistance to fatigue*. British Standard Institution. London.

Collis, L. and Fox, R. A., (1985). *Aggregates: Sand, Gravel and Crushed Rock Aggregates for Construction Purposes*. The Geological Society. London.

Collop, A. C. and Elliott, R. C., (1999). *Assessing the mechanical performance of Densiphalt*. 3rd European Symposium of "Performance and Durability of Bituminous Materials and Hydraulic Stabilised Composites". Leeds.

Collop, A. C., Thom, N. H. and Brown, S. F., (2001). *Mechanical performance of high modulus roadbase materials*. University of Nottingham. Nottingham.

Colombier, G. and Marchand, J. P., (1993). *The precracking of pavements underlays incorporating hydraulic binders*. 2nd International RILEM Conference on "Reflective Cracking in Pavements - State of the Art and Design Recommendations". Liege.

Contec ApS, (2005). The new generation semi-flexible wearing course. <URL:http://www.confalt.com> [Accessed 8 August 2005]

COST 333, (1999). *Development of New Bituminous Pavement Design Method*. Final Report of the Action. European Commission Directorate General Transport. Brussels.

Croney, D. and Croney, P., (1991). *The design and performance of road pavements*. McGraw -Hill Book Company Europe. Maidenhead.

Darter, M., (1992). *Report on the 1992 U.S. Tour of European Concrete Highways (U.S. Tech)*. Federal Highway Administration. Washington, D.C.

Densit a/s, (2000). *Densiphalt$^®$ Handbook*. Aalborg.

Di Benedetto, H., De La Roche, C., Baaj, H., Pronk, A. and Lundström, R., (2003). *Fatigue of Bituminous Mixtures: Different Approaches and RILEM group contribution*. 6th RILEM Symposium on Performance Testing and Evaluation of Bituminous Materials. Zurich.

Di Benedetto, H., De La Roche, C., Baaj, H., Pronk, A. and Lundström, R., (2004). *Fatigue of Bituminous Mixtures*. RILEM TC 182-PEB. Materials and Structures, Vol.37, pp. 202-216.

Ekdahl, P. and Nilsson, R., (2005). *How may the variation of traffic loading effect measured asphalt strains and calculated pavement service life?* 7th International Conference on the Bearing Capacity of Roads, Railways and Airfields (BCRA). Trondheim.

Ellis, S. J., Dudgeon, R. P. and Megan, M. A., (2000). *Induced cracking, developing an analytical design method with performance validation.* 4th International RILEM Conference on "Reflective Cracking in Pavements - Research in Practice". Ottawa.

Ellis, S. J., Megan, M. A. and Wilde, L. A., (1997). *Construction of full-scale trials to evaluate the performance of induced cracked CBM roadbases.* TRL Report 289. Transport Research Laboratory. Crowthorne.

Francken, L., (1993). *Laboratory Simulation and Modelling of Overlay Systems.* 2nd International RILEM Conference on "Reflective Cracking in Pavements - State of the Art and Design Recommendations". Liege.

Freitas, E., Pereira, P. and Picado-Santos, L., (2003). *Assessment of Top-Down Cracking Causes in Asphalt Pavements.* MAIREPAV03 - Third International Symposium on Maintenance and Rehabilitation of Pavements and Technological Control. University of Minho, Guimaraes.

Ghuzlan, K. A. and Carpenter, S. H., (2000). *Energy-Derived, Damage-Based Failure Criterion for Fatigue Testing.* Transportation Research Record 1723: 141-149. Washington, D.C.

Highways Agency, (1994$_a$). *Design Manual for Roads and Bridges.* HD 25/94 - Volume 7 - Section 2 - Part 2 - Foundations. London.

Highways Agency, (1994$_b$). *Design Manual for Roads and Bridges.* HD 32/94 - Volume 7 - Section 4 - Part 2 - Maintenance of Concrete Roads. London.

Highways Agency, (1999). *Design Manual for Roads and Bridges.* HD 23/99 - Volume 7 - Section 1 - Part 1 - General Information. London.

Highways Agency, (2001). *Design Manual for Roads and Bridges.* HD 26/01 - Volume 7 - Section 2 - Part 3 - Pavement Design. London.

Highways Agency, (2004). *Manual of Contract Documents for Highway Works.* Volume 1 - Specification for Highway Works - Series 900. London.

Highways Agency, (2005). *Design Manual for Roads and Bridges.* HD 26/05 (Draft 4) - Volume 7 - Section 2 - Part 3 - Pavement Design. London.

Hunter, R. N., (1994). *Bituminous mixtures in road construction*. Thomas Telford Ltd. London.

Hunter, R. N., (2000). *Asphalt in road construction*. Thomas Telford Ltd. London.

Jofré, C., Vaquero, J. and Alvarez-Loranca, R., (2000). *15 Years of Precracking in Spain: An Evaluation*. 4th International RILEM Conference on "Reflective Cracking in Pavements - Research in Practice". Ottawa.

Kazarnovsky, V. D., Kretov, V. A. and Yumashev, V. M., (2000). *Quantitative estimation of thermal crack resistance of road Pavements with asphalt surfacings and cement concrete bases*. 4th International RILEM Conference on "Reflective Cracking in Pavements - Research in Practice". Ottawa.

Khweir, K. and Fordyce, D., (2003). *Influence of layer bonding on the prediction of pavement life*. Proc. Institution of Civil Engineers, Transport 156, Issue TR2, pp. 73-83.

Kim, Y. R., Lee, H. J. and Little, D. N., (1997). *Fatigue Characterisation of Asphalt Concrete Using Viscoelasticity and Continuum Damage Theory*. Journal of the Association of Asphalt Paving Technologists, Vol. 66, pp. 520-569.

Kim, Y. R., Little, D. N. and Lytton, R. L., (2003). *Fatigue and Healing Characterization of Asphalt Mixtures*. Journal of Materials in Civil Engineering, Vol. 15, No. 1. pp. 75-83. ASCE.

Lemlin, M., (1997). *Cement concrete roads in Belgium*. Britpave Seminar.

Lundstrom, R., Di Benedetto, H. and Isacsson, U., (2004). *Influence of Asphalt Mixture Stiffness on Fatigue Failure*. Journal of Materials in Civil Engineering, Vol. 16, No. 6. pp. 516-525. ASCE.

Mayer, J. and Thau, M., (2001). *Joint Less Pavements for Heavy-Duty Airport Application: The Semi-Flexible Approach*. Proc. ASCE Airfield Pavement Speciality Conference - Advancing Airfield Pavements. Chicago.

MetOffice, (2005). M*ean annual temperature in the UK*. <URL:http://www.metoffice.com/climate/uk/location/england/> [Accessed 2 December 2005]

Nunn, M., (1997). *Long-life Flexible Roads*. 8th International Conference on Asphalt Pavements. Seattle. Vol. 1, pp.3-16.

Nunn, M. E. and Potter, J. F., (1993). *Assessment of methods to prevent reflection cracking*. 2nd International RILEM Conference on "Reflective Cracking in Pavements - State of the Art and Design Recommendations". Liege.

Nunn, M., (2004). *Development of a more versatile approach to flexible and flexible composite pavement design*. TRL Report TRL615. TRL Limited. Crowthorne.

Osman, S. A., (2004). *The role Bitumen and Bitumen/Filler Mortar in Bituminous Mixture Fatigue*. PhD thesis. University of Nottingham. Nottingham.

Parry, A. R., Phillips, S. J., Potter, J. F. and Nunn, M. E., (1999). *Design and performance of flexible composite road pavements*. Proc. Institution of Civil Engineers. Transport 135: 9-16.

Pelgröm, L. J. W., (2000). *Engineering mechanical properties Densiphalt*. Report prepared for Densit a/s by KOAC-WMD. Aalborg.

Pell, P. S. and Taylor, I. F., (1969). *Asphaltic Road Materials in Fatigue*. Journal of the Association of Asphalt Paving Technologists, Vol. 38, pp. 371-422.

Pell, P. S. and Cooper, K. E., (1975). *The Effect of Testing and Mix Variables on the Fatigue Performance of Bituminous Materials*. Journal of the Association of Asphalt Paving Technologists, Vol. 44, pp. 1-37.

Potter, J. F., Dudgeon, R. and Langdale, P. C., (2000). *Implementation of crack and seat for concrete pavement maintenance*. 4th International RILEM Conference on "Reflective Cracking in Pavements - Research in Practice". Ottawa.

Powell, W. D., Potter, J. F., Mayhew, H. C. and Nunn, M. E., (1984). *The structural design of bituminous roads*. TRRL Laboratory Report 1132. Transportation and Road Research Laboratory. Crowthorne.

Rao Tangella, S. C. S., Craus, J., Deacon, J. A. and Monismith, C. L., (1990). *Summary Report on Fatigue Response of Asphalt Mixtures*. Prepared for Strategic Highway Research Program, Project A-003-A, Institute of Transportation Studies, University of California. Berkeley.

Read, J. and Whiteoak, D., (2003). *The Shell Bitumen Handbook*. Published for Shell Bitumen by Thomas Telford Ltd. London.

Rowe, G. M., (1993). *Performance of Asphalt Mixtures in the Trapezoidal Fatigue Test*. Journal of the Association of Asphalt Paving Technologists, Vol. 62, pp. 344-384.

Saraf, C. L., (1998). *Pavement Condition Rating System - Review of PCR Methodology*. FHWA/OH-99/004. Ohio Department of Transportation. Westerville.

Scholz, T. V., (1995). *Durability of Bituminous Paving Mixtures*. PhD thesis. University of Nottingham. Nottingham.

Setyawan, A., (2003). *Development of Semi-Flexible Heavy-Duty Pavements*. PhD thesis. University of Leeds. Leeds.

Shahid, M. A. and Thom, N. H., (1996). *Performance of Cement Bound Bases with controlled cracking*. Third Int. RILEM Conference on Reflective Cracking in Pavements. pp. 55-66.

Shahid, M. A., (1997). *Improved Cement Bound Base Design for Flexible Composite Pavements*. PhD thesis. University of Nottingham. Nottingham.

Shell International Petroleum Company Ltd., (1978). *Shell Pavement Design Manual*. London.

Shell International Oil Products BV, (1998). *BISAR 3.0 – BItumen Stress Analysis in Roads*. User Manual. The Hague.

Sousa, J. B., (1994). *Asphalt-Aggregate Mix Design Using the Simple Shear Test (Constant Height)*. Journal of the Association of Asphalt Paving Technologists Vol. 63: 298-334.

Taherkhani, H. and Collop, A. C., (2005). *Characterisation of Uniaxial Creep Deformation Behaviour of Asphalt Mixtures*. 7th International Conference on the Bearing Capacity of Roads, Railways and Airfields (BCRA). Trondheim.

Tayebali, A. A., Rowe, G. M. and Sousa, J. B., (1992). *Fatigue Response of Asphalt-Aggregate Mixtures*. Journal of the Association of Asphalt Paving Technologists, Vol. 61, pp. 333-360.

Tayebali, A. A., Deacon, J. A., Coplantz, J. S. and Monismith, C. L., (1993). *Modeling Fatigue Response of Asphalt-Aggregate Mixes*. Journal of the Association of Asphalt Paving Technologists, Vol. 62, pp. 385-421.

Tayebali, A. A., Deacon, J. A., Coplantz, J. S., Finn, F. N. and Monismith, C. L., (1994a). *Fatigue Response of Asphalt-Aggregate Mixes - Part II - Extended test Program*, (SHRP-A-404). Strategic Highway Research Program, National Research Council. Washington, DC.

Tayebali, A. A., Deacon, J. A., Coplantz, J. S., Harvey, J. T. and Monismith, C. L., (1994b). *Fatigue Response of Asphalt-Aggregate Mixes - Part I - Test Method Selection*, (SHRP-A-404). Strategic Highway Research Program, National Research Council. Washington, DC.

Thom, N. H., (2000). *A simplified computer model for grid reinforced asphalt overlays*. 4th International RILEM Conference on "Reflective Cracking in Pavements - Research in Practice". Ottawa.

Thom, N. H., (2003a). *Grid Reinforced overlays: predicting the unpredictable*. MAIREPAV03 - Third International Symposium on Maintenance and Rehabilitation of Pavements and Technological Control. University of Minho, Guimaraes. pp. 317-326.

Thom, N. H., (2003b). *Implementation of a Performance Specification for Capping and Subgrade*. Final Report prepared for The Highways Agency by Scott Wilson Pavement Engineering Ltd. Nottingham.

van de Ven, M. F. C. and Molenaar, A. A. A., (2004). *Mechanical Characterization of Combi-layer*. Journal of the Association of Asphalt Paving Technologists, Vol. 73, pp. 1-22.

Van Dijk, W., (1975). *Practical Characterization of Bituminous Mixes*. Journal of the Association of Asphalt Paving Technologists, Vol. 44, pp. 38-74.

Van Dijk, W. and Visser, W., (1977). *The Energy Approach to Fatigue for Pavement Design*. Journal of the Association of Asphalt Paving Technologists, Vol. 46, pp. 1-40.

Visscher, J. D. and Vanelstraete, A., (2003). *Comparative Low-Temperature Thermal Cracking Investigations on Different Reinforcing Interface Systems*. MAIREPAV03 - Third International Symposium on Maintenance and Rehabilitation of Pavements and Technological Control. University of Minho, Guimaraes.

Watanabegumi, (2005). RP-Pavement (Semi-Flexible Pavement). <URL:http://www.watanabegumi.co.jp/pavements/rps/rpse.html> [Accessed 8 August 2005]

Whiteoak, D., (1990). *The Shell Bitumen Handbook*. Shell Bitumen U.K. Surrey.

Zoorob, S. E., Hassan, K. E. and Setyawan, A., (2002). *Cold mix, cold laid semi-flexible Grouted Macadams, mix design and properties*. 4th European Symposium on Performance of Bituminous and Hydraulic Materials in Pavements. Nottingham.

APPENDICES

234

APPENDICES

APPENDICES

Engineering mechanical properties of *Densiphalt*®

Report prepared by KOAC·WMD for Densit a/s

KOAC · WMD
Schuttersweg 43
7328 AB Apeldoorn

Tel   +31-55-5432100
Fax   +31-55-5430111
E-mail apeldoorn@koac-wmd.nl
Homepage www.koac-wmd.nl

Instituut voor materiaal- en wegbouwkundig onderzoek

KOAC WMD

Engineering mechanical properties Densiphalt

Project number	:	A00.1011
Proposal number & date	:	O996319/kkw/nja, 10 December 1999
Title report	:	Engineering mechanical properties Densiphalt
Status report	:	Final report
Name principal	:	Densit a/s
Address	:	Rordalsvej 44
Town	:	9100 Aalborg
Country	:	Denmark
Name contact person	:	Mr. P. Aarsleff
Date of agreement	:	Thursday 23 December 1999
Remark of agreement	:	E-mail, 15:02:37
Contact person KOAC·WMD	:	Maarten M.J. Jacobs Ph.D.
Author report	:	Leo J.W. Pelgröm B.Sc.

Report

Name: Leo J.W. Pelgröm B.Sc.

Signature:

Date: June 28, 2000

Authorization

Name: Maarten M.J. Jacobs Ph.D.

Signature:

Date: June 28, 2000

Zonder schriftelijke toestemming van KOAC·WMD mag het rapport (of certificaat) niet anders dan in zijn geheel worden gereproduceerd.

KOAC·WMD Apeldoorn is STERLAB-geaccrediteerd onder nr. L103 voor de met een "Q" gemerkte verrichtingen).

A00.1011

- page 2 of 12 -

Contents

A00.1011

- page 3 of 12 -

---

1   Introduction

In assignment of COWI A/S Denmark, KOAC·WMD Apeldoorn carried out a research program for the determination of the engineering properties of Densiphalt. This research program consists of the determination of the stiffness and fatigue properties of Densiphalt. For this purpose the client delivered 4 platens of material where the test specimens has been taken from.

In this report the research program is explained and the results of the research program are presented.

2   Research program

2.1   General

For the determination of the mechanical properties a four point bending test is used. In figure 1 a picture of this test is given.

Figure 1: Overview of the test facility

In the test a prismatic specimen with the dimensions of $(450 \pm 2) * (50 \pm 1) * (50 \pm 1)$ mm is subjected to four-point periodic bending with free rotation and translation at all load and reaction points. The bending is realised by the centre bearing, in the vertical direction, perpendicular to the longitudinal axis of the specimen. The vertical position of the end-bearings is fixed. The applied force or displacement is sinusoidal and symmetrical around zero without rest period. During the test the displacement (strain controlled) amplitude remains constant. During the test the load, needed for the bending of the specimen,

A00.1011

- page 4 of 12 -

KOAC WMD

the displacement and the phase angle between force and displacement are measured as a function of time. From these properties the stiffness and fatigue properties of the material are derived.
The test performance to determine the stiffness and fatigue properties of a mixture is described in a test prescription of the Dutch Road and Hydraulic Engineering Division of Rijkswaterstaat (DWW). For the performance of this test according to this W-DWW-94530 document, KOAC·WMD is accredited by STERLAB (Q).

2.2 Determination of the dynamic stiffness modulus

For the determination of the dynamic stiffness modulus and the phase angle the following loading frequencies are used (frequency sweep): 0.1, 0.5, 1.0, 4.9, 9.8, 19.5, 29.3 and subsequently at 1.0 Hz. The displacement is chosen in such a way that the specimen will not be damaged during the test. The second test at a loading frequency of 1Hz is to make sure that this has not occurred. These tests are performed at 3 temperatures: 0, 20 and 40°C on 3 different specimens.

Based on the results of these tests a so-called mastercurve of the stiffness modulus can be determined. With this mastercurve the stiffness modulus of the Densiphalt can be determined at any loading frequency of temperature. This mastercurve is determined in the same way Francken and Vanelstraete suggested in their article "Complex Moduli of Bituminous materials: A rational method for the interpretation of test results", which was presented in the Proceedings of the RILEM Symposium on Mechanical Tests for Bituminous Materials in Lyon, France (May 1997).

2.3 Determination of the fatigue properties

In order to determine the fatigue properties of Densiphalt, dynamic tests are carried out. These tests are performed at a loading frequency of 29.3 Hz. During the test, the dynamic stiffness and the material phase angle are recorded as a function of the number of load repetitions. The test is continued until the fatigue life N_f is reached. For strain controlled tests the fatigue life is defined as the number of load repetitions which are needed to reduce the initial stiffness of the material to half of its initial value; in stress controlled tests, which are not carried out in this research program, the fatigue life is defined as the number of load repetitions until break down of the specimen.

The fatigue tests are performed at two temperatures: 0 and 20 °C at a constant strain level. At each temperature two strain levels are used: a lower strain level to attain a life span of about 10^6 load repetitions and a higher strain level to attain a life span of about 10^5 load repetitions. For each loading condition three specimens are tested. To determine the strain level two specimens have been used in a pre-test.

Based on the results of the fatigue tests a relationship between the applied strain (= ε) and the number of load repetitions (= N_f) is calculated for each temperature. To this end linear regression analysis based upon the method of least squares is performed on the number pairs (log N, log ε). The results of these analyses is the determination of the regression parameters k and n in the relationship:

$$N_f = k(\varepsilon)^{-n}$$

A00.1011

KOAC WMD

2.4 Fatigue curves

According to Van Dijk and Visser in their paper "The energy approach to fatigue for pavement design", presented at the AAPT Conference of 1977 the energy dissipation in fatigue specimens can be calculated with the equation:

$$W_f = \sum_{N=1}^{N=N_f} \pi \cdot \varepsilon_N \cdot S_N \cdot \sin \varphi_N = A \cdot N_f^z$$

Where:
W_f	=	total dissipated energy
ε_n	=	applied strain at cycle number n
S_n	=	stiffness modulus of the test specimen at cycle number N
φ_n	=	phase angle at cycle number n
A, z	=	material parameters
N	=	load cycle number
N_f	=	number of load cycles to fatigue.

This approach is also discussed in de Shell Pavement Design Manual (SPDM).

For the two temperatures the individual test results of N_f and W_f are combined to determine the regression or material parameters A and z.

To calculate the permissible strain the relation between the total dissipated energy to fatigue and the fatigue life on one hand is used and the description of the total dissipated energy per unit volume on the other hand. Hereby the ratio between the calculated "total" dissipated energy and the real total dissipated energy per volume is used. In formula:

$$\psi = \frac{W_{real}}{W_f} = \frac{N_f \pi S_{ini} \varepsilon^2 \sin \varphi_{ini}}{A N_f^z}$$

with S_{ini} and φ_{ini} being the initial values for, respectively, stiffness modulus of the beam and the phase angle in the fatigue test.

This formula can be also derived explicit in a relation between the permissible strain (ε_p) and the fatigue life (N_f):

$$\varepsilon_p = \sqrt{\frac{A \cdot \psi}{\pi \cdot S_{ini} \cdot \sin(\varphi)} \cdot \frac{1}{N_f^{1-z}}}$$

The relation between S_{ini} and respectively φ_{ini} and can also be determined. These relations are respectively $\varphi_{ini} = C_1 + C_2 \log S_{ini}$ and $= C_3 + C_4 \log S_{ini}$. These two relations can we substitute in the main formula of the permissible strain and we get the following equation:

$$\varepsilon_p = \sqrt{\frac{A \cdot (C_3 + C_4 \log S_{ini})}{\pi \cdot S_{ini} \cdot \sin(C_1 + C_2 \log S_{ini})} \cdot \frac{1}{N_f^{1-z}}}$$

With the last equation, different stiffness moduli and assuming $N_f = 10^5$, 10^6, 10^7 and 10^8 fatigue curves for the tested specimen can be determined.

A00.1011

KOAC WMD

3 Test results

3.1 Fatigue tests

In table 1 the results of the fatigue tests are presented.

Table 1: Results of the fatigue tests

Specimen number	Temperature	Strain					
Temperature 20 °C							
5	20	136.6	70	13811	14.3	92140	16975141	1.087
7	20	181.2	70	13378	14.7	28015	8928427	1.098
8	20	75.4	70	13634	13.3	1001015	55104907	1.018
13	20	75.7	70	13189	15.0	1644047	92298653	1.091
14	20	138.8	70	12707	16.2	69936	13651474	1.100
16	20	226.5	70	11276	17.7	11663	5883577	1.098
19	20	138.4	70	12174	17.0	75103	14105843	1.140
20*	20	82.0	70	13213	14.6	2198015	123086603	1.256
Mean				12923	15.4			
Stnd. Dev.				843	1.5			
Temperature 0 °C								
2	0	136.3	70	24215	6.1	118664	17444411	1.021
4	0	73.2	70	25224	5.6	1729015	76620190	1.013
9	0	131.8	70	25031	6.5	149892	22886935	1.012
12	0	71.2	70	25541	6.5	2353652	108081307	1.002
15	0	137.8	70	24770	6.7	111607	18995900	1.006
18	0	82.5	70	25494	6.1	885751	54381113	1.006
Mean				25046	6.2			
Stnd. Dev.				499	0.4			

In figures 2, 3 and 4 the relations are presented graphically.

A00.1011

KOAC WMD

Log Eps - log Nf
@ 0 & 20 °C

y = -4.6665x + 14.962
R² = 0.9665

y = -4.3385x + 14.339
R² = 0.9936

- 20 °C
- 0 °C
- Lineair (20 °C)
- Lineair (0 °C)
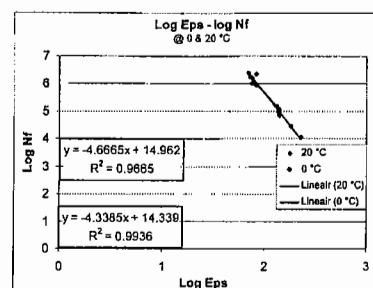
Figure 2: Relation between fatigue life and strain level

Log Nf - log Wf
@ 0 & 20 °C

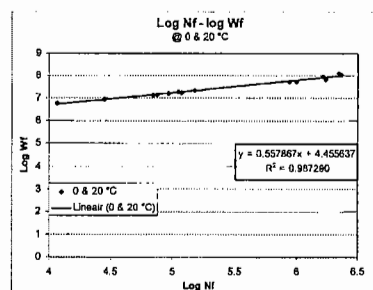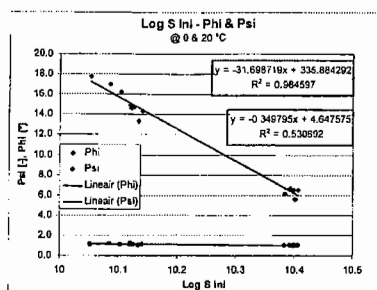y = 0.557867x + 4.455637
R² = 0.987280

- 0 & 20 °C
- Lineair (0 & 20 °C)

*Figure 3: Relation between dissipated energy and fatigue life*

A00.1011

Figure 4: Relation between φ resp. ψ and initial stiffness modulus

3.2 Fatigue curves of Densiphalt

With the regression parameters from figure 3 and 4 on one hand and the relation between the permissible strain and the number of load repetitions until failure the fatigue curve of Densiphalt can be determined (see figure 5).
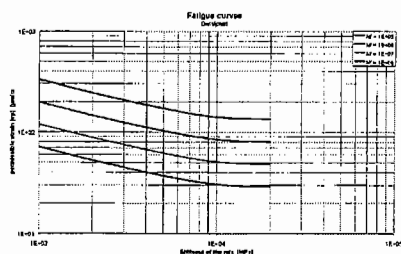
A00.1011

3.3 Dynamic stiffness

For the determination of the dynamic stiffness modulus and the phase angle the following loading frequencies are used (frequency sweep): 0.1, 0.5, 1.0, 4.9, 9.8, 19.5, 29.3 and subsequently at 1.0 Hz. The displacement is chosen in such a way that the specimen will not be damaged during the test. The second test at a loading frequency of 1 Hz is to make sure that this has not occurred. These tests are performed at 3 temperatures: 0, 20 and 40°C on 3 different specimens.

The results of the tests are presented in table 2. In figure 6 the mean results as a function of the loading frequency is presented.

Table 2: Results of the frequency sweep

40	0.1	1585	1359	946	1297	324
40	0.5	2290	2150	1545	1995	396
40	1	2872	2687	1897	2485	518
40	4.9	4336	4310	3273	3973	606
40	9.8	5255	5139	4079	4824	648
40	19.55	6153	6119	5086	5786	606
40	29.3	6619	6723	5677	6340	576
20	0.1	5848	5595	4384	5276	783
20	0.5	7743	7618	6497	7286	686
20	1	8491	8444	7538	8158	538
20	4.9	10827	11103	10424	10785	341
20	9.8	12146	12528	11750	12135	399
20	19.55	13128	13502	13132	13254	215
20	29.3	14192	14497	13955	14215	271
0	0.1	15771	15781	15456	15669	185
0	0.5	18398	18586	18624	18536	121
0	1	19812	19851	20032	19899	117
0	4.9	22462	22833	23032	22776	289
0	9.8	23482	24003	24074	23853	324
0	19.55	25057	25384	25645	25362	295
0	29.3	25289	25935	25941	25722	375

A00.1011

Figure 6: The mean of the individual results of the frequency sweep tests

Based on the results of these tests a so-called mastercurve of the stiffness modulus can be determined. With this mastercurve the stiffness modulus of the Densiphalt can be determined at any loading frequency of temperature. This mastercurve is determined is the same way Francken and Vanelstraete suggested in their article "Complex Moduli of Bituminous materials: A rational method for the interpretation of test results", which was presented in the Proceeding of the RILEM Symposium on Mechanical Tests for Bituminous Materials in Lyon, France (may 1997). To construct the mastercurve the mean value per (test condition (temperature and loading frequency) of the three individual results is used.

The technique of the establishment of the master curve is based on the principle of time-temperature correspondence of the equivalence between frequency and temperature. This equivalence is a result of the thermorheological behaviour of the bitumen. With this behaviour it is possible to shifting the results horizontally using a shift factor α_T. The shift factor is calculated by means of an Arrhenius type of equation:

$$\alpha_T = \exp\left[\frac{\Delta H}{R}\left(\frac{1}{T} - \frac{1}{T_r}\right)\right]$$

where:
- ΔH = apparent activation energy (in J/mole);
- R = universal gas constant = 8.31441 J/K/mole;
- T = the considered temperature (in K);
- T_r = the reference temperature (in K, in this case 293.15 K = 20 °C);
- α_t = f/f;
- f_r = reduced frequency (in Hz);
- f = loading frequency (in Hz).

Based on the described procedure an ΔH-value for Densiphalt of 186 kJ/mole is found. In figure 7 the master curve of Densiphalt is presented.

For comparing the results in table 3 some results of other specimens the ΔH-values is presented.

A00.1011

Table 3: ΔH-values of some other specimens

Specimen	ΔH [in kJ/mole]	
	Mean	Std. Dev.
Sand asphalt	154	43
DAC 0/8	142	46
DAC 0/16	130	43
DAC modified	150	31
SMA	154	32

The relation of the regression analysis of the master curve is:

$${}^{10}\log(\text{Smix}) = -0.01944*{}^{10}\log(f_r)^2 + 0.20079*{}^{10}\log(f_r) + 3.921162 \quad (R^2 = 0.998)$$
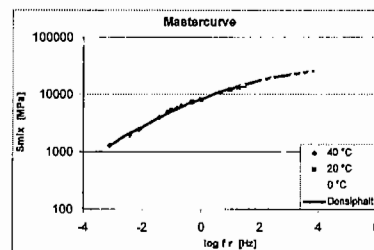
Figure 7: Master curve of Densiphalt

A00.1011

Stiffness Modulus and Phase Angle of the studied mixtures (four-point bending test results)
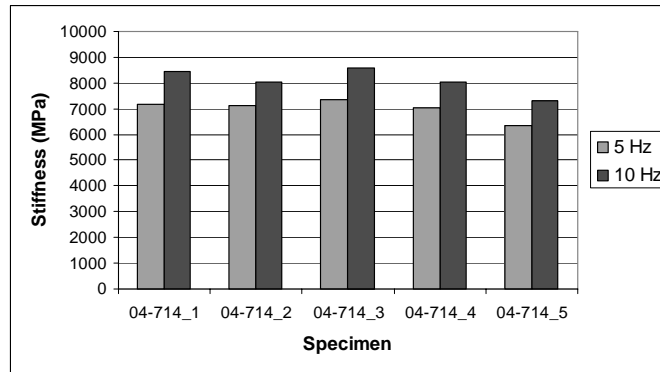

Figure B1 – Stiffness Modulus of Slab 04-0714 (Standard mixture, 7 days, 20 ºC)
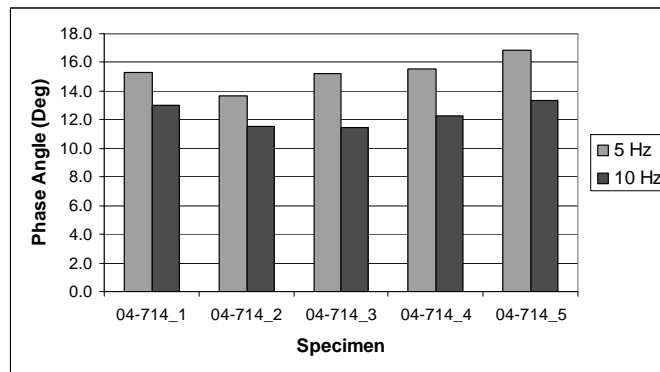

Figure B2 – Phase Angle of Slab 04-0714 (Standard mixture, 7 days, 20 ºC)
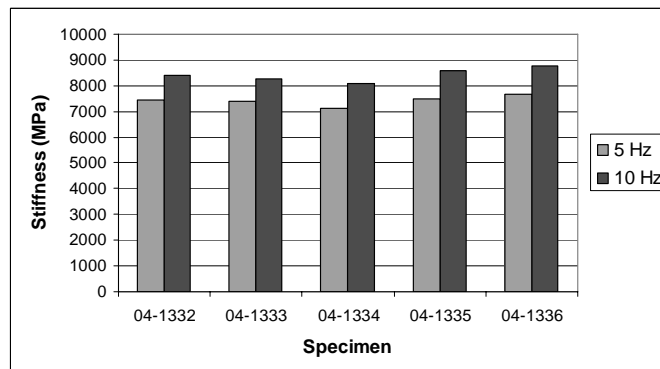

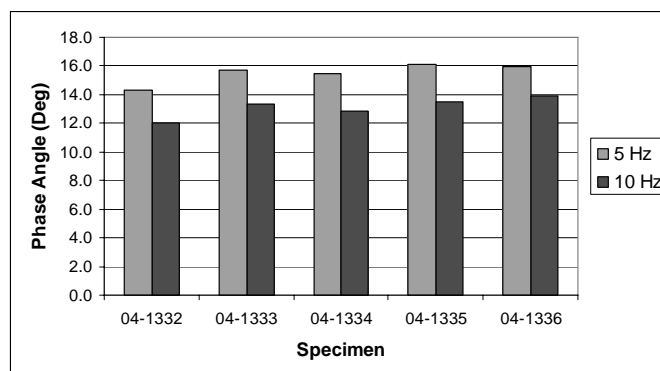Figure B3 – Stiffness Modulus of Slab 04-0936 (Standard mixture, 28 days, 20 ºC)

Figure B4 – Phase Angle of Slab 04-0936 (Standard mixture, 28 days, 20 ºC)
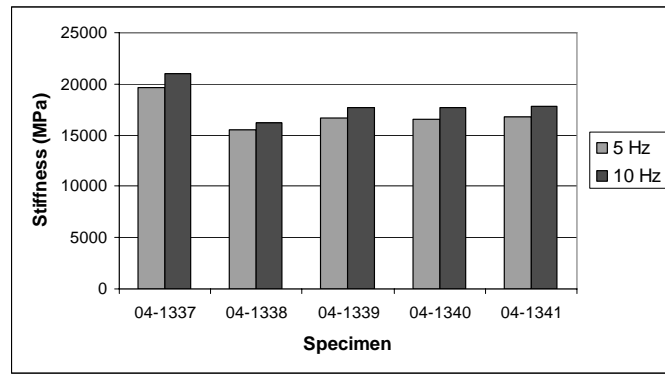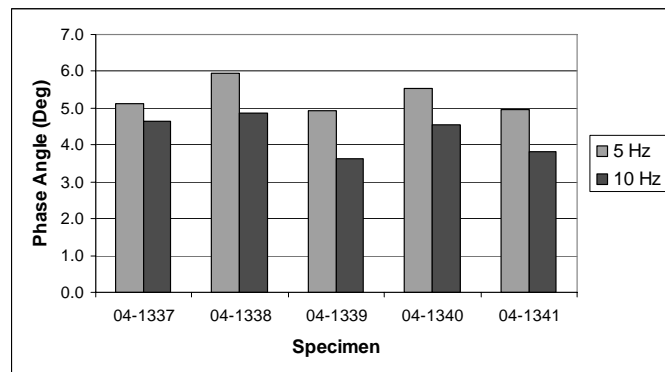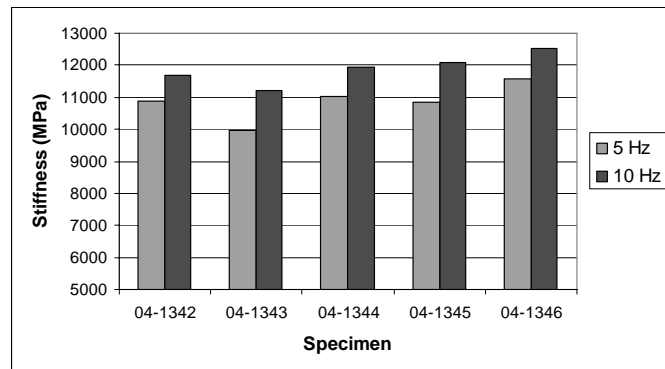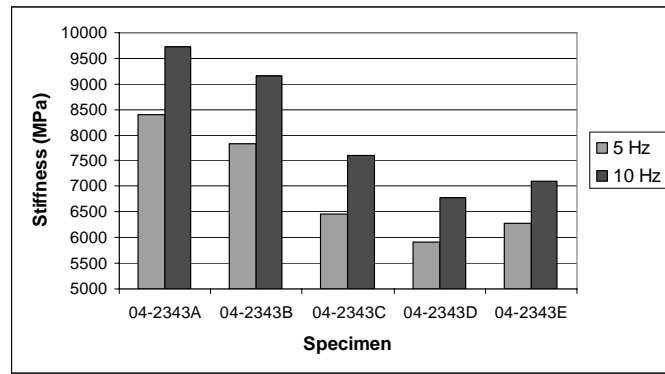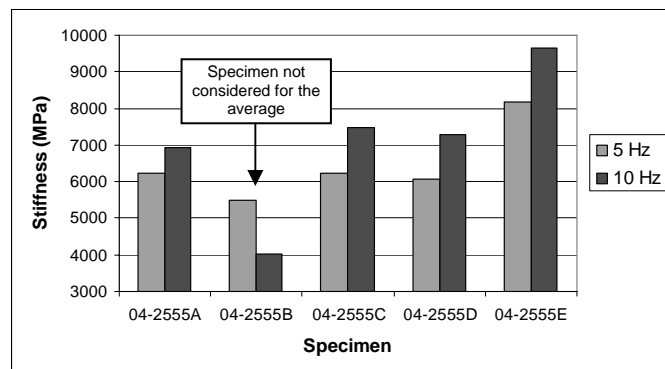
Figure B5 – Stiffness Modulus of Slab 04-1309 (Standard mixture, 28 days, 0 ºC)

Figure B6 – Phase Angle of Slab 04-1309 (Standard mixture, 28 days, 0 ºC)

Figure B7 – Stiffness Modulus of Slab 04-1310 (50 pen bitumen, 7 days, 20 ºC)
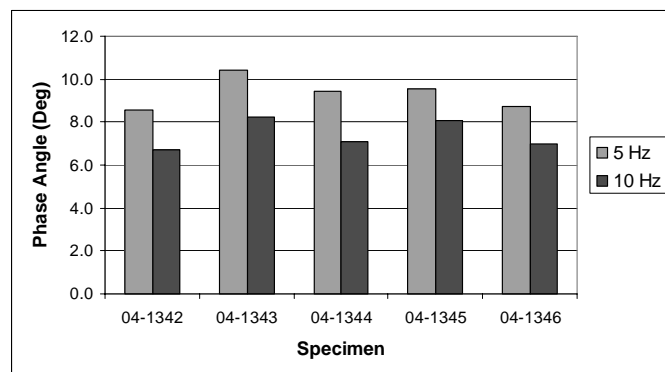
Figure B8 – Phase Angle of Slab 04-1310 (50 pen bitumen, 7 days, 20 ºC)
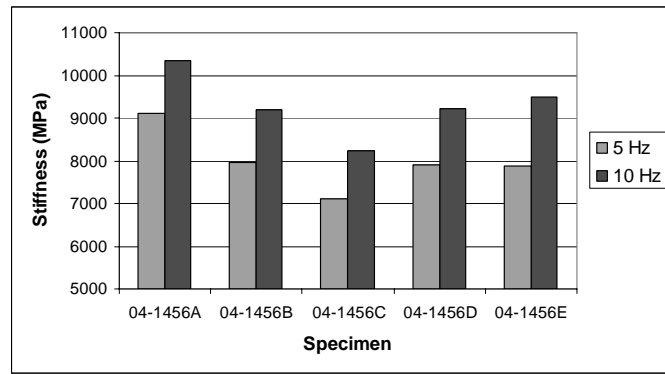
Figure B9 – Stiffness Modulus of Slab 04-1456 (3% binder, 7 days, 20 ºC)
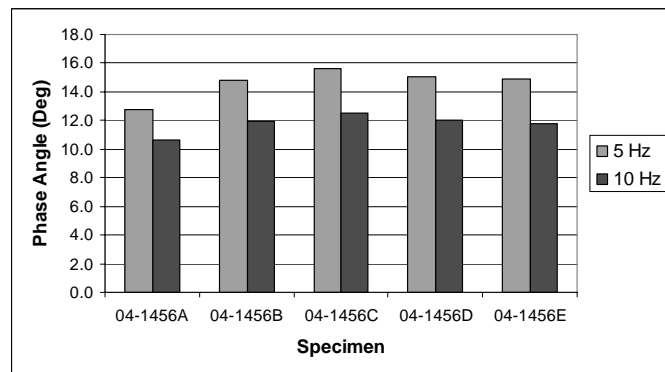
Figure B10 – Phase Angle of Slab 04-1456 (3% binder, 7 days, 20 ºC)
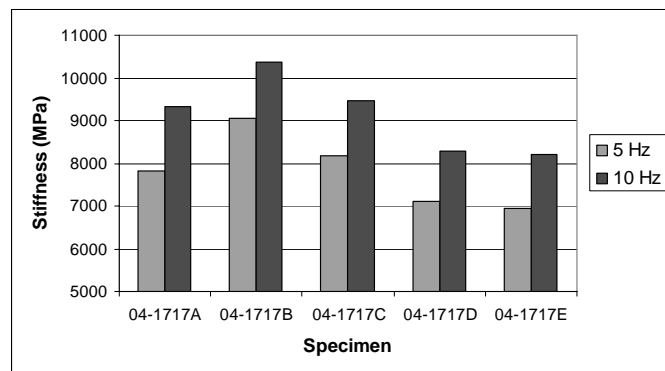
Figure B11 – Stiffness Modulus of Slab 04-1717 (more continuous grading, 7 days, 20 ºC)
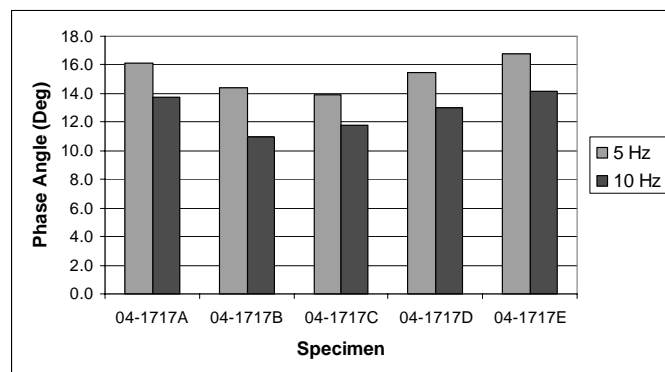
Figure B12 – Phase Angle of Slab 04-1717 (more continuous grading, 7 days, 20 ºC)
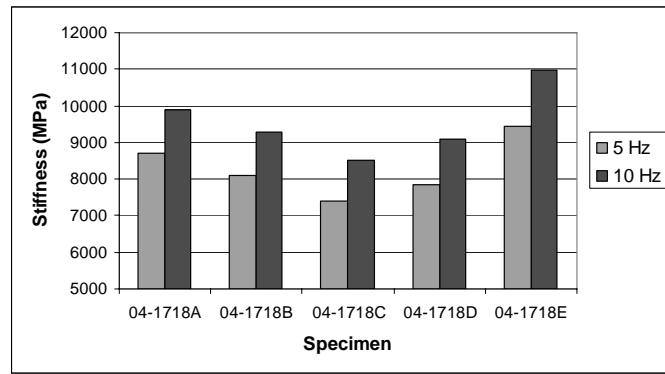
Figure B13 – Stiffness Modulus of Slab 04-1718 (14 mm aggregate, 3% binder, 7 days, 20 ºC)
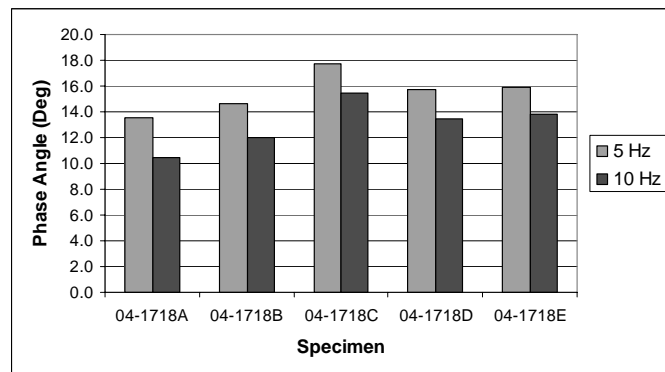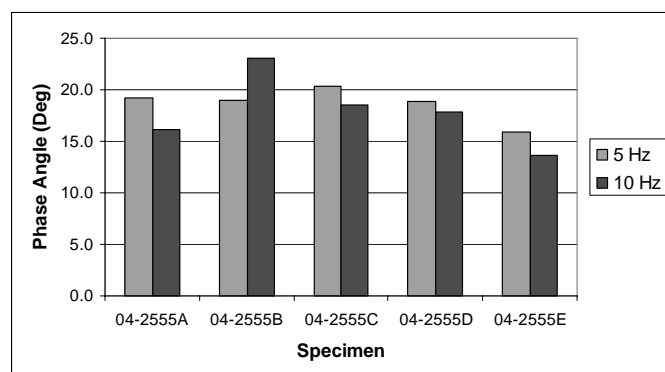

Figure B14 – Phase Angle of Slab 04-1718 (14 mm aggregate, 3% binder, 7 days, 20 ºC)
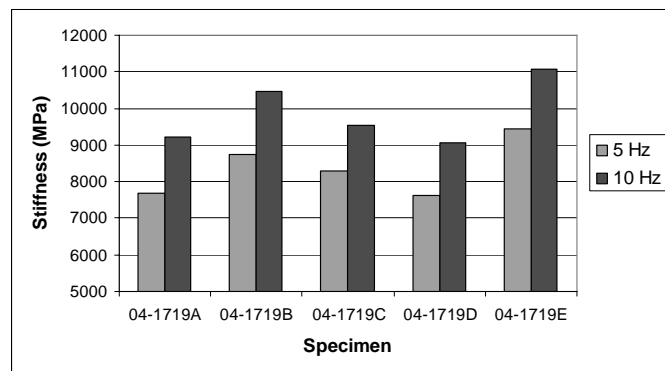
Figure B15 – Stiffness Modulus of Slab 04-1719 (limestone aggregate, 3% binder, 7 days, 20 ºC)
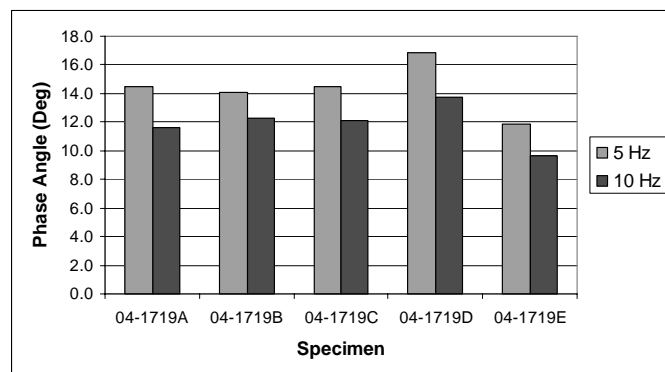
Figure B16 – Phase Angle of Slab 04-1719 (limestone aggregate, 3% binder, 7 days, 20 ºC)
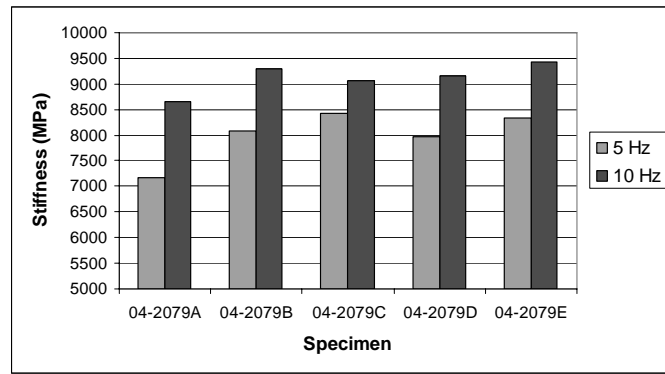
Figure B17 – Stiffness Modulus of Slab 04-2079 (limestone aggregate, 7 days, 20 ºC)
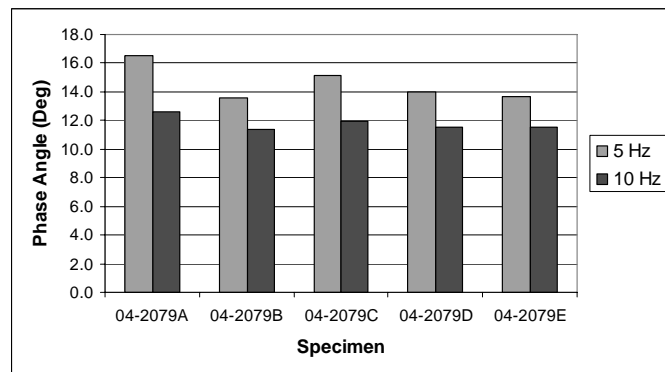
Figure B18 – Phase Angle of Slab 04-2079 (limestone aggregate, 7 days, 20 ºC)
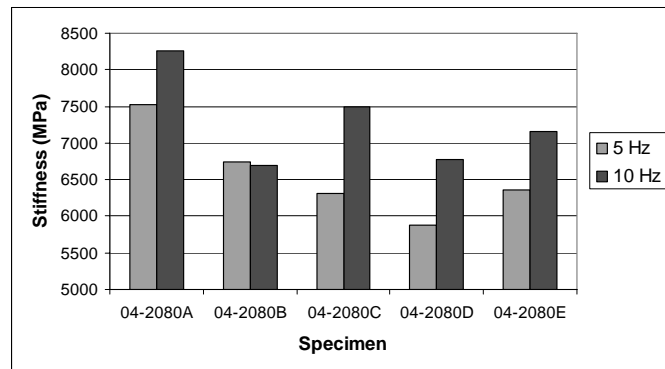
Figure B19 – Stiffness Modulus of Slab 04-2080 (14 mm aggregate, 4.1% binder, 7 days, 20 ºC)
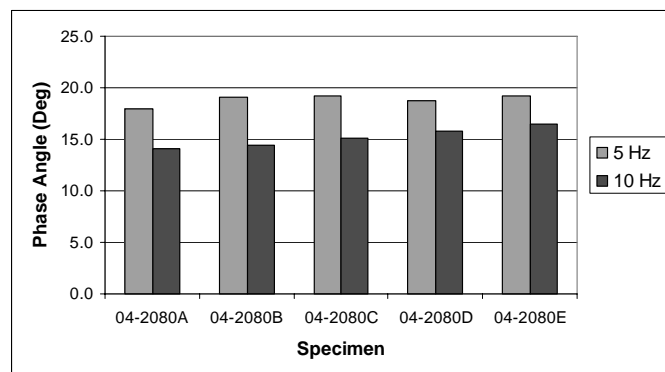
Figure B20 – Phase Angle of Slab 04-2080 (14 mm aggregate, 4.1% binder, 7 days, 20 ºC)

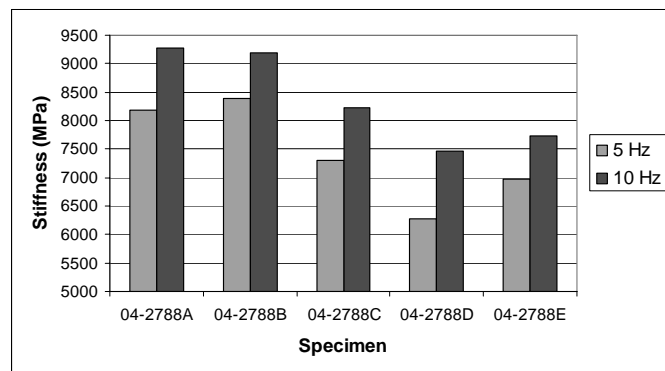Figure B21 – Stiffness Modulus of Slab 04-2343 (Standard mixture, 7 days, 20 ℃)
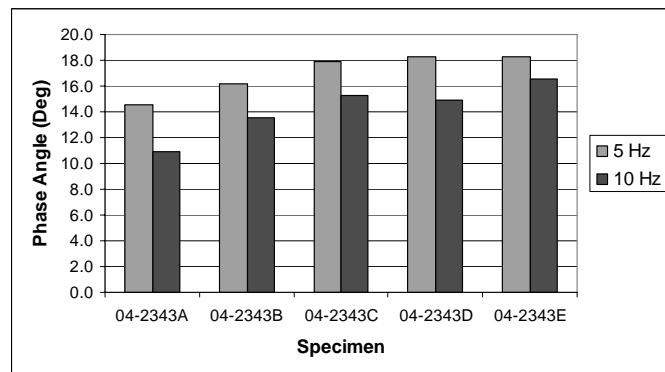
Figure B22 – Phase Angle of Slab 04-2343 (Standard mixture, 7 days, 20 ℃)

Figure B23 – Stiffness Modulus of Slab 04-2555 (20 mm aggregate, 4.1% binder, 7 days, 20 ℃)

Figure B24 – Phase Angle of Slab 04-2555 (20 mm aggregate, 4.1% binder, 7 days, 20 ℃)
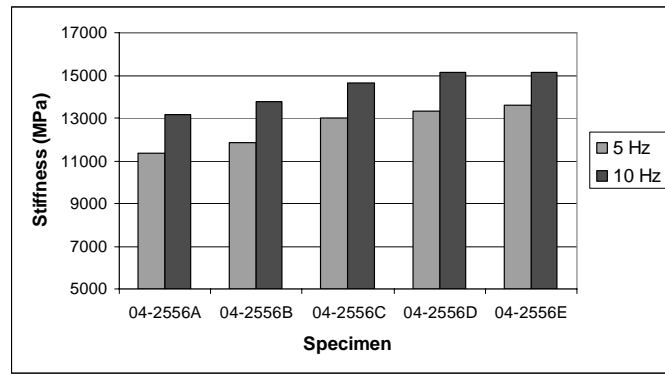
Figure B25 – Stiffness Modulus of Slab 04-2556 (1.5% binder, 7 days, 20 ºC)
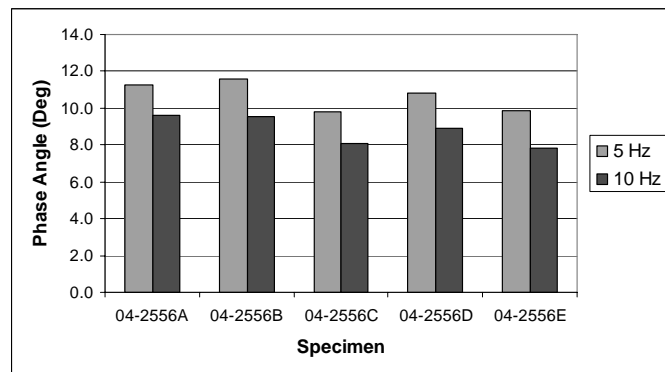
Figure B26 – Phase Angle of Slab 04-2556 (1.5% binder, 7 days, 20 ºC)

Figure B27 – Stiffness Modulus of Slab 04-2788 (4.1% PMB binder, 7 days, 20 ºC)
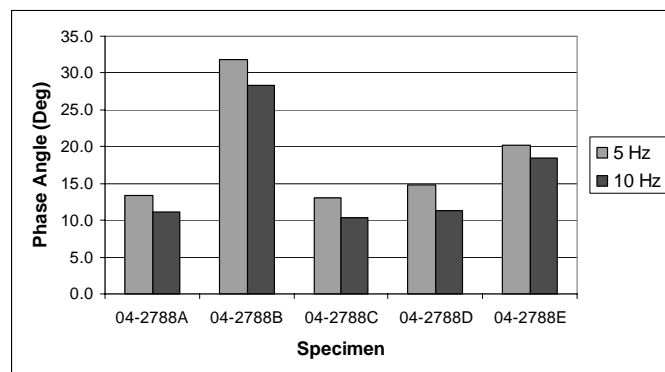
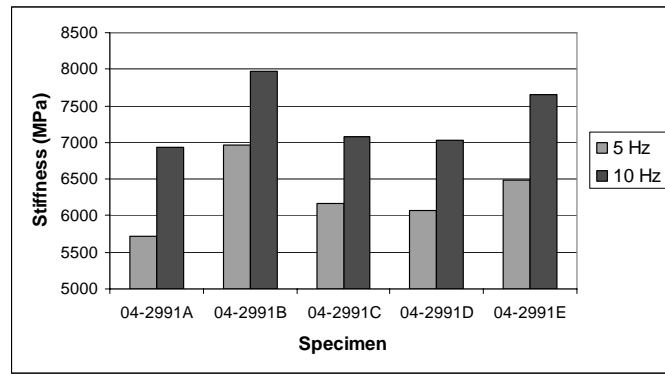Figure B28 – Phase Angle of Slab 04-2788 (4.1% PMB binder, 7 days, 20 ºC)

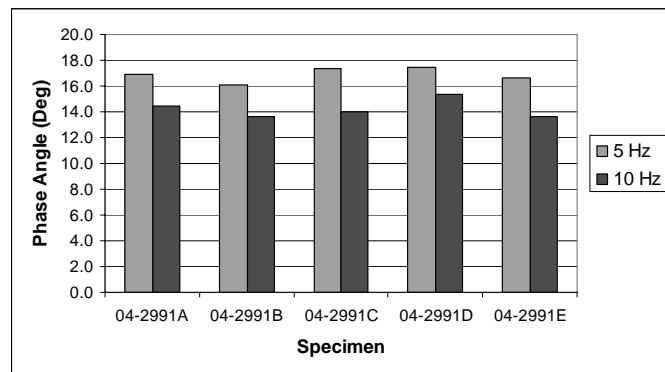Figure B29 – Stiffness Modulus of Slab 04-2991 (low strength grout, 7 days, 20 ºC)

Figure B30 – Phase Angle of Slab 04-2991 (low strength grout, 7 days, 20 ºC)
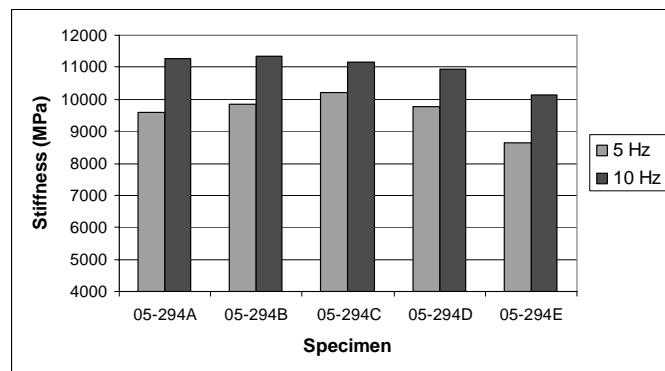

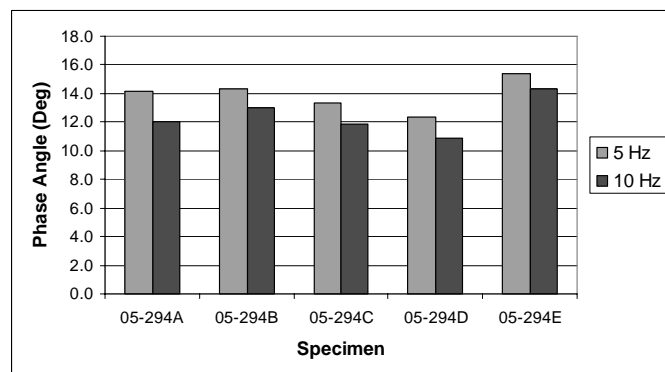Figure B31 – Stiffness Modulus of Slab 05-0294 (PTF – Standard mixture, 5 months, 20 ºC)

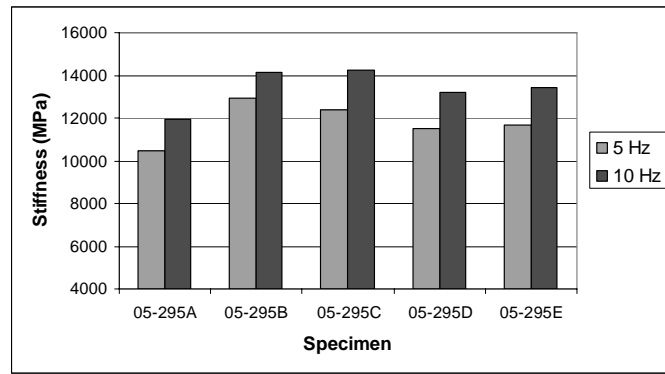Figure B32 – Phase Angle of Slab 05-0294 (PTF – Standard mixture, 5 months, 20 ºC)

Figure B33 – Stiffness Modulus of Slab 05-0295 (PTF – 2% PMB, 5 months, 20 ºC)
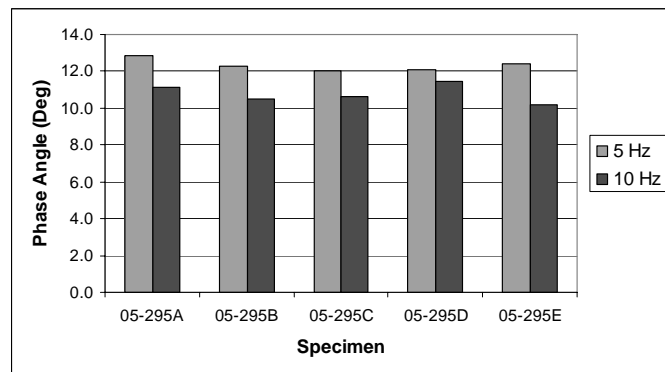

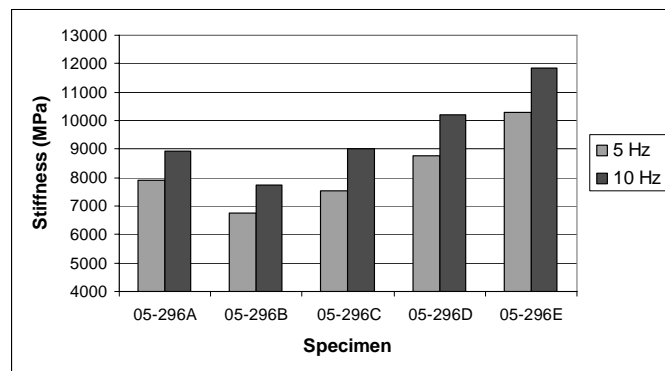Figure B34 – Phase Angle of Slab 05-0295 (PTF – 2% PMB, 5 months, 20 ºC)

Figure B35 – Stiffness Modulus of Slab 05-0296 (PTF – Standard mixture, 5 months, 20 ºC)
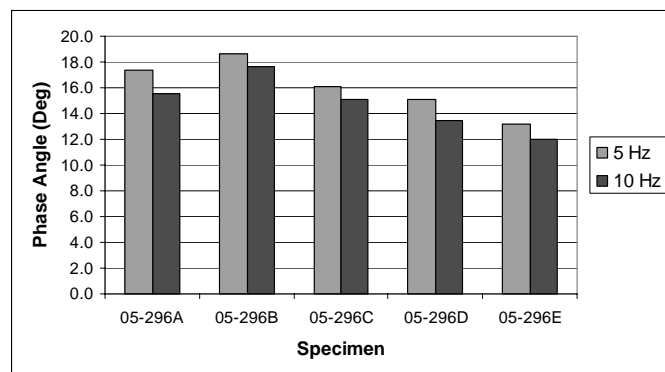

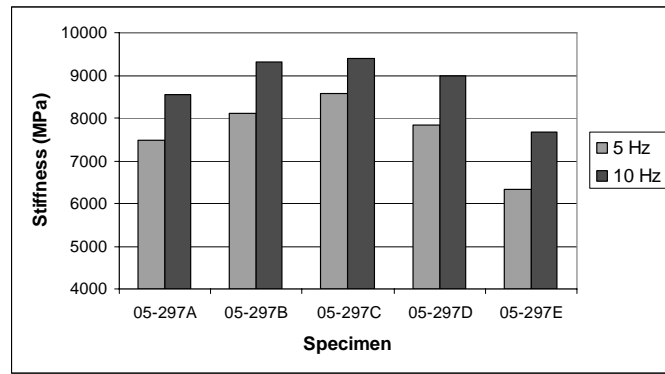Figure B36 – Phase Angle of Slab 05-0296 (PTF – Standard mixture, 5 months, 20 ºC)

Figure B37 – Stiffness Modulus of Slab 05-0297 (PTF – Modified Densit grout, 5 months, 20 ºC)

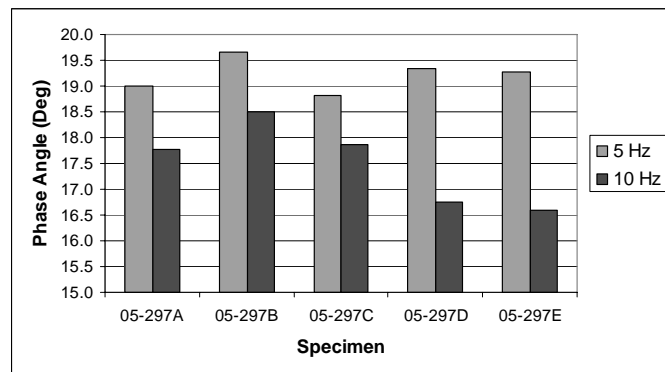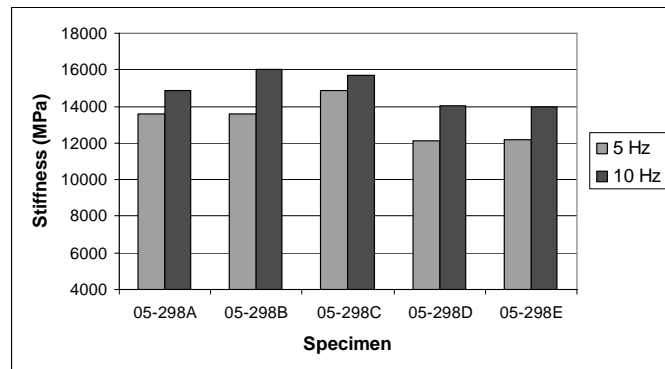Figure B38 – Phase Angle of Slab 05-0297 (PTF – Modified Densit grout, 5 months, 20 ºC)

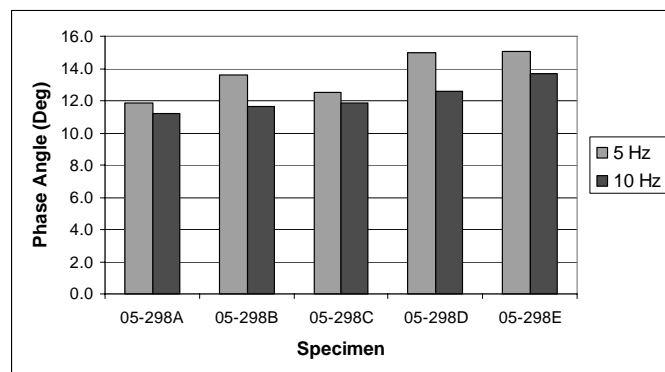Figure B39 – Stiffness Modulus of Slab 05-0298 (PTF – 2% Binder, 5½ months, 20 ºC)

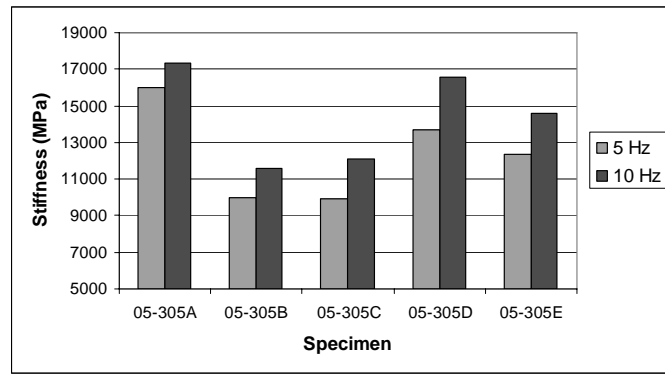Figure B40 – Phase Angle of Slab 05-0298 (PTF – 2% Binder, 5½ months, 20 ºC)

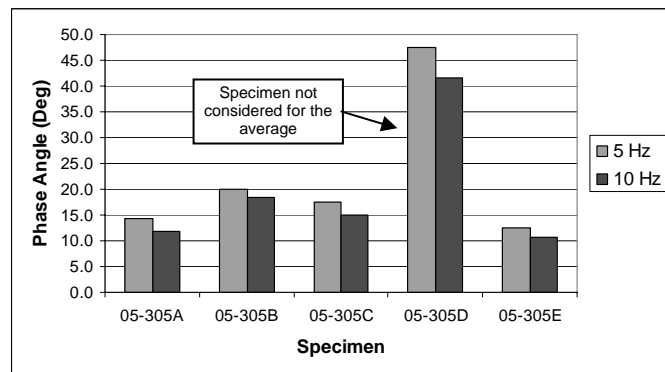Figure B41 – Stiffness Modulus of Slab 05-0305 (20 mm aggregate, 7 days, 20 ℃)

Figure B42 – Phase Angle of Slab 05-0305 (20 mm aggregate, 7 days, 20 ℃)

Fatigue life of the studied mixtures (four-point bending test results)

Mixture	Specimen	Strain level (με)	No. of cycles to failure (Nf)
Slab 04-0714 Standard mixture (7 days, 20 ℃)	A	178	61001
	B	--	--
	C	371	3142
	D	278	4370
	E	453	884
Slab 04-0936 Standard mixture (28 days, 20 ℃)	A	456	1134
	B	360	2552
	C	268	6808
	D	173	43283
	E	130	179354
Slab 04-1309 Standard mixture (28 days, 0 ℃)	A	279	13205
	B	220	37075
	C	142	189563
	D	358	3183
	E	98	815083
Slab 04-1310 50 pen bitumen (7 days, 20 ℃)	A	323	8304
	B	413	1584
	C	159	91671
	D	252	20557
	E	79	1526524
Slab 04-1456 3% binder (7 days, 20 ℃)	A	155	100076
	B	354	3111
	C	453	1648
	D	264	10221
	E	208	21853
Slab 04-1717 More continuous grading (7 days, 20 ℃)	A	350	2204
	B	254	5525
	C	434	888
	D	212	10879
	E	160	41706
Slab 04-1718 14 mm aggregate, 3% binder (7 days, 20 ℃)	A	354	3108
	B	451	1664
	C	274	6618
	D	210	16545
	E	149	118136
Slab 04-1719 Limestone aggregate, 3% binder (7 days, 20 ℃)	A	360	4102
	B	444	966
	C	210	16376
	D	269	4326
	E	128	1170760

Mixture	Specimen	Strain level (με)	No. of cycles to failure (Nf)
Slab 04-2079 Limestone aggregate (7 days, 20 ºC)	A	375	2907
	B	454	1458
	C	273	8651
	D	215	25841
	E	160	130224
Slab 04-2080 14 mm aggregate, 4.1% binder (7 days, 20 ºC)	A	355	2032
	B	460	1747
	C	272	8511
	D	222	18874
	E	163	131777
Slab 04-2343 Standard mixture (7 days, 20 ºC)	A	376	2330
	B	482	927
	C	441	1166
	D	291	6030
	E	587	455
Slab 04-2555 20 mm aggregate, 4.1% binder (7 days, 20 ºC)	A	376	2365
	B	491	550
	C	278	3328
	D	582	254
	E	217	4459
Slab 04-2556 1.5% binder (7 days, 20 ºC)	A	376	1596
	B	449	692
	C	257	5289
	D	570	251
	E	216	12899
Slab 04-2788 4.1% PMB binder (7 days, 20 ºC)	A	541	1865
	B	461	7917
	C	370	16577
	D	424	6264
	E	287	97575
Slab 04-2991 Low strength grout (7 days, 20 ºC)	A	386	2378
	B	476	1339
	C	592	767
	D	440	1373
	E	281	3895
Slab 05-0294 PTF – Standard mixture (5 months, 20 ºC)	A	377	1900
	B	465	346
	C	578	512
	D	281	6029
	E	166	40451
Slab 05-0295 PTF – 2% PMB (5 months, 20 ºC)	A	370	4203
	B	560	466
	C	271	10254
	D	465	2294
	E	158	140139

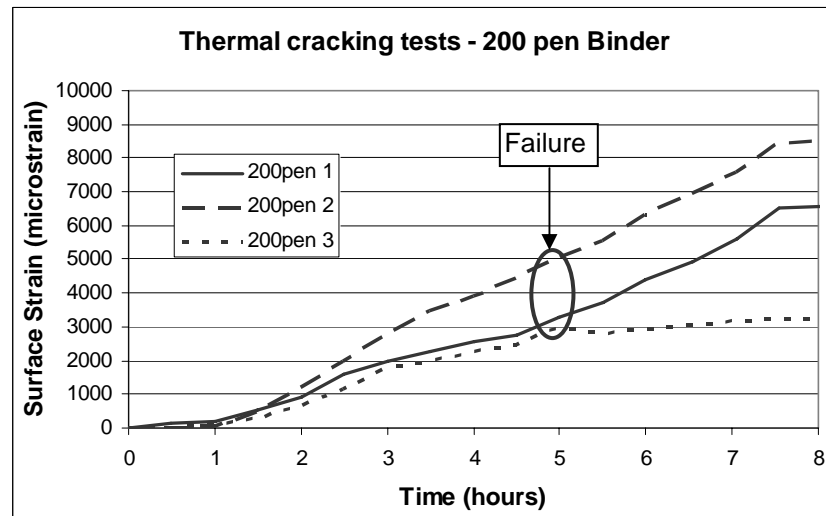| Mixture	Specimen	Strain level (με)	No. of cycles to failure (Nf)
Slab 05-0296 PTF – Standard mixture (5 months, 20 ºC)	A	374	669
	B	164	27077
	C	280	3408
	D	466	814
	E	575	527
Slab 05-0297 PTF – Modified Densit grout (5 months, 20 ºC)	A	366	2134
	B	578	286
	C	282	3786
	D	478	464
	E	172	13286
Slab 05-0298 PTF – 2% Binder (5½ months, 20 ºC)	A	378	316
	B	569	451
	C	281	1828
	D	225	3671
	E	135	45540
Slab 05-0305 20 mm aggregate (7 days, 20 ºC)	A	380	608
	B	577	121
	C	289	491
	D	232	2654
	E	139	15081

Thermal cracking test results

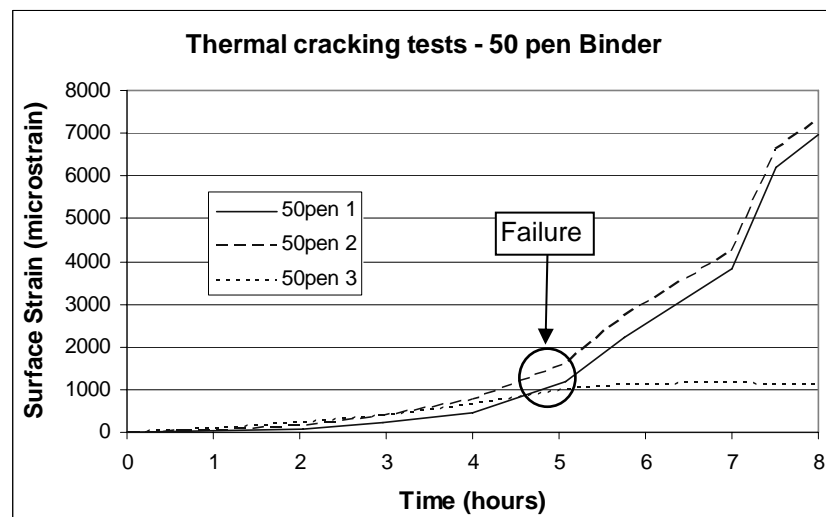Figure E1 – Thermal cracking test (Standard mixture, -5 ℃)

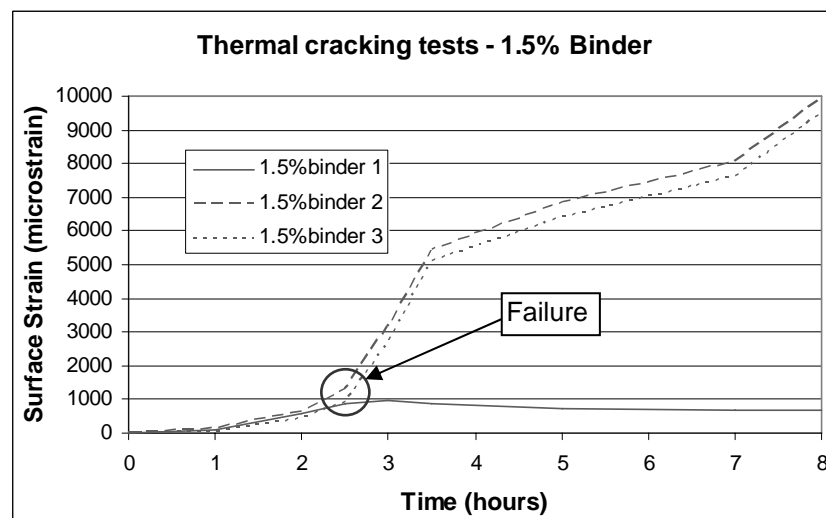Figure E2 – Thermal cracking test (50 pen Binder, -5 ℃)

Figure E3 – Thermal cracking test (1.5% Binder, -5 ℃)

Stiffness Modulus of DBM 50 and standard Grouted Macadam mixtures (two-point bending tests)

Table D1 – Stiffness and Fatigue Life of DBM50 (two-point bending test results)

Specimen identification	Initial Stiffness [MPa]	Strain level [µε]	No. of Cycles to failure
04-2121	6196	150	33674
04-2123	5760	300	2554
04-2124	4623	400	6034
04-2125	7432	120	465900
04-2126	4223	500	814
04-2127	7187	130	59074
04-2128	5179	350	2914
04-2130	6262	250	22694
04-2131	4235	450	2714
04-2132	7180	80	5735450
04-2133	5026	400	1954
04-2134	6422	125	470900
04-2138	5309	200	9300
	Average	**5772**	

Table D2 – Stiffness and Fatigue Life of Grouted Macadam (two-point bending test results)

Specimen identification	Initial Stiffness [MPa]	Strain level [µε]	No. of Cycles to failure
05-668 A	4541	90	1398850
05-668 B	4726	300	4550
05-668 C	5465	400	1800
05-668 E	5887	200	11150
05-668 F	3037	500	1750
05-668 G	5057	100	160600
05-668 H	6490	170	15600
05-668 I	7106	160	32350
05-668 J	4987	150	48500
05-668 L	8166	110	87700
	Average	**5546**	